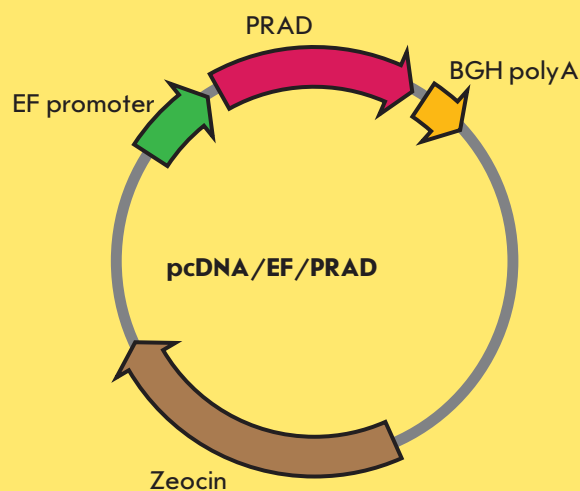
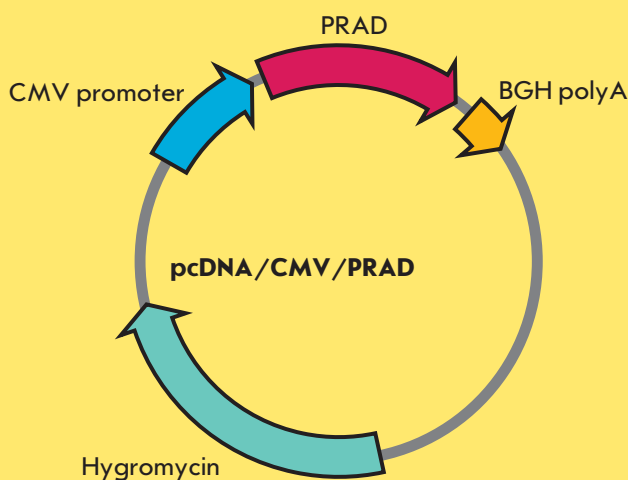
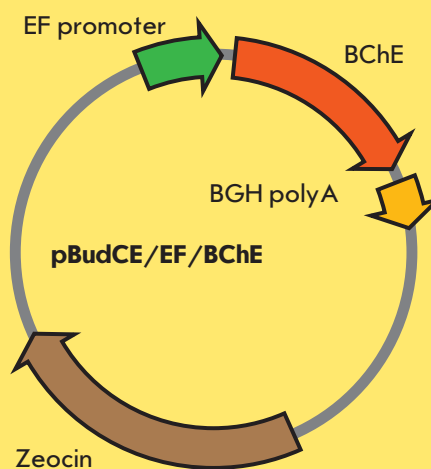
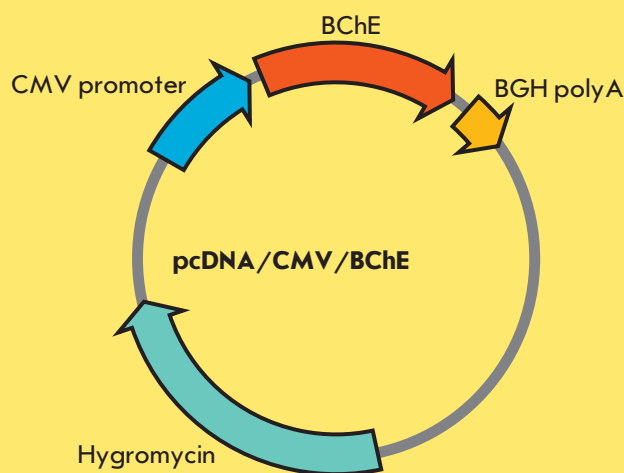


ActaNaturae

Use of Transgenic Animals in Biotechnology: Prospects and Problems



PULSED ELECTRON DOUBLE RESONANCE IN STRUCTURAL STUDIES OF SPIN-LABELED NUCLEIC

P. 9

RECOMBINANT HUMAN BUTYRYLCHOLINESTERASE AS A NEW-AGE BIOSCAVENGER DRUG

P. 73

Letter from the Editors

Dear readers,
We are elated to bring you the 16th issue of *Acta Naturae*, the first for 2013. We take this opportunity to wish you and us (especially our journal) further success and much luck in 2013!

Let us comment on the current issue. The 38th Congress of the Federation of European Biochemical Societies (FEBS), which is set to take place this summer in St. Petersburg, is shaping up to be the most significant event for Russian and foreign biologists in 2013. Our journal is closely connected to the event; therefore, we want to announce it and invite all our readers to participate in the Congress in its Forum section.

The research section of this issue contains three reviews; their titles once again show the broad character of the subject matters covered in *Acta Naturae*. Indeed, the first

review is devoted to the physical chemistry of nucleic acids (O.S. Fedorova and Yu.D. Tsvetkov), the second one focuses on bioengineering (O.G. Maksimenko, A.V. Deikin, Yu.M. Khodarovich, and P.G. Georgiev), while the third review is devoted to population genetics (V.I. Glazko and T.T. Glazko). We hope that researchers involved in interdisciplinary life sciences will find these materials useful.

Commenting on the research articles, we would like to bring your attention to the increasing number of publications by foreign authors or joint research by Russian and foreign scientists. We believe that this is a result of the inclusion of *Acta Naturae* into PubMed and other databases. In turn, we encourage further cooperation between our journal and foreign authors.

See you in the next issue of *Acta Naturae*. ●

ActaNaturae

SUBSCRIPTION TO

Acta Naturae journal focuses upon interdisciplinary research and developments at the intersection of various spheres of biology, such as molecular biology, biochemistry, molecular genetics, and biological medicine.

Acta Naturae journal is published in Russian and English by Park Media company. It has been included in the list of scientific journals recommended by the State Commission for Academic Degrees and Titles of the Ministry of Education and Science of the Russian Federation and the Pubmed abstracts database.



SUBSCRIBE AT THE EDITORIAL OFFICE

Leninskie Gory, 1-75G, Moscow, 119234 Russia
Telephone: +7 (495) 930-87-07, 930-88-51
Bio-mail: podpiska@biorf.ru
Web site: www.actanaturae.ru

SUBSCRIBE USING THE CATALOGUES OR VIA THE INTERNET:

ROSPECHAT (The Russian Press)
Indices: 37283, 59881
www.pressa.rosp.ru

INFORMNAUKA
Index: 59881
www.informnauka.com

INTER-POCHTA
17510
www.interpochta.ru

INFORMATION FOR AUTHORS:

If you would like to get your research paper published in *Acta Naturae* journal, please contact us at journal@biorf.ru or call +7 (495) 930-87-07.

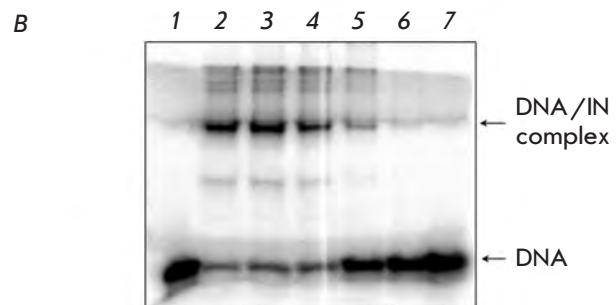
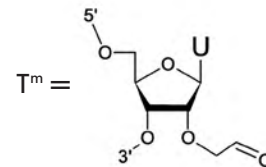


Structural-Functional Analysis of 2,1,3-Benzoxadiazoles and Their N-oxides As HIV-1 Integrase Inhibitors

S. P. Korolev, O. V. Kondrashina,
D. S. Druzhilovsky, A. M. Starosotnikov,
M. D. Dutov, M. A. Bastrakov,
I. L. Dalinger, D. A. Filimonov, S. A. Shevelev,
V. V. Poroikov, Y. Y. Agapkina, M. B. Gottikh

Human immunodeficiency virus type 1 integrase is one of the most attractive targets for the development of anti-HIV-1 inhibitors. The capacity of a series of 2,1,3-benzoxadiazoles (benzofurazans) and their N-oxides (benzofuroxans) selected using the PASS software to inhibit the catalytic activity of HIV-1 integrase was studied in the present work. Only the nitro-derivatives of these compounds were found to display inhibitory activity. The study of the mechanism of inhibition by nitro-benzofurazans/benzofuroxans showed that they impede the substrate DNA binding at the integrase active site. These inhibitors were also active against integrase mutants resistant to raltegravir, which is the first HIV-1 integrase inhibitor approved for clinical use.

A USB 5'-GTGTGGAAAATCTCTAGCAGT-3'
USA^m 3'-CACACCTTTTAGAGATCGT^mCA-5'



The influence of compound **6** on the efficiency of covalent binding of a DNA-substrate analog containing the aldehyde group to IN

Sources of Contradictions in the Evaluation of Population Genetic Consequences after the Chernobyl Disaster

V.I. Glazko, T.T. Glazko

The review covers population and genetic consequences in various mammalian species under conditions of high levels of ionizing radiation as a result of the Chernobyl accident.

Table 1. The frequency of micronuclei occurrence per 1,000 erythrocytes (EMN) isolated from the peripheral blood of CC57W/Mv mice of various ages from the Chernobyl and Kiev populations during different seasons

Season	EMN, control, ‰		EMN, Chernobyl, ‰	
	2.5–3.5 months	14–16 months	2.5–3.5 months	14–16 months
Winter 1993	2.5 ± 0.7	2.7 ± 0.9	10.0 ± 1.0	4.0 ± 1.0
Summer 1994	3.0 ± 0.8	3.2 ± 0.7	6.5 ± 1.0	3.8 ± 0.3

Founders

Ministry of Education and
Science of the Russian Federation,
Lomonosov Moscow State University,
Park Media Ltd

Editorial Council

Chairman: A.I. Grigoriev
Editors-in-Chief: A.G. Gabibov, S.N. Kochetkov

V.V. Vlassov, P.G. Georgiev, M.P. Kirpichnikov,
A.A. Makarov, A.I. Miroshnikov, V.A. Tkachuk,
M.V. Ugryumov

Editorial Board

Managing Editor: V.D. Knorre
Publisher: A.I. Gordeyev

K.V. Anokhin (Moscow, Russia)
I. Bezprozvanny (Dallas, Texas, USA)
I.P. Bilenkina (Moscow, Russia)
M. Blackburn (Sheffield, England)
S.M. Deyev (Moscow, Russia)
V.M. Govorun (Moscow, Russia)
O.A. Dontsova (Moscow, Russia)
K. Drauz (Hanau-Wolfgang, Germany)
A. Friboulet (Paris, France)
M. Issagouliants (Stockholm, Sweden)
A.L. Konov (Moscow, Russia)
M. Lukic (Abu Dhabi, United Arab Emirates)
P. Masson (La Tronche, France)
K. Nierhaus (Berlin, Germany)
V.O. Popov (Moscow, Russia)
I.A. Tikhonovich (Moscow, Russia)
A. Tramontano (Davis, California, USA)
V.K. Švedas (Moscow, Russia)
J.-R. Wu (Shanghai, China)
N.K. Yankovsky (Moscow, Russia)
M. Zouali (Paris, France)

Project Head: M.N. Morozova
Editor: N.Yu. Deeva
Strategic Development Director: E.L. Pustovalova
Designer: K.K. Oparin
Photo Editor: I.A. Solovey
Art and Layout: K. Shnaider
Copy Chief: Daniel M. Medjo

Address: 119234 Moscow, Russia, Leninskiye Gory, Nauchny
Park MGU, vlad.1, stroeniye 75G.
Phone/Fax: +7 (495) 930 88 50
E-mail: vera.knorre@gmail.com, mmorozova@strf.ru,
actanaturae@gmail.com

Reprinting is by permission only.

© ACTA NATURAE, 2013

Номер подписан в печать 5 марта 2013 г.
Тираж 200 экз. Цена свободная.
Отпечатано в типографии «МЕДИА-ГРАНД»

Letter from the Editors 1

FORUM

Federation of European Biochemical
Societies CONGRESS 2013
“Mechanisms in Biology” 6

REVIEWS

O. S. Fedorova, Yu. D. Tsvetkov
Pulsed Electron Double Resonance
in Structural Studies of Spin-Labeled
Nucleic Acids 9

O. G. Maksimenko, A. V. Deykin,
Yu. M. Khodarovich, P. G. Georgiev
Use of Transgenic Animals
in Biotechnology: Prospects
and Problems 33

V.I. Glazko, T.T. Glazko
**Sources of Contradictions
in the Evaluation of Population
Genetic Consequences after
the Chernobyl Disaster**47

N. V. Punina, V. S. Zotov, A. L. Parkhomenko,
T. U. Parkhomenko, A. F. Topunov
**Genetic Diversity of *Bacillus thuringiensis*
from Different Geo-Ecological Regions
of Ukraine by Analyzing the 16S rRNA
and *gyrB* Genes and by AP-PCR
and saAFLP**90

RESEARCH ARTICLES

S. P. Korolev, O. V. Kondrashina,
D. S. Druzhilovsky, A. M. Starosotnikov,
M. D. Dutov, M. A. Bastrakov, I. L. Dalinger,
D. A. Filimonov, S. A. Shevelev,
V. V. Poroikov, Y. Y. Agapkina, M. B. Gottikh
**Structural-Functional Analysis of
2,1,3-Benzoxadiazoles and Their N-oxides
As HIV-1 Integrase Inhibitors**63

Guidelines for Authors..... 101

D.G. Ilyushin, O.M. Haertley, T.V. Bobik,
O.G. Shamborant, E.A. Surina, V.D. Knorre,
P. Masson, I.V. Smirnov, A.G. Gabibov,
N.A. Ponomarenko
**Recombinant Human Butyrylcholinesterase
As a New-Age Bioscavenger Drug:
Development of the Expression System**73

Z. Shevchuk, M. Y. Yurchenko, S. D. Darekar,
I. Holodnuka-Kholodnyuk, V. I. Kashuba,
E. V. Kashuba
**Overexpression of MRPS18-2
in Cancer Cell Lines Results in Appearance
of Multinucleated Cells**85

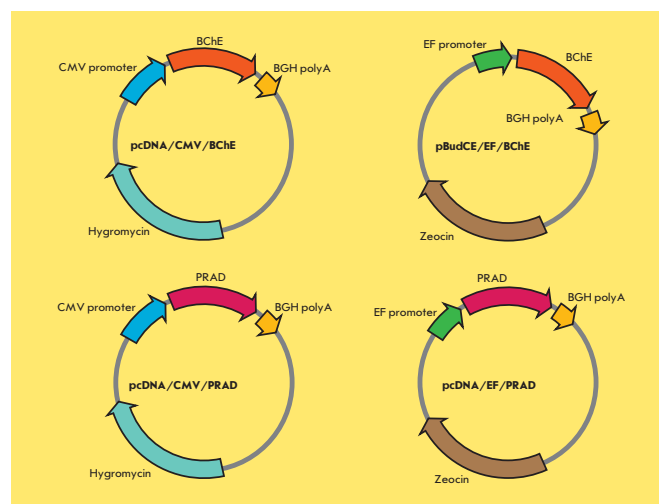


IMAGE ON THE COVER PAGE
Expression vectors used in this study
(D.G. Ilyushin *et al.*)



Dear readers of *Acta Naturae*,

We are elated to share information that the 38th Congress of the Federation of European Biochemical Societies (FEBS) will be held in Russia. Our journal is one of the sponsors of the Congress, while Park-Media Ltd., a cofounder of our journal, is one of the main co-organizers. Vice President of the Russian Academy of Sciences A.I. Grigoriev (chairman of *Acta Naturae* Journal), corresponding members of the RAS S.N. Kochetkov and A.G. Gabibov (editors-in-chief), and Candidate of Chemical Sciences V.D. Knorre (Managing Editor) will be responsible for the scientific program and the main activities of the Congress.

The decision to host the 2013 Congress in Saint Petersburg was made at the 36th FEBS Congress in Torino, Italy. This decision was received with tremendous enthusiasm by the Russian scientific community and has drawn wide applause from the international community. It took a relatively short time to outline the scientific program. The International Advisory Board headed by Nobel Laureate, Prof. Richard Roberts (USA) and Secretary of the Advisory Board Michael Blackburn (UK), has made an invaluable contribution to its preparation.

The event will be unique in that almost all scheduled lecturers at the Congress are amongst the most prominent contemporary scientists and Nobel Prize winners: Aaron Ciechanover, Jules Hoffmann, Robert Huber, Roger D. Kornberg, Jean-Marie Lehn, Richard Roberts, Jack W. Szostak, Jöhl E. Walker, Kurt Wüthrich, Ada E. Yonath, Sidney Altman, and Susumu Tonegawa.

FEBS Congresses rank among the top five world forums in the field of life sciences. A congress of such status has been held in Russia only once, in 1984, and it was headed by Yu.A. Ovchinnikov, Vice President of the USSR Academy of Sciences. The president of the current 38th Congress is Academician V.P. Skulachev. The National Committee of Biochemists and Molecular Biologists of the Russian Academy of Sciences is responsible for the research section of the Congress. The general organizational events are regulated by the Decree of the Government of the Russian Federation No. 1965-r dated October 22, 2012, and are discussed at the meetings of the Organizing Committee chaired by Dmitry Livanov, the minister of education and science of the Russian Federation.

The Congress' Theme is "Mechanisms in Biology," and the Organ-

izing Committee of the Congress is seeking to put in place a powerful and diverse program to support this key theme. The Congress program will consist of 37 symposia. The list of symposia is currently in the final stage of consideration; it includes such sections as Immunology, RNA, Carbohydrate Biochemistry, Stem Cell Biology, Mechanisms of Proteolysis, Bacteriology, Bioinformatics, Techniques of Biochemistry, etc. A strong list of symposium speakers from Europe, the U.S., Japan and other countries are expected to participate in the Congress.

The Congress program also includes a number of symposia dedicated to the memories of outstanding scientists: A symposium dedicated to the memory of prominent contemporary scientist Professor Marianne Grunberg-Manago (the former President of the French Academy of Sciences, a foreign member of the Russian Academy of Sciences) and a symposium dedicated to the memory of the famous Russian biochemist Academician Alexander Evseevich Braunstein. A special lecture by Nobel Laureate John E. Walker will be dedicated to the memory of Academician Yuri Anatolievich Ovchinnikov. The symposia lecturers are invited by the Organizing Committee. A competition of poster applications will be held; the winners will be invited to make short oral presentations at the corresponding symposia.

A number of sessions traditional to FEBS Congresses will also be held (in particular, ones devoted to the issues of biochemical education and to the role of women in science). The Science and Society workshop will be devoted to cancer diseases. The Congress will be immediately preceded by the Young Scientists' Forum. An exhibition of scientific and biomedical equipment will be arranged during the entire Congress.

The Congress will be held on July 6–11, 2013, in Saint Petersburg at the Lenexpo exhibition complex located on Vasilyevsky Island. A number of hotels are located in direct proximity to the Congress venue. The Congress delegates will be offered special Congress room rates.

St. Petersburg is one of the most beautiful cities in Europe with rich cultural and scientific traditions. The delegates to the 38th FEBS congress will have an opportunity to visit the Hermitage museum, as well as numerous other famous landmarks in St. Petersburg and its suburbs, and to enjoy a classical ballet program.

We believe you can only share our enthusiasm for the Congress, and we exhort all members of the scientific community to participate in this momentous event. Should you need further information, please follow the links on our website www.febs-2013.org.

Here is the program of plenary lectures at the Congress:

July 6, 17.00–18.00

Jules Hoffmann, UPR 9022 du CNRS, Institut de Biologie Moléculaire et Cellulaire, Strasbourg, France
"Evolutionary perspectives of innate immunity"

July 7, 11.00–12.00

Aaron Ciechanover, Tumor and Vascular Biology Research Center, The Rappaport Faculty of Medicine and Research Institute, Technion – Israel Institute of Technology, Haifa, Israel
"The end of the polyubiquitin chain as the hallmark proteasomal signal"

July 7, 12.00–13.00

Yuri Ovchinnikov Lecture
John E. Walker, MRC Mitochondrial Biology Unit, Cambridge, UK

July 7, 14.30–15.30

Theodor Bücher Lecture
Kurt Wüthrich, The Scripps Research Institute, La Jolla, California, USA

“Structural genomics with soluble and membrane proteins”

July 7, 15.30–16.30

Ada E. Yonath, The Helen and Milton A. Kimmelman Center for Biomolecular Structure and Assembly Structural Biology Department, Weizmann Institute of Science, Rehovot, Israel

“An ancient chemical bonding machine functioning nowadays”

July 8, 11.00–12.00

Lecture of International Union Biochemistry and Molecular Biology
Jack W. Szostak, Howard Hughes Medical Institute; Harvard Medical School; Massachusetts General Hospital, USA

“The origin of cellular life and the emergence of Darwinian evolution”

July 8, 12.00–13.00

Special Science and Society Lecture
Gottfried Schatz, Biozentrum, Universität Basel, Switzerland

“What it takes to succeed in science – and what Europe should do for its young scientists”

July 8, 14.30–15.30

FEBS Journal Award Lecture

July 8, 15.30–16.30

FEBS Letters Young Group Leader Lecture

July 9, 11.00–12.00

Chris Walsh, Department of Biological Chemistry & Molecular Pharmacology, Harvard Medical School, Boston, MA, USA

“The chemical logic and enzymatic machinery of natural product assembly lines”

July 9, 12.00–13.00

Susumu Tonegawa, RIKEN-MIT Center for Neural Circuit Genetics, Department of Biology, USA

“Engrams for genuine and false memories”

July 9, 13.30–14.30

Prakash Datta Lecture

Roger D. Kornberg, Stanford University Medical School, Department of Structural Biology, Stanford, USA

“The molecular basis of eukaryotic transcription”

July 9, 14.30–15.30

Women in Science Award Plenary Lecture

July 10, 11.00–12.00

Hans Krebs Lecture

Richard Roberts, New England Biolabs, Ipswich, MA, USA

“Bacterial methylomes”

July 10, 12.00–13.00

Pavel Georgiev, Institute of Gene Biology, Russian Academy of Sciences, Moscow, Russia

“Chromatin insulators and long-distance interactions”

July 10, 14.30–15.30

Robert Huber, Max-Planck-Institut für Biochemie, Emeritusgruppe Strukturfor- schung, Martinsried, Germany; Technische Universität München, Fakultät für Chemie, Garching, Germany; Universität Duisburg-Essen, Zentrum für Medizinische Biotechnologie, Essen, Germany; Cardiff University, School of Biosciences, Cardiff, UK

“Proteases and their control in health and disease”

July 10, 15.30–16.30

Sidney Altman, Department of Molecular, Cellular and Developmental Biology (MCDB), Yale University, New Haven, Connecticut, USA

“Antibiotics: present and future”

July 11, 12.30–13.30

EMBO Lecture

Jean-Marie Lehn, ISIS, Université de Strasbourg, France

“Perspectives in chemistry: From supramolecular chemistry towards adaptive chemistry”

Pulsed Electron Double Resonance in Structural Studies of Spin-Labeled Nucleic Acids

O. S. Fedorova^{1*}, Yu. D. Tsvetkov²

¹Institute of Chemical Biology and Fundamental Medicine, Siberian Branch, Russian Academy of Sciences, Lavrentyev Ave., 8, Novosibirsk, 630090

²Institute of Chemical Kinetics and Combustion, Siberian Branch, Russian Academy of Sciences, Institutskaya Str. 3, Novosibirsk, 630090

*E-mail: fedorova@niboch.nsc.ru

Received 06.08.2012

Copyright © 2013 Park-media, Ltd. This is an open access article distributed under the Creative Commons Attribution License, which permits unrestricted use, distribution, and reproduction in any medium, provided the original work is properly cited.

ABSTRACT This review deals with the application of the pulsed electron double resonance (PELDOR) method to studies of spin-labeled DNA and RNA with complicated spatial structures, such as tetramers, aptamers, riboswitches, and three- and four-way junctions. The use of this method for studying DNA damage sites is also described.

KEYWORDS pulsed electron double resonance (PELDOR); spin-labels; DNA; RNA; oligonucleotides.

INTRODUCTION. FOUNDATIONS OF THE PELDOR THEORY

Pulsed electron double resonance (PELDOR), or DEER (abbreviation used for pulsed electron double resonance or double electron-electron resonance; the former abbreviation is used hereinafter), which was developed at the Institute of Chemical Kinetics and Combustion (Siberian Branch of the Russian Academy of Sciences) in 1981 [1], is today considered the most popular EPR method. It is widely used in structural studies of systems containing paramagnetic centers.

Reviews that cover the PELDOR theory and provide examples of its application to structural investigations are published virtually every year. Only the works that have been published over the past 5 years are mentioned here [2–8]. The most significant success in the research into biomacromolecules using PELDOR has been achieved undoubtedly due to the development of effective methods of site-directed spin labeling. Many of these works cover investigations of DNA and RNA in specific biochemical systems. However, these efforts are only briefly discussed in the reviews [2–8] and only in combination with the other examples of PELDOR application. This review aims to present the results of PELDOR application in structural studies of the important classes of biomacromolecules, DNA and RNA, in a systematic manner. The review covers studies that were carried out mostly during the period between 2003 and the first half of 2012.

Two spin labels are typically introduced into molecules for PELDOR investigations. Nitroxide radicals are usually used as labels. The dipole and exchange magnetic interactions between the labels contain information regarding the distances between the labels, their mutual orientation, the aggregation and complexation of labeled molecules, and the spatial distribution of the spin labels in the investigated system. What makes PELDOR so important and unique is the possibility of using it in *systems of randomly oriented* particles.

Let us provide the most important information on the PELDOR theory required for the analysis of PELDOR results in this review. Detailed information regarding the PELDOR theory can be found in [2, 4, 9], and a description of methodological questions and PELDOR spectrometers can be found in [10].

The magnetic dipole–dipole interaction between the A and B spin labels is determined by a dipole frequency [4, 9, 11]:

$$\omega_{dd} = 2\pi\nu_{dd} = \frac{D}{r^3}(1 - 3\cos^2\theta) + J. \quad (1)$$

Here, $D = 327 \text{ rad nm}^3/\mu\text{s}$ is the dipole–dipole interaction constant, r is the interspin distance, θ is the angle between the direction of the external magnetic field and the vector connecting the spins, and J is the exchange integral. Three-pulse PELDOR (3pPELDOR) is used to determine the dipole frequency and, hence, the distance between the spins. This sequence is shown in *Fig. 1A* and consists of 2 types of pulses at the frequen-

cies ν_A and ν_B . Pulses $\pi/2$ and π at the frequency ν_A acting upon the spins A in the EPR spectrum (Fig. 1B) are used to form the spin echo signal, which is then used to detect the PELDOR effect. The interval τ between the pulses at the frequency ν_A is fixed. The pumping pulse π at the frequency ν_B , which acts on the spins B with a delay T counted from the first $\pi/2$ pulse, lies in this interval. The pumping pulse changes the orientation of the spins B, resulting in a change in the dipole interaction between the spins A and B. This change is recorded as the decay of the amplitude of the spin echo signal, $V(T)$, when the delay T changes in the interval $0 - \tau$. The time trace $V(T)$ is modulated at the frequency ν_{dd} , which allows one to determine the interspin distance r . Modulation in the PELDOR time trace was first observed and investigated in [12, 13].

A four-pulse PELDOR sequence (4pPELDOR) is also used. Here, an echo signal is formed under the influence of three pulses $\pi/2$, π , π at frequency ν_A and change in it occurs due to the π pumping pulse, which is applied in the interval between the second and third pulses at ν_B .

The PELDOR time trace for a randomly oriented pair of spin labels with a fixed r under the approximation of short microwave pulses is described by the following relationship [4, 9]:

$$V(r, T) = 1 - p_b \{1 - f(r, T)\}, \quad (2)$$

where

$$f(r, T) = \langle \cos \left[\left(\frac{\gamma^2 \hbar}{r^3} (1 - 3 \cos^2 \theta) + J \right) T \right] \rangle_\theta. \quad (3)$$

Here, p_b is the probability of rotation of one of the spins in a pair when the pumping pulse is applied: $\langle \dots \rangle_\theta$ denotes the averaging on the θ angle. The integration of (2) and (3) yields a decreasing function modulated by attenuating oscillations at frequency ν_{dd} (Fig. 2A, curve 1). A Fourier analysis of this PELDOR time trace yields a so-called Pake dublet (Fig. 2B), which allows one to obtain data on the distance r and the exchange integral J [4, 9], since

$$\nu_{\parallel} = |2\nu_{dd} - J|, \quad \nu_{\perp} = |\nu_{dd} + J|. \quad (4)$$

At rather large time periods ($T \rightarrow \infty$), the function $V(r, T)$ approaches the limit value V_p (Fig. 2A),

$$V_p = (1 - p_b)^{N-1} \approx 1 - (N - 1)p_b, \quad (5)$$

whose value is determined by the number (N) of dipole-dipole interacting spins [4, 9], which enables to determine the number of spin-labeled molecules in the aggregates and the complexes.

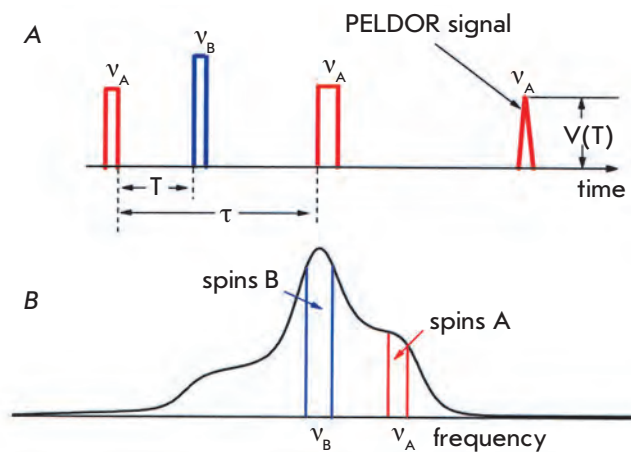


Fig. 1. (A) 3p PELDOR pulse sequence. The spin echo signal is the result of the action of two pulses at frequency ν_A . When the third pumping pulse at ν_B acts on the spin system, the PELDOR effect arises and can be registered as a time scale function, $V(T)$. (B) The positions of the pumping (B) and registration (A) pulses in the EPR frequency scale

The maximum distance that can be measured using PELDOR is determined as the maximum time of the phase relaxation in the spin system under study and typically lies in a range of ~ 8 nm. The minimum distance depends on the duration of the pumping pulse and is typically ~ 1.5 nm under optimal experimental conditions [4].

The distance between a spin-label pair can remain unfixed for different reasons. In this case, a distance distribution function $F(r)$ between the labels (distance spectrum) is introduced, which is determined as $F(r) = dn(r)/dr$, where $dn(r)$ is the fraction of spin-label pairs with the distance between the labels in a pair in the range between r and $r+dr$. In the case of continuous distance distribution, the function describing the PELDOR time trace can assume the following form [14]:

$$V(T) = V_p + (1 - V_p) p_b \int_{r_1}^{r_2} F(r) f(r, T) dr. \quad (6)$$

The limits of integration r_1 and r_2 in (6) restrict the physically reasonable range of distances between spin labels. Expression (6) is a first-kind Fredholm equation whose solution is unstable due to the inaccuracies in the experimental value $V(T)$. The calculation of $F(r)$ basically reduces to a solution of the inverse problem using the Tikhonov regularization techniques [15]. Meanwhile, one should bear in mind that the unstable properties of the solution to the equation are not eliminated. The methods for estimating the distance distribution function in radical pairs from experimental PELDOR data

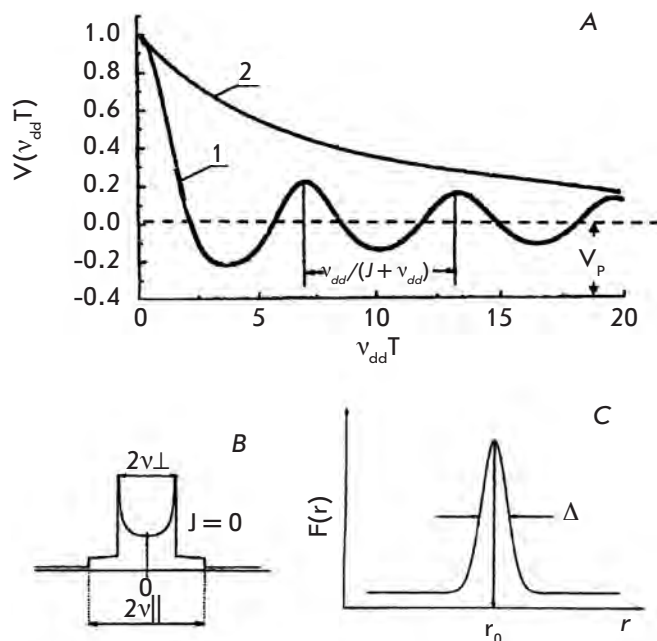


Fig. 2. A – The PELDOR time trace $V(T)$ modulated at the $(v_{dd} + J)$ frequency (curve 1) and its limiting value V_p at $T \rightarrow \infty$. The exponential PELDOR time trace for paramagnetic particles uniformly distributed in the volume (curve 2). B – Fourier conversion of the modulated PELDOR time scale ($J = 0$). C – The distance distribution function (distance spectrum) $F(r)$, r_0 – distance in radical pairs, Δ – half width at half height of $F(r)$ function

were developed in [16–19], and the method for three spin labels was shown in [20]. The program for estimating $F(r)$ using the PELDOR time trace was provided in [21]. The maximum of the function $F(r)$ corresponds to the distance between the spin labels r_0 , and its width Δ corresponds to the spatial distribution of the distances (Fig. 2B). Let us note that in accordance with (5) and (6), estimation of $F(r)$ enables to independently determine N (the number of spins in a group).

Two types of dipole interactions exist in real systems containing spin groups: those between the paramagnetic centers within a group ($V(T)_{INTRA}$) and those between the paramagnetic centers of different groups ($V(T)_{INTER}$). The dipole interaction within the pairs or inside specific groups of spin labels was discussed above. If these interactions are considered independent, then the entire function describing the time trace $V(T)$ can be written as [4, 9]:

$$V(T) = V(T)_{INTRA} V(T)_{INTER}. \quad (7)$$

In most cases, PELDOR is used to investigate systems of spin labels or groups of labels which are uni-

formly distributed over a volume. The PELDOR time trace for paramagnetic centers randomly distributed over a three-dimensional space can be described using the exponential function [4]

$$V_{INTER}(T) = V(0)\exp[-2p_b\Delta\omega_{1/2}T] = V(0)\exp[-\alpha T^{A/3}], \quad (8)$$

where $\Delta\omega_{1/2} = 8.2 \times 10^{-13} \cdot C$, $\text{cm}^3 \cdot \text{s}^{-1}$ is the dipole bandwidth, and C is the concentration of the paramagnetic centers (in cm^{-3}). In general, the α and A values depend on the spatial dimensions. For instance, $A = 3$ for a 3-dimensional space (Fig. 2A, curve 2), $A = 2$ for a plane, and $A = 1$ for a line [4, 9]. The α and A values can be also calculated for more complex situations of spatial distribution of paramagnetic centers [22]. The comparison of the experimentally determined and the estimated α and A values opens the doors to investigating the features of spatial distribution using PELDOR.

The techniques based on recording the exponential time trace $V(T)_{INTER}$ and its dependence on the concentration of paramagnetic centers, which enable separation of $V(T)_{INTER}$ and $V(T)_{INTRA}$ for further analysis, have been devised [23, 24].

The pulses A and B act selectively in the different narrow frequency ranges of the EPR spectrum. The orientational selectivity of the effect of microwave pulses on the spin system emerges if the value of the anisotropy of the magnetic-resonance parameters of the paramagnetic centers is relatively high (like that for nitroxide spin labels). This selectivity means that the radicals differently oriented in space are excited to different extents by the echo forming pulses and by the pumping pulse. The theoretical analysis and the experimental data demonstrated that the data on the mutual orientation of spin labels and their orientation relative to the vector r , which connects a label pair, can be obtained from PELDOR time traces. The measurements should be carried out while varying the positions of the A and B pulses in the spectrum or Δv_{AB} [25–27]. The scheme for conducting these experiments for a typical EPR spectrum obtained for a nitroxide spin label in the X-band is shown in Fig. 3.

The contemporary PELDOR theory and experimental techniques allow one to obtain and study the structure and properties of numerous biologically important molecules. The results of DNA and RNA studies using this method are discussed below.

PELDOR STUDY OF SPIN-LABELED DNA AND RNA

Spin labels for DNA and RNA

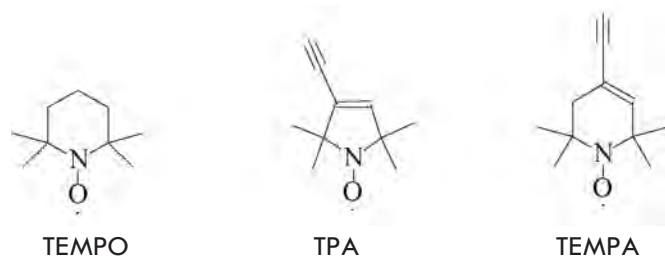
The development of site-directed spin labeling has enabled to elaborate a wide range of EPR spectroscopy applications in biochemistry and biophysics. These

comprise the determination of the elements of the secondary and tertiary structures of membrane proteins, including the environmental influence; research into the orientation and motion of separate protein fragments under physiological conditions; detection of the conformational transitions in the functioning of membrane protein complexes; etc.

These investigations are usually performed using conventional stationary EPR methods and are published regularly in a series of collected articles entitled *Biological Magnetic Resonance* edited by L. Berliner *et al.* (a total of 28 books had been published by 2011). Let us discuss only the articles dealing with the application of PELDOR for the structural investigation of DNA and RNA. The results of the first experiments in this field were published in volumes 19 and 21 of this series [28, 29].

The elaboration of efficient methods for the synthesis of site-directed spin-labeled biologically important compounds was the most significant stage in these experiments and made them feasible. The reviews [30–32] discuss a series of methods that resolve this problem for nucleic acids and oligonucleotides. A brief review devoted to spin labeling of DNA and RNA has recently been published [33].

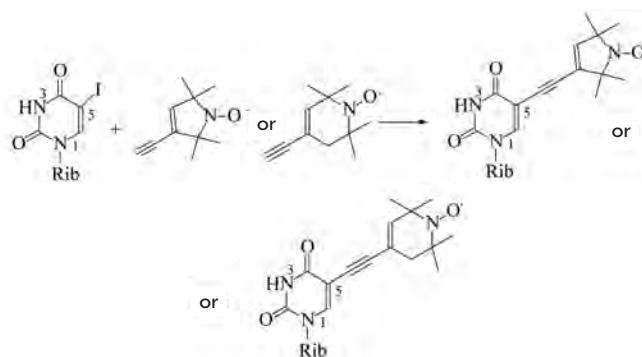
2,2,6,6-Tetramethylpiperidine-N-oxyl (TEMPO), 2,2,5,5-tetramethyl-pyrrolin-1-oxyl-3-acetylene (TPA), and 2,2,6,6-tetramethyl-3,4-dehydropiperidin-N-oxyl-4-acetylene (TEMPEA) are the most popular spin labels used to label proteins and nucleic acids:



An unpaired electron in these molecules is localized on the N-O-fragment.

In the first studies, the label was introduced into the C5 position of the uracil residue of the nucleic acid [34]. Since the limitation of the conformational mobility of spin labels increases accuracy in distance determination using PELDOR, rigid linkers have recently been used to introduce spin labels into nucleic acids. The Sonogashira method, which is based on the replacement of iodine in the organic compound with an alkynyl residue, is one of such methods commonly used today [35, 36]. The reaction is catalyzed by Pd(II) and Cu(I) salts. For the nucleic acids, TPA and TEMPEA residues are introduced into the C5 position of iodouridine via reaction A [34, 37–40] giving rise to adducts.

Reaction A:



where Rib is the ribosomal residue.

This technique enables to introduce spin labels both into the monomers used in the phosphoramidite method for oligonucleotide synthesis and into the complete ribo- and deoxyribo-oligonucleotides. In the course of the ribooligonucleotide synthesis, the TPA spin label is also introduced into the adenine and cytosine residues containing protected amino groups via the Sonogashira reaction [41].

Azide-alkyne cycloaddition, known as “click chemistry,” is also commonly used today to introduce spin labels into oligonucleotides [42]. In this case, the spin label is introduced into the oligonucleotide via the Cu(I)-catalyzed reaction between the acetylene group

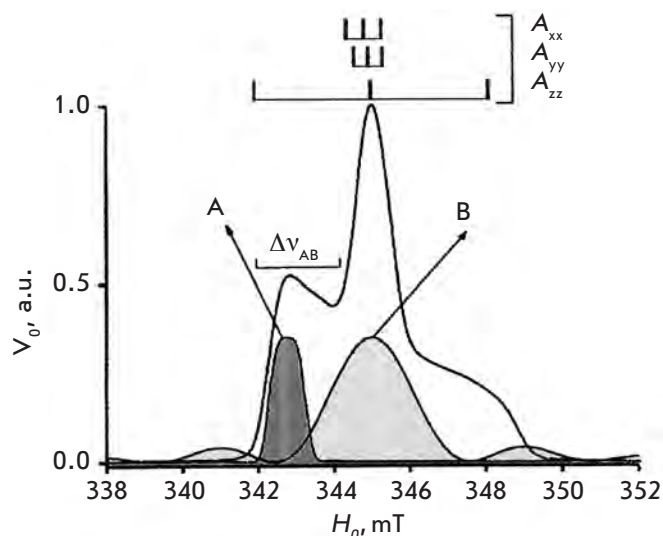
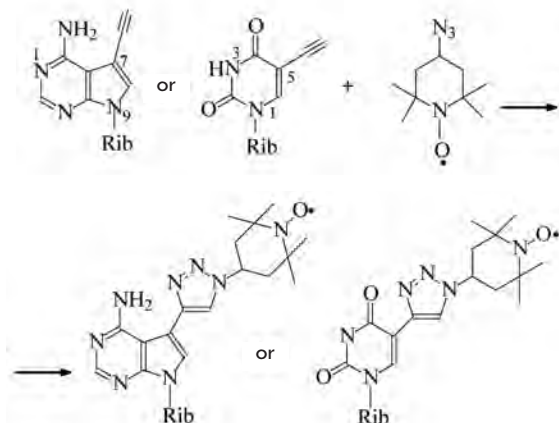


Fig. 3. Schematic representation of the experiments on orientation selectivity measurements for the nitroxide spin labels. The EPR spectrum shape is the function of the main anisotropic hyperfine tensor elements A_{xx} , A_{yy} , A_{zz} . A and B denote the recording and pumping pulses. PELDOR time traces $V(T)$ recorded at different Δv_{AB} fixed on the A_{zz} component of the EPR spectrum

(incorporated into the heterocyclic base at the C7 position of 7-deazaadenine or the C5 position of uracil) and 4-azido-TEMPO in solution [43], or in the course of solid-phase synthesis of oligonucleotides [44] coupled with adduct formation.

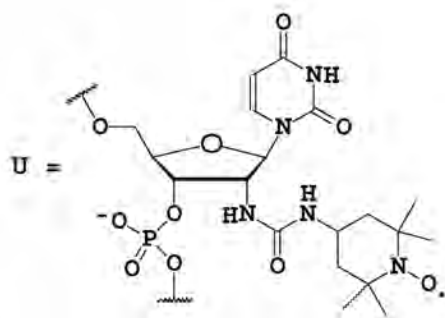
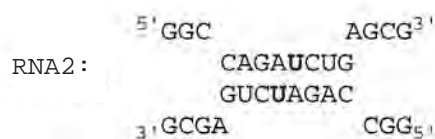
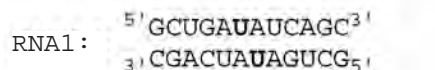
Reaction B:



This reaction is stereospecific, characterized by a high yield, and is used to synthesize spin-labeled DNA and RNA.

Linear duplexes of nucleic acids

The structures of 12-bp (base pairs) duplexes (RNA1) and 15-bp - duplexes (RNA2) were investigated in work [45]. The TEMPO labels were introduced into the 2'-NH₂-groups of ribose in uridine (U) residues via the reaction with TEMPO isothiocyanates:



The modulated PELDOR time trace was recorded only for RNA1. The distance between the spin labels (3.5 ± 0.2 nm) was determined by Fourier analysis. Only

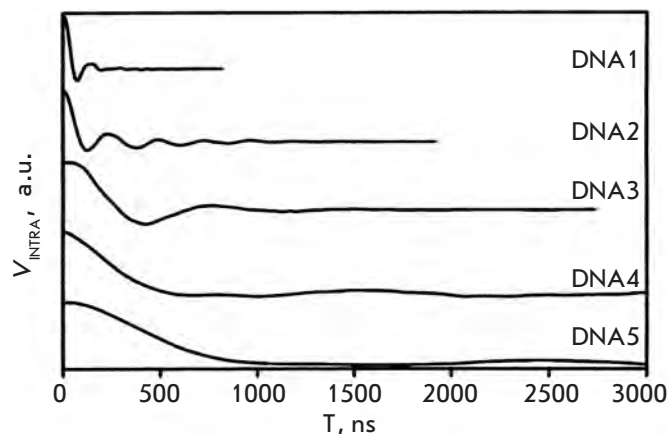
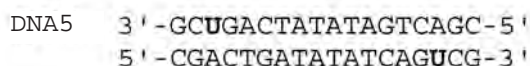
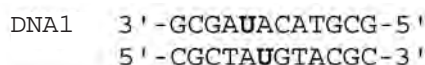


Fig. 4. PELDOR time traces V_{INTRA} for five spin-labeled DNA [46]. (Reproduced by permission from the American Chemical Society:[Schiemann, O., Piton, N., Mu Y., Stock, G., Engels, J.W., Prisner, T.F. (2004) *Am. Chem. Soc.* 126, 5722-5729], copyright 2004)

the exponential PELDOR time trace was recorded for RNA2, which was testament to the uniform distribution of the spin labels. This means that no duplexes were formed between the spin-labeled oligonucleotides of RNA2 in a water solution (buffer 0.1 M NaCl, 0.01 M Na-phosphate, 0.1 mM Na₂EDTA, pH 7.2) at a concentration of 0.3 mM. This fact suggests that intramolecular hairpin structures could have formed, the process being predominant over the bimolecular process of duplex formation.

The distances between the TPA spin labels introduced via the reaction A into the residues of 2'-deoxyuridine (U) of the DNA duplex helices were determined using the 4pPELDOR [46]. The labels were introduced into the U residues located at 5 different positions in the duplex, so that the number of bases between the labels, n , was different: $n = 0, 2, 8, 10, 12$, respectively, for the DNA1-DNA5; for instance (spin-labeled U residues are in shown in bold):



Frozen (35 K) aqueous buffer solutions of the duplexes with the addition of 20% ethylene glycol for vitrification were investigated. The modulation of the PELDOR time trace was recorded for all DNA molecules (Fig. 4). The period of beating of the time traces increased with an increase in the distance between the

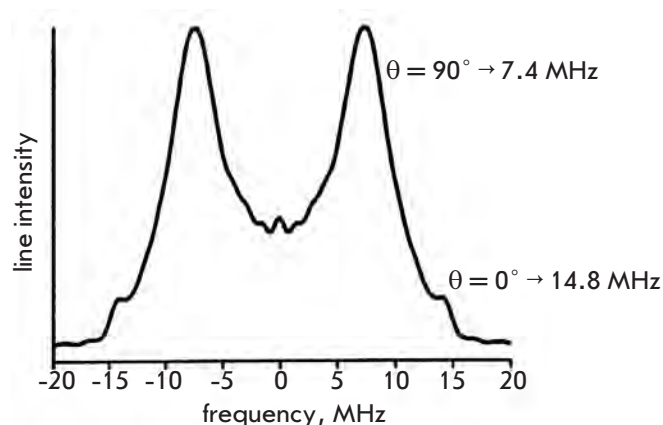


Fig. 5. Fourier spectrum of V_{INTRA} for DNA-1. Lines at ν_{\perp} ($\theta = 90^\circ$) and ν_{\parallel} ($\theta = 0^\circ$). [46]. (Reproduced by permission from the American Chemical Society:[Schiemann, O., Piton, N., Mu Y., Stock, G., Engels, J.W., Prisner, T.F. (2004) *Am. Chem. Soc.* 126, 5722-5729], copyright 2004)

spin labels. The Fourier spectra in all the cases had the shape of Pake doublets. An example of this doublet for DNA1 is shown in *Fig. 5*. The lines in this doublet (at a frequency of 7.4 and 14.8 MHz) correspond to a parallel ($\theta = 0^\circ$) and a perpendicular ($\theta = 90^\circ$) orientations of the vector connecting the spin labels r relative to the direction of the external magnetic field. The distance between the labels can be determined using the ratios (1) and (4). In this case, $r = 1.92$ nm and the J -exchange integral is equal to 0.

The distances determined from the Fourier spectrum for DNA2-DNA5 were equal to 2.33, 3.47, 4.48, and 5.25 nm, respectively. These distances for the investigated spin-labeled DNA were calculated using molecular dynamic (MD) simulations [46]. The results of a comparison of the theoretical and experimentally obtained values listing all probable errors are shown in *Fig. 6*. The correlation coefficient of these results is equal to 0.997, which is believed [46] to support the existence of B-conformation in the duplex helix in frozen aqueous solutions. A detailed comparison of the PELDOR and FRET (fluorescence resonance energy transfer) [46] methods demonstrated that these methods complement each other in the investigations of spin-labeled systems.

Six TPA-labeled RNA duplexes were synthesized [41]. A sufficiently deep modulation recorded for the PELDOR time traces enabled to calculate the distribution function, $F(r)$, and accurately determine the distances in the duplexes, which lie in a range from 1.93 ± 0.12 to 3.87 ± 0.13 nm, depending on the number of base pairs between the labels. The comparison of the

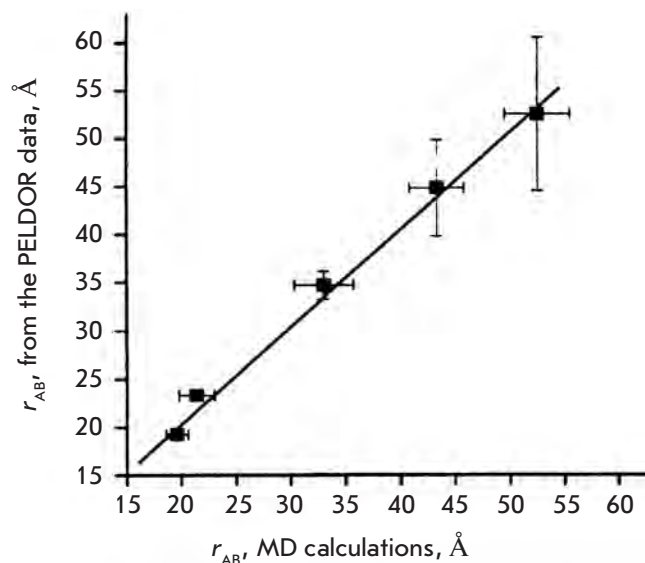


Fig. 6. Correlation of the distances r_{AB} obtained by PELDOR experiment and MD calculations [46]. (Reproduced by permission from the American Chemical Society:[Schiemann, O., Piton, N., MuY., Stock, G., Engels, J.W., Prisner, T.F. (2004) *Am. Chem. Soc.* 126, 5722-5729], copyright 2004)

experimental results in [41] and [46] with the results of a measurement of the distances in DNA demonstrated that given an identical number of base pairs, the distances between the labels in DNA and RNA located in different helices of the duplex are different. Hence, when the labels are located in bases at a distance of 10 bp, these values are equal to 4.48 ± 0.5 nm and 3.87 ± 0.13 nm in DNA and RNA, respectively [41]. This difference cannot be accounted for by a measurement error; it corresponds to two different conformations: the A-form in RNA and the more stretched B-form in DNA. It turned out that the results obtained were in close agreement with those obtained by MD simulations; the correlation coefficient was 0.976 [41]. The authors believe that this result shows that the DNA and RNA duplexes maintain their conformations in frozen (40 K) aqueous phosphate buffer solutions.

In the paper of Q. Cai *et al.* [47], the TPA labels were introduced via a methylene linker not into a heterocyclic base but into the phosphorothioate groups at specific positions of the sugar-phosphate backbone. The duplex formed from polynucleotides labeled at different positions enabled one to measure the distances between arbitrary points of DNA duplexes. The samples prepared in this manner (the measurements were taken at 50 K in frozen aqueous solutions of DNA duplexes) were used to determine eight interspin distances in a

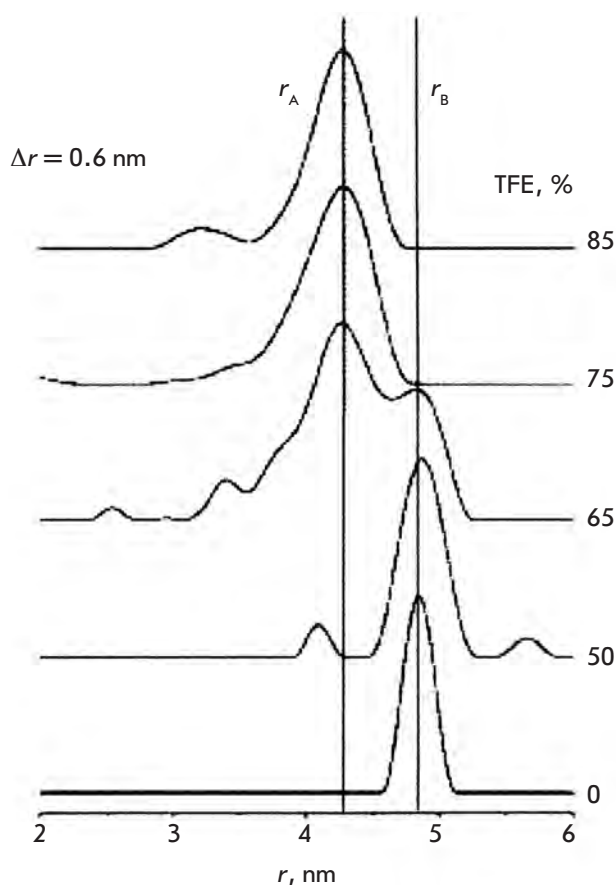


Fig. 7. PELDOR-measured distance spectrum change after TFE was added to a water solution of a 4; 18' labeled DNA duplex. [49]. (Reproduced by permission from John Wiley & Sons, Inc.: [Sicoli, G., Mathis, G., Delalande, O., Bou-lard, Y., Gasparutto, D., Gambarelli, S. (2008) *Angew. Chem. Int. Ed.* 47, 735-737], copyright 2008)

12 bp DNA duplex by PELDOR on the basis of the position of the maximum values of the distance spectrum. The minimum and maximum distances were equal to 2.56 and 3.88 nm, respectively, for DNA. According to the authors, this method of labeling is not limited by the polynucleotide length [47]. The data for a 68bp-long DNA fragment containing labels located opposite each other at a distance of 9 nucleotides from one end of the duplex are provided in this article. The distance measured using PELDOR (2.52 nm) was equal to that obtained with MD simulation (2.5 nm).

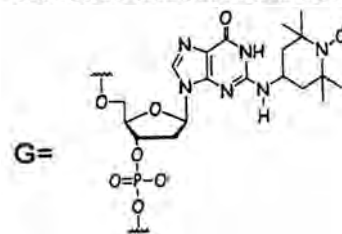
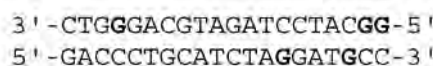
Q. Cai *et al.* [47] also compared the results of the PELDOR measurement with those calculated using NMR spectroscopy, which takes into account the probable conformations of the DNA under study, and found an excellent correlation ($R^2 = 0.98$) between the PELDOR and NMR measurements. They believe that the method proposed for label introduction can be widely

used in structural studies of DNA- and RNA-protein complexes.

An investigation very similar to [47] is described in [48], where spin labels were introduced into phosphorothioate groups of RNA; six sets of interspin distances ranging from 2.5 to 4.72 nm were compared to the X-ray data. A positive correlation between these measurements was found ($R^2 = 0.97$). This fact indicates that the introduction of a label does not significantly alter the RNA structure.

It was shown in the investigations described above that the methods developed for spin labeling of linear DNA and RNA duplexes allow an appreciably accurate ($\sim 1\%$) determination of the distance between the spin-labeled nucleotides. The strict correlation between the PELDOR and MD results is of significance. The MD simulations were typically carried out at room temperatures and for aqueous solutions; the PELDOR measurements were carried out using rapidly frozen vitreous solutions. It can be concluded that the conformations existing in DNA and RNA molecules at room temperature is instantaneously fixed as the molecules froze. This fact substantiates future PELDOR studies of DNA and RNA in different environments or in the course of various interactions and reactions.

The inter-nucleotide distance changes in a transition from the B- to the A-conformation of DNA. This change was recorded and studied using PELDOR [49]. In this case, spin-labeled complementary DNA duplexes were investigated:



The 4-amino-TEMPO label was introduced into the N2 atom of the guanine residue located either in the same (top) helix (positions (4; 19), (4; 20)) or in both helices. In the latter case, the labels occupied the positions (4; 14') or (4; 18') in different helices.

The transition between the B and A forms of DNA occurs in polar media. The spin-labeled DNA duplexes were investigated at 60–70K in an aqueous buffer with the addition of 10 vol. % glycerol (as a cryoprotectant). Trifluoroethanol (TFE) was added to stimulate the B \rightarrow A transition. The changes in the distance spectrum in response to the changes in the volumetric content of TFE are shown in *Fig. 7*. The B-form is converted into the A-form at a TFE concentration exceeding 70%.

Table 1. Experimental and calculated distances between the spin labels (nm) for the A- and B-form of DNA

DNA duplex	PELDOR	B-form, O–O distance, MD calculation	PELDOR	A-form, O–O distance, MD calculation
(4;20)	5.6 ± 0.2	5.6 ± 0.3	4.8 ± 0.2	4.5 ± 0.4
(4;19)	5.1 ± 0.2	5.1 ± 0.3	4.6 ± 0.3	4.4 ± 0.4
(4;18')	4.9 ± 0.2	4.8 ± 0.4	4.3 ± 0.3	4.2 ± 0.4
(4;14')	3.2 ± 0.2	3.6 ± 0.3	2.8 ± 0.3	3.3 ± 0.3

The difference between the average distances for the A- and B-forms is 0.8 nm. The interspin distances for all the investigated samples of DNA in the A- and B-forms are shown in *Table 1*. The MD simulation values for the distances between the oxygen atoms of the >NO groups of the spin labels in the investigated duplexes are also provided for comparative purposes.

According to [49], PELDOR sensitivity in distance determination in the nanometric range is considerably higher than that for any other method, such as stationary EPR or circular dichroism (CD). This fact justifies the investigation of the transitions between different conformers of the A- and B-forms of RNA and DNA under various conditions of molecular environment and polarity.

It was shown using an MD simulation [50] that localization of the TPA spin label in the major DNA or RNA groove results in a change in the mutual orientation of the base pairs in the molecule. This effect is less significant for the labels located in the minor groove. Nonetheless, the conformational changes that occur during the incorporation of the labels into DNA or RNA should be taken into account when interpreting the orientational effects in PELDOR.

The distances between the spin labels in 4 hybrid DNA/RNA-duplexes were measured [51]. The TPA spin labels were incorporated into the heterocyclic bases in such a way that they were oriented towards either the major or the minor groove of the duplex. This allowed one to choose between the A- and B- conformations of the hybrid. The B-conformation was found in 50% of the cases, and the A-conformation typically occurred in the rest of the cases. During the interaction of sufficiently long DNA and RNA duplexes with proteins and membranes, formation of conformational bending and disruptions of the linear structure, as well as the emergence of differently spatially oriented short duplex segments, are likely to occur. This heterogeneous system was formed using mixtures of DNA duplexes

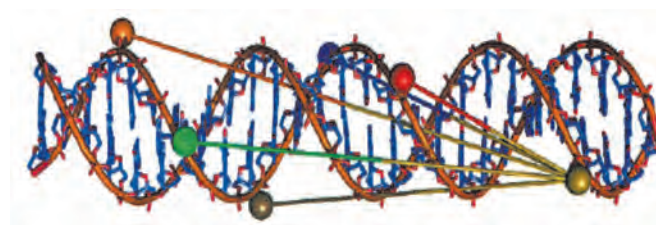
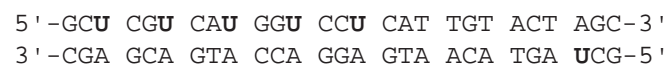


Fig. 8. Molecular model showing the positions of spin label pairs for the distance measured in [52]. (Reproduced by permission from John Wiley & Sons, Inc.: [Ward, R., Keeble, D.J., El-Mkami, H., Norman, D.G. (2007) *Chem-BioChem.* 8, 1957-1964], copyright 2007)

of identical length with spin labels incorporated into different segments [52]. The spin labels in the present work were introduced into the 2'-amino groups of uridine residues in the DNA duplexes in a stepwise manner via a reaction with isocyanate TEMPO in such a manner that the interspin distances were equal to 9, 12, 15, 18 or 21 bp:



(spin-labeled nucleotides are shown in bold).

A total of five double spin-labeled duplexes were synthesized. The optimally prepared samples (DNA solutions frozen at 77 K were studied) for the X-band of the PELDOR spectrometer (relatively high signal-to-noise ratios, long relaxation time $T_f \approx 8 \mu\text{s}$) contained $12.5 \times 10^{-6} \text{ mol l}^{-1}$ of the DNA duplex in a 50% solution of deuterated ethylene glycol in D_2O . The spin-label pairs (with the distances between them determined in different duplexes) are schematically shown in *Fig. 8*.

The PELDOR time trace was recorded; the distance spectrum estimated using Tikhonov's regularization method were analyzed [15]. Six interspin distances in the range from 2.8 to 6.8 nm were determined. The results of the study of the mixtures containing the aforementioned spin-labeled duplexes are of particular interest (*Fig. 9*). It was ascertained [52] that for a mixture of two different duplexes, deconvolution of a composite function $F(r)$ through the introduction of the distribution function in the form of a Gaussian curve for each duplex allows one to determine the average distance in each duplex and its concentration in the mixture with good accuracy. Meanwhile, certain difficulties arise during the analysis of the $F(r)$ of mixtures containing large numbers of duplexes. These difficulties are apparently connected with both the inaccuracies and ambiguities in the solution of the inverse problem of recovery $F(r)$ from the time trace $V(T)$, as well as

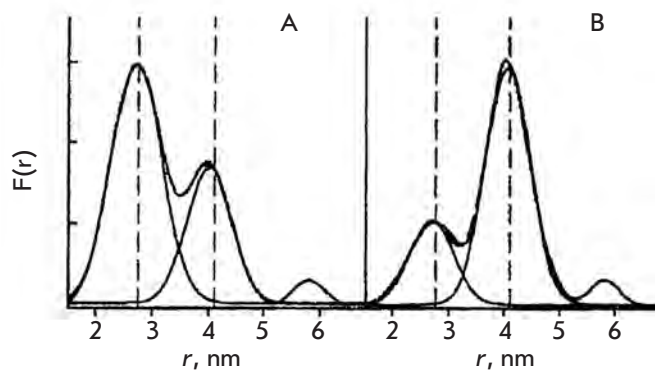
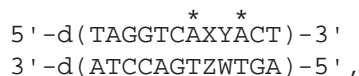


Fig. 9. Investigation of spin-labeled DNA mixtures [52]. The distance distribution spectra are shown for a mixture of the DNA duplex labeled at distances 2.8 nm and 4.1 nm; A – at a 3:1 ratio; B – at a 1:3 ratio. (Reproduced by permission from John Wiley & Sons, Inc.: [Ward, R., Keeble, D.J., El-Mkami, H., Norman, D.G. (2007) *Chem-BioChem.* 8, 1957-1964], copyright 2007)

with the probable transformations under the influence of such factors as stacking interactions in the complex mixture, which changes the spatial geometry of the duplexes [52].

The duplexes containing AA and TT mismatches (non-canonical pairs) were studied in [53]. Two TEMPO spin labels were introduced via the reaction of catalyzed cycloaddition (“click chemistry”) into one of the oligonucleotides on each side of the mismatches:



where $*$ is 7-deazaadenosine containing the TEMPO spin label at C7; XY is the noncanonical pair dA x dA or dT x dT at positions 8 or 9 of the duplex. The distance between the spin labels in the canonical duplex, when XY/ZW = AT/TA, was 1.83 nm. The distance between the unpaired electrons in the duplexes **TT**/TA and **AT**/AA containing the **TT** or **AA** noncanonical pair at position 8 was 1.73 nm. The distances between the spin labels were 1.87 and 2.08 nm if the duplexes contained noncanonical pairs (AT/TT and AA/TA, respectively) at position 9. Thus, the introduction of a noncanonical pair into position 8 reduces the interspin distance, while the introduction into position 9 increases it as compared to the canonical duplex. Therefore, the DNA mismatch formation affects the structure of the adjacent base pairs, thus causing their convergence or divergence.

The DNA duplexes containing three TEMPO spin labels were also studied [54]. These Y labels were attached to the C5 atom of the uridine residue of the

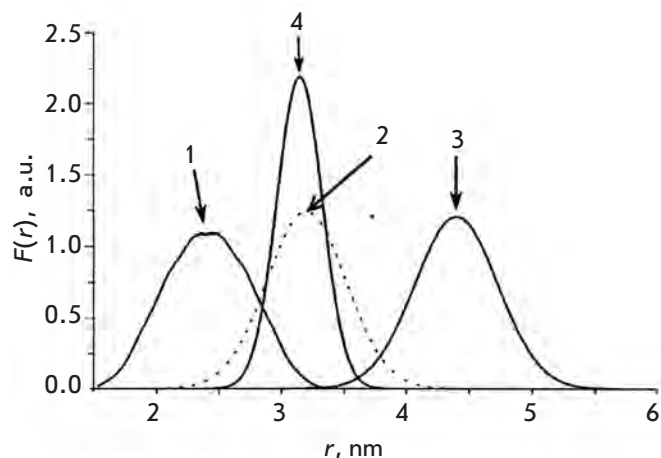
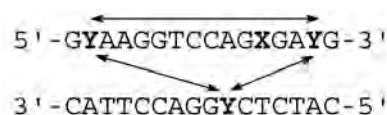


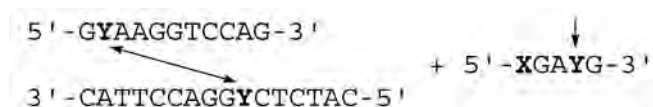
Fig. 10. Distance distribution function $F(r)$ for the tri-labeled DNA duplex (arrows 1, 2, 3) and the same after treatment with Endo IV resulting to double-labeled DNA cleavage (arrow 4) [54]. (Reproduced by permission from John Wiley & Sons, Inc.: [Flaender, M., Sicoli, G., Aci-Seche, S., Reignier, T., Maurel, V., Saint-Pierre, C., Boulard, Y., Gambarelli, S., Gasparutto, D. (2011) *Chem-BioChem.* 12, 2560-2563], copyright 2011)

alkynyl-oligonucleotide using the “click chemistry” approach. Tetrahydrofuran X insertion (THF damage, see Tables 3 and 5 below) was also introduced into one of the DNA strands in addition to two spin labels. Hence, the original system in the buffer solution contained three spin labels and one damaged site.



The PELDOR time traces in this 3-spin system were analyzed using the conventional procedure [21], which was modified for the 3-spin system [20]. As was expected, the distance spectrum in this system consisted of three lines with the peaks corresponding to the distances of 2.50, 3.15, and 4.60 nm and the widths of 0.05, 0.45, and 0.75 nm, respectively (Fig. 10).

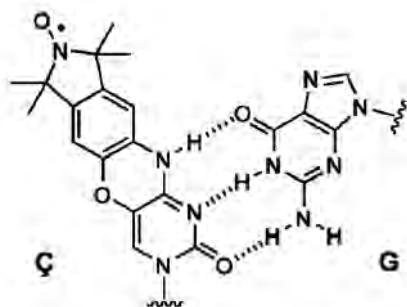
The interaction between this DNA duplex and apurinic/aprimidinic endonuclease IV isolated from *Escherichia coli* (EndoIV) was also investigated [54]. DNA degradation is known to occur under the influence of EndoIV [55] at the apurinic/aprimidinic (AP) sites and at the AP site analogs containing tetrahydrofuran (THF) residues instead of ribose. Duplex dissociation occurs at the THF residue, yielding a duplex containing only two spin labels and a DNA fragment with one label and a THF residue:



A single line (Fig. 10) was detected in the distance spectrum after denaturation during the investigation of the PELDOR time traces (with the maximum at 3.20 nm and a width of 0.75 nm), which was attributed to the spin-labeled duplex that remained after the degradation.

The results obtained demonstrate the potential for using PELDOR in the investigation of 3-spin DNA systems and, more importantly, expand the range of systems that can possibly be used for the analysis of the mechanisms of interaction between DNA and proteins and enzymes.

The data concerning the distances between the spin labels, as well as their mutual orientation, can be determined by studying the orientational selectivity using PELDOR spectroscopy. Orientation selectivity was investigated in [25–27, 56]. A special rigid spin label ζ was developed to study DNA [57]. It was rigidly bound to cytosine, which in turn was rigidly oriented and fixed by hydrogen bonds with the corresponding complementary base in the DNA structure:



In accordance with the DNA structure, label planes are coplanar to the nucleotide pairs in DNA. Thus, the normal vectors to the label plane are parallel to each other (Fig. 11A), and the β angle between the vector r connecting the labels and the normal to the plane of different labels will be the same. This finding made it possible to analytically determine this angle from the PELDOR time traces recorded at different frequencies of recording A and pumping B pulses; i.e., at different $\Delta\nu_{AB}$. A detailed theory of this analysis and the experimental results are provided in [56]. The PELDOR time traces in the X-band of the EPR were measured for different frequency difference values ($\Delta\nu_{AB}$) in a range from 90 to 40 MHz with a 10 MHz increment. The position of the second label in the investigated series of DNA samples varied from N3 to N14 (Fig. 11A). The re-

sults obtained for angle β in DNA with varied positions of the labels are provided in Fig. 11B. It is clear that the angle estimated from the geometry of the DNA duplex fully corresponds to the experimentally obtained angle value. The obtained results create possibilities for investigating the orientation of spin labels in structures that are more complex than simple linear single- and double-stranded DNA and RNA.

The dynamic properties of nucleic acid molecules are of significance for understanding the kinetics and the mechanisms of cellular processes, such as replication and transcription, when DNA is twisted and bent upon the interaction with protein active centers. One of the urgent problems of modern biophysics is the investigation of the mechanisms of the molecular dynamics of nucleic acids. It was believed at the early stages of theoretical and experimental research that the dynamic properties of DNA duplexes can be described using the elastic cylinder model [58]. Various modern physical methods used to study the mechanisms of mobility of DNA helices [59–61] allow one to determine at least three types of possible motion, including change in the helical pitch without any changes in the helix radius (A), change in the helix radius with a constant helix pitch – elongation and twisting (B), and bending of the helix without changes in the radius and the pitch (C).

We have repeatedly mentioned before that the linewidth in the distance spectrum obtained in the PELDOR experiments at low temperatures in frozen glasses correlates with the spectrum of the possible conformational states of the spin system estimated for that same system using modern MD methods in liquids. This means that PELDOR provides snapshots of the dynamic situation for a given molecular system.

A. Marko *et al.* [62] used these features of PELDOR to separate the A, B and C mechanisms by studying the conformational flexibility of double spin-labeled DNA (20 nucleotides). Rigid spin labels ζ were incorporated into the duplex nucleotides. The paired labels were introduced into 10 duplexes in such a way that the position of one of them was fixed at one end of the duplex, and the distance R to the other labels was consistently increased for each pitch of the helix. The PELDOR measurements were carried out at the frequencies of the X-band (9 GHz) and the G-band (180 GHz). The PELDOR time traces and their dependency on $\Delta\nu_{AB}$ for all the duplexes from (1.5) to (1.14) were measured; the linewidth $\Delta = \langle \Delta R^2 \rangle^{1/2}$ for $F(r)$ was determined in the distance spectrum in the Gaussian approximation (Fig. 12A). The linewidth was determined by averaging the orientational selectivity data [26], which eliminate the correlation between the label orientations when the distances between them are measured. During the investigation of the orientational selectivity at different

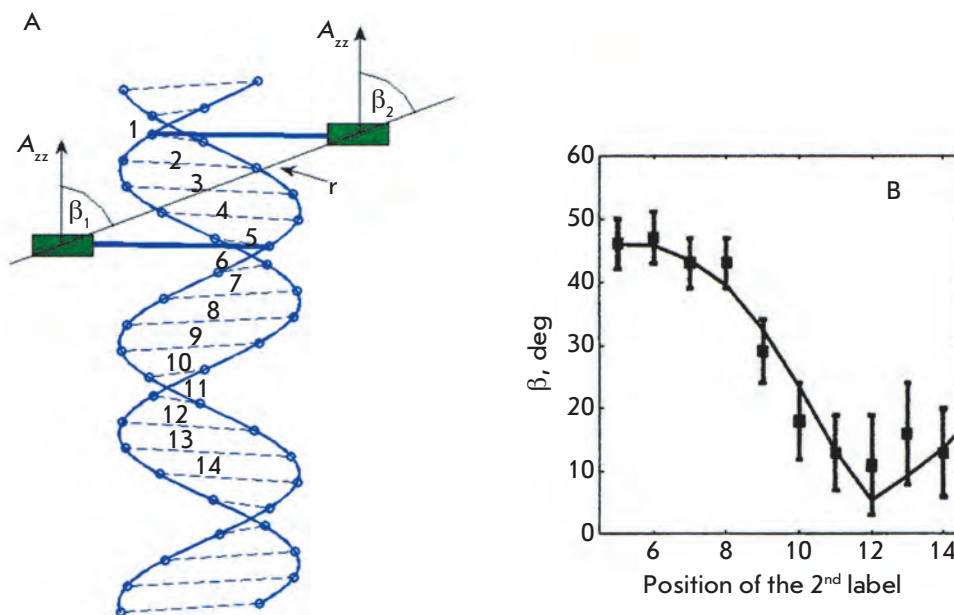


Fig. 11. (A) Orientation of spin labels in the DNA structure. The spin labels are attached to the base pairs with the numbers 1 and 5. The principal axis of the hyperfine interaction tensor A_{zz} is normal to the labels planes; angles β_1 and β_2 are approximately equal. (B) Experimental and calculated dependence of $\beta = \beta_1 = \beta_2$ on the position of the second label [27]. (Reproduced by permission from The American Physical Society: [Marko, A., Margraf, D., Cekan, P., Sigurdsson, S.T, Schiemann, O., Prisner, T.F. (2010) *Phys. Rev. E.* 81,021911], copyright 2010)

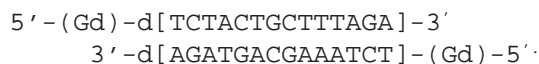
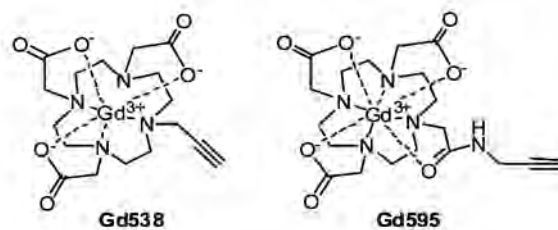
Δv_{AB} , the mutual orientations of the labels for all spin pairs were determined using the methods described in [25–27]. The theoretical computation of the modulated PELDOR time traces, the linewidth of the $F(r)$ function, and the mutual orientation of the labels for different A, B, C motion models became an important phase of the investigation.

It was found that the relationship between the width of the spectrum lines and the position of a label can be used to interpret the experimental data (Fig. 12B) only for model B (helix winding). Twisting and stretching of the helix in this model can be determined from the data on spin-specific orientation obtained in the course of the experiments at 180 GHz. It was found that the angle variation between the relative orientations of the closest labels in the N–O bond was $\pm 22^\circ$.

As mentioned in [62], the results obtained completely agree with the model of cooperating fluctuations, the so-called model of “respiratory” movements of the DNA duplex, when the pitch of a helix remains constant, while the helix radius and the length of the DNA molecule vary in a correlated manner. According to the PELDOR data, the helix radius changes by 11% and the DNA length can change by $\pm 6\%$. All these PELDOR results correlate with the small angle X-ray scattering data (SAXS) [61] and with the results obtained via fluorescent microscopy [59] for short DNA polynucleotides. It should be mentioned that the wide variety of experimental approaches (the unique set of spin-labeled DNA, studies of the orientational selectivity, measurements carried out in various frequency ranges) used in this work [62] presumably for the first

time demonstrated the potential of this method not only for structural studies, but for thorough studies of the dynamics of biomacromolecules as well.

Gd(III) [63–65] or Cu(II) [66] complexes have been recently suggested for use as labels. These labels are typically characterized by a rather complex EPR spectrum in polyoriented systems. However, when conducting measurements at high frequencies ~ 30 GHz (K_a -range) and at cryogenic temperatures of ~ 10 K, in the case of Gd(III) one line corresponding to the $-\frac{1}{2} \rightarrow +\frac{1}{2}$ transition prevails in the spectrum; this line is used in the PELDOR experiments. The structure of the duplex containing 14 base pairs was investigated using Gd(III) (Gd538 and Gd595) complexes as labels incorporated into the terminal thymidine molecules using the “click chemistry” method [65]:



The measurements carried out by 4pPELDOR demonstrated that the distance between the ions in these DNA duplexes was approximately 5.9 ± 1.2 nm, while

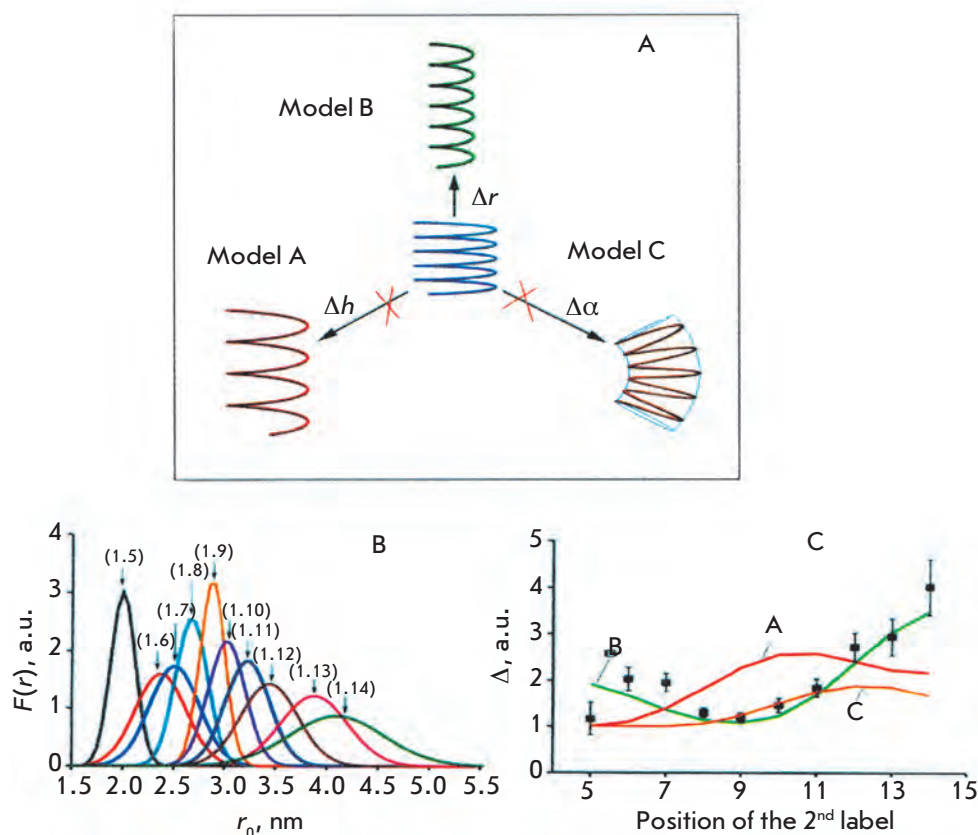


Fig. 12. (A) Three models of cooperative motion in a double-stranded DNA molecule (see text). (B) Distance spectrum lines found from the X-band PELDOR data in a Gaussian approximation for $F(r)$. The orientation selectivity for ζ labels in DNA duplexes was studied for spin labels pairs (shown in brackets). (C) Experimental spectra line widths, $\Delta = \langle \Delta R \rangle^{1/2}$, upon the distances between the labels and the theoretical mobility calculations for different mobility types A, B, C. (text). The minimal Δ value corresponds to the distance between the 1 and 9 labels of DNA [62]. (Reproduced by permission from the American Chemical Society: [Marko, A., Denysenkov, V., Margraf, D., Cekan, P., Schiemann, O., Sigurdsson, S.Th., Prisner, T.F. (2011) *J. Am. Chem. Soc.* 133, 13375-13379], copyright 2011)

the width of the distance spectrum line was ~ 2 nm. The authors [65] believe that the use of these ions can increase the range of PELDOR-measured distances to ~ 10 nm, which is significant in the case of the conformations of complex biomolecules. A relatively large distance (1.2–1.5 nm) between the ions and the position at which they attach to the investigated molecule results in a wide distance spectrum and a decrease in the measurement accuracy due to the mobility of these labels. This is an obvious drawback of these labels in comparison to nitroxide labels. It should be mentioned that a number of features of the PELDOR analysis methods for Gd(III) and Cu(II) were thoroughly examined in [65] and [66].

Nonlinear duplexes and tertiary structures of DNA and RNA

The secondary structure of DNA and RNA not only can appear as a linear helix, but can also have more complex configurations related to the tertiary structure of biopolymers. Relatively long 180° bent single-stranded RNA form duplexes with their complementary segments, while non-complementary segments form rings, hairpins, and loops, which contain several nucleotides. The distances in these secondary struc-

tures differ from those between nucleotides in ordinary helices.

Data on the distances in the hairpin structure of spin-labeled RNA containing 20 nucleotides was obtained in [67]. Nitroxide TEMPO labels were introduced into the NH_2 groups of guanine, adenine, and cytosine of certain nucleotides in single-stranded RNA (Fig. 13A). The number of nucleotides between the labels was fixed and equal to 10. The interlabel distance was determined using PELDOR during the formation of the complementary helix of spin-labeled and non-labeled RNA, as well as in the hairpin structures. In the first case, regardless of the nucleotide type and the position of the label pair in the RNA duplex, the interlabel distance remained the same and was equal to 3.1 nm, which corresponds to the calculated values for the A-form of the duplex.

In the RNA hairpin structure consisting of 20 nucleotides, six complementary nucleotides form a double helix (the hairpin stem), four nucleotides form the loop, and the remaining nucleotides form a monohelix. The duplex with labels located only in one strand was formed after a completely complementary RNA molecule without spin labels had been added to the system (Fig. 13B). The experiments with samples containing different amounts of spin-labeled RNA were carried

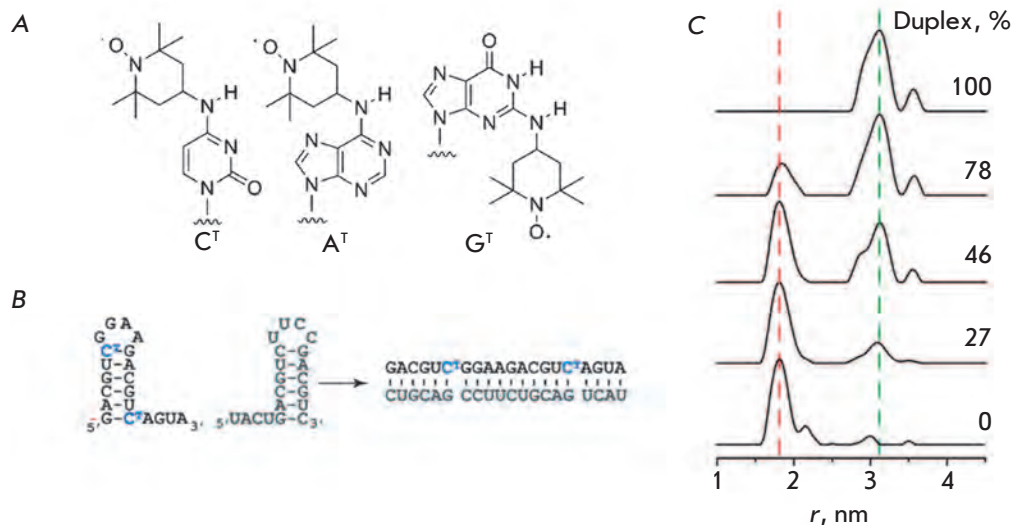
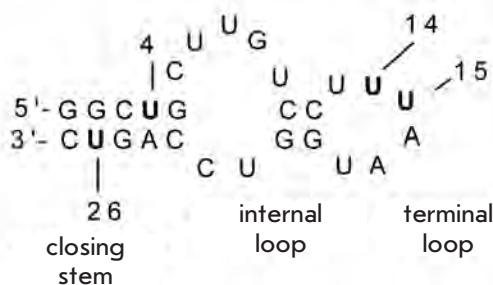


Fig. 13. RNA hairpin structures investigated by PELDOR [67]. (A) RNA with spin-labeled nucleosides. (B) RNA duplex formation from two hairpins. (C) The distance spectrum in mixtures with different contents of the RNA duplex. (Reproduced by permission from John Wiley & Sons, Inc.: [Sicoli, G., Wachowius, F., Bennati, M., Höbartner, C. (2010) *Angew. Chem. Int. Ed.* 49, 6443-6447], copyright 2010)

out using PELDOR. The distance spectrum obtained in these experiments (Fig. 13C) attest to the existence of spin-labeled hairpins with a distance of 1.8 nm between the labels, as well as duplexes with a distance of 3.1 nm in frozen buffer solutions.

Single RNAs can form hairpins along with more complex structures, such as rings (or semi-rings) in conjunction with hairpins. These structural elements may accept certain molecules; they are known as RNA riboswitches and play a crucial role in the mechanisms regulating the transfer of genetic information in cells.

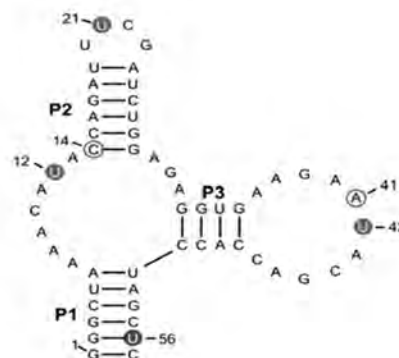
Artificially synthesized RNA riboswitches consisting of 27 nucleotides and capable of accepting neomycin have been investigated using PELDOR [68]:



The TPA spin labels were introduced into uracil residues (highlighted in bold). The interspin distances between positions 4-14, 4-15, 14-26, 15-26 were determined. An attempt was made to determine the conformational changes in the RNA riboswitch during the formation of a neomycin complex [68]. It was found, however, that the distance spectrum between the spin-labeled uridine molecules virtually did not change in this complex as compared to the initial structure of the RNA riboswitch. According to [68],

this fact suggests a conformational stability of the structure.

The structure of another enzyme capable of performing the functions of an RNA-riboswitch and/or of an RNA aptamer in respect to tetracycline (Tc) molecules was investigated [69]. Spin labels were introduced into the synthetic 57-mer ribooligonucleotide either via the reaction between (1-oxyl-2,2,5,5-tetramethylpyrroline-3-methyl)methanethiosulfonate and 4-thiouridine or via the reaction between 4-isocyanate-2,2,6,6-tetramethylpiperidine-N-oxyl and the 2'-amino groups of the ribose molecule.



Here, the filled circles represent spin-labeled 4-thiouridine molecules and the hollow ones represent the nucleotides, which were spin-labeled at the 2'-amino groups.

The tentative structure of this RNA fragment contained three stems (P1, P2, and P3) and three loops. The distances between the spin labels incorporated at the positions (U12/U21), (U12/U56), (U42/U56), and (C14/A41) were measured using PELDOR in the absence and in the presence of Tc. It was determined that the free RNA aptamer exists in two different

Table 2. Nucleic acids studied in [70]

Sample	Nucleotide sequence*
RNA hairpin (U6–U11)	5'-GGC- ACU -UCG-GUG-CC-3'
Neomycin riboswitch (U14–U26)	5'-GGC-UGC-UUG-UCC-UUU-AAU-GGU-CCA-GUC-3'
DNA duplex	5'-GCT-GAT- ATC -AGC-3' 3'-CGA-CTA-TAG-TCG-5'

* Spin-labeled nucleotides are shown in bold.

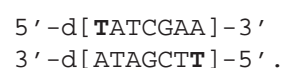
conformations. In the presence of the Tc ligand, an equilibrium shift towards one of the conformations occurs.

The first attempt at using PELDOR to study the influence of the intracellular surrounding on spin-labeled DNA and RNA structures was reported in [70, 71]. In both works, which were published almost simultaneously, the behavior of spin-labeled nucleic acids was investigated in relatively large cells (~ 1 mm in diameter): oocytes of *Xenopus laevis*.

A 12-bp DNA duplex, a 14-mer RNA hairpin, and a 27-mer RNA riboswitch sensitive to neomycin were studied in [70] (Table 2). The TPA spin label was incorporated into the heterocyclic bases via the Sonogashira reaction. Approximately 50 cells were used for the PELDOR experiments. Each cell was infused with 30–50 nl of 2.5- to 5.0-mM free spin label or a double-labeled nucleic acid using microinjections. These manipulations took around 10 min. The cells were subsequently washed with a buffer, transferred into an EPR cuvette, and frozen in liquid nitrogen; then, the measurements were carried out.

The distances between the spin labels in the RNA hairpin and the neomycin RNA riboswitch did not depend on the localization of the specimen: whether inside the oocytes or outside the cell (in the buffer). This fact means that these RNA molecules had rigid structures, which are identical both *in vivo* and *in vitro*. In contrast, the interlabel distance in the short DNA duplex depended on the conditions experienced by the specimen: in the solution or inside the cell. The distance between the spin labels in the solution was smaller compared to that for a sample inside the cell. The authors attributed this fact to the existence of base stacking interactions when the duplex was localized in the solution and to stacking disruption when DNA was located inside the cell and interacted with cellular proteins and other molecules.

In [71], the TEMPA label was attached to the terminal residues of thymidine of each strand (shown in bold) in the DNA duplex via the Sonogashira reaction:



This spin-labeled duplex was introduced through a microinjection into the oocytes of *X. laevis*. The properties of spin-labeled DNA in cells frozen at 45 K and the physiological buffer solution were compared. In both cases, the concentration of paramagnetic particles after freezing decreased considerably: this did not hinder the assessment of the interlabel distance in DNA: 3.20 and 3.22 nm in buffer and inside the cells, respectively. The main impact consisted in a considerable increase in the width of the spectrum line. This value was equal to 0.43 nm in buffer and increased to 1.04 nm inside the cells. Based upon the presented PELDOR data, the latter value can be even higher; i.e. it can correspond to the virtually uniform spin distribution. This effect is presumably conditioned upon a relatively rapid degradation of DNA in the cellular environment, which occurs prior to freezing of the samples.

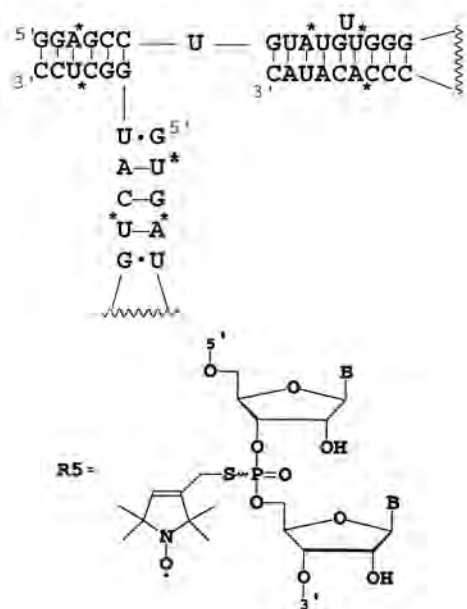
The increase in the stability of the spin labels in the cellular environment remains one of the main problems of this important research. Furthermore, it is possible also to reduce the time from the moment when a spin-labeled DNA is introduced into the cell to its freezing.

Numerous functional DNA and RNA molecules form specific tertiary structures, whose organization and dynamics determine their functions. The distances between the incorporated spin labels in these tertiary structures depend both on the biopolymer conformation and on the spatial orientation of its individual units.

The effect of Mg²⁺ ions on a ribozyme with a branched “hammerhead” structure (“hammerhead ribozyme,” HHRz) was also studied [72]. The distance spectrum for the TEMPO spin labels incorporated into various loops of the HHRz structure was determined. It was demonstrated that at the addition of Mn²⁺ ions into the HHRz solution, the number of ribozymes containing loops with the smallest interlabel distances (~ 2.4 nm) increases with the increase in Mn²⁺ concentration. It

was assumed that these RNA-metal ion complexes participate in the catalyzed RNA cleavage.

The changes in the distances between the spin labels that are due to the conformational transformations were also estimated using PELDOR in other, more complex RNA and DNA molecules with various tertiary structures (e.g., RNA containing a three-way-junction) [73]. A similar structure is formed in the packaging motor of ϕ 29-bacteriophage during the packaging of double-stranded genomic DNA into a preformed capsid. The packaging motor is an RNA-protein complex, which utilizes the energy from the ATP hydrolysis to condense genomic DNA. The structure of the RNA within this motor has yet to be studied thoroughly; hence, the significance of the investigation of its structure using PELDOR is not in doubt. This RNA is a dimer whose structure used to be regarded as a possible intermediate formed during this process. The R5 spin labels were introduced into the internucleotide phosphorothioate groups. A unit of this structure is shown below; the positions where the spin labels were incorporated are marked with asterisks:



Seventeen distances between the spin-label pairs were measured. The analysis of these data allows one to determine the possible spatial orientations of three helices in the packaging motor. It was demonstrated that two out of three RNA helices in this structure formed a sharp angle with respect to each other, which does not correspond to the previously proposed model, where these helices were attached to each other along a single line. This work demonstrated all the advantages of the method used to study the spatial geometry of complex RNA structures.

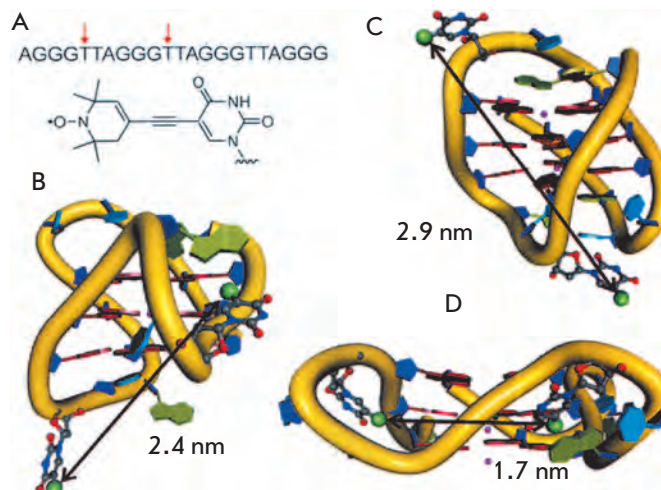


Fig. 14. Human telomeric quadruplexes [74]. The DNA sequence was examined, arrows indicate the sites of the spin-labels in the conformers shown. Parallel propeller (A), hybrid 3 + 1 (B) and antiparallel basket (C). (Reproduced by permission from John Wiley and Sons: [Singh, V., Azarkh, M., Exner, T.E., Hartig, J.S., Drescher, M. (2009) *Angew. Chem. Int. Ed.* 48, 9728-9730], copyright 2009)

PELDOR was used to study the conformations of the quadruplexes formed in telomeric sequences at chromosome termini [74] (in humans, they consist of GGGTTA repeats [75]). The structure of the quadruplex-forming oligonucleotide double labeled with TEMPA, in which the spin labels were incorporated into positions 5 and 11, was studied (Fig. 14A) [74]. It has been proven that a mixture of two structures exists in a solution containing K^+ ions: an antiparallel basket and a parallel propeller at a 1:1 ratio (Fig. 14B,D). Moreover, the sequence $TT(GGGTTA)_3GGGA$, which is slightly different from the previous sequence, folded into a new hybrid 3+1 structure in the solution in the presence of K^+ ions (Fig. 14C).

The four-way DNA junction (also known as the “Holliday junction”) and the changes in its structure during its interaction with endonuclease I of bacteriophage T7 were also investigated [76]. The DNA was made up of two strands: the Y strand (marked in red) and the Z strand (marked in blue), which formed a structure consisting of four different helices linked together at a single location:



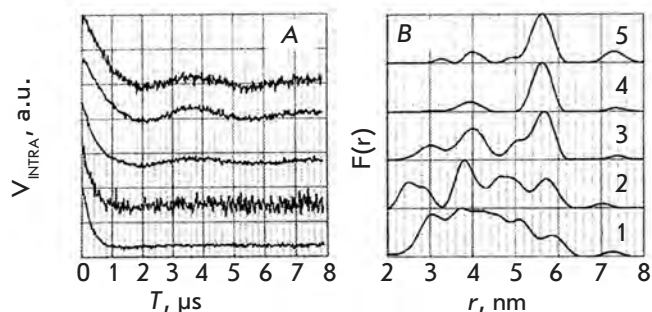


Fig. 15. PELDOR time trace (A) and distance spectrum (B) changes as the function of the duplex/enzyme ratios in frozen buffer solutions: 1/0.00 (1), 1/0.25 (2), 1/0.50 (3), 1/1.00 (4), 1/1.25 (5) [76]. (Reproduced by permission from the American Chemical Society: [Freeman, A.D.J., Ward, R., Mkami, H.E., Lilley, D.M.J., Norman, D.G. (2011) *Biochemistry* 50, 9963-9972], copyright 2011)

The TEMPO labels were introduced into the uridine residues of different duplex branches (the labels are denoted with the letter U and are highlighted in bold). The frozen buffer solutions contained D₂O and deuterio-glycerol. The PELDOR time traces were recorded and analyzed using the conventional procedures [21]. The result of endonuclease action on the four-way DNA junction is shown in *Fig. 15*. Prior to the introduction of the enzyme, a broad distance distribution between the TEMPO labels in the 3- to 6-nm range was observed. With enzyme concentration increasing (presumably due to the stabilization of the DNA–enzyme complex), the distance spectrum, with the interlabel distance in this complex being 5.6 nm, contained a single line (*Fig. 15*).

Data on the changes in the distances between the labels introduced into T7-endonuclease I during the formation of the duplex–enzyme complex were also obtained [76]. These changes in the distances, which occurred during the reorganization of the protein structure, were shown to be insignificant (not more than several Å) but to be reliably recordable using PELDOR.

Thus, it has been reliably established that the induced fitting of the conformations in both biopolymers between T7-endonuclease I and the 4-way DNA-junction occurs during the complex formation. The conformational changes observed during the duplex–enzyme complex formation were confirmed using MD-simulations. It is worth mentioning that this work was characterized by high experimental quality (reliability and accuracy in the PELDOR experiment and its processing).

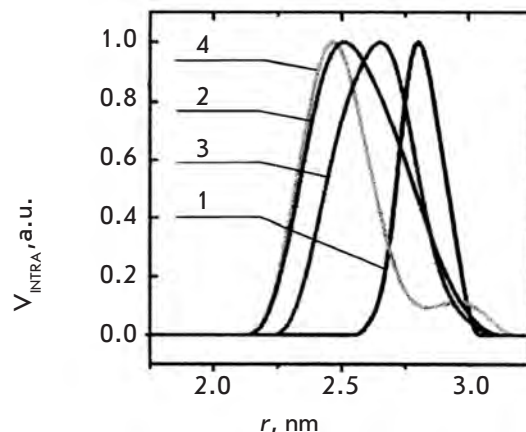


Fig. 16. Distance distribution functions $F(r)$ for undamaged DNA (1) and its changes when damages as propyl (2), ethyl (3), THF (4) (see Table 3) are introduced into DNA. Orientation selectivity was considered for $F(r)$ calculated in the standard experiment [77]. (Reproduced by permission from Oxford University Press: [Sicoli, G., Mathis, G., Aci-Seche, S., Saint-Pierre, C., Boulard, Y., Gasparutto, D., Gambarelli, S. (2009) *Nucleic Acids Res.* 37, 3165-3176], copyright 2009)

Effect of the deficiencies on the DNA structure

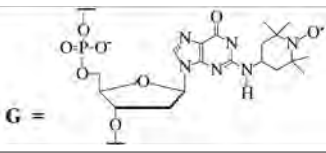
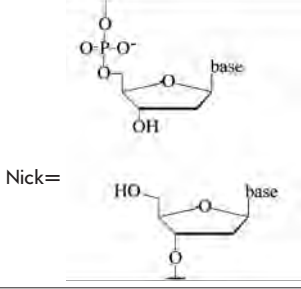
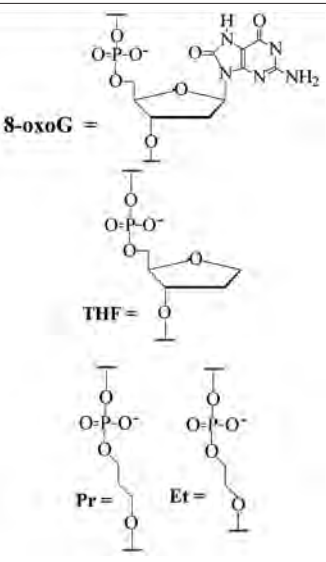
The effect of various lesions modifying the DNA structure (in particular, changing the distances between the introduced spin labels) was studied in [77–79]. These defects can be caused by many factors, such as structural aggregates or groups binding DNA at a certain location, nucleotide substitution with various structures, nicks in one of the DNA strands in the duplex, etc. All these factors that chemically modify DNA become evident in the endogenous metabolism; their investigation employing physical methods is of particular interest for biologists and biochemists.

The changes in the interlabel distances in the DNA duplexes containing various structural defects and insertions in one of the duplex strands were analyzed in [77]. 4-Amino-TEMPO spin labels were introduced into the guanine residues of the other DNA strand (see reference [49]) into positions (4;11) (A) and (4;19) (B); the second strand of the duplex contained various lesions – nicks (C), gaps (D), modified nucleotides (E1–E5), and bulges (F) (*Table 3*).

4pPELDOR and conventional methods for data analysis were used in each case. The measurements were carried out at 60 or 70 K. The samples contained 50 or 100 μM of spin-labeled DNA in saline with 15–20% of glycerol added.

The data for the undamaged duplexes (4;11) and for those with various lesions are provided in *Fig. 16*

Table 3. Spin-labeled DNA duplexes with nicks and insertions [77]

A	3'-C-T-G-G-A-C-G-T-A-G-A-T-C-C-T-A-C-G-G-5' 5'-G-A-C-C-C-T-G-C-A-T-C-T-A-G-G-A-T-G-C-C-3'	
B	3'-C-T-G-G-A-C-G-T-A-G-A-T-C-C-T-A-C-G-G-5' 5'-G-A-C-C-C-T-G-C-A-T-C-T-A-G-G-A-T-G-C-C-3'	
C	3'-C-T-G-G-A-C-G-T-A-G-A-T-C-C-T-A-C-G-G-5' 5'-G-A-C-C-C-T-G C-A-T-C-T-A-G-G-A-T-G-C-C-3'	
D	3'-C-T-G-G-A-C-G-T-A-G-A-T-C-C-T-A-C-G-G-5' 5'-G-A-C-C-C-T-G ■ A-T-C-T-A-G-G-A-T-G-C-C-3'	Gap
E	3'-C-T-G-G-A-C-G-T-A-G-A-T-C-C-T-A-C-G-G-5' 5'-G-A-C-C-C-T-X ₁ -C-A-T-C-T-A-G-G-A-X ₂ -G-C-C-3'	
E1	X1=8-oxoG	
E2	X1=G	
E3	X1=THF	
E4	X1=Et	
E5	X1=Pr	
F	3'-C-T-G-G-A-C-G-T-A-G-A-T-C-C-T-A-C-G-G-5' 5'-G-A-C-C-C-T-G C-A-T-C-T-A-G-G-A-T-G-C-C-3' ∨ A ₁	Insertion A ₁

as an example of the distance spectra obtained from the modulated PELDOR time traces. In order to eliminate the orientational selectivity, the PELDOR time trace (averaged over 10 measurements) obtained via the variation of the magnetic field for the position of the detection pulse in the EPR spectrum was analyzed. The authors [77] believe that all these measures allow one to reliably assess the error in determining the average distance and the width of the lines in the distance spectrum (error ~10%) (Table 4).

All the results obtained for the duplexes labeled at positions (4;11) were separated into two groups [77].

The first group contained the duplexes with structural lesions of C, D, F, E1 and E2 types. The changes in the interspin distances in this group were insignificant in comparison with the undamaged DNA and were mostly due to measurement errors. A significant decrease in the distance, along with widening of the distance spectrum lines leading to its asymmetry, was found in the second group, which contained duplexes with E3, E4, E5 lesion types. A similar situation was observed for the duplexes labeled at positions (4;19), where the distances change from 5.21 ± 0.04 nm for the initial, undamaged structure to 5.02 ± 0.03 nm for the damaged duplexes

Table 4. Experimental distances r_{\max} between the spin labels and widths of the Δ -bands of the spectra lines (nm) in the duplexes with spin labels at positions (4;11) [77]

DNA duplex	r_{\max}	Δ
Undamaged duplex	2.81 ± 0.01	0.21 ± 0.02
Nick	2.87 ± 0.01	0.22 ± 0.02
Gap	2.84 ± 0.01	0.26 ± 0.02
Insertion A ₁	2.85 ± 0.02	0.23 ± 0.02
8-oxoG (E ₁ duplex)	2.81 ± 0.01	0.22 ± 0.02
8-oxoG (E ₂ duplex)	2.84 ± 0.01	0.27 ± 0.02
THF	2.46 ± 0.02	0.35 ± 0.02
Ethyl	2.65 ± 0.02	0.38 ± 0.04
Propyl	2.48 ± 0.02	0.45 ± 0.03

of (5.4), (5.5) type; the width of the distribution function changes from 0.33 ± 0.02 to 0.44 ± 0.05 nm.

When discussing the results, it is usually assumed that the width of the distance spectrum line characterizes the conformational flexibility of the duplexes. Following special MD calculations, G. Sicoli *et al.* [77] concluded that the significant changes in the distances in the second group of damaged duplexes could be attributed to the local changes in the conformations at lesions sites and in the complementary nucleotide of the duplex.

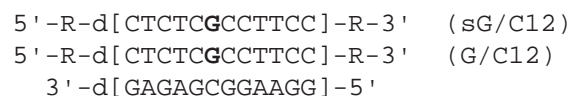
In general, the results in study [77] (where the changes in the damaged DNA were examined) in a number of cases are in qualitative agreement with the data obtained using such methods as NMR. It is also considered that the use of pulse EPR spectroscopy in

combination with MD techniques for spin-labeled DNA is complementary (to conventional methods, such as NMR, CD, FRET, and X-ray crystallography) and a highly informative method for studying various DNA lesions and weak interactions between DNA and other molecules and complexes.

The sensitivity of the PELDOR parameters determined to the changes in the nucleic acid structure was found to be considerably higher than that in [77], when the spin labels were introduced into the termini of relatively short nucleotides and their duplexes [78, 79].

3pPELDOR was used to identify the distance spectrum for the labels at the termini of 12-mer oligonucleotides and their DNA duplexes [78]. The synthesized substrates contained TEMPO spin labels at their 5'- and 3'- terminal phosphate groups.

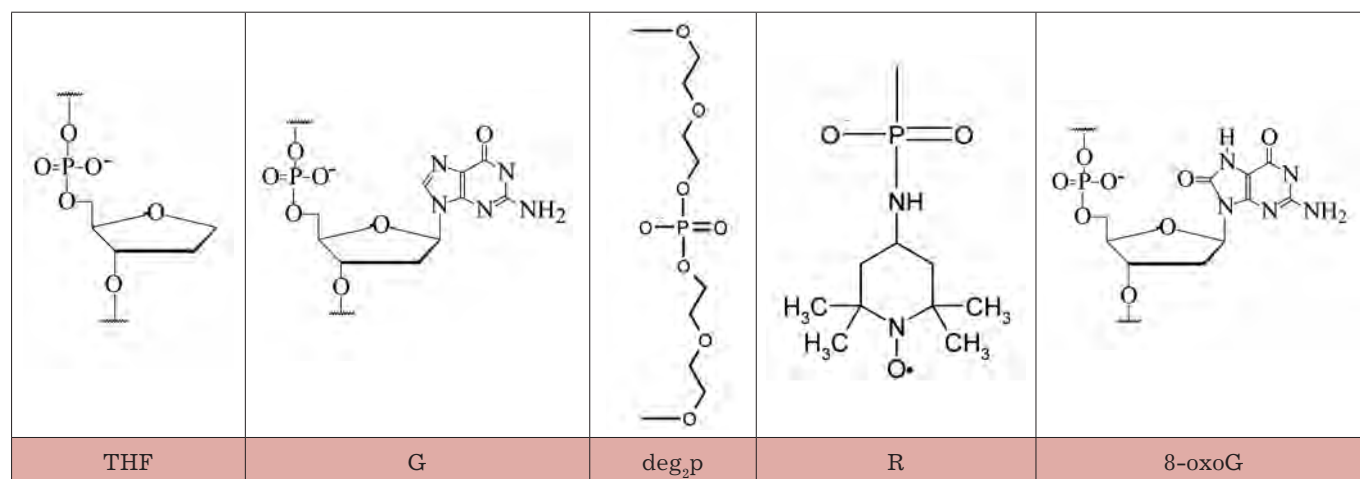
The structures of 12-mer single-stranded DNA and DNA duplexes, as well as their denotation, are provided below:



One of the nucleotides located in the center of the G strand could be modified by various insertions and substitutions. The structures of the spin labels and introduced insertions are listed in Table 5.

Frozen glassy solutions of spin-labeled DNA were studied in a water/glycerol mixture at 77 K using 3pPELDOR in order to obtain the distance spectrum between the labels. These distance spectra were determined from the experimental V_{INTRA} time traces by the Tikhonov's regularization method with the use of both

Table 5. Structures of radical R, nucleotides, and non-nucleotide insertions [78, 79]



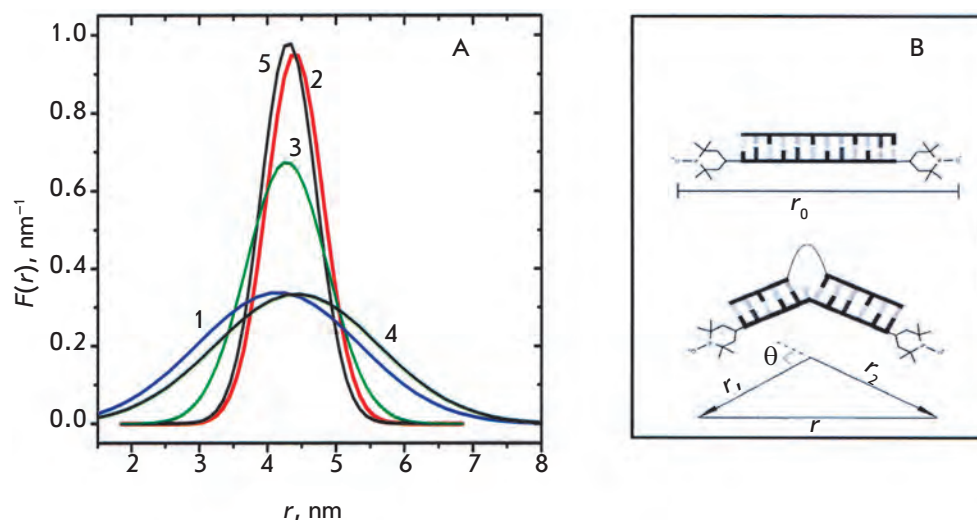


Fig. 17. (A) Gaussian approximations of the spectra lines for two spin labels in DNAs in a frozen glassy water/glycerol mixture at 77 K [78]. (1) – single-stranded oligonucleotide ssG, (2), thick line – duplex dsG, (3 – duplex dsG-looped, 4 – single-stranded oligonucleotide ssF, 5 – duplex dsF. (B) Schematic representation of the spin-labeled DNA molecule without (top) and with (bottom) a non-nucleotide insert, which demonstrates the bending of the molecule and shortening of the distance between two labels. (Reproduced by permission from The Royal Society of Chemistry: [Kuznetsov, N.A., Milov, A.D., Koval, V.V., Samoilo, R.I., Grishin, Yu.A., Knorre, D.G., Tsvetkov, Yu.D., Fedorova, O.S., Dzuba, S.A. (2009) *Phys. Chem. Chem. Phys.* 11, 6826-6832], copyright 2009)

the standard algorithm and the Gaussian approximation for $F(r)$.

The distance spectra shown in Fig. 17A and the data listed in Table 6 demonstrate that a 2- to 3-fold narrowing of the spectrum lines as compared to those for single-stranded DNA occurs during the duplex formation. The insertion of nucleotide analogues results in a reduction in the average interspin distance in the duplexes. In case of the **deg₂p** insertion, a noticeable widening of the distance spectrum as compared to **G/C12** duplexes was observed. It is obvious that the line narrowing of the distance spectrum can be attributed to the formation of the DNA double helix, which is characterized by a more rigid structure as compared to that of single-stranded DNA. The observed width of the spectrum line for the undistorted duplex (**G/C12**) was apparently caused by the random orientation of spin labels due to rotation around the P–N bonds. Considering the fact that the distance between the nitrogen atom and the N–O moiety of the spin label is ~ 0.4 nm, the maximum widening of the spectrum line due to the reorientation of spin labels will be equal to 1.6 nm. The magnitude of the experimental value of the width of the distance spectrum $\Delta = 0.98 \pm 0.1$ nm for the undamaged duplex lies within this range. It should be mentioned that the effects associated with the orientational selectivity in PELDOR were observed neither in this study nor in [77], which

Table 6. Parameters of the distance spectra (nm) for 12-meric oligonucleotides and their DNA duplexes [78]

Sample*	Average distance, r	Width, Δ
sG/C12	4.05 ± 0.05	2.8 ± 0.2
sTHF/C12	4.32 ± 0.05	2.85 ± 0.2
G/C12	4.35 ± 0.03	0.98 ± 0.1
deg ₂ p/C12	4.23 ± 0.03	1.39 ± 0.1
THF/C12	4.26 ± 0.03	0.95 ± 0.1

* Symbol **s** denotes the single-stranded DNA.

can also presumably be attributed to the uncorrelated spread of spin label orientations.

The introduction of non-nucleotide insertions into the duplex structure affects the average interspin distance. A decrease in the distance denotes the possibility of duplex bending with respect to the insertion sites, due to the emergence of an additional degree of freedom in the insertion site. The scheme illustrating the estimation of the conformational distortion angle

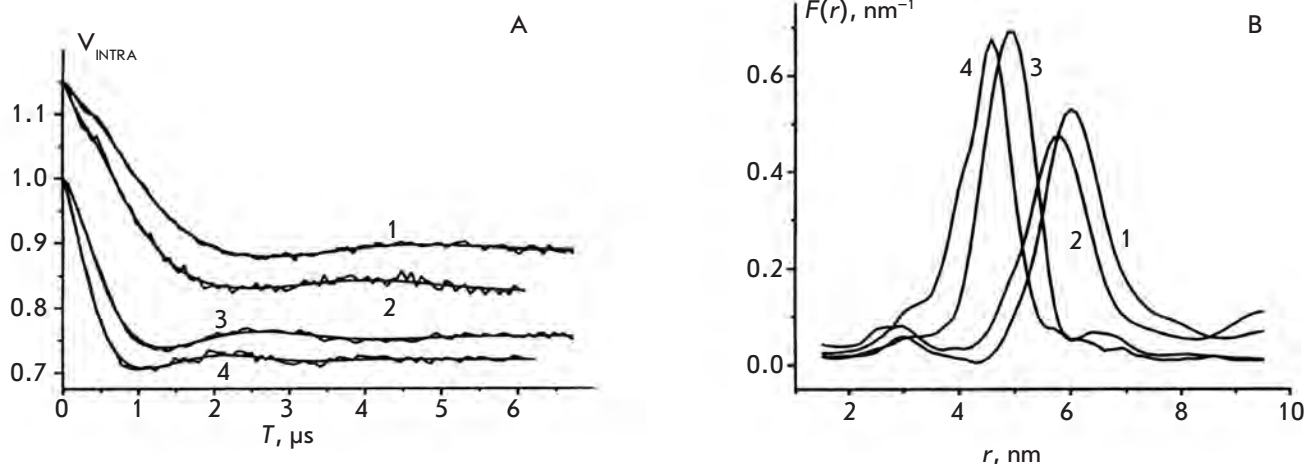


Fig. 18. The intramolecular contribution to the PELDOR signal obtained for complexes of DNA with Fpg [79]. (A) Curves 1 and 2 refer to DNA G/C¹⁷ and F/C¹⁷/Fpg, respectively; curves 3 and 4 refer to DNA G/C¹³ and F/C¹³/Fpg, respectively. For convenience of comparison, curves 1 and 2 are shifted upwards relative to curves 3 and 4. The smooth curves were calculated using the distribution functions shown in Fig. 18B. (B) The distance distribution function between labels, $F(r)$, obtained from the data in Fig. 18 (A) neglecting the orientational selectivity. Curves 1 and 2 refer to DNA G/C¹⁷ and F/C¹⁷/Fpg, respectively; curves 3 and 4 refer to DNA G/C¹³ and F/C¹³/Fpg, respectively. (Reproduced by permission from The Royal Society of Chemistry: [Kuznetsov N.A., Milov A.D., Isaev N.P., Vorobjev Yu.N., Koval V.V., Dzuba S.A., Fedorova O.S., Tsvetkov Yu.D. (2011) *Mol. BioSystems* 7, 2670-2680], copyright 2009)

is shown in Fig. 17B. The experimentally determined values of r_0 (the duplex without the insertion) and r for the distorted duplex can be used to estimate the angle ($\theta = 23^\circ$) in the **THF/C12** duplex and ($\theta = 27^\circ$) in the looped **deg_p/C12** duplex.

An increase in the length and flexibility of the insertion in the **deg_p/C12** duplex as compared with those in the other two duplexes results in additional line broadening ($\Delta = 1.39$ nm) of the distance spectrum. The broadening value is too large to simply attribute it to the spread in the bending angle of the duplex without taking into account the possible elongation of the duplex.

Hence, the aforementioned estimation of the bending angle of this insertion can only be used as the lower boundary of the average bending angle for this duplex. Therefore, the provided estimates show that the incorporation of a non-nucleotide insertion into a DNA molecule opens the possibility of duplex bending with respect to the insertion site. An increase in the number of bonds in the insertion increases insertion flexibility. A decrease in duplex rigidity near the insertion causes a considerable increase in the dispersion of the bending angle and the total duplex length.

N.A. Kuznetsov *et al.* [79] used the same approach as that used in [78] to study the lesions in stretched DNA duplexes (13 and 17 nucleotides). However, the main aim of this work was to investigate the features of the

conformational transformations of DNA during its interaction with the Fpg protein from *E.coli*. This protein is considered to be one of the key factors involved in the process of DNA repair. The structure of the investigated duplexes is shown below:



The structures of the R spin labels, nucleotides, and non-nucleotide insertions are presented in Table 5.

The analysis of the PELDOR time traces (Fig. 18A) allowed to obtain the distance spectra (Fig. 18B) and to determine the structural parameters: the distance values at the maximum of the distribution lines, r_{max} (0.8% accuracy), and the width of the lines at half-height Δ (10% accuracy) (Table 7).

Similar to that in [78], the positions of the spin labels at the 5'- and 3'- terminal ends of the complementary second oligonucleotide of the DNA duplex made them sensitive to the formation of the DNA curves caused by either the existence of damaged sites or the formation of complexes with an enzyme. The Fpg protein from *E. coli* was found to cause bending even in the undamaged 13-bp duplex. A similar result has been obtained only

with the use of an X-ray structure analysis of Fpg from *Bacillus stearothermophilus* [80–82]. However, no bend formation has been detected for the undamaged 17-bp duplex in the presence of the enzyme. This could be attributed to the fact that the enzyme occupying a 10-bp DNA segment cannot move (slide) along the strand of the short DNA duplex, while sliding is possible during binding to the 17-bp DNA duplex. It cannot be ruled out, however, that the conformational mobility of the spin labels of the 17-bp duplex is higher than that of the 13-bp duplex, which is supported by an increase in the width of the spectrum line for the 17-bp duplex (see Table 7).

In free DNA duplexes containing 8-oxoG, changes in the interspin distances as compared with the undamaged duplex have not been identified. This is not surprising, since 8-oxoG hardly changes the DNA structure. A considerable reduction in the interspin distance was observed for the duplexes containing the cyclic THF site. This result was confirmed by computer simulations using the molecular dynamics method [79].

During the interaction between the duplexes and the Fpg protein from *E. coli*, bending occurred both in 13- and 17-unit duplexes. This result correlates with the X-ray structural data for the cross-linked adduct of Fpg and the apurinic/apyrimidinic site [80–82]. It is important to mention that the X-ray data provide information on the local DNA segments in the damaged region, whereas PELDOR provides data on the global changes in the structure. Hence, structural studies of both types agree with and complement each other.

The bending of the DNA helix in the region of the damaged nucleotide recorded using PELDOR [78, 79] provides new information regarding the mechanism of the search for lesions in DNA by DNA repair enzymes. The emergence of the bendings allows one to understand why the enzymes that slide along the DNA strand stop at the damaged sites to repair them. The data obtained are also important for understanding the mechanisms of action of other enzymes that perform the search for specific DNA sites.

CONCLUSIONS

Let us summarize the results of these PELDOR studies of DNA and RNA. It has been demonstrated that the PELDOR method can be used to determine DNA and RNA conformations and the conformational changes that are due to structural modifications and transformations, to assess the dispersion in the distances between individual groups and structure rigidity, and to determine the orientation of the spin labels introduced into DNA and RNA by measuring the distances between various fragments of poly- and oligonucleotides. Studies of the effect of the surrounding environment

Table 7. Parameters (nm) of the distance distribution function $F(r)$ between two spin labels in the DNA duplexes [79]

Sample	r_{\max} , nm*	Δ , nm*
G/C13	4.96	1.1
8-oxoG/C13	4.96	1.1
THF/C13	4.83	1.1
THF/C13/Fpg	4.60	1.2
G/C13/Fpg	4.78	1.1
G/C17	6.00	1.2
8-oxoG/C17	6.02	1.2
THF/C17	5.98	1.2
THF/C17/Fpg	5.76	1.2
G/C17/Fpg	5.99	1.4

* r_{\max} and Δ were measured with errors of 0.8 and 10%, respectively.

and complex formation on the structural parameters of DNA and RNA have been launched.

The studies summarized in this review describe the features, advantages, and drawbacks of PELDOR as compared with similar structural methods. Among the most obvious and most important advantages, let us mention in particular the relatively wide range of distances between the spin labels (1.5–8 nm) measured with high accuracy. The fact that it is not only the distances but also the distance distribution spectra that can be determined makes PELDOR prominent among the other structural methods. Relatively simple methods for analyzing the experimental data obtained for randomly oriented systems, in mixtures and solutions (which are convenient media for chemists and biologists), have been elaborated. Pulse EPR spectrometers are commercially available. All these factors determine the popularity of PELDOR in modern chemical radiospectroscopy, especially for biologically important systems.

Meanwhile, we attribute the necessity of introducing spin labels into the investigated molecule to the disadvantages of this method as compared with such methods as NMR. However, despite the fact that a series of chemical methods have been developed, site-directed spin labeling still remains a relatively labor-consuming manipulation. Moreover, one needs to make sure that a

spin-labeled molecule does not lose its initial physical-chemical properties. Because of the “molecule–label” effects of a linker, the measured interspin distance can differ from the molecular distance. All these problems have typically existed and were solved in one way or the other in most of the aforementioned works. One also needs to select a special solvent that has to undergo glassing during freezing, since all the measurements are carried out in glassy matrices at low temperatures. We would like to point out that the same disadvantages were encountered when measuring the distances using the dipole widening of the lines in a stationary EPR spectrum confined to distances of less than 2–2.5 nm [29].

In methodological terms, PELDOR is similar to the commonly used FRET method [83], which helps study the excitation transfer between the incorporated donor and acceptor labels. It is worth mentioning that the two fluorescent labels, which are introduced to carry out FRET measurements, differ in their structures (as opposed to similar labels for the PELDOR method) and are typically relatively larger as compared to spin labels. The efficiency in FRET is proportional to the $1/[1 + (r/R_0)^6]$ value, where R_0 is the Förster radius and r is the interlabel distance [84]. The Förster radius depends on a number of parameters, such as the overlap integral of the donor spectrum with the acceptor one, the fluorescence quantum yield, and the orientation of electrical dipoles. Unlike that in PELDOR, all these factors require additional experiments and calibrations in order to determine the interlabel distances. This reduces accuracy in determining these distances. The extremely high sensitivity of FRET is its major drawback. Similar to most modern optical methods, it can be used to perform measurements with a resolution of up to single molecules, including quick transformations

in liquids. PELDOR has a maximum sensitivity of approximately 10^{12} particles per sample [10].

Hence, the choice of the investigation method to study the structure and properties of poly- and oligonucleotides is determined primarily by the aims of the study and experimental capabilities. Ideally, a combination of PELDOR and FRET provides the most comprehensive information on the structure and physical-chemical properties of biologically important structures. Such studies are currently under way. For instance, studies employing these methods to investigate the features of the protein–nucleic complexes structure have already been published [85, 86]. Among them, a relatively complex supramolecular complex regulating the structure of chromatin histones has been studied [87].

In our opinion, the data obtained with the use of PELDOR significantly contributes to the investigation of the structure and properties of DNA and RNA. This method opens new perspectives for studying complex nonlinear structures, interactions between polynucleotides and enzymes, proteins, and membranes. The potential of PELDOR as a method for structural studies will undoubtedly increase with the development of pulse ERP spectroscopy. ●

The authors would like to thank O.V. Polukarikova for her assistance during the preparation of this review.

This work was supported by the Russian Foundation for Basic Research (grants № 13-04-00013a, 11-03-0011a, and 11-04-01377a), NSh-64-04-2012, Department of Chemistry and Material Sciences of the Russian Academy of Sciences (project 5.6.3, grant 5.6), Federal Target-Oriented Program “Scientific and Scientific-Pedagogical Personnel” (№ 8092, 8473).

REFERENCES

- Milov A. D., Salikhov K. M., Shirov M.D. // *Fiz. Tverd. Tela*. 1981. V. 23. P. 975–982.
- Schiemann O., Prisner T.F. // *Quart. Rev. Biophys.* 2007. V. 40. P. 1–53.
- Jeschke G., Polyhach Ye. // *Phys. Chem. Chem. Phys.* 2007. V. 9. P. 1895–1910.
- Tsvetkov Y. D., Milov A. D., Maryasov A. G. // *Russ. Chem. Rev.* 2008. V. 77. P. 487–520.
- Sowa Z., Qin P.Z. // *Prog. Nucl. Acid Res. Mol. Biol.* 2008. V. 82. P. 147–197.
- Schiemann O. // *Meth. Enzymol.* 2009. V. 469. Ch. 16. P. 329–351.
- Reginsson G.W., Schiemann O. // *Biochem. Soc. Trans.* 2011. V. 39. P. 128–139.
- Reginsson G.W., Schiemann O. // *Biochem. J.* 2011. V. 434. P. 353–363.
- Milov A.D., Maryasov A.G., Tsvetkov Yu.D. // *Appl. Magn. Reson.* 1998. V. 15. P. 107–143.
- Tsvetkov Y. D., Grishin Y.A. // *Instruments and Experimental Techniques*. 2009. V. 52. P. 615–636.
- Maryasov A.G., Tsvetkov Yu.D. // *Appl. Magn. Reson.* 2000. V. 18. P. 583–605.
- Ponomarev A.B., Milov A.D., Tsvetkov Yu.D. // *J. Struct. Chem. (Russ.)*. 1984. V. 25. P. 51–54.
- Milov A.D., Ponomarev A.V., Tsvetkov Yu.D. // *Chem. Phys. Lett.* 1984. V. 110. P. 67–72.
- Milov A.D., Samoilova R.I., Tsvetkov Yu.D., Jost M., Peggion C., Formaggio F., Toniolo C., Handgraaf J.-W., Raap J. // *Chem. Biodiv.* 2007. V. 4. C. 1275–1298.
- Tikhonov A.N., Arsenin V.Y. *Solutions of ill-posed problems*. N.Y.: Wiley, 1977.
- Bowman K., Maryasov A.G., Kim N., DeRose V.J. // *Appl. Magn. Reson.* 2004. V. 26. C. 23–39.
- Jeschke G., Koch A., Jonas U., Godt A. // *J. Magn. Reson.* 2002. V. 155. P. 72–82.
- Jeschke G., Panek G., Godt A., Bender A., Paulsen H. // *Appl. Magn. Reson.* 2004. V. 26. P. 223–244.

19. Chiang Y.-W., Borbat P.P., Freed J.H. // *J. Magn. Reson.* 2005. V. 172. P. 279–295.
20. Jeschke G., Sajid M., Schulte M., Godt A. // *Phys. Chem. Chem. Phys.* 2009. V. 11. P. 6580–6592.
21. Jeschke G., Chechik V., Ionita P., Godt A., Zimmermann H., Bbanham J., Timmel C.R., Hilger D., Jung H. // *Appl. Magn. Reson.* 2006. V. 30. P. 473–498.
22. Milov A.D., Samoilova R.I., Tsvetkov Yu. D., Gusev V.A., Formaggio F., Grisma M., Toniolo C., Raap J. // *Appl. Magn. Reson.* 2002. V. 23. P. 81–95.
23. Milov A.D., Tsvetkov Yu.D., Formaggio F., Oancea S., Toniolo C., Raap J. // *J. Phys. Chem. B.* 2003. V. 107. P. 13719–13727.
24. Tsvetkov Yu.D. / *Biological Magnetic Resonance*. V. 21. (EPR: Instrumental Methods) // Eds C.J. Bender, L.J. Berliner. New York: Kluwer Academic/Plenum Publishers, 2004. V. 21. P. 385.
25. Savitsky A., Dubinskii A.A., Flores M., Lubitz W., Möbius K. // *J. Phys. Chem. B.* 2007. V. 111. P. 6245–6262.
26. Marko A., Margraf D., Yu H., Mu Y., Stock G., Prisner T. // *J. Chem. Phys.* 2009. V. 130. 064102.
27. Marko A., Margraf D., Cekan P., Sigurdsson S.T., Schiemann O., Prisner T.F. // *Phys. Rev. E.* 2010. V. 81. 021911.
28. *Biological Magnetic Resonance. Spin Labeling: The Next Millennium* / Ed. L. Berliner. New York: Kluwer Academic/Plenum Publishers, 1998. V. 14.
29. *Biological Magnetic Resonance. Distance Measurements in Biological Systems by ESR* / Eds L. Berliner, S. Eaton, G. Eaton. New York: Kluwer Academic/Plenum Publishers, 2000. V. 19.
30. *Biological Magnetic Resonance. EPR: Instrumental Methods* / Eds C. Bender, L. Berliner. New York: Kluwer Academic/Plenum Publishers, 2004. V. 21.
31. Schiemann O., Piton N., Plackmeyer J., Bode B.E., Prisner T.F., Engels J.W. // *Nat. Protocols.* 2007. V. 2. C. 904–923.
32. Krstić I., Endeward B., Margraf D., Marko A., Prisner T.F. // *Top. Curr. Chem.* 2012. V. 321. P. 159–198.
33. Shelke S.A., Sigurdsson S.T. // *Eur. J. Org. Chem.* 2012. V. P. 2291–2301.
34. Spaltenstein A., Robinson B., Hopkins P.B. // *J. Am. Chem. Soc.* 1988. V. 110. P. 1299–1301.
35. Rossi R., Carpita A., Bellina F. // *Org. Prep. Proc. Int.* 1995. V. 27. P. 127–160.
36. Chinchilla R., Nájera C. // *Chem. Rev.* 2007. V. 107. P. 874–922.
37. Gannett P.M., Darian E., Powell J.H., Johnson E.M. // *Synthetic Communications.* 2001. V. 31. P. 2137–2141.
38. Gannett P.M., Darian E., Powell J., Johnson E.M. II, Munday C., Greenbaum N.L., Ramsey C.M., Dalal N.S., Budil D.E. // *Nucleic Acids Res.* 2002. V. 30. P. 5328–5337.
39. Frolow O., Bode B.E., Engels J.W. // *Nucleosides Nucleotides Nucl. Acids.* 2007. V. 26. P. 655–659.
40. Piton N., Schiemann O., Mu Y., Stock G., Prisner T.F., Engels J.W. // *Nucleosides Nucleotides Nucl. Acids.* 2005. V. 24. P. 771–775.
41. Piton N., Mu Y., Stock G., Prisner T.F., Schiemann O., Engels J.W. // *Nucleic Acids Res.* 2007. V. 35. P. 3128–3143.
42. Kolb H.C., Finn M.G., Sharpless K.B. // *Angew. Chem. Int. Ed.* 2001. V. 40. P. 2004–2021.
43. Ding P., Wunnicke D., Steinhoff H.-J., Seela F. // *Chem. Eur. J.* 2010. V. 16. P. 14385–14396.
44. Jakobsen U., Shelke S.A., Vogel S., Sigurdsson S.T. // *J. Am. Chem. Soc.* 2010. V. 132. P. 10424–10428.
45. Schiemann O., Weber A., Edwards T.E., Prisner T.F., Sigurdsson S.T. // *J. Am. Chem. Soc.* 2003. V. 125. P. 3434–3435.
46. Schiemann O., Piton N., Mu Y., Stock G., Engels J.W., Prisner T.F. // *J. Am. Chem. Soc.* 2004. V. 126. P. 5722–5729.
47. Cai Q., Kusnetzow A.K., Hubbell W.L., Haworth I.S., Gacho G.C., Eps N.V., Hideg K., Chambers E.J., Qin P.Z. // *Nucl. Acids Res.* 2006. V. 34. P. 4722–4730.
48. Cai Q., Kusnetzow A.K., Hideg K., Price E.A., Haworth I.S., Qin P.Z. // *Biophys. J.* 2007. V. 93. P. 2110–2117.
49. Sicoli G., Mathis G., Delalande O., Boulard Y., Gasparutto D., Gambarelli S. // *Angew. Chem. Int. Ed.* 2008. V. 47. P. 735–737.
50. Yu H., Mu Y., Nordenskiöld L., Stock G. // *J. Chem. Theory Comput.* 2008. V. 4. P. 1781–1787.
51. Romainczyk O., Endeward B., Prisner T.F., Engels J.W. // *Mol. BioSystems.* 2011. V. 7. P. 1050–1052.
52. Ward R., Keeble D.J., El-Mkami H., Norman D.G. // *ChemBioChem.* 2007. V. 8. P. 1957–1964.
53. Wunnicke D., Ding P., Seela F., Steinhoff H.-J. // *J. Phys. Chem. B.* 2012. V. 116. P. 4118–123.
54. Flaender M., Sicoli G., Aci-Seche S., Reignier T., Maurel V., Saint-Pierre C., Boulard Y., Gambarelli S., Gasparutto D. // *ChemBioChem.* 2011. V. 12. P. 2560–2563.
55. Takeuchi M., Lillis R., Demple B., Takeshita M. // *J. Biol. Chem.* 1994. V. 269. P. 21907–21914.
56. Schiemann O., Cekan P., Margraf D., Prisner T.F., Sigurdsson S.Th. // *Angew. Chem. Int. Ed.* 2009. V. 48. P. 3292–3595.
57. Barhate N., Cekan P., Massey A.P., Sigurdsson S.Th. // *Angew. Chem. Int. Ed. Engl.* 2007. V. 119. P. 2655–2658.
58. Hagerman P.J. // *Annu. Rev. Biophys. Chem.* 1988. V. 17. P. 265–286.
59. Gore J., Bryant Z., Nöllmann M., Le M.U., Cozzarelli N.R., Bustamante C. // *Nature.* 2006. V. 442. P. 836–839.
60. Marko J.F. // *Europhys. Lett.* 1997. V. 38. P. 183–188.
61. Mathew-Fenn R.S., Das R., Harbury P.A. // *Science.* 2008. V. 322. P. 446–449.
62. Marko A., Denysenkov V., Margraf D., Cekan P., Schiemann O., Sigurdsson S.Th., Prisner T.F. // *J. Am. Chem. Soc.* 2011. V. 133. P. 13375–13379.
63. Raitsimring A.M., Gunanathan C., Potapov A., Efemenko I., Martin J.M.L., Milstein D., Goldfarb D. // *J. Am. Chem. Soc.* 2007. V. 129. P. 14138–14139.
64. Potapov A., Song Y., Meade T.J., Goldfarb D., Astashkin A.V., Raitsimring A. // *J. Magn. Res.* 2010. V. 205. P. 38–49.
65. Song Y., Meade T.J., Astashkin A.V., Klein E.L., Enemark J.H., Raitsimring A. // *J. Magn. Res.* 2011. V. 210. P. 59–68.
66. Yang Z., Kise D., Saxena S. // *J. Phys. Chem. B.* 2010. V. 114. P. 6165–6174.
67. Sicoli G., Wachowius F., Bennati M., Höbartner C. // *Angew. Chem. Int. Ed.* 2010. V. 49. P. 6443–6447.
68. Krstić I., Frolow O., Sezer D., Endeward B., Weigand J.E., Suess B., Engels J.W., Prisner T.F. // *J. Am. Chem. Soc.* 2010. V. 132. P. 1454–1455.
69. Wunnicke D., Strohbach D., Weigand J.E., Appel B., Feresin E., Suess B., Müller S., Steinhoff H.-J. // *RNA.* 2011. V. 17. P. 182–188.
70. Krstić I., Hänsel R., Romainczyk O., Engels J.W., Dötsch V., Prisner T.F. // *Angew. Chem. Int. Ed.* 2011. V. 50. P. 5070–5074.
71. Azarkh M., Okle O., Singh V., Seemann I.T., Hartig J.S., Dietrich D.R., Drescher M. // *ChemBioChem.* 2011. V. 12. P. 1992–1995.
72. Kim N.-K., Bowman M.K., DeRose V.J. // *J. Am. Chem. Soc.* 2010. V. 132. P. 8882–8884.
73. Zhang X., Tung C.-S., Sowa G.Z., Hatmal M.M., Haworth I.S., Qin P.Z. // *J. Am. Chem. Soc.* 2012. V. 134. P. 2644–2652.

REVIEWS

74. Singh V., Azarkh M., Exner T.E., Hartig J.S., Drescher M. // *Angew. Chem. Int. Ed.* 2009. V. 48. P. 9728–9730.
75. Wright W.E., Tesmer V.M., Huffman K.E., Levene S.D., Shay J.W. // *Genes Dev.* 1997. V. 11. P. 2801–2809.
76. Freeman A.D.J., Ward R., Mkami H.E., Lilley D.M.J., Norman D.G. // *Biochemistry.* 2011. V. 50. P. 9963–9972.
77. Sicoli G., Mathis G., Aci-Seche S., Saint-Pierre C., Boulard Y., Gasparutto D., Gambarelli S. // *Nucl. Acids Res.* 2009. V. 37. 3165–3176.
78. Kuznetsov N.A., Milov A.D., Koval V.V., Samoiloa R.I., Grishin Yu.A., Knorre D.G., Tsvetkov Yu.D., Fedorova O.S., Dzuba S.A. // *Phys. Chem. Chem. Phys.* 2009. V. 11. P. 6826–6832.
79. Kuznetsov N.A., Milov A.D., Isaev N.P., Vorobjev Yu.N., Koval V.V., Dzuba S.A., Fedorova O.S., Tsvetkov Yu.D. // *Mol. BioSystems.* 2011. V. 7. P. 2670–2680.
80. Banerjee A., Santos W.L., Verdine G.L. // *Science.* 2006. V. 311. P. 1153–1157.
81. Qi Y., Spong M.C., Nam K., Karplus M., Verdine G.L. // *J. Biol. Chem.* 2010. V. 285. P. 1468–1478.
82. Gilboa R., Zharkov D.O., Golan G., Fernandes A.S., Gerchman S.E., Matz E., Kycia J.H., Grollman A.P., Shoham G. // *J. Biol. Chem.* 2002. V. 277. P. 19811–19816.
83. Lacowicz J.R. *Principles of Fluorescence Spectroscopy.* 2nd Ed. New York: Kluwer Academic/Plenum Publishers, 1999.
84. Förster T. // *Ann. Physik.* 1948. V. 437. P. 55–74.
85. Grohmann D., Klose D., Klare J.P., Kay C.W.M., Steinhoff H.-J., Werner F. // *J. Am. Chem. Soc.* 2010. V. 132. P. 5954–5955.
86. Sarver J. L., Townsend J. E., Rajapakse G., Jen-Jacobson L., Saxena S. // *J. Phys. Chem. B.* 2012. V. 116. P. 4024–4033.
87. Ward R., Bowman A., El-Mkami H., Owen-Hughes T., Norman D.G. // *J. Am. Chem. Soc.* 2009. V. 131. P. 1348–1349.

Use of Transgenic Animals in Biotechnology: Prospects and Problems

O. G. Maksimenko¹, A. V. Deykin¹, Yu. M. Khodarovich², P. G. Georgiev^{1*}

¹Institute of Gene Biology of the Russian Academy of Sciences, Vavilov St., 34/5, Moscow, Russia, 119334

²Shemyakin-Ovchinnikov Institute of Bioorganic Chemistry of the Russian Academy of Sciences, Miklucho-Maklai St., 16/10, Moscow, Russia, 117997

*E-mail: georgiev_p@mail.ru

Received 28.06.2012

Copyright © 2013 Park-media, Ltd. This is an open access article distributed under the Creative Commons Attribution License, which permits unrestricted use, distribution, and reproduction in any medium, provided the original work is properly cited.

ABSTRACT During the past two decades, there have been numerous attempts at using animals in order to produce recombinant human proteins and monoclonal antibodies. However, it is only recently that the first two therapeutic agents isolated from the milk of transgenic animals, C1 inhibitor (Ruconest) and antithrombin (ATryn), appeared on the market. This inspires hope that a considerable number of new recombinant proteins created using such technology could become available for practical use in the near future. In this review, the methods applied to produce transgenic animals are described and the advantages and drawbacks related to their use for producing recombinant human proteins and monoclonal antibodies are discussed.

KEYWORDS bioreactor; milk protein production; production of monoclonal antibodies; recombinant proteins; therapeutic drugs; transgenic animals.

ABBREVIATIONS mAb – monoclonal antibodies; MI – intranuclear microinjection of DNA; NT – nuclear transfer; RP – recombinant protein; RHA – recombinant human albumin; rhBChE – recombinant human butyrylcholinesterase; TA – transgenic animal; FDA – United States Food and Drug Administration; EMEA – European Medicines Evaluation Agency; CHO cells – Chinese hamster ovary cells; ES cells – embryonic stem cells; UTR – untranslated region of a gene.

INTRODUCTION

After the successful expression of the first recombinant proteins (RPs) in bacteria and yeast, it became clear that a large number of human RPs could not be efficiently produced using such systems. Thus, human proteins do not undergo post-translational modifications in bacterial cells, and the nature of the modifications in yeast cells is different from those that take place in human cells. Additionally, these expression systems cannot ensure the proper folding of a number of complex human RPs [1, 2]. Therefore, the research community faced the challenge of developing alternative expression systems capable of ensuring correct post-translational modifications in RPs. A simultaneous development of two technological models (based on transgenic animals and mammalian cell cultures) was started as a result.

The first successful production of transgenic mammals by the microinjection of genetically engineered constructs into the pronucleus of a mouse zygote was carried out over 20 years ago [3]. A large number of transgenic animals (TAs) have been produced since for scientific purposes, to improve livestock and to produce RPs [4–9]. Until the end of the past century, TAs

had been considered to be the most promising models for producing human RPs and monoclonal antibodies (mAb). Yet, it was mammalian cell cultures (Chinese hamster ovary cells (CHO) in particular) that played the dominant role in the production of RPs. Thus, 312 therapeutic products obtained using living organisms had been introduced to the U.S. market by 2012 [10]. A total of 193 products were obtained using mammalian cell cultures, and 42 of them were produced using CHO cell cultures. This has been largely attributed to the fact that it was not until 2006 that the European Medicines Evaluation Agency (EMEA) approved antithrombin, the first recombinant protein derived from the milk of transgenic goats [11]. This protein was subsequently approved for commercialization by the United States' Food and Drug Administration (FDA) as a drug that prevents blood clotting in patients with hereditary antithrombin deficiency. In 2011, the EMEA approved the use of the recombinant C1-esterase inhibitor produced in rabbits for the treatment of hereditary angioedema. The arrival on the market of the first therapeutic products produced using TAs and their approval for medical use suggest that RPs could carve out a significant niche in biotechnology in the near future. Some biotechnol-

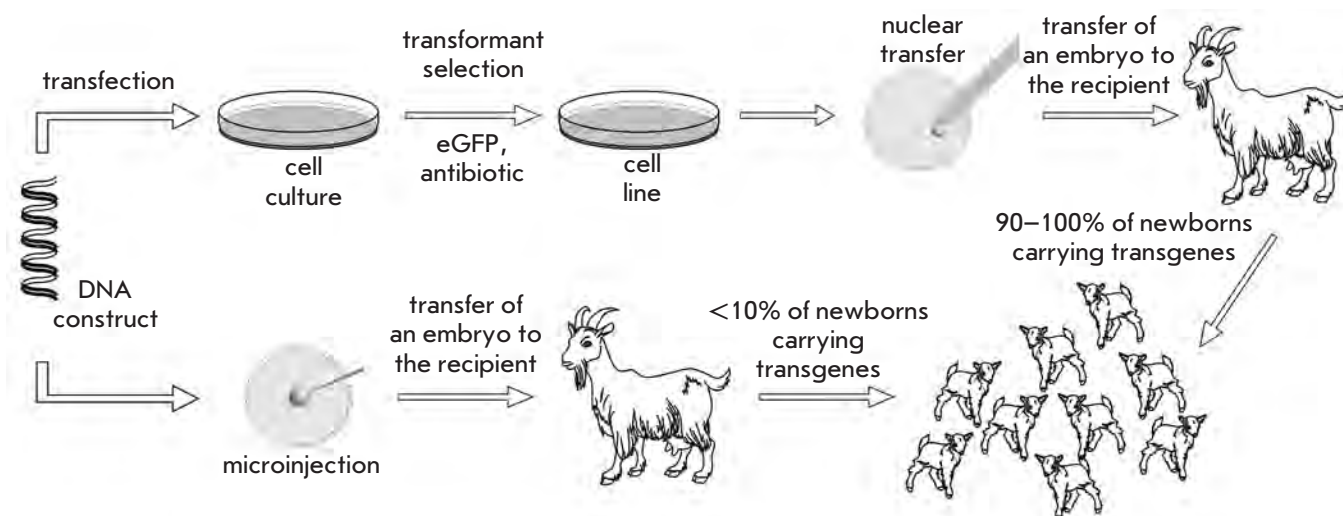


Fig. 1. Scheme for producing transgenic animals using the methods of nuclear transfer (upper panel) and intranuclear microinjection of DNA (lower panel)

ogy companies (PPL Therapeutics (England), GTC Biotherapeutics (USA) (acquired by LFB Biotechnologies, France, in 2010), Hematech (USA), Genzyme (USA), ZymoGenetics (USA), Nexia Biotechnologies (Canada), Pharming (Netherlands), BioProtein Technologies (France), Avigenics (USA), Viragen (USA), and TranX-enoGen (USA)) are actively working on developing this technology. This review discusses the general concepts behind generating TAs for the production of human RPs and mAb.

THE MAIN METHODS USED TO PRODUCE TRANSGENIC ANIMALS

The contemporary methods that allow one to obtain RP-producing livestock that contain the required transgene in all the cells of their organism and pass it on to their offspring include intra-pronuclear zygotic DNA microinjection (MI) and somatic cell nuclear transfer (NT). Today, DNA microinjection into the male pronucleus of a zygote is the most commonly used method [12] (Fig. 1). As it enters the nucleus, linear DNA is capable of integrating into the genome of cell lines or living organisms [13]. DNA is usually integrated into transcriptionally inactive gene-poor regions and into heterochromatin. From one to several or even hundreds of copies of the injected construct can integrate into one genomic site. This technology was initially tested on mice, and it remains a reliable method for the production of TAs. This method was used to produce the first agricultural TAs. However, MI is now used mainly to produce transgenic mice, rabbits and pigs. This is attributed to the insufficient efficiency of the method due

to the low frequency of incorporation of recombinant DNA into the genome and the availability of zygotes at the two pronuclear stages. The result depends on carrying out a large number of surgical procedures, which entails the need to keep a substantial number (200–300 heads) of experimental livestock and perform skilled animal handling. Furthermore, the only way to determine the expression level of the integrated transgene is to examine the original TAs and their offspring. The reproductive cycle in large animals (including the time before they reach physiological maturity and the need to obtain females producing RPs in milk from the original transgenic males) is approximately 0.9/2.3 years for goat females/males, 1.0/2.3 years for pigs, and 2.3/4.5 years for cows. These limitations increase the cost of obtaining the original TAs and the time required to organize the work.

In 1997, a sheep clone was produced by nuclear transfer (NT) of a somatic mammary gland cell into an oocyte [14]. This achievement opened the possibility of developing cheaper and easier procedures for producing agricultural TAs (Fig. 1), since most of the manipulations in this case are moved from a farm to a laboratory, where the transfection of somatic cells is carried out and clones characterized by the integration of the transgene into the genome are selected. The nucleus of the somatic cell is then injected into the enucleated oocyte, which is transplanted into female recipients. Fibroblast cells are typically used for NT. The majority of recently generated large farm animals have been obtained by NT [12]. However, the transfected cells in this case are selected using antibiotic resistance marker

genes, which complicates the approval of the produced recombinant proteins by the FDA and EMEA [15]. Fluorescent proteins, such as the enhanced green fluorescent protein (eGFP), are often used as an additional selective agent in order to increase efficiency in such selection [16]. Systems based on site-specific recombinases are additionally used to remove selection markers from the genome of the selected cell lines [17].

The adverse effects of the NT technique include a low *in utero* embryo survival rate and poor health of the newborn animals [12]. This is attributed, among other things, to incomplete reprogramming of the somatic nucleus, resulting in impaired expression of several of the genes required for the proper progression of embryogenesis. Moreover, the process of obtaining suitable oocytes and their activation requires considerable expenditures of time and financial resources. As a result, one of the world leaders in the use of NT for the production of agricultural TAs, the AgroResearch company (New Zealand), has rejected the method. The company is now developing alternative methods for producing agricultural TAs.

The site-specific transgenesis technology using embryonic stem (ES) cells could be an alternative to the MI and NT methods [18]. This method involves the insertion of a transgene into the genome of ES cells, followed by the selection of clones with a proper integration of the required number of copies, before transgenic ES cells are introduced into the cavity of a blastocyst, which is transplanted into a recipient female. After these cells are transplanted into the ovaries of adult mice, up to 30% of newborn mice can carry the transgene. All animal handling can be performed using nonsurgical methods, which are widely used in animal husbandry. The production of transgenes requires a relatively small number of blastocysts and, hence, a small experimental herd. However, this method has only been perfected for mice and rats; ES cell lines for farm animals have yet to be obtained. A similar approach involves the transformation of stem cells, the precursors of sperm cells, and their subsequent transplantation into seminiferous tubules of infertile males [19].

The other methods for obtaining TAs are relatively rarely used. Thus, TAs can be effectively produced using retroviruses containing the required transgene [12]. In order to achieve this objective, the zygotes lacking protective coating are cultured in a medium supplemented with lentiviral particles, followed by transplantation into female recipients. The integration of one to several copies of the transgene occurs depending on the lentiviral titer; almost 100% of the offspring can be transgenic in this case [12]. The advantages of this method include efficient production of any species of

TAs and the opportunity to produce TAs carrying only one transgene copy, which is sometimes necessary for scientific purposes. The main drawbacks of the method include the inability to use the introns present in the gene construct and the limitation of the transgene length (approximately 8000 bp), which is determined by the size of the viral particle. As a result, it is very difficult to achieve a high level of transgene expression using this method.

A promising method for obtaining TAs is the use of vectors based on mobile genetic elements, which are integrated into the genome by transposase [12]. The gene encoding transposase and the transgene flanked by terminal repeats of transposon are coinjected into the zygote. The reaction catalyzed by transposase results in the integration of a single copy of the transgene into one or several sites of the animal's genome. This approach has been used to produce large farm animals (e.g. pigs [20]). The efficiency of the integration of the transgene in this case depends on the type of transposon, transgene length, concentration and site of DNA injection, and can be as high as 50% [20]. However, no data regarding the levels of expression of the target gene in the TAs produced using this method have been obtained thus far.

The group of methods based on infecting the organs or tissues of an organism with a replication-defective adenovirus containing the gene of the target protein should be specifically mentioned. This approach results in a short-term nonhereditary production of RPs in the organ or tissue under consideration.

Today, it remains difficult to compare the efficiency of new and traditional methods for producing TAs.

THE EXPRESSION VECTORS USED TO OBTAIN TRANSGENIC ANIMALS

The expression vectors used to produce RPs in milk contain regulatory regions of genes whose protein products comprise the major fraction of milk. The most popular examples of the latter include the regulatory regions of the lactoglobulin sheep gene, the acidic protein gene of rodents (mouse, rat) and rabbit, the α -lactalbumin and α -S1-casein genes of cow, and the goat β -casein gene [5]. An expression vector typically includes a long 5'-region (1–7 kb) which consists of a promoter, tissue-specific enhancers that increase the expression in mammary glands, the first non-coding exons and introns located between them (*Fig. 2A*). The first introns of the genes are likely to contain the regulatory elements which can enhance gene transcription. The expression vector also includes the 3'-untranslated region (UTR) of a gene, whose size can vary from 0.5 to 10 kb and even more. The 3'-UTR typically includes the last non-coding exons and introns, a polyadenyla-

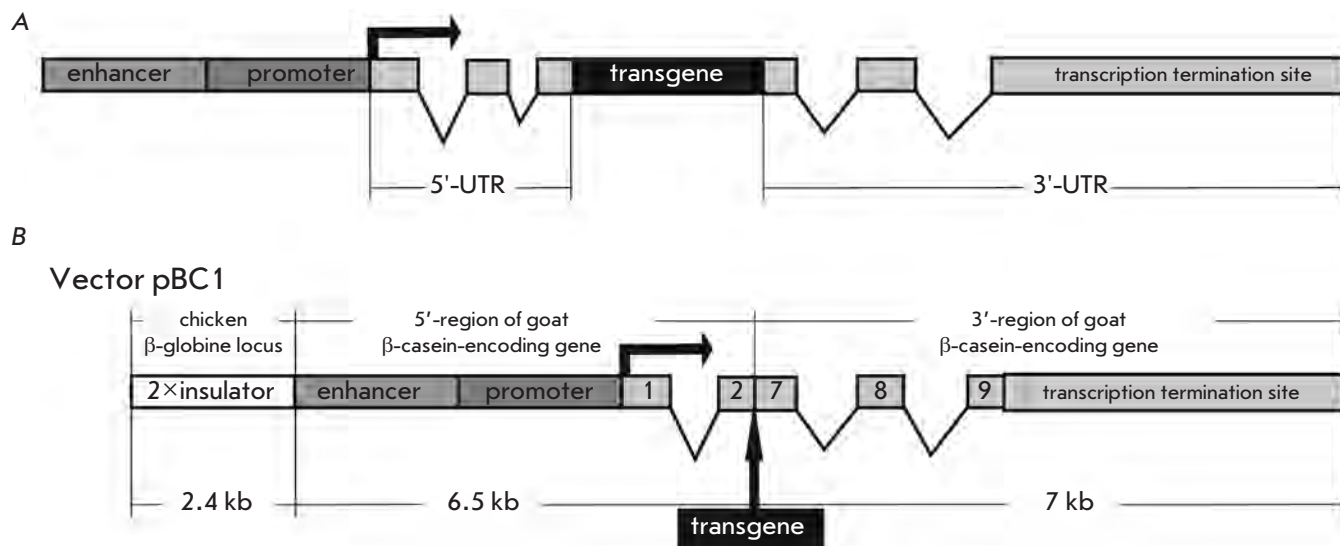


Fig. 2. Vectors used for the production of recombinant proteins. (A) Vector structure used in the production of recombinant proteins in transgenic animals and cell lines. (B) Structure of the pBC1 vector used for the production of recombinant proteins in the milk of transgenic animals

tion site, and the adjacent sequences, which have the potential to enhance transcription termination. The 5'- and 3'-UTRs in a vector may belong to either one or different genes.

Among the promoters used for expression in mammary glands, the β -casein gene promoter is one of the most efficient and is used for the production of target proteins in the mammary glands of mice, goats and cows (Table 1). The most popular commercial vector for the production of RPs in the milk of TAs – pBC1 (Invitrogen) – was produced using the aforementioned promoter (Fig. 2B). This vector allowed one to obtain most of the transgenic goat lines characterized by a high level of target protein production. The regulatory region of the β -casein gene with a length of 6.2 kb and consisting of a promoter and a hormone-dependent enhancer that stimulates the promoter only in the mammary gland cells is used in this vector [31]. The structure of the vector also includes a 7.8-kb-long 3'-region of the β -casein gene, which ensures efficient transcription termination. The latter is required for the formation of a stable mRNA encoding the target protein and for the prevention of the transcription of the adjacent genomic regions capable of causing the formation of repressed chromatin by RNA interference. In order to accumulate the target protein in milk, the coding region of the gene must contain the signal peptide sequence required for secretion. This sequence can be obtained from any gene encoding the secreted protein.

Depending on the aim, either a complete gene with introns or its cDNA or a mini-gene containing only some of the introns is inserted into the vector. The use of a gene with an unmodified exon–intron structure allows one to obtain much higher levels of target protein production in TAs in comparison with the use of cDNA [32, 33]. For instance, the human lactoferrin gene was expressed using the same vector, pBC1, in several independent studies (Fig. 2B). The concentration of recombinant lactoferrin did not exceed 4 mg/ml of mouse milk and 0.7 mg/ml of transgenic goat milk if cDNA was used to produce the TAs (Table 1). Transgenic mice were produced using the native lactoferrin gene with introns (50 kb long). The concentration of recombinant lactoferrin in their milk was as high as 160 mg/ml (Table 1). Transgenic goats carrying one copy of the construct but expressing up to 10 mg/ml of the recombinant human lactoferrin in their milk have also been produced [22]. The difference in the expression of recombinant lactoferrin using the α S1-casein promoter of cows was similar (Table 1). This example demonstrates that the presence of introns in the coding region of the transgene results in a two-fold increase in the amount of the target protein in milk.

The site at which the construct is integrated into the genome plays a crucial role in ensuring efficient transgene expression. Injected DNA is typically incorporated into the gene-poor regions, which are characterized by frequent DNA breaks [13]. The chromatin in these regions typically exerts a negative influence on the

REVIEWS

Table 1. Comparison of production of human milk recombinant proteins (RPs) in transgenic animals (TAs) using various variants of the gene construct

RP/construct	Regulatory elements	TA/method of production	Maximum level of RP production, mg/ml	Reference
Lactoferrin				
Native gene	Bacmid	Cow/NT	3.4	[16]
Native gene	WAP-gene (21 kb) (mouse)	Mouse/MI	30	[21]
–“–	β -casein promoter (goat) + insulator	Mouse/MI	160	[22]
–“–	β -casein promoter (goat) + insulator	Goat/MI	10.8	[22]
–“–	α S1-casein promoter (cow)	Cow/MI	3	[23]
cDNA	β -casein promoter (goat) + insulator	Goat/MI	0.7	[24]
cDNA	α S1-casein promoter (cow)	Mouse/MI	0.036	[25]
–“–	β -casein promoter (goat) + insulator	Mouse/MI	4	[26]
Lysozyme				
cDNA	β -casein promoter (goat) + insulator	Cow/NT	0.026	[17]
–“–	β -casein promoter (goat) + insulator	Pig/NT	0.00032	[27]
–“–	α -S1- casein (cow)	Goat/MI	0.27	[28]
–“–	α -S1- casein (cow)	Mouse/MI	0.00071	[29]
α-Lactalbumin				
Native gene	Bacmid	Cow/NT	1.55	[30]

expression of the transgene integrated nearby. In addition, several copies of the construct are typically integrated onto the same genomic site, which can, in turn, lead to repression of transcription due to the formation of heterochromatin in repetitive sequences.

A number of regulatory elements are used to protect the transgene expression from repression and to maintain the direct relationship between the number of copies and the level of transgene expression in mammalian cell cultures: A/T-rich regions of DNA, which bind to the nuclear matrix fraction (known as MAR/SAR-elements) [34, 35]; regulatory elements (UCOE) that activate the promoters of the “household” genes [36]; STAR-elements that can block the spread of heterochromatin [37]; and insulators [38, 39].

Among the mentioned regulatory elements, only insulators are used in vector constructs to produce TAs. Insulators are the regulatory elements that block the interaction between an enhancer and a promoter, if located between them [40, 41]. Moreover, some insulators can act as a boundary between the transcriptionally active chromatin and heterochromatin. The insulator from a cluster of chicken β -globin genes (HS4 insulator)

is one of the most intensely studied vertebrate insulators. It is 1200 bp long and is located at the 5'-end of the β -globin locus [42]. A 250-bp-long core region characterized by full insulator activity has been found in it. This segment contains the binding site for the CTCF protein, which is the only characterized vertebrate insulator protein [43]. The CTCF protein is responsible for the ability of the HS4 insulator to block enhancers. It also assists the USF1 and USF2 proteins (which form the boundary between active chromatin and heterochromatin) to bind to the insulator [44]. The HS4 insulator sequence also binds to the BGP1/Vezf1 protein [45], which protects the GC-rich sequences of an insulator against methylation, which leads to a disruption of the binding of insulator proteins to DNA and, as a result, to inactivation of the insulator. According to the existing model, BGP1/Vezf1 also terminates the weak transcription initiated in the heterochromatic region, which can play an important role in protecting the β -globin locus against the propagation of inactive chromatin [46]. The pBC1 vector constructed by Invitrogen (USA) for TAs production contains two 1.2-kb-long copies of the HS4 insulator at the 5'-end of the vector (*Fig. 2B*).

A thorough analysis of the effect of the HS4 insulator on the transcriptional activity of several promoters, including the goat β -casein promoter and rabbit WAP-promoter, demonstrated that the insulator significantly increases the level of transgene expression and the number of transgenic lines that are characterized by a significant production of the target protein [22, 47–50]. Meanwhile, the HS4 insulator neither affects the variability of the transgene expression and its ectopic expression in other tissues of the organism nor ensures a direct correlation between the number of transgene copies and its level of expression. Thus, the HS4 insulator acts as a universal transcription regulator that can be used to increase the activity of weak promoters. However, it does not allow to achieve efficient transgene expression exclusively in a mammary gland, which is important for the production of many target proteins that can adversely affect the health of TAs.

Increasing the size of the regulatory sequences in the transgene construction can be an alternative to insulators and other regulatory elements. Multiple loci expressing milk protein genes possess extended 5'- and 3'-regions, which can contain both tissue-specific enhancers and insulators capable of providing protection against the influence of adjacent genes. For instance, a 50-kb-long construct was synthesized in which the coding region (3 kb) of the mouse WAP gene consisting of 24 kb was replaced with a structural part of the human lactoferrin gene (29 kb) [21]. As a result, transgenic mice have been obtained whose mammary glands are characterized by high tissue-specific transgene expression, and the production of recombinant human lactoferrin in their milk was as high as 30 mg/ml (*Table 1*).

Another method for obtaining TAs that efficiently produce target proteins is the integration of large DNA segments (up to 250 kb) into the genome. Vectors based on bacterial artificial chromosomes (bacmids), which enable cloning of sequences up to 400 kb long, can be used to prepare these extended gene constructs [51, 52]. The regulatory regions of tissue-specific genes can occupy large genomic regions and be a part of the neighboring genes. For example, several enhancers that stimulate the pig WAP gene are found 140 kb away from the gene they regulate and are separated from it by the other genes [53]. When large DNA fragments are used, it is highly likely that all of the regulatory elements of this gene are included in the transgene. It is assumed that the use of this approach results in specific transgene expression exclusively in the mammary gland and that the influence of the surrounding chromatin on transgene expression is minimized. This approach allows one to obtain TAs whose level of transgene expression closely corresponds to the expression of the endogenous counterpart. For instance, transgenic

cows expressing the genes of human lactoferrin and human α -lactalbumin have been produced (*Table 1*). In general, this method allows one to achieve stable transgene expression at a level similar to that of native genes. Thus, the levels of production of lactoferrin and alpha-lactalbumin in transgenic cows were 3.4 and 1.55 mg/ml, respectively (*Table 1*). The problem is associated with the other genes, which are a part of the bacmid structure and whose expression can adversely affect the health of the TAs. It should also be mentioned that the use of a bacmid does not completely suppress the effect of the genomic surrounding: the expression is partially dependent on the genome integration site [54, 55]. In this case, there is no direct observable relationship between the number of bacmid copies and the expression level. This can be attributed to the fact that the initiated RNA interference adversely affects the gene expression in a bacmid.

PRODUCTION OF HUMAN RECOMBINANT PROTEINS USING TRANSGENIC ANIMALS

Since the early 1990s, attempts have been made to produce TAs that synthesize a variety of human proteins. Today, these proteins are produced in other expression systems (bacteria, yeast, mammalian cells). Most of the recombinant human proteins that are produced in mammalian cell cultures are plasma proteins [56]. The use of recombinant plasma proteins grows every year as the scope of their application expands and the use of human tissues for isolating native proteins is constrained by the existing risk of viral contamination, the small number of donors, and ethical considerations. The coagulation factors VII, VIII and IX are used for life-long treatment of hereditary diseases. An immune response to therapeutic agents develops in most patients over time, despite the highly efficient purification of the proteins produced in bacterial or yeast systems. This fact creates the need for replacing the drug with an analog produced in a different manner. Therefore, the production of recombinant coagulation factors in the milk of TAs is of significant medical importance [57]. *Table 2* shows some examples of TAs whose milk contains human blood clotting factors. Treatment of blood diseases in most cases requires a comparatively small amount (calculated in grams) of RPs. Consequently, a rabbit is the optimal TA for producing RPs: each transgenic rabbit female can produce approximately 5 liters of milk per lactation or 20 g of RPs per year. The results obtained demonstrate that the expression of coagulation factors does not affect animal health and lactation [74, 75].

Unlike the coagulation factors VII, VIII and IX, the demand for recombinant albumin is calculated in tons, since albumin is used not only in medicine, but also in

Table 2. Examples of the expression of human recombinant proteins (RPs) in the milk of transgenic animals (TAs)

RP (construct)	Regulatory elements	TA/method of production	Maximum level of RP production in milk, mg/ml	Reference
Albumin (native gene)	β -casein promoter (goat) + insulator	Cow/NT	40	[15]
α -fetoprotein (native gene)	β -casein promoter (goat) + insulator	Goat/NT	1.1	[58]
Butyrylcholinesterase (cDNA)	—“—	Goat/NT	5	[59]
Granulocyte colony-stimulating factor (native gene)	—“—	Goat/MI	0.05	[60]
Growth hormone (native gene)	β -casein promoter (goat)	Goat/NT	0.07	[61]
Antithrombin (cDNA)	β -casein promoter (goat)	Goat/MI	2	[62]
Coagulation Factor IX (mini-gene)	—“—	Mouse/MI	0.026	[63]
Tissue plasminogen activator (cDNA)	—“—	Goat/MI	3	[64]
Coagulation Factor IX (cDNA)	β -casein promoter (cow)	Goat/MI	9.5×10^{-5}	[65]
Growth hormone (native gene)	β -casein promoter (cow)	Cow/NT	5	[66]
Granulocyte colony-stimulating factor (native gene)	α -S1- casein promoter (goat)	Mouse/MI	0.04	[67]
Erythropoietin (cDNA)	β -lactoglobulin promoter (cow)	Mouse/rabbit/MI	0.3 (mouse) 0.5 (rabbit)	[68]
Lysostaphin (native gene)	β -lactoglobulin promoter (sheep)	Cow/NT	0.014	[69]
Lysostaphin (cDNA)	β -lactoglobulin promoter (sheep)	Mouse/MI	1.3	[70]
C1-esterase inhibitor (native gene)	WAP-promoter (mouse)	Rabbit/MI	1.8	[71]
Coagulation Factor IX (cDNA)	WAP-promoter (mouse)	Pig/MI	4	[72]
Coagulation Factor VIII (cDNA)	WAP-promoter (mouse)	Rabbit/MI	0.1	[73, 74]

biotechnology to stabilize other proteins. Albumin is the major blood protein, which is usually isolated from plasma. The production of recombinant albumin is more expensive than its isolation from blood plasma, since a very high degree of purification is required for its medical application. Nowadays, recombinant albumin is produced mostly in yeasts *Saccharomyces cerevisiae* (Recombunin™) and *Pichia pastoris* (Albrec™). The huge demand for recombinant albumin has determined the choice of transgenic cows for its production. Thus, GTC Biotherapeutics (USA) has recently created transgenic cows whose average level of recombinant human albumin (rhAB) production in milk is 1–5 mg/ml [15] or up to 30 kg per producing cow per year. The same work described a line of transgenic cows whose RHA concentration in milk was as high as 48 mg/ml, which corresponds to the integration of 250 copies of the con-

struct. Transgenic cows of this line are characterized by a shorter period of lactation and a decrease in the milk yield. Thus, it can be assumed that the production of rhAB in the milk of transgenic cows must be below 48 mg/ml.

Certain proteins, such as hormones and cytokines, have a negative effect on the lactation and health of TAs. This makes maintenance of the transgenic herd problematic. The most notable project undertaken by the PharmAthene Inc. company (USA) on the instructions of the Ministry of Defense is connected with the production of butyrylcholinesterase (Table 2), a highly active enzyme that efficiently protects against organophosphate poisons. As a result, a herd of goats has been produced whose level of production of recombinant human butyrylcholinesterase (rhBChE) in milk is 1–5 mg/ml [59]. The main problem the company en-

countered was the effect of rhBChE on lactation. The latter significantly reduced the productivity of transgenic goats [76]. As a result, a question regarding the economic feasibility of using transgenic goats to obtain rhBChE has arisen.

There are several approaches that allow one to produce RPs that adversely affect lactation and the health of the TAs; however, they only resolve the problem partially. First of all, a promoter that stably functions only in the mammary gland at a relatively low level can be selected. For instance, a recombinant human granulocyte colony stimulating factor (rhG-CSF) was produced using the β -casein gene promoter without an enhancer in transgenic goats (Table 2) [60]. However, the rhG-CSF concentration in the milk of the goats did not exceed 0.05 mg/ml. Transgenic mice with milk containing 0.02–0.04 mg/ml of rhG-CSF have also been produced. An expression vector containing the 5'-regulatory region of the *CSN1S1* gene of a goat (3387 bp), including the first intron and the 3'-region of the *CSN1S1* gene of a cow (1518 bp) with non-coding exons 18 and 19, was also used [67]. As a result, it was demonstrated that transgenic mice carrying this vector express rhG-CSF exclusively in milk, but not in other tissues. However, the low level of RPs in the milk reduces the economic attractiveness of this approach.

An alternative way to produce RPs, which adversely affects the health of the producing TAs, is infection of a mammary gland with replication-defective vectors based on adenoviruses. Thus, an adenoviral vector designed to express recombinant human erythropoietin was produced at the Laboratory of Transgenesis and Animal Cloning (Havana, Cuba). The erythropoietin concentration in the milk of the goats infected with this adenovirus reached 2 mg/ml, but it exhibited a low biological activity, which was presumably due to insufficient glycosylation of the protein produced using this approach [77]. The production of the recombinant human growth hormone in mice (2 mg/ml) and goats (0.3 mg/ml) using adenoviral vectors has been described [78]. A similar approach was used in the case of recombinant human lactoferrin, whose concentration in the milk of goats was as high as 2 mg/ml [79]. Despite the simplicity of using an animal adenoviral vector to create TAs expressing the target protein in milk, this method does not allow one to obtain a stable expression of the recombinant protein at a level sufficient for its commercial production. A high expression level (1.5–2 mg/ml) was observed exclusively during the first 25 days of lactation, which can be explained by either natural death of the transfected cells or the immune response to the infection.

Finally, the production of the inactive forms of proteins is considered to be a promising approach. For in-

stance, an expression vector containing erythropoietin cDNA integrated into the fifth exon of the lactoglobulin gene of a cow [68] in such a manner that there was a region cleavable by IgA-protease between the coding regions of two genes was constructed in order to produce recombinant human erythropoietin. As a result, transgenic mice and rabbits were produced in whose milk the concentration of chimeric protein reached 0.3 and 0.5 mg/ml, respectively. Following the cleavage of the chimeric protein by IgA-protease, the activity of erythropoietin was restored and lactation and the health of the TAs were not affected. It is also possible to use the co-expression of RPs and an inhibitor that blocks its activity. Thus, the recombinant human prourokinase expressed in milk almost immediately transforms into its active form, urokinase, which makes this bioreactor unpromising with respect to the production of a therapeutic form of the protein (prourokinase). Prourokinase was co-expressed with the bacterial serine protease inhibitor in the milk of transgenic mice in order to resolve this problem [80]. This allowed to purify the milk of transgenic mice from the processed prourokinase (urokinase) and to dramatically increase the yield of the therapeutic form of the protein.

It should be mentioned that sialylation of RPs in the milk of transgenic rabbits and pigs is most similar to sialylation in human cells, which is essential for reducing the immunogenicity of the drugs used in long-term therapy [81, 82]. Incorrect post-translational modifications that reduce the activity of the recombinant protein can occur in the milk of transgenic goats and cows. The easiest way to remove the incorrect modification is mutation in the protein site where the undesired modification occurs. For example, alpha-fetoprotein, a single chain glycosylated plasma protein with a molecular weight of 68 kDa, is used to treat autoimmune diseases. The demand for a properly folded recombinant human alpha-fetoprotein (rh-AFP) is extremely high (kilograms of protein are needed); hence, the Merrimack Pharma company (USA), together with GTC Biotherapeutics (USA), have launched a project for the production of transgenic goats that produce rh-AFP in their milk. The human alpha-fetoprotein isolated from the milk of transgenic goats was glycosylated at the asparagine residue located at position 233, which greatly reduced its activity. Therefore, the glutamine residue replaced the asparagine residue in rh-AFP, which caused inactivation of the glycosylation site [58, 83]. It was demonstrated that the biological activity and pharmacokinetics of the mutant variant of alpha-fetoprotein are similar to those of the native protein.

The mAb market is the fastest growing segment of the pharmaceutical industry. Therapeutic mAbs, most of which are used to treat cancer and autoimmune dis-

Table 3. Examples of mAb production in the milk of transgenic animals (TAs)

Antibody binding antigen	Regulatory elements	TA/constructs	Maximum level of antibody production in milk, mg/ml	Reference
CD6-receptor	WAP-promoter (rabbit)	Mouse/two native genes	0.4	[90]
Envelope glycoprotein S (gastroenteritis coronavirus)	WAP-promoter (mouse)	Mouse/two native genes	5	[89]
Envelope glycoprotein S (gastroenteritis virus)	β -lactoglobulin promoter (sheep)	Mouse/two cDNA	6	[91]
BR96 anti-Lewis Y	β -casein promoter (goat)	Mouse/two native genes	14	[86]
BR96 anti-Lewis Y	β -casein promoter (goat)	Mouse/two native genes	4	[86]
CD20-receptor	β -casein promoter (goat) + insulator	—“—	22.3	[92]
Surface antigen (Hepatitis A virus)	β -casein promoter (goat) + insulator	—“—	32	[93]
Surface antigen (Hepatitis B virus)	—“—	—“—	17.8	[94]

eases, generated profit of over \$26 billion for American biotechnological companies in 2007 [84].

The mAbs currently used in medicine are produced exclusively in mammalian cell cultures, since proper post-translational modifications are required to ensure therapeutic efficiency. The most important modifications include the attachment of oligosaccharides and sialic acid, which considerably increase the mAbs bloodstream circulation time and reduce their immunogenicity. However, the RPs produced in cell cultures have a relatively high cost. Hence, an attempt to use TAs to produce antibodies was made at the end of the 1990s [85, 86]. Since mAbs are composed of two polypeptide chains, two constructs containing the genes encoding heavy and light subunits were used for their expression in TAs. When producing TAs, several constructs encoding the heavy and light chains of the antibody are typically incorporated into the same genomic site. During the initial experiments, mAbs were expressed using various gene promoters of milk proteins, e.g., sheep β -lactoglobulin [87] and mouse WAP [88, 89]. Transgenic mice whose milk contains mAbs at relatively high concentrations of 0.4–5 mg/ml have been produced as a result (Table 3). mAbs for pharmaceutical production were subsequently obtained from transgenic goats; mAbs for testing expression vectors, evaluating the quality of mAbs, and refining the methods used for their isolation were obtained from transgenic mice. The pBC1 vector described above has been widely used for the expression of mAbs (Fig. 2B). The highest expression levels of mAbs in transgenic mice (as high as 32 mg/

ml of milk) were obtained using this vector (Table 3). However, published data on the expression level of mAbs in the milk of transgenic goats are virtually absent. Transgenic goats, one of which showed an expression level approaching 14 mg/ml, have been mentioned in only one review [86].

According to the data provided by the GTC Biotherapeutics company (USA), mAbs isolated from the milk of transgenic goats are typically stable and highly efficient; even high levels of mAb expression do not affect the health and lactation of transgenic goats. The company has developed relatively simple methods for obtaining highly purified mAbs that are suitable for medical applications [95, 96]. The conducted investigations led to regarding transgenic goats as the optimal model for the production of mAbs [97]. The attractiveness of transgenic goats is attributed to the fact that they rarely get infected with BSE, in comparison with sheep and cows. Transgenic goats from New Zealand or Australia are currently being used for the production of RPs in milk, since it is officially believed that there is no cow disease in these countries.

The demand for mAbs recently hit the several-hundred-kilograms-per-year mark. For example, world demand for anti-receptor CD20 mAbs exceeds 600 kg per year. It is estimated that a herd consisting of 210 transgenic goats whose milk contains mAbs at a concentration of 8 g/l can fully meet the world demand in anti-CD20 mAbs at an approximate cost of \$100/g [85]. Meanwhile, 51,000 l of cell culture with the capacity of 1g/l and an approximate cost of \$300/g are required to obtain an equal amount of mAbs.

Despite the relatively low cost of mAb production in transgenic goats, there are some drawbacks associated with their use in comparison with the use of mammalian cell cultures. Firstly, the antibodies must be properly glycosylated and sialylated, which is important for their stability, immunogenicity, and biological activity. Sialylation and glycosylation occur in the mammary glands of transgenic goats, but it may be incomplete. In addition, an increase in the level of mAb expression is associated with a decrease in glycosylation efficiency. Therefore, 2–4 mg/ml is considered to be an optimal level of mAbs in milk. The second problem is associated with the fact that sialic acid is present in transgenic goats in the form of N-acetylneuraminic acid (NANA) [98], while human antibodies contain N-glycolylneuraminic acid (NGNA). There is a possibility that antibodies containing the “wrong” sialic acid could be immunogenic to patients in some cases. Recombinant proteins in mammalian cell cultures also undergo heterogeneous glycosylation and sialylation. These processes are usually not completely identical to their native counterparts. In order to overcome this hurdle, additional genes encoding transporters and enzymes, which increase the level of glycosylation and sialylation, and/or genes whose RNA-product induces inactivation of the genes encoding the proteins that adversely affect glycosylation, are introduced into the cell lines producing the recombinant proteins [99, 100]. An opportunity to inactivate the genes involved in the glycosylation of RPs in the cell lines, which is different from glycosylation in human cells, recently became available due to the development of the new technologies of site-directed mutagenesis. Similar approaches cannot be used for producing animals, since the changes in the genome can adversely affect the viability of the TAs. The only potential option is to create TAs using a vector under strict control of expression exclusively in the mammary gland. This vector must express additional genes which increase/modify glycosylation and genes that encode groups of RNA capable of inactivating the genes whose protein products are responsible for the abnormal glycosylation of RPs. Finally, the presence of approximately 0.3–0.5 mg/ml of endogenous immunoglobulins in goat milk poses an additional problem during mAb purification. Therefore, an efficient chromatographic separation of goat and human immunoglobulins is required in order to obtain highly purified mAbs [86]. Meanwhile, the introduction of synthetic media for the cultivation of cell cultures significantly simplifies the stage of recombinant protein purification, which somewhat reduces the cost of obtaining highly purified mAbs.

It has recently been demonstrated that the absence of fucose in the glycol chain of an antibody results in an induction of cytotoxicity at an antibody concentra-

tion ten times lower than in the case when conventional antibodies are used [101]. A model based on transgenic rabbits could be cost-effective for producing these defucosylated antibodies. Interestingly, no fucose residues have been identified in the recombinant human C1-inhibitor isolated from the milk of transgenic rabbits, suggesting the absence of active fucosylation in rabbit mammary glands. Thus, transgenic rabbits can become an attractive model for the production of this new class of highly active antibodies.

A large-scale project to obtain mAbs in TAs was initiated in the late 1990s by Genzyme Transgenic company (currently known as GTC Biotherapeutics), which signed contracts with a large number of companies developing mAbs as therapeutic agents. During the initial stage, mAbs were obtained in transgenic mice in order to assess their overall activity. If the levels of expression and biological activity of mAbs in transgenic mice were comparable to the expected values, goats-producers were created during the second stage. GTC Biotherapeutics is currently developing a technology for the production of several widely used mAbs (Rituximab®, Herceptin®, Humira®, and Erbitux®) in transgenic goats. Work aimed at producing RPs in transgenic goats is being actively conducted in China and New Zealand.

POTENTIAL ROLE OF TRANSGENIC ANIMALS IN AGRICULTURE

At the moment, the FDA is nearing approval for salmon which expresses the growth hormone for commercial use (AquAdvantage) (according to the findings, it is safe for humans and the environment) [11, 102]. The economic impact in the case of transgenic salmon is associated with an almost twofold increase in growth, which significantly reduces the cost of cultivation. Therefore, it can be assumed that in the near future permission for the commercial application of various TAs will be obtained. These TAs can be used to achieve such important objectives as 1) producing modified milk containing human RPs; 2) altering the composition of milk to increase efficiency in dairy products production; 3) improving the characteristics of farm animals (fast growth, recycling); and 4) improving the resistance of farm animals to bacterial, viral, and prion infections [103].

The issues of artificial infant feeding and nutrition of newborns is gaining in importance. In terms of its composition, breast milk is significantly different from goat and cow milk. Thus, human milk contains much higher concentrations of lactoferrin (2.0–5.8 mg/ml), lysozyme (0.03–3 mg/ml), and lactalbumin (1.8–3.1 mg/ml). These proteins protect the organism against infections, improve the structure of the intestinal epithelium, have a positive effect on the intestinal microflora,

and enhance immunity. Meanwhile, the concentration of these proteins is significantly lower in cow milk: 0.03–0.49 mg/ml for lactoferrin, 0.05–0.22 mg/ml for lysozyme, and 1.47 mg/ml for lactalbumin. The mixtures for artificial feeding produced using animal milk do not provide optimal infant nutrition, since they are prepared from hydrolysates and contain no functional proteins.

Transgenic cows expressing recombinant lactoferrin (3.4 mg/ml) [16], lysozyme (0.03 mg/ml) [17] or human lactalbumin (1.5 mg/ml) [33] have been obtained in China to produce modified milk. Milk containing all three human RPs at the optimal concentration is intended for production next. Transgenic goats whose milk contains recombinant human lysozyme at a concentration of 0.27 mg/ml [31] (corresponding to 67% of the lysozyme concentration in breast milk) have been obtained in the USA. It was demonstrated that pasteurized milk with human lysozyme has a positive effect on the health of young goats and pigs [104, 105]. The University of California, Davis (USA), and the Institute of Biomedicine of the Federal University of Ceará (Brazil) received a grant from the Government of Brazil to explore the possibility of using milk containing recombinant human lysozyme to treat diarrhea in children from low-income families. Production of transgenic goats expressing recombinant lactoferrin in milk for the subsequent production of milk simultaneously containing a combination of two human proteins is also scheduled.

The government-owned AgroResearch company in New Zealand produces transgenic cows with the aim of increasing efficiency in cheese production. Caseins, the most valuable proteins, comprise approximately 80% of milk proteins. The casein fraction in cow milk consists of α -S1-, α -S2-, β - and k-caseins, encoded by a single copy of each gene [106]. Caseins aggregate into large micelles. The micellar structure and its stability may vary depending on the ratio of caseins, which affects the physical and chemical properties of the milk. Cheese is made via the aggregation of casein micelles, which retain water and fat by forming a protein network. An increased content of β - and k-caseins leads to a reduction in the micellar size and increases thermal stability, which is necessary for cheese production [107]. In order to increase the amount of β - and k-caseins in milk, transgenic cows with additional copies of the gene were produced [108]. The endogenous β -casein gene of cows with its regulatory sequences was used. Since the k-casein gene is characterized by a relatively low expression level, a chimeric gene containing the regulatory region of the β -casein gene and the coding region of the k-casein was used for the production of transgenic cows. The transgenic cows were eventually produced; their milk was characterized by a 20% increase in the

level of β -casein expression and a twofold increase in k-casein synthesis. This result clearly demonstrates the fact that the milk content can be altered by transgenesis, which can increase efficiency in the multi-billion-dollar cheese production industry.

One of the problems in swine breeding is the high mortality of piglets attributed to the insufficient content of α -lactalbumin in milk. In order to tackle the problem, we produced transgenic pigs with the α -lactalbumin gene of cows inserted into their genome, which resulted in an increase in the lactose concentration in milk [109]. This significantly decreased the mortality rate among the piglets that were fed the modified milk. Another problem in swine breeding is the pollution of the environment with their feces, which contain high levels of phosphorus. This problem was resolved by producing transgenic pigs whose genome contained an inserted phytase-encoding gene of bacterial origin [110]. As a result, the level of phosphates in the feces of the transgenic pigs decreased by 75%.

Resistance to diseases is another extremely important aspect in the application of transgenesis in agriculture. Thus, the losses inflicted by mastitis (inflammation of the mammary gland caused by bacterial infection) in cattle exceed 1.7 billion dollars a year in the USA alone [111]. Mastitis is typically caused by staphylococci. Lysostaphin, a powerful peptidoglycan hydrolase secreted by *Staphylococcus simulans*, exhibits a bactericidal effect against staphylococci, causing mastitis. Transgenic cows [69] whose milk contains lysostaphin at a concentration of 0.014 mg/ml have been obtained. It was demonstrated that such cows are characterized by increased resistance to staphylococcal infections.

Bovine spongiform encephalopathy (BSE, also known as mad cow disease) is the most lethal disease affecting cattle in countries of the Northern Hemisphere. Removal of the prion protein gene that causes the disease was proposed as a way to combat it [112]. As a result, transgenic cows lacking the gene (and, thus, resistant to BSE) have been produced [113]. It is obvious that the use of such cows can reduce the incidence and spread of the disease epidemics.

These examples demonstrate that the use of TAs in agriculture is highly promising. The main restriction to the widespread distribution of TAs is the fear of the wider public regarding the safety of transgenic food products. More stringent regulatory requirements are imposed as a result, making it difficult to obtain permission to use TAs. In 2009 (the current edition from May 17, 2011), after more than 10 years of development, the FDA approved a procedure for considering applications for using TAs [114]. The procedure for the approval of new products is simpler in developing countries, and both the government and the public view TAs as one

of the ways to resolve the problem of food security and improvement of living standards. As a result, most of the projects on the applications of TAs in agriculture are currently being implemented in countries, such as Brazil, Argentina, and China.

CONCLUSIONS

Efficient methods for producing TAs expressing RPs have been developed over the past 20 years. TAs offer opportunities to significantly reduce costs in producing mAb and human RPs with post-translational modifications that closely match those of human proteins.

Until recently, the main reasons behind the reluctance to produce RPs using TAs in developing countries included a lack of developed laws regulating the use of TAs, strict ethical standards, and protests in the public against the use of animals as bioreactors.

However, the situation has begun to change. Detailed regulations to accompany the use of TAs for the production of RPs have been developed. The establishment of two manufacturing productions of RPs in the milk of TAs approved by regulatory agencies in the USA and EU has removed many issues related to the organization of production, while the expiration of patents on many biological preparations has increased competition between manufacturers, forcing companies to search for the most economically efficient technological models of production. Thus, it is very likely that in the near future the use of TAs in the biotechnology and food industries will expand. ●

This work was supported by the federal target contracts № 16.512.12.2007 and № 16.552.11.7067.

REFERENCES

- Demain A.L., Vaishnav P. // *Biotechnology Advances*. 2009. V. 27. P. 297–306.
- Durocher Y., Butler M. // *Curr. Opin. Biotech.* 2009. V. 20. P. 700–707.
- Hammer R.E., Brinster R.L., Rosenfeld M.G., Evans R.M., Mayo K.E. // *Nature*. 1985. V. 315. P. 413–416.
- Dyck M.K., Lacroix D., Pothier F., Sirard M.A. // *Trends Biotechnol.* 2003. V. 21. P. 394–399.
- Echelard Y. // *Curr. Opin. Biotechnol.* 1996. V. 7. P. 536–540.
- Houdebine L.-M. // *Comp. Immunol. Microbiol. Infect. Dis.* 2009. V. 32. P. 107–121.
- Redwan el-R.M. // *J. Immunoassay Immunochem.* 2009. V. 30. P. 262–290.
- Rudolph N.S. // *TIBTECH*. 1999. V. 17. P. 367–374.
- Soler E., Thepot D., Rival-Gervier S., Jolivet G., Houdebine L.-M. // *Reprod. Nutr. Dev.* 2006. V. 46. P. 579–588.
- BIOPHARMA: Biopharmaceutical Products in the US and European Markets. http://biopharma.fmsdb.com/biopharma7.lasso?S=index&DB_test=DD&-nothing
- Vázquez-Salat N., Salter B., Smets G., Houdebine L.-M. // *Biotechnology Advances*. 2012. V. 30. № 6. P. 1336–1343.
- Kues W.A., Niemann H. // *Prev. Vet. Med.* 2011. V. 102. P. 146–156.
- Goldman I.L., Kadullin S.G., Razin S.V. // *Med. Sci. Monit.* 2004. V. 10. P. RA274–285.
- Wilmot I., Schnieke A.E., McWhir J., Kind A.J., Campbell K.H. // *Nature*. 1997. V. 385. P. 810–813.
- Echelard Y., Williams J.L., Destrempe M.M., Koster J.A., Overton S.A., Pollock D.P., Rapiejko K.T., Behboodi E., Masiello N.C., Gavin W.G., et al. // *Transgenic Res.* 2009. V. 18. P. 361–376.
- Yang P., Wang J., Gong G., Sun X., Zhang R., Du Z., Liu Y., Li R., Ding F., Tang B., et al. // *PLoS One*. 2008. V. 3. P. e3453.
- Whyte J.J., Prather R.S. // *Mol. Reprod. Dev.* 2011. V. 78. P. 879–891.
- Zhang Y., Yang Z., Yang Y., Wang S., Shi L., Xie W., Sun K., Zou K., Wang L., Xiong J., et al. // *J. Mol. Cell Biol.* 2011. V. 3. P. 132–141.
- Honaramooz A., Yang Y. // *Vet. Med. Int.* 2010. pii: 657860.
- Garrels W., Mátés L., Holler S., Dalda A., Taylor U., Petersen B., Niemann H., Izsvák Z., Ivics Z., Kues W.A. // *PLoS One*. 2011. V. 6. P. e23573.
- Shi G., Chen H., Wu X., Zhou Y., Liu Z., Zheng T., Huang P. // *Transgenic Res.* 2009. V. 18. P. 573–582.
- Goldman I.L., Georgieva S.G., Gurskiy Ya.G., Krasnov A.N., Deykin A.V., Popov A.N., Ermolkevich T.G., Budzevich A.I., Chernousov A.D., Sadchikova E.R. // *Biochem. Cell Biol.* 2012. V. 90. P. 513–519.
- van Berkel P.H., Welling M.M., Geerts M., van Veen H.A., Ravensbergen B., Salaheddine M., Pauwels E.K., Pieper F., Nuijens J.H., Nibbering P.H. // *Nat. Biotechnol.* 2002. V. 20. P. 484–487.
- Zhang J., Li L., Cai Y., Xu X., Chen J., Wu Y., Yu H., Yu G., Liu S., Zhang A., et al. // *Protein Expression and Purification*. 2008. V. 57. P. 127–135.
- Platenburg G.J., Kootwijk E.P., Kooiman P.M., Woloshuk S.L., Nuijens J.H., Krimpenfort P.J.A., Pieper F.R., de Boer H.A., Strijker R. // *Transgenic Res.* 1994. V. 3. P. 99–108.
- Deykin A.V., Ermolkevich T.G., Gurskiy Ya.G., Krasnov A.N., Georgieva S.G., Kuznetsov S.L., Derevyanko V.G., Novikova N.I., Murashev A.N., Goldman I.L., et al. // *Dokl. Biochem. Biophys.* 2009. V. 427. P. 195–198.
- Tong J., Wei H., Liu X., Hu W., Bi M., Wang Y., Li Q., Li N. // *Transgenic Res.* 2011. V. 20. P. 417–419.
- Maga E.A., Shoemaker C.F., Rowe J.D., BonDurant R.H., Anderson G.B., Murray J.D. // *J. Dairy Sci.* 2006. V. 89. P. 518–524.
- Maga E.A., Anderson G.B., Huang M.C., Murray J.D. // *Transgenic Res.* 1994. V. 3. P. 36–42.
- Wang J., Yang P., Tang B., Sun X., Zhang R., Guo C., Gong G., Liu Y., Li R., Zhang L., et al. // *J. Dairy Sci.* 2008. V. 91. P. 4466–4476.
- Kabotyanski E.B., Rijnkels M., Freeman-Zadrowski C., Buser A.C., Edwards D.P., Rosen J.M. // *J. Biol. Chem.* 2009. V. 284. P. 22815–22824.
- Choi T., Huang M., Gorman C., Jaenisch R. // *Mol. Cell Biol.* 1991. V. 11. P. 3070–3074.
- Whitelaw C.B., Archibald A.L., Harris S., McClenaghan M., Simons J.P., Clark A.J. // *Transgenic Res.* 1991. V. 1. P. 3–13.

34. Girod P.A., Zahn-Zabal M., Mermod N. // *Biotech. Bioeng.* 2005. V. 91. P. 1–11.
35. Girod P.A., Nguyen D.Q., Calabrese D., Puttini S., Grandjean M., Martinet D., Regamey A., Saugy D., Beckmann J.S., Bucher P., et al. // *Nat. Methods.* 2007. V. 4. P. 747–753.
36. Benton T., Chen T., McEntee M., Fox B., King D., Crombie R., Thomas T.C., Bebbington C. // *Cytotechnology.* 2002. V. 38. P. 43–46.
37. Kwaks T.H.J., Barnett P., Hemrika W., Siersma T., Sewalt R.G., Satijn D.P., Brons J.F., van Blokland R., Kwakman P., Kruckeberg A.L., et al. // *Nat. Biotech.* 2003. V. 21. P. 553–558.
38. Kwaks T.H.J., Otte A.P. // *Trends Biotechnol.* 2006. V. 24. P. 137–142.
39. Recillas-Targa F., Valadez-Graham V., Farrell C.M. // *BioEssays.* 2004. V. 26. P. 796–807.
40. Maksimenko O., Chetverina D., Georgiev P. // *Genetika.* 2006. T. 42. C. 845–857.
41. Herold M., Bartkuhn M., Renkawitz R. // *Development.* 2012. V. 139. P. 1045–1057.
42. Chung J.H., Bell A.C., Felsenfeld G. // *Proc. Natl. Acad. Sci. USA.* 1997. V. 94. P. 575–580.
43. Bell A.C., West A.G., Felsenfeld G. // *Cell.* 1999. V. 98. P. 387–396.
44. West A.G., Huang S., Gaszner M., Litt M.D., Felsenfeld G. // *Mol. Cell.* 2004. V. 16. P. 453–463.
45. Dickson J., Gowher H., Strogantsev R., Gaszner M., Hair A., Felsenfeld G., West A.G. // *PLoS Genetics.* 2010. 6:e1000804.
46. Giles K.E., Gowher H., Ghirlando R., Jin C., Felsenfeld G. // *Cold Spring Harbor Symp. Quantitative Biol.* 2010. V. 75. P. 1–7.
47. Giraldo P., Martinez A., Regales L., Lavado A., Garcia-Diaz A., Alonso A., Busturia A., Montoliu L. // *Nucl. Acids. Res.* 2003. V. 31. P. 6290–6305.
48. Giraldo P., Rival-Gervier S., Houdebine L.-M., Montoliu L. // *Transgenic Res.* 2003. V. 12. P. 751–755.
49. Potts W., Tucker D., Wood H., Martin C. // *Biochem. Biophys. Res. Commun.* 2000. V. 273. P. 1015–1018.
50. Rival-Gervier S., Pantano T., Viglietta C., Maeder C., Prince S., Attal J., Jolivet G., Houdebine L.-M. // *Transgenic Res.* 2003. V. 12. P. 723–730.
51. Chandler K.J., Chandler R.L., Broeckelmann E.M., Hou Y., Southard-Smith E.M., Mortlock D.P. // *Mamm. Genome.* 2007. V. 18. P. 693–708.
52. Tong J., Lillico S.G., Bi M.J., Qing T., Liu X.F., Wang Y.Y., Zheng M., Wang M., Dai Y.P., Bruce C., Whitelaw A., Li N. // *Transgenic Res.* 2011. V. 20. P. 933–938.
53. Saidi S., Rival-Gervier S., Daniel-Carlier N., Thépot D., Morgenthaler C., Viglietta C., Prince S., Passet B., Houdebine L.-M., Jolivet G. // *Gene.* 2007. V. 401. P. 97–107.
54. Saux A.L., Houdebine L.-M., Jolivet G. // *Transgenic Res.* 2010. V. 19. P. 923–931.
55. van Keuren M., Gavrilina G., Filipiak W., Zeidler M., Saunders T. // *Transgenic Res.* 2009. V. 18. P. 769–785.
56. Burnouf T. // *Vox. Sanguinis.* 2011. V. 100. P. 68–83.
57. Lubon H. // *Biotechnol. Annu. Rev.* 1998. V. 4. P. 1–54.
58. Parker M.H., Birck-Wilson E., Allard G., Masiello N., Day M., Murphy K.P., Paragas V., Silver S., Moody M.D. // *Protein Expr. Purif.* 2004. V. 38. P. 177–183.
59. Huang Y.J., Huang Y., Baldassarre H., Wang B., Lazaris A., Leduc M., Bilodeau A.S., Bellemare A., Côté M., Herzkovits P., et al. // *Proc. Natl. Acad. Sci. USA.* 2007. V. 104. P. 13603–13608.
60. Ko J.H., Lee C.S., Kim K.H., Pang M.G., Koo J.S., Fang N., Koo D.B., Oh K.B., Youn W.S., Zheng G.D., et al. // *Transgenic Res.* 2000. V. 9. P. 215–222.
61. Lee C.S., Lee D.S., Fang N.Z., Oh K.B., Shin S.T., Lee K.K. // *Reprod. Dev. Biol.* 2006. V. 30. P. 293–299.
62. Edmunds T., van Patten S.M., Pollock J., Hanson E., Bernasconi R., Higgins E., Manavalan P., Ziomek C., Meade H., McPherson J.M., et al. // *Blood.* 1998. V. 91. P. 4561–4571.
63. Yan J.-B., Wang S., Huang W.-Y., Xiao Y.-P., Ren Z.-R., Huang S.-Z., Zeng Y.-T. // *Biochem. Genet.* 2006. V. 44. P. 349–360.
64. Ebert K.M., DiTullio P., Barry C.A., Schindler J.E., Ayres S.L., Smith T.E., Pellerin L.J., Meade H.M., Denman J., Roberts B. // *Biotechnology (N.Y.).* 1994. V. 12. P. 699–702.
65. Huang S., Zhang K., Huang Y., Chen M., Li H., Lu D., Lu J., Chen Y., Qiu X., Xue J., et al. // *Chin. Sci. Bull.* 1998. V. 43. P. 1317–1319.
66. Salamone D., Baranao L., Santos C., Busmann L., Artuso J., Werning C., Prync A., Carbonetto C., Dabsys S., Munar C., et al. // *J. Biotechnol.* 2006. V. 124. P. 469–472.
67. Serova I.A., Dvoryanchikov G.A., Andreeva L.E., Burkov I.A., Dias L.P., Battulin N.R., Smirnov A.V., Serov O.L. // *Transgenic Res.* 2012. V. 21. P. 485–498.
68. Korhonen V.P., Tolvanen M., Hyttinen J.M., Uusi-Oukari M., Sinervirta R., Alhonen L., Jauhiainen M., Jänne O.A., Jänne J. // *Eur. J. Biochem.* 1997. V. 245. P. 482–489.
69. Wall R.J., Powell A.M., Paape M.J., Kerr D.E., Bannerman D.D., Pursel V.G., Wells K.D., Talbot N., Hawk H.W. // *Nat. Biotechnol.* 2005. V. 23. P. 445–451.
70. Kerr D.E., Plaut K., Bramley A.J., Williamson C.M., Lax A.J., Moore K., Wells K.D., Wall R.J. // *Nat. Biotechnol.* 2001. V. 19. P. 66–70.
71. Van Cott K.E., Lubon H., Russell C.G., Butler S.P., Gwazdauska F.C., Knight J., Drohan W.N., Velander W.H. // *Transgenic Res.* 1997. V. 6. P. 203–212.
72. van Cott K.E., Butler S.P., Russell C.G., Subbramanian A., Lubon H., Gwazdauskas F.C., Knight J., Drohan W.N., Velander W.H. // *Biomol. Engineering.* 1999. V. 15. P. 155–160.
73. Chrenek P., Vasicek D., Makarevich A.V., Jurcik R., Suvegova K., Bauer M., Parkanyi V., Rafay J., Batorova A., Paleyanda R.K. // *Transgenic Res.* 2005. V. 14. P. 417–428.
74. Chrenek P., Ryban L., Vetr H., Makarevich A.V., Uhrin P., Paleyanda R.K., Binder B.R. // *Transgenic Res.* 2007. V. 16. P. 353–361.
75. Hiripi L., Makovics F., Halter R., Baranyi M., Paul D., Carnwath J.W., Bosze Z., Niemann H. // *DNA Cell Biol.* 2003. V. 22. P. 41–45.
76. Baldassarre H., Deslauriers J., Neveu N., Bordignon V. // *Transgenic Res.* 2011. V. 20. P. 1265–1272.
77. Toledo J.R., Sánchez O., Seguí R.M., García G., Montañez M., Zamora P.A., Rodríguez M.P., Cremata J.A. // *J. Biotechnol.* 2006. V. 123. P. 225–235.
78. Sanchez O., Toledo J.R., Rodriguez M.P., Castro F.O. // *J. Biotechnol.* 2004. V. 114. P. 89–97.
79. Han Z.S., Li Q.W., Zhang Z.Y., Xiao B., Gao D.W., Wu S.Y., Li J., Zhao H.W., Jiang Z.L., Hu J.H. // *Protein Expr. Purif.* 2007. V. 53. P. 225–231.
80. Gursky Y., Bibilashvili R., Minashkin M., Krasnov A., Deikin A., Ermolkevich T., Popov A., Verbovaya L., Rutkevich N., Shevelev A., et al. // *Transgenic Res.* 2009. V. 18. P. 747–756.
81. Gil G.-C., Velander W.H., van Cott K.E. // *Glycobiology.* 2008. V. 18. P. 526–539.
82. Koles K., van Berkel P.H., Pieper F.R., Nuijens J.H., Manne M.L., Vliegthart J.F., Kamerling J.P. // *Glycobiology.* 2004. V. 14. P. 51–64.

REVIEWS

83. Parkera M.H., Birck-Wilsonb E., Allardb G., Masiello N., Dayb M., Murphya K.P., Paragasa V., Silverb S., Moody M.D. // *Protein Exp. Purif.* 2004. V. 38. P. 177–183.
84. Shukla A.A., Thommes J. // *Trends Biotech.* 2010. V. 28. P. 253–261.
85. Young M.W., Meade H., Curling J.M., Ziomek C.A., Harvey M. // *Res. Immunol.* 1998. V. 149. P. 609–610.
86. Pollock D.P., Kutzko J.P., Birck-Wilson E., Williams J.L., Echelard Y., Meade H.M. // *J. Immunol. Meth.* 1999. V. 231. P. 147–157.
87. Simons J.P., McClenaghan M., Clark A.J. // *Nature.* 1987. V. 328. P. 530–532.
88. Shamay A., Solinas S., Pursel V.G., McKnight R.A., Alexander L., Beattie C., Hennighausen L., Wall R.J. // *J. Anim. Sci.* 1991. V. 69. P. 4552–4562.
89. Castilla J., Pintado B., Sola I., Sanchez-Morgado J.M., Enjuanes L. // *Nat. Biotechnol.* 1998. V. 16. P. 349–354.
90. Limonta J., Pedraza A., Rodriguez A., Freyre F.M., Barral A.M., Castro F.O., Leonart R., Gracia C.A., Gaviolondo J.V., de la Fuente J. // *Immunotechnology.* 1995. V. 1. P. 107–113.
91. Sola I., Castilla J., Pintado B., Sanchez-Morgado J.M., Whitelaw C.B., Clark A.J., Enjuanes L. // *J. Virol.* 1998. V. 72. P. 3762–3772.
92. Tang B., Yu S., Zheng M., Ding F., Zhao R., Zhao J., Dai Y., Li N. // *Transgenic Res.* 2008. V. 17. P. 727–732.
93. Zhang R., Rao M., Li C., Cao J., Meng Q., Zheng M., Wang M., Dai Y., Liang M., Li N. // *Transgenic Res.* 2009. V. 18. P. 445–453.
94. Zhang R., Cui D., Wang H., Li C., Yao X., Zhao Y., Liang M., Li N. // *Transgenic Res.* 2012. DOI 10.1007/s11248-012-9589-z
95. Baruah G.L., Belfort G. // *Biotech. & Bioengineering.* 2004. V. 87. P. 274–285.
96. Baruah G.L., Nayak A., Wenkelman E., Belfort G. // *Biotech. & Bioengineering.* 2005. V. 93. P. 747–754.
97. Houdebine L.-M. // *Curr. Opin. Biotech.* 2002. V. 13. P. 625–629.
98. Raju T.S., Briggs J.B., Borge S.M., Jones A.J. // *Glycobiology.* 2000. V. 10. P. 477–486.
99. Bork K., Horstkorte R., Weidemann W. // *J. Pharm. Sci.* 2009. V. 98. P. 3499–3508.
100. Lim Y., Wong N.S.C., Lee Y.Y., Ku S.C.Y., Wong D.C.F. // *Biotech. Appl. Biochem.* 2010. V. 55. P. 175–189.
101. Shinkawa T., Nakamura K., Yamane N., Shoji-Hosaka E., Kanda Y., Sakurada M., Uchida K., Anazawa H., Satoh M., Yamasaki M., et al. // *J. Biol. Chem.* 2003. V. 278. P. 3466–3473.
102. van Eenennaam A.L., Muir W.M. // *Nat. Biotechnol.* 2011. V. 29. P. 706–710.
103. Murray J.D., Maga E.A. // *Transgenic Res.* 2010. V. 19. P. 357–361.
104. Maga E.A., Cullor J.S., Smith W., Anderson G.B., Murray J.D. // *Foodborne Pathog. Dis.* 2006. V. 3. P. 384–392.
105. Brundige D.R., Maga E.A., Klasing K.C., Murray J.D. // *J. Nutr.* 2008. V. 138. P. 921–926.
106. Karatzas C.N., Turner J.D. // *J. Dairy Sci.* 1997. V. 80. P. 2225–2232.
107. Kang Y., Jimenez-Flores R., Richardson T. // *Basic Life Sci.* 1986. V. 37. P. 95–111.
108. Brophy B., Smolenski G., Wheeler T., Wells D., L’Huillier P., Laible G. // *Nat. Biotechnol.* 2003. V. 21. P. 157–162.
109. Wheeler M.B., Bleck G.T., Donovan S.M. // *Reprod. Suppl.* 2001. V. 58. P. 313–324.
110. Golovan S.P., Meidinger R.G., Ajakaiye A., Cottrill M., Wiederkehr M.Z., Barney D.J., Plante C., Pollard J.W., Fan M.Z., Hayes M.A., et al. // *Nat. Biotechnol.* 2001. V. 19. P. 741–745.
111. Kerr D.E., Wellnitz O. // *J. Anim. Sci.* 2003. V. 81. P. 38–47.
112. Weissmann C., Enari M., Klöhn P.C., Rossi D., Flechsig E. // *Proc. Natl. Acad. Sci. USA.* 2002. V. 99. P. 16378–16383.
113. Richt J.A., Kasinathan P., Hamir A.N., Castilla J., Sathiyaseelan T., Vargas F. // *Nat. Biotechnol.* 2007. V. 25. P. 132–138.
114. 187 Guidance for Industry Regulation of Genetically Engineered Animals Containing Heritable Recombinant DNA Constructs. U.S. Department of Health and Human Services, Food and Drug Administration, Center for Veterinary Medicine (CVM). 2009, 2011.

Sources of Contradictions in the Evaluation of Population Genetic Consequences after the Chernobyl Disaster

V.I. Glazko*, T.T. Glazko

The Ministry of Agriculture of the Russian Federation, Orlikov Pereulok, 1/11, Moscow, Russia, 107139
Russian State Agrarian University – Moscow Timiryazev Agricultural Academy,
Timirjazevskaia Str., 49, Moscow, Russia, 127550

* E-mail: vglazko@yahoo.com

Received 14.08.2012

Copyright © 2013 Park-media, Ltd. This is an open access article distributed under the Creative Commons Attribution License, which permits unrestricted use, distribution, and reproduction in any medium, provided the original work is properly cited.

ABSTRACT The review covers the analysis of our own and published data pertaining to population and genetic consequences in various mammalian species under conditions of high levels of ionizing radiation as a result of the Chernobyl accident. The findings indicate that these conditions have promoted the reproduction of heterozygotes in polyloci spectra of molecular genetic markers and animals with a relatively increased stability of the chromosomal apparatus. The prospects of using the reproductive “success” of the carriers of these characteristics as an integral indicator of the selective influence of environmental stress factors are discussed.

KEYWORDS ionizing radiation; molecular genetic markers; reproductive “success”; cytogenetic anomalies; ecological stress.

INTRODUCTION

It has been 26 years since the largest technogenic catastrophe of the 20th century – the Chernobyl disaster – which highlighted many of the global issues facing industrial and post-industrial societies. From the point of view of a systemic-evolutionary approach, the processes of anthropogenesis and sociogenesis are the results of employing unique strategies of survival pertaining exclusively to *Homo sapiens*, whose core elements include the simultaneous combination of biological, socio-cultural and technological adaptations. The Chernobyl accident revealed the incompatibility of these elements. Technological adaptation being the most mobile of the listed adaptations, it determines the general direction of the history of humankind. Domestication of plants and animals as a condition of the transition to sedentary life characterized the first phase of the formation of the agrarian civilization and, hence, the creation of novel technologies capable of adapting to dynamic environmental factors. Culture itself (including the production culture) must play a major role in the coordination of all three components of the adaptive strategy. The Chernobyl accident and the attitude towards its consequences and the consequences of numerous technogenic accidents and disasters of the 20th century indicate that culture is developing significantly slower than technological process and its biospheric

consequences. The persistent controversies regarding the evaluation of the consequences for the health of the human population not only after the Chernobyl disaster, but also those of the atomic bombings of the cities of Hiroshima and Nagasaki serve as an illustrative example of the latter fact.

Thus far, the consequences of ecological changes for living objects are merely declarative: species on the brink of extinction are counted, their reproductive function is assessed, and changes in communities are evaluated. The inconsistency in the evaluation of the consequences of the Chernobyl accident for biota yet again brings forward an even more global problem; that is a lack of relatively reliable and consistent evaluations of biological safety in human habitats. The urgent need to develop novel approaches for the assessment of biological safety has two reasons: the abrupt increase in the spread of contaminants and the complexity of their composition. The conventional methods for the detection of toxic agents in the air, ground and water do not take into account the constantly emerging novel contaminants and neglect their combined effects, thus requiring an additional analysis of the complex of living organisms which act as a target for toxic agents. It is evident that the selection of indicator species in which population genetic changes can be used as an objective indicator of the

biological safety of the region under surveillance remains among the key issues today.

However, the genetic consequences of genotoxic effects are most commonly considered exclusively from the point of view of the risk of emergence of mutant organisms, i.e., the carriers of constitutional mutations that are present in all the cells of a multicell organism. The frequency of occurrence (especially for carriers of such large-scale genetic defects as cytogenetic anomalies) can be used as an indirect measure of the “sensitive” part of the gene pool which does not participate in the reproduction of the population anymore, since the carriers of constitutive mutations in the populations of higher organisms are typically less fertile than the normal individuals.

The main reasons complicating an objective assessment of the damaging effects of ionizing radiation include the following ones: heterogeneity in the radiosensitivity of the investigated groups of organisms at the level of species, populations, individual organisms, various tissues and organs; volatility of the radiosensitivity of the cells isolated from the same organism during the ontogenesis and under the influence of environmental factors (in particular those increasing or suppressing the activity of various parts of the antioxidant system; the complexity of the mutational spectra and their contribution to somatic pathologies, their connection with the reproductive function abnormalities in the organisms.

In order to assess the genotoxicity of a particular factor or the level of regional contamination, the incidence of gene mutation and the number of chromosomal aberrations are typically determined, along with performing a micronuclear test in the members of various indicator species. Thus, for instance, the cytogenetic characteristics of the bone marrow of small mammals are widely used as a biological test to assess the ecological situation in various regions [1–5]. However, the accumulated data clearly indicate that a widespread individual variability exists with respect to the spontaneous frequencies of cytogenetic anomalies and their alterations in response to the genotoxic impact.

The stability of the chromosomal apparatus is a polygenic trait controlled by a large number of various factors and genes, which are not limited to DNA repair enzymes [6]. Thus, aneuploidy is closely connected with the gene mutations that control the synchronism of centrosome division and stages of mitosis. Synchronism impairment results in multicentric mitosis with subsequent errors in chromosome segregation into daughter cells [7–10]. Chronic or transient abnormalities in the telomeric function, mutations or dysfunctions of the genes encoding telomeric proteins lead to their fusion, which causes significant genomic instability [11, 12]. A

large number of various sources and mechanisms of genomic instability have been identified at the level of nucleotide sequences; their only common trait is the formation of double-strand breaks (DSB) [13]. It should be emphasized that the frequency of the mutations in various genome segments depends on a number of genomic parameters (nucleotide context, replication duration, nucleosome density, histone modifications, chromatin packing, etc.) [14]. This specific feature typically complicates the assessment of genotoxic effects in genetically heterogeneous populations, including human populations.

The problem is further complicated by the fact that the “release” of mutations in somatic cells, the number of mutants in the progeny, is the final phase of a multiphase process. The observed effect of any genotoxic impact depends on several parameters, including 1) the individual sensitivity of a given organism to the factor under investigation (in particular, the activity of the enzymes participating in the biotransformation of xenobiotics and in antioxidant protection systems), 2) the genotypical characteristics of the activity of the enzymes participating in the repair of the induced defects, 3) the enzymes facilitating the detoxification of the toxic agents that enter the cells and are formed during the intracellular metabolism, and 4) the rate of removal of the damaged cells.

The polygenic nature of the listed functions presumably leads to the widespread individual variability in mammalian groups in response to genotoxic impacts of identical intensity.

It should be emphasized that the underdeveloped conceptions related to the multiplicity of targets for the damaging effect of ionizing radiation in the cytoplasm and nucleus, in various DNA segments and to the no less complex ways of formation of these damages in the form of mutations, and to the protection systems of a multicellular organism, which prevent the accumulation of mutant cells, results in the fact that the predicted damaging effects (for humans in particular) are drastically different from empirically collected data.

Taking into account the lack of information regarding the cascades of mutagenesis-related molecular events, the problematic nature of predicting the consequences of an ionizing radiation impact becomes apparent in case this prognosis is based on the assessment of the actual mutational events. The specific features of the mutagenesis of various genomic elements, whose mechanisms, initiation rate, and biological consequences significantly differ from each other, usually are not discussed.

Meanwhile, without changing our views regarding the mechanism of the effect of ionizing radiation on the genetic material of biological objects, it is impossible to

expect that the contradictions between the experimental data and predictions based on simplified conceptions and models of the mutagenic action of ionizing radiation on living objects will be resolved.

Heterogeneity of target sensitivity in living objects. Molecular, cellular, organ, species diversity of the damaging effects of ionizing radiation

One of the reasons behind the existing difficulties is the fact that mutational events also occur at a relatively high frequency due to endogenous events. Thus, the frequency of spontaneous mutations in the structural genes in human cells is 5×10^{-11} per base per round of cell division [15]. The frequency of nucleotide substitutions in genes leading to substitutions in the amino acid sequences in the corresponding protein products is discussed in this case. The diploid genome of higher mammals contains approximately 6×10^9 nucleotides, and roughly 10% of those are found in the coding regions; i.e., this frequency is typical of 6×10^8 genomic nucleotides. Hence, approximately 1×10^{-3} mutations emerge in the coding regions of the structural genes in each genome in each round of replication.

Today the frequency of mutations is determined per nucleotide in the human haploid set (3×10^9 nucleotides) using a comparative analysis of the completely sequenced genomes of parents and two monozygotic twins. The frequency of spontaneous substitutions estimated using this method reaches $\sim 1.1 \times 10^{-8}$ per nucleotide per round of replication [16].

Every second 10^7 cells in a normal human organism undergo division [17]; hence, every second 10^3 new cells containing nucleotide substitutes exclusively in the protein-coding regions are formed. It is important to point out that actual mutations are discussed in this review.

However, these mutations are preceded by DNA lesions at the potential mutation sites, since they can either be easily repaired or become actual mutations. They usually emerge due to hydrolysis, oxidation, or electrophilic influence on DNA molecules. These reactions occur as a result of an exogenous impact, including the impact of ionizing radiation; they can also result from endogenous metabolic processes. The endogenous events cause a large number of various DNA lesions [17]. Thus, for instance, apurine/aprimidine (AP) sites in DNA may occur as a result of spontaneous hydrolysis or DNA-glycosylase-aided excision repair. AP sites are quickly repaired by AP endonuclease, which catalyses the hydrolysis of the 5'-phosphodiester bond with subsequent removal of 3'-phosphate (aided by the lyase activity of DNA polymerase β) [18]. Nakamura and Swenberg [19] determined the number of AP sites in DNA from tissues. They found out that the num-

ber of such sites in the genomes of cells isolated from most human and rodent tissues reaches 50,000–200,000 (i.e. $\sim 10^{-5}$ – 10^{-4} per nucleotide). It is clear that such lesions occur 6–7 orders of magnitude more frequently as compared to the nucleotide substitutions in the structural genes. The typical AP sites induce nucleotide substitutions (typically A→T) or may result in frameshift mutations. These mutations have been found in the microsatellite loci of a plasmid treated with H_2O_2 . The number of AP sites increases when the cells are treated with oxidizing or methylating agents.

It has been known for a relatively long time that the action of oxygen radicals leads to the emergence of a large number of oxidized bases in DNA, as well as to DNA breaks. Base modifications that occur due to the other oxidizing processes are discussed less frequently. Thus, polyunsaturated fatty acids, one of the main components of membrane phospholipids, are characterized by high sensitivity to oxidation and are the main target of oxygen radicals [18]. During the oxidation of polyunsaturated fatty acids, bifunctional electrophilic groups capable of interacting with DNA bases are synthesized, giving rise to exocyclic compounds. These modified bases carrying the exocyclic groups disrupt the double-stranded DNA and are considered to be potentially highly mutagenic.

Exocyclic ethylene groups (denoted by ϵ : ϵA , ϵC and $N^2,3-\epsilon G$) have been identified in the DNA isolated from various human tissues; their level increases with an increase in the concentration of oxygen radicals. $N^2,3-\epsilon G$ can be found in rodent tissues subjected to oxidizing stress. The amounts of ϵA , ϵC are increased in patients with Wilson's disease and the diseases associated with accumulation of copper and iron in the liver [20]. The rate of oxidation of unsaturated fatty acids increases during the accumulation of metal ions. The level of ethylene groups is also increased in DNA isolated from the polyps of patients suffering from familial adenomatous polyposis, and, interestingly, in the DNA of leucocytes isolated from the blood of women whose food contains large amounts of unsaturated fatty acids; this effect is absent in males [20].

The amounts of ϵA , ϵC increase during the promotion stage of a tumor in a two-stage mouse skin carcinogenesis model [21]. The treatment of a tumor promoter using phorbol ester (tetradecanoylforbol-13-acetate) has resulted in a 9- to 12-fold increase in ϵA and ϵC , respectively. The increase in the amount of DNA lesions correlates with the induction of fatty acid oxygenase (8-lipoxygenase).

Special attention has recently been brought to bear on the C → T transitions in CpG-islets, since these mutations are commonly found in organisms affected by cancer and in a number of other pathologies. Cytosine

methylation is considered to be an important factor in the occurrence of such transitions.

The rearrangements in large DNA segments may underlie the occurrence of chromosomal translocations, resulting in particular in a loss of heterozygosity, which is very commonly observed in tumor cells. The chromosomal alterations begin with breaks in both DNA strands, which are induced by oxidative stress or enzymatic cleavage during chromatin reorganization (e.g., DNA topoisomerase II). Approximately 10 double-strand DNA breaks per cell cycle in the form of blocked replication forks occur during DNA replication [22]. It is evident that the factors giving rise to double-strand breaks and the methods to repair them significantly contribute to the processes of endogenous mutagenesis.

Studies of animals with various knock-outs of the genes encoding the enzymes used to repair double-strand breaks have demonstrated the significance of these modifications for the occurrence of mutational events at the nucleotide and chromosome levels.

It is obvious that the high frequency of spontaneous mutational events leads to the fact that mutagenic effects are attributed not to the occurrence of the lesions but to the activity of their repair (e.g., those in radiation-resistant species known as *Deinococcus radiodurans*, which are capable of withstanding 5000 Gy [23]).

The investigation into the mechanisms of spontaneous lesions in the genetic material (each of which can be converted into a mutation with an unpredictable effect for the cell, its clonal progeny, and the multicellular organism in general) indicates that these events are multistage by their nature. Supplementing this cascade with ionizing radiation will be an additional factor increasing the probability of conversion of potential DNA lesions into mutations.

The next level of control of the genetic stability in a multicellular organism, which prevents the accumulation of mutant cell clones, is based on the various options of cell death available to genetically deficient cells, as well as the participation of immune system cells in the elimination of mutant clones [24]. It is obvious that during this stage the ionizing radiation can have a dual effect: it can increase the portion of dying mutant cells and reduce the rate at which they are eliminated by suppressing the effector cells of the immune system.

The reproduction of mutant cell clones of the germinative line and the emergence of mutant progeny are controlled by a cascade of events, each of which can be modified by ionizing radiation.

It is interesting to point out that embryonic preimplantation mortality is increased and embryonic fission is slowed down *in vitro* in CC57W/Mv mice under

the influence of absorbed ionizing radiation at a dose of 0.4–0.5 Gy (with respect to the control) as was confirmed in our experiments [25]. It should be emphasized that the preimplantation embryonic losses in mammals are difficult to control, and they manifest themselves through a decrease in the fertility of the population.

The analysis of the events of mutagenesis at the gene, cell and organism levels demonstrate that the characteristics of its alterations under the influence of low-dose ionizing radiation depend on many factors, which are connected both with genetically determined processes and with the modifying effect of the environmental factors. The complexity of the interactions between the genetic and environmental components prevents the examination of individual characteristics of mutagenesis as an integral indicator of the effect of low doses of ionizing radiation on multicellular organisms. A decrease in population fertility seems to be the most objective indicator.

Conceptions of the radiation doses capable of causing damage to living objects

Significant amounts of experimental observations of the consequences of increasing the level of ionizing radiation in various species, including the human one, have been accumulated. The most commonly used methods for assessing the health consequences of increased levels of ionizing radiation are as follows: determining the growth in the incidence of oncological diseases; the frequency of occurrence of dividing cells (generally in the peripheral blood) containing lesions in the genetic apparatus; and the proportion of children born with congenital anomalies [26]. Today an increase in the incidence of thyroid cancer remains the only indicator of worsening of population health as a result of the Chernobyl accident that generates no disputes [26]. The features of the data regarding the cytogenetic anomalies in somatic cells include high individual variability of the characteristics of chromosomal apparatus destabilization and a lack of clearly defined linear relationships between the degree of karyotype destabilization and radionuclide contamination of the habitat [27] and the amount of cesium isotopes in an organism [28, 29].

Laboratory and field studies have demonstrated that an increase in the level of ionizing radiation in a number of cases (even in the low-dose range, up to 20–30 mGy) is accompanied by an increase in the frequency of individual species characterized by an increased proportion of somatic cells with various mutations [27, 29]. Meanwhile, after the bombing of the cities of Hiroshima and Nagasaki, it is generally considered that an increase in the frequency of cancer due to the increased level of ionizing radiation can be definitively traced only if the

absorbed dose exceeds 100 mSv/year. The data accumulated following the Chernobyl accident indicate that even significantly lower doses can be damaging; this fact requires the theory of damaging doses to be reconsidered [30]. The explicit contradiction between the observation of the effects at the levels of cell populations and individual species and the statistical analyses of average populations can be due to a number of reasons. It is of significant importance to elucidate these reasons in order to develop objective techniques to predict the damaging effects of low-dose ionizing radiation and to search for integral indicators of this effect.

Leukemia was the first oncological disease whose incidence was connected to the consequences of the atomic bombings in Hiroshima and Nagasaki. The maximum incidence was observed 5 years after the bombings. Ten years later, an increase in the growth of solid tumors was recorded. Chronic lymphocytic leukemia, pancreatic and prostate cancer, and endometrial cancer were the most frequently identified types. Even 55 years after the atomic bombings, 40% of the people initially included in the Atomic-bomb Survivor Research Program are still alive; this fact makes it possible to assess the long-term consequences of the exposure. It was determined that the relative risk of developing various conditions per dose unit is higher among survivors of the bombings than among those who were subjected to medical radiation exposure. The risk of developing a disease among employees of atomic stations and miners is on average comparable to that observed among some population groups which survived the atomic bombings. The risk of somatic conditions among those who were subjected to primary exposure of identical doses decreases with increasing age at which the exposure occurred. The frequency of various conditions of respiratory, gastrointestinal, and vascular systems is increased among survivors of the atomic bombings [31, 32].

The connection between the doses absorbed by the embryos and the incidence of leukemia in children was analyzed in England, Scotland, Greece, Germany, and Belarus following the Chernobyl accident. The total doses absorbed by the embryos varied from 0.02 mSv in England to 0.06 mSv in Germany, 0.2 mSv in Greece and 2 mSv in Belarus. A statistically significant increase in the risk of developing leukemia in newborns was identified at the peak of the exposure, between July 1, 1986, and December 31, 1987, as compared with children born between January 1, 1980, and December 31, 1985, and between January 01, 1988, and December 31, 1990. In certain countries, the risk increases non-monotonously with respect to the dose absorbed: it increases abruptly at low doses, followed by a decrease at high doses. The findings have been discussed in connection with the mechanisms of embryo/cell death at

high doses and dose-dependent induction of DNA repair. The accumulated results show the need for reconsidering our views on the absorbed doses that could be harmful to embryos [33]. In children who received high doses of ionizing radiation in the period between 0 and 5 years after birth, an increase in leukemia incidence was also observed, which correlated with the absorbed doses (over 10 mGy) [34]. Nonetheless it is important to emphasize that the relationship between cancer development and various factors exerting influence simultaneously (especially for leukemia), the difficulties of diagnosing and classification, as well as treatment success, hinder the assessment of the contribution of radionuclide contamination following the Chernobyl accident to the dynamics of oncopathology and early mortality in European countries [35].

Meanwhile, there are data available that indicate that the incidence of congenital developmental anomalies among children born to fathers who participated in the cleanup effort after the Chernobyl accident exceeds the average frequency recorded in the Russian Federation [36]. An increase in the incidence of congenital developmental anomalies in children born in the regions with high levels of radionuclide contamination following the Chernobyl accident was revealed by the analysis of the Belarus National registry of congenital anomalies for the period of 1983–1999 performed by G.I. Lazyuk *et al.* [37].

It was demonstrated that high and low doses of ionizing radiation have a nonthreshold effect on the cardiovascular system. At least two mechanisms are involved in the formation of these effects: the impact on the formation of macrophage-enriched atherosclerotic plaques due to inflammation processes on the vessel wall and a decrease in the cardiac muscle blood supply as a result. The manifestation of the pathology of the cardiovascular system following the irradiation exhibits a large lag-phase, especially after exposure to a low dose [38].

It was discovered that the number of boys born in Bavaria and Denmark in 1987 after the Chernobyl Nuclear Power Plant accident was higher than that of girls [39]. The mortality rate among newborns increased considerably in 1987–1988 [40].

Young people who received doses of ionizing radiation *in utero* had considerably lower IQ scores as compared to those in the control group of the same age. The differences were limited to the verbal IQ score; the nonverbal IQ score was not affected. These effects were not identified in the group of people who were exposed to radiation after 16 weeks of prenatal development [41].

The incidence of cytogenetic anomalies in cells isolated from the peripheral blood and bone marrow at

Table 1. The frequency of micronuclei occurrence per 1,000 erythrocytes (EMN) isolated from the peripheral blood of CC57W/Mv mice of various ages from the Chernobyl and Kiev populations during different seasons

Season	EMN, control, ‰		EMN, Chernobyl, ‰	
	2.5–3.5 months	14–16 months	2.5–3.5 months	14–16 months
Winter 1993	2.5 ± 0.7	2.7 ± 0.9	10.0 ± 1.0	4.0 ± 1.0
Summer 1994	3.0 ± 0.8	3.2 ± 0.7	6.5 ± 1.0	3.8 ± 0.3

various laboratory and wild-type small murine rodents that reproduced in the alienation zone of the Chernobyl Nuclear Power Plant (CNPP) was determined. This zone is a unique system model to study the population genetic transformations caused by a change in the direction and intensity of natural selection. An abrupt change in the entire complex of ecological factors occurred on a limited territory following the accident. Representatives of various taxonomic groups, including higher mammals, dwell successfully in spite of these changes. It is important to emphasize that the main culprit in the ecological catastrophe (the emission of radionuclides) has been well established. It should be highlighted that it is impossible to simulate the action of interdependent and interrelated changes in various conditions of population reproduction under the influence even of a single environmental stress factor in a laboratory (e.g., an increase in radionuclide contamination), whereas it is typically impossible to analyze the inheritance of induced changes in generations of families under field conditions.

In order to evaluate the possible direction of population genetic changes under the influence of an increase in ionizing radiation in the alienation zone of the CNPP, with allowance for the genetic heterogeneity of bioindicator species in field conditions, a comparative analysis of long-term changes in generations of genetically homogenous laboratory CC57W/Mv mice and in species of field voles captured between 1994 and 2001 in the alienation zone of the CNPP in locations with various levels of radionuclide contamination was carried out in the present study. The cytogenetic variability in generations of the genetically homogenous population was analyzed using two populations of CC57W/Mv mice bred at the Institute of Molecular Biology and Genetics of the National Academy of Sciences of Ukraine: the Chernobyl group (a specialized vivarium located in a 10-km radius from the CNPP) and the control group (a vivarium in Kiev). These populations were kindly provided by S.S. Malyuta, an academician of the National Academy of Sciences of Ukraine. The bone marrow cells isolated from mice of first and second generations of the Kiev population (K-1, K-2) and the first, second, fifth, seventh, and tenth generations of the Chernobyl population (Ch-1, Ch-2, Ch-5, Ch-7 and Ch-10) repro-

ducing in the specialized vivarium at a rated dose of absorbed radiation of approximately 0.6 Gy per animal were analyzed.

The mutational spectra were determined in representatives of the field vole species (*Microtus arvalis* and *Clethrionomys glareolus*) captured in the alienation zone of the CNPP at locations with low levels of radionuclide contamination (< 5 Cu/km²), which were considered spontaneous (conditional control) under conditions of an intermediate level of radionuclide contamination (~200 Cu/km² – Yanov, rated dose of absorbed radiation of approximately 0.6–0.8 Gy/year) and with high levels (500–1000 Cu/km², Glubokoe lake, Chistogalovka, “Red Forest,” rated dose of absorbed radiation of approximately 0.9–1.1 Gy/year).

The following cytogenetic characteristics were taken into consideration in the animal bone marrow cells: two types of aneuploidy, polyploidy, the frequency of occurrence of metaphases with chromosomal aberrations (CA), centric fusions known as Robertsonian translocations (RB) and asynchronous separation of chromosomal centromeric regions at the end of the metaphase (ASCR). The percentage of aneuploid cells was determined in two different variants: the cells with a loss or gain of the chromosome number, more than one (general aneuploidy, A1) and aneuploid cells with a number of chromosomes $2n \pm 1$ (A2). The numbers of binuclear leukocytes (BL) and leukocytes with micronuclei (LM) were determined in cells with an intact cytoplasm using the same preparations. The mitotic index (MI) and the frequency of occurrence of BL and LM were determined per 1,000 cells.

A significant increase in the frequency of cytogenetic anomalies was identified in the mutational spectra of the Chernobyl population of CC57W/Mv mice (in particular, the metaphases with chromosomal aberrations: $0.9 \pm 0.2\%$ in the control group and $6.0 \pm 2.0\%$ in the test group). Meanwhile, the responses to identical levels of increased ionizing radiation were different to the statistically significant level in groups of linear mice of various ages (Table 1, 2) and in generations of the experimental population (Table 3).

The data in Table 1 show that the frequencies of occurrence of erythrocytes with micronuclei in the con-

REVIEWS

Table 2. The frequencies of cell deletions and cytogenetic anomalies in "young" and "old" CC57W/Mv mice from the control (Kiev) and the Chernobyl groups

Mice group	Age, months	MI, ‰	BL, ‰	LM, ‰
Mice from the "Young" control group (Kiev)	2–3	6.8 ± 0.5***	4.5 ± 0.7	5.2 ± 0.3**
Mice from the "Young" experimental group (Chernobyl)	2–3	5.6 ± 0.7	9.0 ± 1.4*	14.4 ± 2.4**
Mice from the "Old" control group (Kiev)	12–18	3.5 ± 0.6***	7.1 ± 1.3	10.5 ± 1.3*
Mice from the "Old" test group (Chernobyl)	12–18	7.0 ± 1.0*	5.0 ± 0.8*	6.0 ± 0.8*

* $P < 0.05$, ** $P < 0.01$, *** $P < 0.001$.

Note. Here and in Tables 3 and 4, MI is the number of metaphases per 1,000 cells; BL is the number of binuclear leucocytes per 1,000 cells; LM is the number of mononuclear leucocytes with micronuclei per 1,000 cells.

Table 3. The variability of cytogenetic characteristics in CC57W/Mv mice in generations (Ch-1, Ch-2, Ch-5, Ch-7, Ch-10) reproducing under conditions of the specialized vivarium of the CNPP as compared with the control populations of K-1 and K-2 (average values)

Population	Aneuploid cells, %		Polyploid cells, %	The frequency of metaphase occurrence, %			Number per 1000 cells, ‰		
	A1	A2		PC	RB	CA	ASCR	MI	BL
K-1	23 ± 1	10 ± 1	8 ± 1	10 ± 1	0.9 ± 0.4	0.7 ± 0.3	6.0 ± 0.7	6.0 ± 0.6	6.0 ± 0.7
K-2	27 ± 5	10 ± 1	4 ± 1	9 ± 3	2.0 ± 0.1	2.0 ± 1.0	7.0 ± 0.6	5.0 ± 0.5	5.0 ± 0.4
Ch-1	30 ± 2	12 ± 1	4 ± 2	11 ± 3	6.0 ± 2.0	5.0 ± 1.0	7.0 ± 1.0	10.0 ± 1.5	14.0 ± 2.0
Ch-2	28 ± 3	5 ± 3	9 ± 2	8 ± 2	6.0 ± 3.0	7.0 ± 1.0	7.0 ± 1.0	5.0 ± 0.9	6.0 ± 1.0
Ch-5	34 ± 5	5 ± 1	4 ± 1	3 ± 1	0.5 ± 0.2	1.0 ± 1.0	8.0 ± 1.0	7.0 ± 0.4	6.0 ± 0.4
Ch-7	35 ± 2	7 ± 1	2 ± 1	8 ± 1	4.0 ± 1.0	4.0 ± 1.0	7.0 ± 0.7	8.0 ± 1.0	5.0 ± 2.0
Ch-10	20 ± 2	3 ± 1	3 ± 1	1.0 ± 0.2	4.5 ± 1.0	2.5 ± 0.4	6.0 ± 0.7	7.0 ± 1.0	5.0 ± 0.4

Note. Here and in Table 4, A1 is general aneuploidy, A2 is aneuploidy $2n \pm 1$ chromosome; PC is the fraction of polyploid cells; RB is the fraction of cells with centric fusion of chromosomes (Robertsonian translocations); CA is the frequency of occurrence of metaphases with chromosomal aberrations; ASCR is the proportion of cells with asynchronous separation of the centromeric regions of the chromosomes at the end of the metaphase.

control groups of "young" and "old" animals determined in different seasons show no statistically significant differences. However, this figure was significantly higher in the Chernobyl "young" animals than that in the control population and in the "old" animals. The results of these experiments (Table 1) gave grounds to assume that the age-related changes are accompanied by a decrease in erythroblast sensitivity to damaging effects. It can be also expected that in this case the processes of physiological adaptation in "old" animals as compared to the "young" group are connected to the long-lasting action of chronic low-dose exposure to radiation. It was determined that this physiological adaptation was accompanied by an increase in the number of dividing cells and a certain acceleration of the cell cycle, if the determination is based on the number of binuclear

leukocytes per round of mitosis in bone marrow cells isolated from the groups of the "old" control and the Chernobyl animals (Table 2).

The analysis of the incidence of cytogenetic anomalies in the bone marrow cells of the "young" CC57W/Mv mice in the sequential generations (Ch-1, Ch-2, Ch-5, Ch-7, Ch-10) reproducing under conditions of chronic exposure to increased levels of ionizing radiation allowed to identify a nonlinearity of the changes in a number of cytogenetic characteristics in generations of genetically homogenous animals (Table 3). It turned out that the incidence of such cytogenetic characteristics as RB, CA, and ASCR, which are directly connected with intra-chromosomal aberrations, decreases in the 5th generation, increases in the 7th generation, and decreases again in the 10th generation. A similar pattern of

REVIEWS

Table 4. The incidence of various cytogenetic anomalies in the bone marrow cells of bank vole species captured at locations characterized by different levels of radionuclide contamination

The frequency of occurrence of metaphases, %						The number per 1,000 bone marrow cells, ‰		
A1	A2	RB	PP	ASCR	CA	MI	BL	LM
Control								
33.7 ± 6	9.0 ± 3.5	14.0 ± 3.5	0.5 ± 0.5	6.2 ± 3.6	1.2 ± 0.7	3.2 ± 0.6	3.5 ± 0.6	5.5 ± 1.5
Total: Janov for the period between 1997 and 1999								
31.2 ± 2.4	8.9 ± 3.7	13.9 ± 6.0	6.9 ± 5.6	10.1 ± 4.1	8.1 ± 4.0	5.7 ± 1.0	5.2 ± 0.8	3.2 ± 0.8
“Red Forest” 1999								
34.6 ± 6.2	10.5 ± 3.0	22.6 ± 3.6	1.2 ± 0.7	9.6 ± 1.3	3.5 ± 0.8	5.2 ± 1.2	3.7 ± 1.1	6.5 ± 0.7
“Red Forest” 2001								
35.2 ± 2.8	6.3 ± 1.1	12.9 ± 3.1	0.5 ± 0.4	11.8 ± 2.8	0.9 ± 0.3	8.0 ± 2.5	9.8 ± 1.7	8.0 ± 1.2

Table 5. The incidence of various cytogenetic anomalies in the bone marrow cells of common vole species captured at locations characterized by different levels of radionuclide contamination

The frequency of occurrence of the metaphases, %						Per 1,000 mononuclear lymphocytes, ‰		
A1	A2	RB	PP	ASCR	CA	MI	BL	LM
Control								
44.4 ± 5.1	8.6 ± 0.8	0.9 ± 0.5	1.0 ± 0.5	2.5 ± 0.6	16.5 ± 4.9	4.5 ± 0.9	5.0 ± 0.8	3.0 ± 0.4
2001, Chistogalovka, Glubokoe lake, ~500 Cu/km ²								
26.5 ± 2.7	3.1 ± 0.8	1.8 ± 0.4	0.3 ± 0.3	2.5 ± 0.3	17.6 ± 4.1	6.1 ± 0.6	7.8 ± 1.6	3.1 ± 0.5

variability in the generations was identified for a fraction of the second type of aneuploid cells ($2n = 40 \pm 1$ chromosome). The incidence of other types of cytogenetic anomalies was higher only in the first generation of Chernobyl mice as compared to that in the control populations (Table 3).

The nonlinear variability in generations of genetically homogenous mice, which was determined from the frequency of occurrence of cells with intrachromosomal deficiencies, may be an indication that the intensity of the aberrations caused by a prolonged action of ionizing radiation in a low-dose range is comparable to the activity of damage repair processes, elimination of damaged cells, and the rate of division of undamaged substituting cell clones. A multitude of factors controlling the mechanisms of physiological adaptation to ionizing radiation in animals, the comparability of the intensity of the action of multidirectional factors may result in a sequential increase and decrease in the incidence of the cytogenetic anomalies that occur in the presence of a relatively constant level of a damaging agent in genetically homogenous animals.

An analysis of genetically heterogeneous populations of field voles captured in various years at locations with various levels of radionuclide contamination allowed to obtain data supporting the fact that the selection for radioresistant animals became clearly evident in 1999 and 2001 among populations of bank voles and common vole which inhabit regions characterized by high levels of radionuclide contamination (Tables 4 and 5).

Thus, the bank vole populations captured in 1999 and 2001 at locations with the highest level of radionuclide contamination mainly contained animals whose bone marrow cells were characterized by an incidence of cytogenetic anomalies that not only was higher than that in the conditional control population, but was sometimes lower with respect to certain characteristics (Table 4). It was determined that an increase in the number of radioresistant species among the bank voles was most prominently evident in the “Red Forest” population (1000 Cu/km²). This selection was not observed at the locations characterized by a significantly lower level of radionuclide contamination (Janov, ~200 Cu/km²).

Similar data were obtained when studying common vole populations (*Table 5*).

Thus, the accumulation of hypothetically radioresistant species in generations of genetically homogenous laboratory mice and a decrease in the incidence of certain types of cytogenetic anomalies at a lower rate than that normally observed in the control populations were revealed in the genetically heterogeneous populations of two types of field vole species captured at locations characterized by high levels of radionuclide contamination.

It seems that the sources of these nonlinear responses to ionizing radiation in the low-dose range can be numerous, can occur at different phases of the ionizing radiation exposure, and at different levels of organization of multicellular organisms. Thus, a complex cascade of biochemical events can be initiated due to the induction of free-radical processes in cells by ionizing radiation [42]. The accumulation of free radicals results in the activation of antioxidant enzymes that limit the free radical processes (they include superoxide dismutase, catalase, glutathione peroxidase, and glutathione reductase [43]). The activation of these enzymes can be tissue- and organelle-specific. For instance, the change in the antioxidant activity in mitochondria was found to be directly connected with the stability of the chromosomal cellular apparatus. Characteristic “radial” markers (Robertsonian translocations, dicentrics, and circular chromosomes) occur in the bone marrow cells of mice lacking functional mitochondrial superoxide dismutase [44]. An increase in the radioresistance of human chromosomes with an increase in the telomerase activity [45] and its decrease due to damage to chromatin proteins, which prevents the occurrence of double-strand breaks in DNA during mutation, have been described [46]. The existence of a “substrate” induction of DNA repair processes was demonstrated: it was discovered that a large number of double-strand breaks in DNA occurring following the irradiation of human fibroblasts at a dose of 2 Gy are repaired much more rapidly as compared to the numerous breaks that occur after irradiation at a dose of 200 mGy [47]. It can also be expected that some contribution to the nonlinear responses of multicellular organisms to the same dose of ionizing radiation can also be made by intracellular interactions, such as changes in the ratio between highly specialized to poorly differentiated cell populations. The ratio between the effector cells of the immune system, which differ from each other in terms of their radiosensitivity, as well as the presence of the antigen structures recognized by killer cells on the surface of the plasma membrane of the damaged cells, can contribute to this response in mammals [48].

Thus, the findings suggest that the incidence of certain types of cytogenic anomalies in generations of ge-

netically homogenous and genetically heterogeneous populations of small murine rodents undergo nonlinear changes under prolonged exposure to low doses of ionizing radiation. It can be surmised that this nonlinearity is due to the multiplicity and multidirectionality of the radiation-induced repair processes existing at the cellular and subcellular levels, as well as to the action of the exogenous factor that is comparable to the former in terms of the intensity of the damaging effect. The nonlinearity of the effects hypothetically disappears only when the intensity of the damaging action of ionizing radiation significantly exceeds the capabilities of the multifactor mechanisms of adaptation.

It was discovered in our experiments using three different strains of laboratory mice (the Chernobyl population – mice from a specialized vivarium in the 10-km zone of influence of the CNPP; the control group – mice from the vivarium in Kiev) that each strain under control conditions has its own spectrum of spontaneous mutations in bone marrow cells, and that only certain characteristics of this spectrum varied with animal age and the season during which the research was carried out [49]. Thus, an increase in aneuploidy (chromosome loss) with an increase in age and during the transition to the summer season was typical of the C57BL/6 mice. In the CC57W/Mv mice, the age and the seasonal changes were mainly associated with intrachromosomal defects (chromosomal aberrations), and in BALB/c mice they were associated with the percentage of polyploid cells. Under conditions of an increased level of ionizing radiation in the specialized vivarium near the CNPP (absorbed doses of approximately 0.5–0.6 Gy/year), an increased incidence was observed only for those anomalies that were characterized by spontaneous instability under control conditions. For instance, an increased frequency of the occurrence of aneuploid cells was observed in the C57BL/6 strain, and an increased frequency of metaphases with chromosomal aberrations was observed in CC57W/Mv mice. Thus, an increase in the doses of ionizing radiation in this case did not result in the development of new characteristics in the mutational spectra of mice but caused an increase in the spontaneous instability of the individual strain-specific characteristics of these spectra.

The same tendency was revealed for the voles captured in the areas with elevated levels of radionuclide contamination. Only cytogenetic abnormalities, whose increased variability is species-specific for voles dwelling in unpolluted areas, accumulate in bone marrow cells: metaphases with Robertsonian interchromosomal fusions for the bank voles and aneuploidy for the common voles. The data obtained suggest that elevated levels of ionizing radiation (within the investigated range) increase the incidence of cytogenetic anomalies in labo-

ratory strains of mice and in voles, which are characterized by high strain- and species-specific variability (in mice) under control conditions. The analysis of these mutational spectra is further complicated by the fact that individual chromosomes of the experimental animals exhibit a pronounced predisposition to a particular type of cytogenetic abnormalities.

A comparative analysis of the incidence of various chromosomal breaks in blood cells extracted from 14- to 15-year-old children was carried out. One group consisted of children who received ionizing radiation at a dose of approximately 30 mSv during their prenatal development; the second group consisted of children who received approximately the same dose, but in the course of their entire lives as they lived in the contaminated areas (approximately 1.5 mSv/year) [50, 51]. The frequencies of occurrence of cells with cytogenetic abnormalities were found to be almost identical in these two groups of children; however, the first group (acute exposure during the prenatal period) was characterized by a statistically significant increase in the number of cells with stable chromosomal abnormalities, such as translocations, inversions, and insertions. These data indicate that cell clones with the aforementioned anomalies are accumulated in the blood of children. Since a certain parallelism between the frequency of mutational events in populations of somatic and generative cells has been identified along with the fact that these types of cytogenetic abnormalities can significantly complicate the progression of meiosis it can be expected that the children who were exposed to ionizing radiation in the prenatal period of their lives will face reproductive problems [50, 51].

It is interesting to mention that the tendency towards increasing sensitivity to ionizing radiation with an increase in the complexity of an organism has been established a long time ago; i.e., the more ancient the species the more resistant it is to ionizing radiation. The mean half-lethal dose of radiation is approximately 4–6 Gy for mammals; it reaches 30 Gy for colibacillus (*Escherichia coli*). The absolute record holder in this respect is the bacterium *D. radiodurans*, whose individual cells survive and retain their reproductive capacity after being exposed to 5000 Gy [23]. It was discovered that immediately after irradiation with a dose of 3000 Gy, nearly all the genomic DNA of this organism decomposes into small fragments; a single double-strand break was on average induced per 27-kb-long DNA segment, and 3 h after the exposure the genome initiates the recovery process without any significant accumulation of mutations in the structural genes. A species-specific ability to restore the genomic integrity rather than a unique stability of the genetic material to ionizing radiation is observed in this case. It was found

that the ability of this species to repair DNA damage is associated with drought-resistance genes, the mutations in which lead to the disappearance of this unique radiation stability of the species.

It is believed that the improvement in the accuracy (“resolution”) of the genetic methods for assessing chromosomal aberrations at low-dose exposures will ensure a more accurate determination of the relationship between low-dose radiations and induced mutational events. This assumption was supported by the data pertaining to the occurrence of new mutations in highly polymorphic DNA sequences in children born to irradiated parents [52, 53]. However, the study by Veynber *et al.* [52], in which RAPD-PCR (Random Amplification of Polymorphic DNA) markers but not ISSR-PCR (Inter Simple Sequence Repeats) markers were used, provided data on the occurrence of new mutations in children born to those who participated in the cleanup effort after Chernobyl. Dubrova *et al.* [53] revealed an increased frequency of mutations in three of the eight investigated minisatellite loci in children whose parents lived in areas with high radionuclide contamination. In other words, the results of the analysis of the mutational events induced by low-dose exposure were dependent on the type of DNA markers used (RAPD-PCR, but not ISSR-PCR) and the investigated loci. Hence it follows that no unambiguous data on the genetic effects of low-dose ionizing radiation, which would be independent of the analysis technique and the variability features of an individual loci, can be obtained using the available methods for detecting mutational events directly in the DNA.

Attempts to assess the genetic consequences of the action of ecotoxic factors have been made for an appreciably long period; two main trends can be distinguished in this development. One consists in searching for the molecular genetic systems associated with detoxification and antioxidant enzymes; the second one is the population genetic investigation of the dynamics of allelic variants in the genetic systems associated with resistance to these factors.

The biomarkers of xenobiotic metabolism are usually subdivided into genes whose products are involved in the metabolic activation of promutagens (procarcinogens) with the occurrence of short-lived, highly toxic derivatives (in particular, cytochrome P450 genes) and genes whose products control their detoxification (e.g., glutathione-S-transferase and N-acetyltransferase). The direct link between the genetically determined polymorphism of these enzymes and the induction of cytogenetic abnormalities by a number of xenobiotics, reproductive function disorders, and the development of certain types of tumors in humans has recently been discovered using PCR [54–56].

The second area is being investigated less successfully. It is based on research into the changes in the structure of the populations that are subjected to environmental stress. The distribution of allelic variants and the genotypes of the structural genes and anonymous (in terms of their function), highly polymorphic DNA, whose involvement in the formation of sensitivity to genotoxic agents has not been established, are being investigated.

Associations have been discovered between human resistance to ionizing radiation and the occurrence of certain genotypes, mainly with respect to the transferrin and haptoglobin loci [57,58]. Japanese researchers have also described an increased frequency of certain genotypes with respect to the MHC genes in “Hibakusha” long-livers (survivors of the atomic bombings of the cities of Nagasaki and Hiroshima), which is presumably associated with a particular state of the immune system. The latter contributes to an increased resistance to a number of common diseases [59].

Success in searching for the biomarkers of resistance to genotoxic effects largely depends on the quality and adequacy of the models used to study the population genetic consequences of various types of environmental stress.

It is obvious that the depth, direction, and characteristics of the population genetic consequences of environmental stress factors can only be assessed for a series of generations of organisms living under the influence of these factors.

The identification of the genes and gene ensembles whose inheritance is preferable and is associated with the selection for resistance to new environmental conditions may result in the development of the so-called individual “genetic passports” of resistance to physical and chemical environmental pollution. These data enable to control the population genetic structure of the species and facilitate its transformation in the desired direction.

The basic data obtained during our investigations were thoroughly described in the monograph [49] and performed on different types of mammals using genetic biochemical, molecular genetics, and cytogenetic methods.

A shift in the spectra of organ-specific isoenzymes occurs in a number of farm animal species under the influence of elevated levels of ionizing radiation (an absorbed dose of 0.6–0.8 Gy/year), mostly in kidney and heart tissues. The heart tissue starts to express a number of isoenzymes, which are typically found in the poorer specialized muscle tissue. No significant increase in the number of individuals with constitutive mutations has been identified during population-based studies of various mammal species. The following ob-

servations have been made with respect to generations of cattle that received absorbed doses of approximately 0.8 Gy/year (^{137}Cs): a) reduced fertility and increased mortality in newborn calves; b) disruption of the equiprobable inheritance of individual allelic variants – elimination of some and preferable inheritance of the other allelic variants; c) displacement of the genetic structure of the parent generation typical of dairy cattle towards less specialized forms; d) changes in the genetic structure that coincided with the population genetic effects of such biotic and abiotic stress factors as the selection for resistance to bovine leukemia infection and introduction into new reproduction conditions. Therefore, the findings suggest that the main response to a prolonged exposure to low-dose ionizing radiation consists not in the induction of the emergence of new genes but in the preferential selection of new gene combinations in the generations. Hence, this concept is consistent with the principles of the evolution theory elaborated by I.I. Schmalhausen [60]: a variation of the selection criteria leads to the preferential reproduction of the least specialized species, as observed in generations of cattle under the influence of various environmental stress factors.

Conventional biochemical and molecular genetic markers were used to investigate the features of the genetic structure of animal groups, which allowed to analyze a number of polymorphisms in a number of loci encoding plasma proteins. Furthermore, markers of the intron sequence of the leptin gene and the exon 4 of the k-casein gene and DNA fragments flanked by microsatellite loci (ISSR-PCR markers) were also employed. The informative nature of utilizing additional characteristics of the genetic structure of the species was also assessed: an analysis of the patterns of inter-loci gene associations was carried out [61]. The investigated loci were parts of various linkage groups [62]. Two groups of syntenic genes (the transferrin and ceruloplasmin genes – chromosome 1; vitamin D receptor, k-casein, and hemoglobin – chromosome 6) and four non-syntenic genes (amylase 1 gene – chromosome 3, leptin – chromosome 4, purine nucleoside phosphorylase – chromosome 10, and post-transferrin 2 – chromosome 19) were investigated.

The following data were obtained during the investigation of the genetic structure of a number of generations of cattle bred under conditions of high radionuclide contamination in the alienation zone of the CNPP. Only one animal with a mutation in the locus encoding transferrin was identified in the second generation. Disruption of the equiprobable transfer of the allelic variants from parent to offspring was detected in certain loci; changes in the results of the assessment of disequilibrium with respect to the linkage in a number

of loci were also recorded. It was demonstrated that, regardless of consanguineous mating under conditions of increased radionuclide contamination, the heterozygosity in the generations did not decrease.

Therefore, the occurrence of population genetic changes in animals under conditions of environmental stress was initially established using this model, and these changes were shown to be directed towards the preferential reproduction of heterozygotes with respect to the structural genes and “anonymous” DNA segments (ISSR-PCR markers).

Next, we compared the population genetic consequences of elevated levels of ionizing radiation and the influence of the other biotic and abiotic environmental stress factors on the genetic structure, which was evaluated using a variety of molecular genetic markers, inbreeding groups of different breeds of cattle. The following mechanisms of the influence of environmental factors were considered. The analysis of the Red Steppe breed included two groups of animals that differed in terms of their resistance to the influence of a biotic stress factor (infected and uninfected with the bovine leukemia virus) – from farms in the Kherson region, which was relatively unaffected by technogeneous pollution; and from farms in Kirovograd and Donetsk, which were characterized by elevated levels of chemical contamination (an abiotic factor). Three groups of animals belonging to the Pinzgau breed were examined in connection with their reproduction in the plains, mountains, and under high-altitude conditions (an abiotic factor). The gray Ukrainian breed was represented by two groups of animals: those from the Kherson region (the original habitat) and from the Altai region and Siberia (new conditions – an abiotic factor). In the Holstein breed, the effect of the abiotic factor was determined by comparing the genetic structure of two groups, one of which reproduced at farms in the relatively uncontaminated Kherson region and the other (experimental herd) reproduced on the “Novoshepeli-chi” farm located in the alienation zone of the CNPP (radionuclide contamination being approximately 200 Cu/km², an abiotic factor). The population genetic studies were conducted using a variety of markers, including electrophoretic variants of proteins, restriction site polymorphism, and ISSR-PCR markers.

It was determined that the influence of environmental stress factors can result in a significant genetic differentiation in animal groups, which in some cases was higher than the interbreed differences. Two genes encoding the vitamin D receptor and apurine-nucleoside phosphorylase have been identified. Obvious differences in the frequencies of the alleles of the latter genes have been found in groups of cattle of the same breed living under various environmental stress conditions

(chemical pollution, introduction into new reproduction conditions, and infection with the bovine leukemia virus). This suggests the existence of universal characteristics of the population genetic response of cattle to the influence of various environmental stress factors [63].

An analysis of the reproductive characteristics of experimental herds of cattle can reveal the mechanisms behind the changes in the genetic structure which occur in the descendants of parents exposed to ecotoxic factors and deletions of a number of alleles and genotypes associated with increased sensitivity. Thus, the experimental herd exposed to high levels of ionizing radiation (absorbed dose of 0.8–1.1 Gy/year) included the parental generation (F0) consisting of three cows (Alpha, Beta, Gamma) and a bull named Uranus captured in 1987 near the CNPP and of 13 cows imported between 1990 and 1993 to the “Novoshepeli-chi” farm (Pripyat) from relatively uncontaminated areas. The F0 generation of cows (a total of 16) from the experimental herd born in the uncontaminated area gave birth to a total of 96 calves (0.93 ± 0.03 calves per cow per year), 20 of which (21%) did not survive 3 months after birth. The first generation (F1) born on the experimental “Novoshepeli-chi” farm was significantly different from the parent generation with respect to this figure. Thus, 21 cows of the 36 cows from the F1 generation were sterile (58%), and only 15 of them yielded offspring (F2 generation, 0.73 ± 0.06); 13 calves died before reaching three months of age (26%). Four cows from the F2 generation gave birth only to 10 calves (F3) in 2–4 years, i.e. 0.94 ± 0.06 calves per cow per year. It should be mentioned that most of the calves from the F1 generation, which did not survive, were bulls (six heifers and 14 calves); the sex ratio amongst 13 dead calves from the F2 generation was approximately the same (seven heifers and six bulls).

Therefore, the changes in the genetic structure of the offspring received from parents exposed to the influence of ecotoxic factors can be attributed to a decrease in fertility and an increase in infant mortality (carriers of the allelic variants associated with increased sensitivity to a given factor).

CONSEQUENCES OF LIVING IN RADIOACTIVE AREAS ON HUMAN HEALTH

There are many “radioactive” areas located in different parts of the earth; various population genetic characteristics of the populations inhabiting them have been identified in some of them. Thus, extensive studies of the populations living in areas characterized by a highly radioactive background were conducted (Kerala state in India, Guangdong province in China), where the exposure of the population to radiation ranges from 0.6 to 10 cGy per year. No increase in the number of human con-

genital diseases was revealed during these investigations [64, 65]. The screening of over 40,000 pregnant women living in areas with a high radioactive background in Brazil demonstrated no increase in the incidence of spontaneous abortions and congenital anomalies, although the incidence of chromosomal aberrations in blood cells isolated from the local population was slightly higher than that in the control areas [66].

Ramsar County in Iran is best known for its annual absorbed dose of 260 mSv; the global average dose is equal to 3.5 mSv/year. The residents of Ramsar County are not characterized by elevated rates of mortality or birth of children with congenital developmental abnormalities.

Meanwhile, distinctive differences in the radioresistance of blood cells isolated from the local population living in this area are observed, in contrast to residents of areas characterized by a low natural radioactive background. Thus, the exposure of the cell cultures of peripheral blood isolated from the inhabitants of Ramsar County to a dose of 1.5 Gy resulted in a significantly smaller increase in the number of cells with cytogenetic anomalies as compared to the blood cells of the control group [67].

The published results of studies of populations living in “radioactive” areas suggest that the selection process for increased radioresistance occurs in these locations from generation to generation. Thus, 125,079 residents of the “radioactive” province were examined in China during the period between 1979 and 1995; 10,415 deaths and 1,003 cancer cases have been analyzed. It was found that the cancer mortality rate in the “radioactive” province was lower than that among residents of the control area [68]. In another study, the authors concluded that a 3- to 5-fold increase in the level of ionizing radiation did not increase the risk of oncological pathologies [69].

No significant differences in the incidence of congenital defects have been identified among newborns (26,151) from the “radioactive” province in India (approximately 35.0 mSv/year) and among newborns (10,654) in the control group [70]. Screening of the inhabitants of another “radioactive” province (over 70 mSv/year) in India (a total of 400,000 people, 100,000 of those lived in the “radioactive” part of the province) showed no differences in the incidence of oncological pathologies due to a high level of external γ -radiation [71].

Annual detection of oncological conditions per 100,000 people in the populations inhabiting Indian regions, which vary from each other by only 0.03 mSv/year with respect to the external radiation exposure proportionately decreases from one area to another one simultaneously with an increase in the background

level of ionizing radiation by 0.03 mSv/year – from the hypothetical incidence of oncological conditions being equal to 79 : 100,000 people, under conditions of “zero” level of external exposure. The authors arrived at conclusion that an increase in ionizing radiation decreases the risk of developing cancer [72].

It should be emphasized that among the 116,000 people evacuated from the Chernobyl zone, only approximately 5% of them received a dose of ionizing radiation exceeding 100 mSv/year, and this very dose (almost 3 times lower than that in Ramsar County) is considered to be the limit exceeding which leads to an increase in the incidence of oncological conditions [73].

Thus, the actual danger is not the received dose of ionizing radiation but its “novelty” to this particular population, species, or species community. It is obvious that an annual increase in the absorbed dose by 3.5mSv will not result in any health consequences among the residents of Ramsar County, but for most European populations whose previous generations have not been exposed to doses exceeding 1 mSv/year such an increase can lead to the elimination of radiosensitive species from the gene pool, thus resulting in a change in the genetic structure of the populations.

Hence, there is a wide range of doses of ionizing radiation within the natural conditions, which are compatible with the ability of various organisms (including humans) to survive and reproduce. This complicates the evaluation of the biological (including genotoxic) effects of low-dose ionizing radiation.

POPULATION GENETIC CONSEQUENCES OF CHRONIC LOW-DOSE EXPOSURE TO IONIZING RADIATION IN VARIOUS SPECIES OF MAMMALS: LABORATORY MICE STRAINS, FIELD VOLES, CATTLE

Our own experimental data suggest that a chronic exposure to elevated levels of ionizing radiation causes no increase in the number of mutant individuals among the investigated species. An increased frequency of somatic cells with cytogenetic anomalies was not accompanied by qualitative changes in comparison to the spontaneous mutational spectra, since the increase was only observed for the indicators of the instability of the chromosomal apparatus that possessed genotypic features in the strains of mice and field vole species.

A comparative analysis of the mutational spectra in field voles conducted in different years showed that the number of individuals of different species with a high frequency of mutant cells in the bone marrow decreased gradually over time despite the persistence of high levels of radioactive contamination at the capture locations. The frequency of occurrence of individual species with high levels of cytogenetic anomalies among the common voles and bank voles was signifi-

cantly higher in 1996 than that in the relatively "uncontaminated" areas, and in animals captured at the same locations but during the later years, in 1999 and 2001. Thus, metaphases with chromosomal aberrations in the common voles were observed in the control group at a frequency of $2.5 \pm 1.5\%$, and in Chistogalovka at a frequency of $3.6 \pm 0.8\%$, $5.0 \pm 2.3\%$, and $2.5 \pm 0.3\%$ in 1996, 1999, and 2001, respectively. These metaphases were encountered in the bank vole species of the control group at a frequency of $1.2 \pm 0.7\%$; in the «Red Forest» in 1996, 1999, and 2001 at a frequency of $7.3 \pm 3.4\%$, $3.5 \pm 0.8\%$, and $0.9 \pm 0.3\%$, respectively.

It is important to emphasize that this decrease indicating the gradual accumulation of radioresistant species among the bank vole species was only observed in the animals captured in the "Red Forest" area, which was characterized by a very high level of radionuclide contamination ($> 1000 \text{ Cu/km}^2$), in contrast to the animals inhabiting the areas with lower levels of radionuclide contamination (Janov, $\sim 200 \text{ Cu/km}^2$). Thus, the rate of selection for radioresistance is higher when the level of radionuclide contamination is higher. It is noteworthy that even in the areas of the alienation zone characterized by a high level of radionuclide contamination (i.e. "Red Forest"), an accumulation of radioresistant species was detected only in 1999; i.e., 13 years after the Chernobyl accident, after 26 generations of voles (voles breed twice a year).

It is interesting to mention that similar data on the selection of the individuals resistant to adverse environmental conditions were obtained by us for various agricultural species reproducing under conditions of the biosphere reserve (Lake Khovsgol, Mongolia) and in the area of risk-associated livestock farming in the southern part of the Gobi Desert. [74] A comparative analysis of the frequency of occurrence of erythrocytes with micronuclei in the blood samples of local Mongolian cattle, sheep, and yaks reproducing under various ecological and geographical conditions was performed: northwestern Mongolia, Khovsgol region, biosphere reserve; southern Mongolia, the area adjacent to the Gobi Desert – a zone of risk-associated livestock farming. The number of erythrocytes containing micronuclei were determined in a smear of 3,000 cells and the value was expressed in parts per million (‰). The frequencies of occurrence of erythrocytes containing micronuclei were similar across various species reproducing under the same environmental conditions, but significantly differed in animals from different ecological and geographical regions. Thus, the frequencies of occurrence of red blood cells containing micronuclei were significantly higher in the area of the biosphere reserve under favorable conditions of reproduction than those in animals of the same species in the risk-associated

livestock farming zone. The frequency of occurrence of erythrocytes containing micronuclei among sheep in the Khovsgol area (22) was found to be $5.3 \pm 0.4 \text{ ‰}$; in cattle (7) – $4.6 \pm 0.7 \text{ ‰}$; in yaks (7) – $3.2 \pm 0.6 \text{ ‰}$; in sheep in the Gobi Desert (10) – $0.9 \pm 0.1 \text{ ‰}$; in cattle (7) – $1.8 \pm 0.6 \text{ ‰}$; and in yaks (7) – $0.3 \pm 0.2 \text{ ‰}$. These findings suggest that the long-term influence of high-intensity environmental stress factors contributes to the selection of animals (over a number of generations) with increased tolerance of the genetic apparatus to unfavorable environmental conditions.

The disruption of equiprobable transmission of allelic variants of several molecular genetic markers and an increase in heterozygosity were observed among generations of the experimental "Novoshepelichi" herd of the black and white Holstein cattle. The frequency of occurrence of leukocytes containing micronuclei in the parental generation was higher at a statistically significant level ($P < 0.05$) as compared to these values in the first, second and third generations of animals born in the zone with an elevated radionuclide contamination. However, this parameter was significantly lower in the third generation ($P < 0.01$) as compared to that in the second generation. The frequency of occurrence of binucleated leukocytes in the peripheral blood smears was also significantly higher in the parental generation than those in the first and second generations of animals. Thus, the radioresistance of animals born under conditions of the elevated levels of ionizing radiation increases over generations as evidenced by the incidence of cytogenetic abnormalities in the peripheral blood smears. No carriers of Robertsonian translocations were identified, which are often found in uncontaminated areas among representatives of species with acrocentric autosomes.

A comparative analysis with respect to a complex of molecular genetic markers in the experimental herd of black and white Holstein cattle from the relatively uncontaminated breeding areas, as well as the representatives of the ancient primitive breed known as the Ukrainian gray breed allowed to observe a convergence of the genetic structure of animals from the experimental herd born under conditions of elevated levels of radionuclide exposure with the gene pool of this ancient breed in contrast to the parental group of individuals. This shift in the genetic structure of the gene pool of the experimental "Novoshepelichi" herd originally belonging to a specialized dairy breed towards a more primitive species was observed with respect to the allelic variants of the structural genes and DNA fragments flanked by inverted microsatellite repeats. It can be expected that these changes are a universal population-genetic response of cattle to the influence of various environmental stress factors.

CONCLUSIONS

The following data are common for our own findings and to the published data. The main problem that populations of different species (including humans inhabiting the areas contaminated with radionuclides after the Chernobyl accident) face is not the absolute value of the dose of ionizing radiation, but the novelty of these doses to the populations. The main genetic effects for populations of various species consist not in the increase in the number of mutant organisms but in the fact that some of the genes are excluded from their reproduction as a result of selection against radiosensitive organisms. In other words, new genes do not emerge, but the "old" ones associated with high sensitivity of the organisms to new conditions of reproduction abandon the population. There is some indirect evidence suggesting that the less specialized organisms of the species turn out to be more adapted to new conditions.

This "reversion" to the more primitive, developmentally and evolutionarily earlier forms of life is observed at various levels of organization of biological material: a shift in the organ-specific isozymatic spectra to developmentally earlier versions; displacement of the population-genetic structure in generations to the predominance of less specialized forms; *in utero* exposure resulted in a decrease exclusively in the verbal IQ score among young people [41], which is a more recent evolutionary acquisition of humans in comparison to the non-verbal IQ score, which is based on older structures. The actual genetic consequences of the Chernobyl dis-

aster for human populations will not be completely elucidated soon, since children born after the year 1986 have only recently entered the reproductive period of their lives.

It is interesting to note that data have been obtained indicating that the first-priority destruction of the youngest biological systems in evolutionary terms is a relatively universal biological rule [75].

The accumulated data allow one to formulate four major laws of the Chernobyl disaster. We believe they can be universally applied to the consequences of all fundamental environmental changes associated with natural and man-made disasters and crises. These laws are as follows: 1) not everyone who was supposed to be born is being born after the Chernobyl accident; 2) the selection against specialized forms of life and preferential reproduction of less specialized forms characterized by higher resistance to adverse environmental factors occurs; 3) the response to the same dose of ionizing radiation depends on its "novelty" for the population of preceding selection for resistance to such doses in the ancestral generations; and 4) the actual consequences of the Chernobyl accident for human populations will be available for analysis no earlier than 20 years from now, since the generation subjected to direct damaging influence has only recently entered its reproductive period. It should be emphasized that the increase in the incidence of even the thyroid pathology resulting from the Chernobyl accident reduces the chances of reproductive success in its carriers. ●

REFERENCES

- Gileva E.A., Bolshakov V.N., Kosareva N.L., Gabitova A.T. The incidence of chromosomal abnormalities in commensal house mice as an indicator of genotoxic effects of environmental pollution // *ASR*. 1992. V. 325. P. 1058–1061.
- Gileva E.A. Ecological and genetic monitoring using rodents (Ural experience). Ekaterinburg: Publishing House of the Ural State University, 1997. P. 105.
- Dmitriev S.G. // *Ecology*. 1997. № 6. P. 447–451.
- Dmitriev S.G. // *Genetics*. 1997. V. 33. № 11. P. 1589–1592.
- Kryukov V.N., Tolstoy V.A., Dolgopalova G.V., Kanevskaya K.T. // *Ecology*. 1995. № 2. P. 169–171.
- Wood R.D., Mitchell M., Lindahl T. // *Mutat. Res.* 2005. V. 577. P. 275–283.
- Ciciarello M., Lavia P. // *EMBO Repts.* 2005. V. 6. № 8. P. 714–716.
- Farina A.R., Tacconelli A., Cappabianca L. // *Mol. Cell. Biol.* 2009. V. 29. № 17. P. 4812–4830.
- Ame J.-C., Fouquerel E., Laurent R., Gauthier L.R. // *J. Cell Sci.* 2009. V. 122. № 12. P. 1990–2002.
- Gisselsson D., Hakanson U., Stoller P. // *PLoS ONE*. 2008. V. 3. № 4. e1871.
- Schoeftner S., Blasco M.A. // *Semin. Cell Devel. Biol.* 2010. V. 21. P. 186–193.
- Begus-Nahrman Y., Hartmann D., Kraus J. // *J. Clin. Invest.* 2012. V. 122. № 6. P. 2283–2288.
- Greaves M., Maley C.C. // *Nature*. 2012. V. 481. № 7381. P. 287–294.
- Schuster-Bockler B., Lehner B. // *Nature*. 2012. V. 488. № 7412. P. 504–507.
- Drake J.W., Charlesworth B., Charlesworth D., Crow J.F. // *Genetics*. 1998. V. 148. P. 1667–1686.
- Roach J.C., Glusman G., Smit A.F.A. // *Science*. 2010. V. 328. P. 636–639.
- Marnett L.J., Plastaras J.P. // *Trends Genet.* 2001. V. 17. № 4. P. 214–221.
- Memisoglu A., Samson L. // *Mutat. Res.* 2000. V. 451. P. 39–51.
- Nakamura J., Walker V.E., Upton P.B., Chiang S.Y., Kow Y.W., Swenberg J.A. // *Cancer Res.* 1998. V. 58. № 2. P. 222–225.
- Nair J., Carmichael P.L., Fernando R.C., Phillips D.H., Strain A.J., Bartsch H. // *Cancer Epidemiol. Biomarkers Prev.* 1998. V. 7. № 5. P. 435–440.
- Nair J., Furstenberger G., Burger F., Marks F., Bartsch H. // *Chem. Res. Toxicol.* 2000. V. 13. № 8. P. 703–709.
- Haber J.E. // *Trends Biochem. Sci.* 1999. V. 24. P. 271–275.
- Battista J.R., Earl A.M., Park M.-J. // *Trends Microbiol.* 1999. V. 7. № 9. P. 362–365.

24. Ilyinskikh N.N. // *Genetics*. 1988. V. 24. № 3. P. 156–162.
25. Stolina M.R., Glazko T.T., Solomko A.P., Maljuta S.S., Glazko V.I. // *NAS of Ukraine Reports*. 1993. № 6. P. 93–98.
26. Mousseau T.A., Nelson N., Shestopalov V. // *Nature*. 2005. V. 437. P. 1089.
27. Gileva E.A., Lyubashevsky M.N., Starichenko V.I., Chibiryak M.R., Romanov G.N. // *Genetics*. 1996. V. 32. № 1. P. 114–119.
28. Pilinskaya M.A. // *Int. Journal of Rad. Med.* 1999. № 2. P. 60–66.
29. Bogdanov I.M., Sorokina M.A., Maslyuk A.I. // *Bul. of Sib. Med.* 2005. № 2. P. 145–151.
30. Busby C., Lengfelder E., Pflugbeil S., Schmitz-Feuerhake I. // *Med. Confl. Surviv.* 2009. V. 25. № 1. P. 20–40.
31. Little M.P. // *J. Radiol. Prot.* 2009. V. 29. № 2A. P. A43–59.
32. Little M.P. // *Mutat Res.* 2010. V. 687. № 1–2. P. 17–27.
33. Busby C.C. // *Int. J. Environ. Res. Publ. Hlth.* 2009. V. 6. P. 3105–3114.
34. Noshchenko A.G., Bondar O.Y., Drozdova V.D. // *Int. J. Cancer*. 2010. V. 127. P. 412–426.
35. Cardis E., Krewski D., Boniolet M. // *Int. J. Cancer*. 2006. V. 119. P. 1224–1235.
36. Liaginskaia A.M., Tukov A.R., Osipov V.A., Ermalitskiĭ A.P., Prokhorova O.N. // *Radiats Biol. Radioecol.* 2009. V. 49. № 6. P. 694–702.
37. Lazyuk G.I., Zatsepin I.O., Kravchuk J.P., Khmel R.D. Radiation monitoring of the residents and their food in the Chernobyl zone of Belarus. Minsk: Inform. Bull. 2003. № 24. P. 41–42.
38. Hildebrandt G. // *Mutat. Res.* 2010. V. 687. № 1–2. P. 73–77.
39. Scherb H., Voigt R. // *Environmetrics*. 2009. V. 20. P. 596–606.
40. Scherb H., Weigelt E. // *Environ. Sci. Pollut. Res.* 2003. Special Issue 1. P. 117–125.
41. Heiervang K.S., Mednick S., Sundet K., Rund B.R. // *Scand. J. Psychol.* 2010. V. 51. № 3. P. 210–215.
42. Kale R.K. // *Ind. J. Exp. Biol.* 2003. V. 41. № 2. P. 105–111.
43. Lee H.C., Kim D.W., Jung K.Y. // *Int. J. Mol. Med.* 2004. V. 13. № 6. P. 883–887.
44. Samper E., Nicholls D.G., Melov S. // *Aging Cell*. 2003. V. 2. P. 277–285.
45. Pirzio L.M., Freulet-Marriere M.A., Bai Y. // *Cytogenet. Genome Res.* 2004. V. 104. № 1–4. P. 87–94.
46. Gutierrez-Enriquez S., Fernet M., Dork T. // *Genes Chromosomes Cancer*. 2004. V. 40. № 2. P. 109–119.
47. Rothkamm K., Loblrich M. // *Proc. Natl. Acad. Sci. USA*. 2003. V. 100. № 9. P. 5057–5062.
48. Gasser S., Orsulic S., Brown E.J., Raulet D.H. // *Nature*. 2005. V. 436. № 7054. P. 1186–1190.
49. Glazko T.T., Arkhipov N.P., Glazko V.I. Population-genetic effects of environmental disasters using Chernobyl accident as an example. M.: FSEI HPE RGAU – MAA of Timiryazev K.A., 2008. P. 556.
50. Nastjukova V.V., Stepanova E.I., Glazko V.I. // *NAS of Ukraine Reports*. 2002. № 11. P. 178–183.
51. Nastjukova V.V., Stepanova E.I., Glazko V.I. // *Cytology and Genetics*. 2002. V. 6. P. 45–52.
52. Weinberg G.S., King A., Nevo E., Shapiro S., Rennert G. // *Int. Journal of Rad. Medicine*. 1999. V. 2. № 2. P. 67–70.
53. Dubrova Y.E., Plumb M., Brown J., Jeffreys A.Jr. // *Int. Journal of Rad. Med.* 1999. V. 1. № 1. P. 90–100.
54. Pluth J.M., Nelson D.O., Ramsey M.J., Tucker J.D. // *Pharmacogenetics*. 2000. V. 10. № 4. P. 311–319.
55. Zusterzeel P.L., Nelen W.L., Roelofs H.M. // *Mol. Hum. Reprod.* 2000. V. 6. № 5. P. 474–478.
56. Schwartz J.L. // *Crit. Rev. Oral. Biol. Med.* 2000. V. 11. № 1. P. 92–122.
57. Beckman L., Nordenson I. // *Hum. Hered.* 1988. V. 38. № 1. P. 56–58.
58. Telnov V.I., Vologodskaya I.A. Zhuntova G.V. // *Genetics*. 1995. V. 31. № 5. P. 715–721.
59. Hayashi T., Kusunoki Y., Seyama T. // *Health Phys.* 1997. V. 73. № 5. P. 779–786.
60. Shmalgausen I.I. Selected Works: The paths and patterns of evolution. Moscow: Nauka, 1983. P. 360.
61. Garnier-Gere P., Dillmann C. // *J. Heredity*. 1992. V. 83. № 3. P. 239.
62. Eggen E., Fries R. // *Animal Genet.* 1995. V. 26. P. 215–236.
63. Glazko V.I. // *TAA news*. 2007. № 5. P. 142–148.
64. Gopal A.A. // *Ind. J. Exp. Biol.* 1970. № 8. P. 313–318.
65. Luxin W. // *J. Radiat. Res.* 1981. V. 22. № 1. P. 88–100.
66. Freire-Maja N. // *Cienc. E cult.* 1977. V. 30. № 2. P. 385–395.
67. Ghiassi-Nejad M., Mortazavi S.M., Cameron J.R., Niroomand-rad A., Karam P.A. // *Health Phys.* 2002. V. 82. № 1. P. 87–93.
68. Tao Z., Zha Y., Akiba S. // *J. Radiat. Res. (Tokyo)*. 2000. V. 41. Suppl. P. 31–41.
69. Zhang W., Wang C., Chen D. // *J. Radiat. Res. (Tokyo)*. 2003. V. 44. № 1. P. 69–74.
70. Jaikrishan G., Andrews V.J., Thampi M.V. // *Radiat. Res.* 1999. V. 152. Suppl. 6. S 149–153.
71. Nair M.K., Nambi K.S., Amma N.S. // *Radiat. Res.* 1999. V. 152. Suppl. 6. S 145–148.
72. Nambi K.S., Soman S.D. // *Health Phys.* 1987. V. 52. № 5. P. 653–657.
73. Masse R. // *Comptes Rendus de l'Academie des Sciences*. 2000. Ser. III. V. 323. № 7. P. 633–640.
74. Glazko T.T., Stolpovsky Yu.A. Genetically and environment components of micronuclei test. In: Book of Abstracts of XXIVth Genetic Days, Brno, Czech Republic, 1–3 September, 2010. Brno, State University of Gregor Mendel's name, 2010. P. 20.
75. Sansom R.S., Gabbott S.E., Purnell M.A. // *Proc. R. Soc. B*. 2010. e-publishing: rspb.royalsocietypublishing.org.

Structural-Functional Analysis of 2,1,3-Benzoxadiazoles and Their N-oxides As HIV-1 Integrase Inhibitors

S. P. Korolev^{1,2*}, O. V. Kondrashina^{1,2}, D. S. Druzhilovsky³, A. M. Starosotnikov⁴, M. D. Dufov⁴, M. A. Bastrakov⁴, I. L. Dalinger⁴, D. A. Filimonov³, S. A. Shevelev⁴, V. V. Poroikov³, Y. Y. Agapkina^{1,2}, M. B. Gottikh^{1,2}

¹Department of Chemistry, Lomonosov Moscow State University, Leninskie gory, 1/3, Moscow, Russia, 119991

²Belozersky Research Institute of Physicochemical Biology, Lomonosov Moscow State University, Leninskie gory, 1/40, Moscow, Russia, 119991

³Orekhovich Institute of Biomedical Chemistry, Russian Academy of Medical Sciences, Pogodinskaya Str., 10/8, Moscow, Russia, 119121

⁴Zelinsky Institute of Organic Chemistry, Russian Academy of Science, Leninskiy prospekt, 47, Moscow, Russia, 119991

*E-mail: spkorolev@mail.ru

Received 1.10.2012

Copyright © 2013 Park-media, Ltd. This is an open access article distributed under the Creative Commons Attribution License, which permits unrestricted use, distribution, and reproduction in any medium, provided the original work is properly cited.

ABSTRACT Human immunodeficiency virus type 1 integrase is one of the most attractive targets for the development of anti-HIV-1 inhibitors. The capacity of a series of 2,1,3-benzoxadiazoles (benzofurazans) and their N-oxides (benzofuroxans) selected using the PASS software to inhibit the catalytic activity of HIV-1 integrase was studied in the present work. Only the nitro-derivatives of these compounds were found to display inhibitory activity. The study of the mechanism of inhibition by nitro-benzofurazans/benzofuroxans showed that they impede the substrate DNA binding at the integrase active site. These inhibitors were also active against integrase mutants resistant to raltegravir, which is the first HIV-1 integrase inhibitor approved for clinical use. The comparison of computer-aided estimations of the pharmacodynamic and pharmacokinetic properties of the compounds studied and raltegravir led us to conclude that these compounds show promise and need to be further studied as potential HIV-1 integrase inhibitors.

KEYWORDS HIV-1 integrase; inhibition; nitrobenzofuroxan; nitrobenzofurazan; PASS; QikProp.

ABBREVIATIONS ADME – absorption, distribution, metabolism, and excretion; AIDS – acquired immunodeficiency syndrome; BFX – benzofuroxan; BFZ – benzofurozan; HIV-1 – human immunodeficiency virus type 1; IN – integrase; IC₅₀ – inhibitor concentration at which the enzyme activity is suppressed by 50 %; IC₉₅ – inhibitor concentration at which the enzyme activity is suppressed by 95 %; PASS – Prediction of Activity Spectra for Substances software program; QikProp – ADME prediction software program.

INTRODUCTION

The human immunodeficiency virus (HIV) is responsible for the acquired immunodeficiency syndrome (AIDS), which is one of the most dangerous diseases. The extremely high rates of growth in the number of HIV-infected patients in Russia make the development of effective medical therapies to combat the virus a particularly pressing challenge for the country. The viral enzyme integrase (IN), catalyzing the integration of viral DNA into cellular DNA, which is the key stage in the replication cycle of HIV, is considered to be one of the most promising targets for HIV-1 inhibitors [1].

Highly active antiretroviral therapy is used to treat HIV infections and currently includes 25 drugs [2]; most of them inhibit two viral enzymes: reverse transcriptase and protease. In late 2007, the first IN inhibitor (Isentress™, or Raltegravir) was approved for use as a new agent for AIDS therapy [3]. However, even combination therapy cannot fully suppress viral replication, and the virus develops resistance to drugs over time. It is now known that resistance to Raltegravir develops in some patients within 12 weeks [4]. The majority of IN inhibitors currently at the stage of clinical trials are similar to Raltegravir in terms of their mechanism of action [5]. Raltegravir-induced cross-resistance to these com-

pounds has already been demonstrated to develop in patients [6]. Thus, designing new integration inhibitors that would differ from Raltegravir in terms of their mechanism of action is currently a pressing need.

Computer-aided design methods are now widely used to search for new physiologically active substances and optimize their structure [7]. In particular, computer-aided methods are used to design HIV-1 IN inhibitors [8–10]. The PASS computer program developed by us [11, 12] was used to perform virtual screening and selection of potential IN inhibitors among commercially available and potentially synthesizable compounds [13, 14]. The derivatives of 2,1,3-benzoxadiazoles (benzofurazans) and their N-oxides (benzofuroxans) were selected using a specialized version of the PASS program [14]. These compounds have been synthesized; their ability to inhibit the catalytic activity of HIV-1 IN was experimentally tested in the present study.

Two reactions are catalyzed by IN during viral replication: the 3'-end processing of viral DNA, resulting in the removal of the dinucleotides GT from both 3'-ends; and the strand transfer reaction, during which viral DNA is incorporated into cellular DNA. Raltegravir and its analogs are known as strand transfer inhibitors, since they suppress this particular reaction more effectively [15]. Benzofurazan (BFZ) and benzofuroxan (BFX) were found to generally exert the same effects on both reactions catalyzed by IN. It was demonstrated that the inhibitory effect of these compounds is highly dependent on the presence of a nitro group. Among a series of substituted 4-nitro-BFZ/BFX, certain compounds capable of blocking IN at a concentration of 0.5–1 μM have been identified. These inhibitors were found to be also active against Raltegravir-resistant IN mutants.

The pharmacodynamic and pharmacokinetic characteristics of BFZ and BFX were assessed using the PASS and QikProp computer programs [16]. The potential benefits of these compounds as compared to those of Raltegravir were demonstrated.

EXPERIMENTAL

Computer programs and databases

A specialized version of the computer program PASS, trained on a sample of 218 compounds with the determined IN suppressive capabilities, was used for virtual screening of the databases of commercially available samples and potentially synthesizable compounds to select substances that are likely to inhibit HIV-1 IN [14]. Thirty-five of these compounds affect the 3'-processing ($\text{IC}_{50} < 100 \mu\text{M}$), Twenty-eight of them inhibit the strand transfer reaction ($\text{IC}_{50} < 100 \mu\text{M}$), the remaining

compounds exhibit no inhibitory properties. The overall pharmacological profile of the new IN inhibitors was evaluated using the contemporary standard version of PASS (12.06.22) [11, 12], which allows one to predict 513 possible toxic and side effects. The result is given to the user as an ordered list of possible biological activities with the estimated Pa and Pi, which characterize the probability of presence/absence of each type of activity, respectively.

QikProp was used to assess the ADME pharmacokinetic parameters of the analyzed molecules [16]. The program enables to assess the physical and chemical characteristics of the drug similarity and is commonly used to screen compounds with undesired pharmacokinetic characteristics [17–19]. The range of parameter values determined by QikProp and recommended for the promising compounds was provided in [14].

1,2,5-benzoxadiazols (benzofurazans) and their N-oxides (benzofuroxans)

1,2,5-benzoxadiazols and their N-oxides were synthesized using the conventional [20–22] or analogous procedures.

Oligodeoxyribonucleotides

Oligodeoxyribonucleotides were synthesized using the amidophosphite method on an ABI 3400 automated DNA synthesizer (Applied Biosystems, USA) in accordance with the standard operating procedures using commercially available reagents (Glen Research, USA). Oligonucleotides U5B (5'-GTGTGGAAAATCTCTAGCAGT-3') and U5A (5'-ACTGCTAGAGATTTTCACAC-3') formed a duplex imitating the end fragment of the U5-moiety of the long terminal repeat of viral DNA, which acts as a substrate for IN during the 3'-processing reaction. The duplex formed from the oligonucleotides U5B-2 (5'-GTGTGGAAAATCTCTAGCA-3') and U5A was used in the chain transfer reaction. The effects of the inhibitors on correct DNA folding at the IN active site was assessed using the U5B/U5A^{m'} duplex (5'-ACT^{m'}GCTAGAGATTTTCACAC-3'), where T^{m'} was 2'-O-(2,3-dihydroxypropyl)-uridine synthesized according to [23]. The N155H (5'-CTGTCCTATAATTTTCTTTAATTCTTTATGCATAGATTCTATTACCCCTGA-3'), G140S (5'-GGGGATCAAGCAGGAATTTAGCATTCCCTACAATC-3'), Q148K (5'-GCATCCCTACAATCCCCAAAGTAAGGGGTAATAG-3') oligonucleotides and their complementary N155H_a, G140S_a, and Q148K_a oligonucleotides were used as primers for site-directed mutagenesis of the HIV-1 integrase gene to produce mutant forms of the integrase gene (N155H, G140S/Q148K).

Enzymes

The recombinant HIV-1 IN was isolated from the cells of the Rosetta *Escherichia coli* producer strain and purified without the addition of a detergent as per [24]. The plasmids containing the mutant forms of the IN genes (N155H and G140S/Q148H substitutions) were obtained by site-directed mutagenesis of a plasmid encoding wild-type IN using the QuikChange II Site-Directed Mutagenesis kit (Agilent Technologies, USA). All procedures were performed in accordance with the manufacturer's instructions. Mutant proteins were isolated and purified as per wild-type of HIV-1 IN [24].

Synthesis of ^{32}P -labeled integrase substrate

Radioactive ^{32}P label was introduced into the 5'-end of the oligonucleotide U5B or U5B-2. To achieve this, 10 pmol of the oligonucleotide was incubated in the presence of T4-polynucleotide kinase (Fermentas, Lithuania) and 50 μCi [γ - ^{32}P]ATP (3000 Ci/mmol) in a buffer containing 50 mM Tris-HCl, pH 7.5, 10 mM MgCl_2 , 5 mM dithiothreitol (DTT), 0.1 mM spermidine, 0.1 mM EDTA, for 1 h at 37°C. Following this procedure, the kinase was inactivated by adding EDTA (25 mM) and heating to 65°C for 10 min. An equimolar amount of the complementary oligonucleotide, U5A, was added, and a duplex was formed by heating the oligonucleotide mixture to 95°C followed by slow cooling to room temperature. The U5B/U5A duplex was completely purified of excess [γ - ^{32}P]ATP and salts on a MicroSpin G-25 column (Amersham Biosciences, USA).

Inhibition of the 3'-end processing reaction

The ^{32}P -labeled U5B/U5A duplex (3 nM) was incubated in 20 μl of the buffer (20 mM HEPES, pH 7.2, 7.5 mM MgCl_2 , 1 mM DTT) in the presence of IN (100 nM) and increasing concentrations of the inhibitor at 37°C for 2 h. The reaction was stopped using 80 μl of a stop solution (7 mM EDTA, 0.3 M NaOAc, 10 mM Tris-HCl, pH 8, 0.125 mg/ml glycogen). The integrase was extracted using phenol-chloroform-isoamyl alcohol = 25 : 24 : 1; the DNA-duplex was precipitated with ethanol (250 μl) and assayed by 20% polyacrylamide gel electrophoresis (PAGE) with 7 M urea. The gel was visualized in a STORM 840TM Phosphorimager (Molecular Dynamics, USA). The reaction was recorded according to the band in electrophoretic pattern, which corresponded in terms of its mobility to oligonucleotide U5B truncated by two residues. The reaction efficiency was assessed using the Image QuANTTM 4.1 program. The results of three independent repetitions of the experiment were used to build a curve representing the relationship between the efficiency of 3'-processing and the inhibitor concentration. The curve was used to identify the value

of IC_{50} as the inhibitor concentration at which the reaction is suppressed to 50%.

Inhibition of the strand transfer reaction

The reaction was carried out as per inhibition of the 3'-processing using the ^{32}P -labeled U5B-2/U5A duplex (10 nM) and IN (100 nM). The reaction was recorded according to the bands in the electrophoretic pattern with a lower mobility as compared to that of the initial oligonucleotide, U5B-2.

Gel shift analysis

The ^{32}P -labeled U5B/U5A duplex (0.05 pmol) was incubated in the presence of integrase (2 pmol) in a buffer containing 20 mM HEPES, pH 7.2, 7.5 mM MgCl_2 , 1 mM DTT, 5% glycerol at 20°C for 30 min. Increasing amounts of the oligonucleotide inhibitor (0.01–10.0 μM) were added to the preformed enzyme-substrate complex; the mixture was incubated at 37°C for 5 min and then applied to an 8% polyacrylamide gel (acrylamide/bisacrylamide ratio = 40: 1) with no urea. The electrophoresis buffer contained 20 mM Tris-acetate, pH 7.2, 7.5 mM MgCl_2 . The gel was visualized with a STORM 840TM Phosphorimager.

The effects of the inhibitor on the correct folding of DNA at the IN active site

The 2,3-dihydroxypropyl group consisting of the oligonucleotide duplex was oxidized to an aldehyde group immediately prior the experiment: 15 μl of a freshly prepared 230 mM aqueous solution of sodium periodate was added to 10 pmol of the U5B/U5A^{m'} duplex containing the ^{32}P -labeled modified oligonucleotide U5A^{m'} in 15 μl of 30 mM sodium acetate (pH 4.5). The mixture was stirred and incubated for 1 h at 25°C in the dark followed by the addition of 170 μl of a 2 M aqueous solution of lithium perchlorate; the oligonucleotide material was precipitated using 1 ml of acetone. The obtained U5B/U5A^m duplex containing the oligonucleotide with a 2'-aldehyde group (U5A^m) was dissolved in a buffer containing 20 mM HEPES, pH 7.2, 7.5 mM MgCl_2 , 1 mM DTT. Covalent attachment of the oxidized U5B/U5A^m duplex (10 nM) to the IN (100 nM) was carried out in 20 μl of a buffer containing 20 mM HEPES, pH 7.2, 7.5 mM MgCl_2 , 1 mM DTT in the presence of increasing concentrations of the inhibitor for 1 h at 37°C. The reaction product was then reduced by adding 2 μl of a freshly prepared 300 mM solution of NaBH_3CN and incubating for 30 min at 37°C. The reaction mixture was analyzed in the Laemmli PAGE system. The labeled products were visualized using the STORM 840TM Phosphorimager. The efficiency of the reaction progress was assessed by observing the intensity of the band corresponding

to the covalently bound IN-DNA complex using Image QuaNT™ 4.1.

RESULTS AND DISCUSSION

Computer-aided screening of new integrase inhibitors

A specialized version of the PASS program was used for computer-aided screening and selection of the substances that are highly likely to possess HIV-1 IN inhibitory potential [14]. The accuracy of anti-integrase activity prediction calculated for the training set of 218 compounds using the leave-one-ROI-out technique was 81%. The biological activity of Raltegravir, which effectively inhibits the chain transfer reaction, was predicted using this particular version of PASS (*Table 1*). The estimated probability of exhibiting this activity was 0.948 for Raltegravir (Pa). These facts suggest that PASS has a significant capability of predicting the anti-integrase activity of compounds.

Over two millions structural formulas of substances belonging to various chemical classes were analyzed. The structures selected using the computer-aided predictions turned out to be the derivatives of benzofurazans and benzofuroxans. In order to perform structural-functional studies, 27 different compounds belonging to these structural classes characterized by an estimated probability of possessing the ability to inhibit the 3'-processing and chain transfer reactions greater than 0.5 were synthesized (*Table 1*).

The effects of the structure of 1,2,5-benzoxadiazols on their ability to inhibit IN activity

The ability of BFZ and BFX to suppress the catalytic activity of IN was investigated in the 3'-end processing and strand transfer reactions using recombinant protein and U5B/U5A and U5B-2/U5A DNA-duplexes corresponding to the terminal fragment of viral DNA prior to and following the cleavage of the GT dinucleotide. The U5B/U5A duplex acted as the IN substrate in the 3'-end processing reaction, while the U5B-2/U5A duplex acted as the IN substrate in the strand transfer. It should be noted that the recombinant IN can use any DNA as a target for incorporation of the processed substrate in the strand transfer reaction; hence, the U5B-2/U5A duplex acted both as a substrate and as a target in this reaction.

The unsubstituted BFX exhibited no inhibitory potential in any of the reactions (*Table 1*, compound **1**). The introduction of an electron-donor (methyl) or electron-acceptor (chlorine) substituent at the 5-position only insignificantly improved the inhibitory activity of BFX during the strand transfer (*Table 1*, **2** and **3**). However, 4-nitro-BFX was a significantly more efficient inhibitor in both reactions (*Table 1*, **4**).

With allowance for such a strong influence of the nitro group, the effects of the substituents at positions 5 and 7 on the activity of 4-nitro-BFX were examined. It was demonstrated that the presence of a methyl residue at any of these positions significantly increases the inhibitory activity of 4-nitro-BFX (*Table 1*, **5** and **6**). In this case, the presence of a methyl group at both positions had no additional positive effect, but instead slightly reduced the inhibition efficiency (*Table 1*, **7**). The enhancement of the inhibitory activity of 4-nitro-BFX after a methyl group was introduced at position 5 or 7 can be attributed to the electron donor effect of a methyl group. To support or refute this assumption, the efficiency of inhibition of processing and strand transfer by 4-nitro-BFX containing other electron-donating substituents at position 7 was assessed (*Table 1*, **8** and **9**). Both of these compounds were found to block IN with an efficiency comparable to that of the unsubstituted 4-nitro-BFX. Thus, the positive inductive effect of the methyl group cannot be the reason for the increased inhibitory activity of compounds **5** and **6**. The ability of the methyl group to form hydrophobic interactions with the protein is also an unlikely reason for the observed effect, since the methoxy group is also theoretically capable of these interactions. It is interesting that the derivative of 4-nitro-BFX containing an electron-acceptor substituent in the form of chlorine at position 7 was a more potent inhibitor as compared to the original 4-nitro-BFX (*Table 1*, **10**) but was inferior to 7-methyl-4-nitro-BFX in terms of its inhibitory properties.

Next, the importance of the role of N-oxide was determined. For this purpose, the inhibitory effect of 4-nitro-BFX derivatives and the corresponding derivatives of 4-nitro-BFZ were compared. Unsubstituted 4-nitro-BFZ inhibited both of the reactions under study to a greater extent than N-oxide did (*Table 1*, **11** and **4**). However, its methyl derivatives (compounds **12** and **13**) were 3–6 times less active than compounds **5** and **6** (*Table 1*). Nevertheless, the patterns observed for the 4-nitro-BFX derivatives were generally valid for a series of 4-nitro-BFZ derivatives (*Table 1*).

Thus, it can be concluded that 4-nitro-BFZ derivatives and the corresponding N-oxides are capable of blocking HIV-1 IN with comparable efficiencies; the level of efficiency depends on the nature of the substituents at position 5 or 7. Methyl-substituted 4-nitro-BFZ and 4-nitro-BFX were found to be the most efficient inhibitors.

In addition to BFX containing a single nitro group, the derivatives of 4,6-dinitro-BFX were also tested as IN inhibitors (*Table 1*, **21–24**). It was found that the introduction of the second nitro group significantly reduced the inhibitory activity (compare **21** and **4**). How-

Table 1. The ability of BFZ and BFX derivatives to inhibit the IN catalytic activity during 3'-processing and strand transfer reactions

Structure	№	R1	R2	Inhibitory activity, IC ₅₀ , μM*	
				3'-processing	strand transfer
Raltegravir				0.50 ± 0.09	0.010 ± 0.003
	1	H	-	> 1000	> 1000
	2	CH ₃	-	> 1000	800 ± 200
	3	Cl	-	> 1000	500 ± 200
	4	H	H	80 ± 20	80 ± 30
	5	CH ₃	H	0.4 ± 0.1	1.0 ± 0.3
	6	H	CH ₃	0.5 ± 0.2	0.4 ± 0.2
	7	CH ₃	CH ₃	1.0 ± 0.3	7 ± 2
	8	H	OCH ₃	70 ± 20	80 ± 20
	9	H		50 ± 10	80 ± 30
	10	H	Cl	20 ± 5	50 ± 10
	11	H	H	30 ± 5	40 ± 10
	12	CH ₃	H	2.0 ± 0.4	3.0 ± 0.6
	13	H	CH ₃	3.0 ± 0.6	3.0 ± 0.5
	14	OCH ₃	H	75 ± 12	150 ± 40
	15	H	OCH ₃	80 ± 30	120 ± 20
	16	H		65 ± 11	70 ± 20
	17	H	Cl	10 ± 2	45 ± 12
	18	H	-SO ₂ -Ph	20 ± 5	15 ± 5
	19	H		10 ± 2	12 ± 3
	20	H		18 ± 6	20 ± 5
	21	H	H	400 ± 100	500 ± 120
	22	H	CH ₃	2.0 ± 0.4	0.3 ± 0.1
	23	H	CH ₂ Br	6 ± 2	2.0 ± 0.5
	24	H		75 ± 15	80 ± 20
	25	H	-	0.5 ± 0.1	5 ± 2
	26	H	-	6 ± 1	5 ± 1
	27	OCH ₃	-	100 ± 20	100 ± 30

* The average values calculated from the results of at least three repeated experiments.

Table 2. The inhibition of the catalytic activity of the Raltegravir-resistant mutant forms of IN by the nitro-BFX/BFZ derivatives

Compound, №	Inhibitory activity during the strand transfer reaction, IC, μM^*					
	wild-type		Q148K/G140S mutant		N155H mutant	
	IC ₅₀	IC ₉₅	IC ₅₀	IC ₉₅	IC ₅₀	IC ₉₅
Raltegravir	0.010 ± 0.003	0.40 ± 0.05	0.15 ± 0.03	3.0 ± 1.0	0.018 ± 0.005	5.2 ± 0.8
6	0.4 ± 0.2	3.5 ± 0.9	0.8 ± 0.3	4.3 ± 0.8	0.9 ± 0.3	8.2 ± 1.7
22	0.3 ± 0.1	6.8 ± 1.1	0.5 ± 0.2	1.0 ± 0.4	0.6 ± 0.1	7.6 ± 1.3
25	5.0 ± 2.0	18.0 ± 2.0	4.0 ± 1.5	15.3 ± 2.8	6.0 ± 1.8	18.8 ± 2.5

* The average values calculated from the results of at least three repeated experiments.

ever, the presence of a methyl substituent at position 7 in the case of 4,6-dinitro-BFX also significantly increased the efficiency of inhibition of integration and strand transfer (the latter process was inhibited 6–7 times more efficiently than 3'-processing) (Table 1, 22). It is interesting to point out that compound 23 containing an electron-accepting bromomethyl substituent also effectively inhibited both reactions, although it was somewhat inferior to 7-methyl-4,6-dinitro-BFX (22) in this respect. Meanwhile, compound 24, which contains a very strong electron acceptor at position 7, exhibited a low inhibitory activity (Table 1).

The integration inhibition properties of 6-nitro-BFX and 6-nitro-BFZ were subsequently studied (Table 1, 25 and 26). Both compounds were found to be significantly more efficient in inhibiting the integration process as compared to 4-nitro-BFX/BFZ and 4,6-dinitro-BFX (Table 1, 4, 11, 21). It is of little interest that the effects of 6-nitro-BFX and 6-nitro-BFZ in the chain transfer reaction were identical, and the 3'-processing was more efficiently inhibited by 6-nitro-BFZ (25). The introduction of the methoxy group at position 4 significantly reduced the inhibition efficiency (Table 1, 27).

The ability of BFX and BFZ containing nitro groups at positions 4 and/or 6 to inhibit both reactions catalyzed by HIV-1 IN with almost identical efficiency gave grounds to assume that the mechanism of integration inhibition used by these compounds differs from the mechanism of action of Raltegravir, which mainly inhibits the stand transfer [15]. In order to verify this hypothesis, the potential of nitro-BFX/BFZ to inhibit the mutant Raltegravir-resistant forms of IN was evaluated.

Inhibition of the mutant forms of IN characterized by increased resistance to Raltegravir

The emergence of resistance to strand transfer inhibitors is attributable to the emergence of mutations at the

IN active site [25]. Patients with Raltegravir resistance typically carry primary mutations, such as Y143R/C, Q148K/R/H, and N155H. Q148R/H/K and N155H amino acid substitutions are also common in patients treated with IN inhibitor Elvitegravir, which has just been approved by the FDA for clinical use in HIV therapy [26]. For this reason, IN proteins containing Q148K and N155N substitutions were used in the present work. With allowance for the fact that the replacement of Q148 dramatically decreases the IN activity, which is reduced due to a secondary mutation in the G140 residue [27], an IN specimen containing the double mutation G140S/Q148K was obtained. The ability of the most active compounds 6, 22 and 25, which represented all three investigated groups of nitro-BFX/BFZ, to inhibit the catalytic activity of the mutant proteins and wild-type IN during the strand transfer reaction was tested. It was found that the inhibitors analyzed suppress the activity of all IN specimens with comparable efficiencies (Table 2). Meanwhile, the two mutant forms of IN were inhibited by Raltegravir to a lower extent than the wild-type IN; the reduction in the inhibition efficiency was particularly evident for the IC₉₅ values (Table 2).

Investigation of the inhibitory mechanism of nitro-BFX/BFZ derivatives

The ability of nitro-BFX/BFZ derivatives to inhibit the mutant forms of IN as efficiently as the wild-type enzyme confirmed the validity of the assumption that the mechanism of integration inhibition by these compounds differs from that of Raltegravir. In order to better understand the inhibitory mechanism of nitro-BFX/BFZ derivatives, the compounds were selected according to two criteria: 1) compounds were selected from all three groups of the derivatives differing by the position and number of nitro groups and 2) compounds with different substituents were selected, since the for-

Table 3. The effects of nitro-BFX and nitro-BFZ on the catalytic activity of IN in 3'-processing and strand transfer reactions, and on the IN DNA-binding activity and binding of the DNA-substrate at the active site of IN

Compound, №	Inhibitory activity, IC ₅₀ , μM *					
	3'-processing		strand transfer		binding of IN to DNA	binding of DNA at the active site of IN
	Mg ²⁺	Mn ²⁺	Mg ²⁺	Mn ²⁺		
	1	2	3	4	5	6
Raltegravir	0.50 ± 0.09	0.15 ± 0.02	0.010 ± 0.003	0.005 ± 0.002	> 500	> 500
6	0.5 ± 0.2	0.5 ± 0.1	0.4 ± 0.2	0.5 ± 0.2	10 ± 2	0.6 ± 0.2
9	50 ± 10	35 ± 10	80 ± 30	70 ± 20	500 ± 100	90 ± 20
18	20 ± 5	20 ± 5	15 ± 5	25 ± 5	50 ± 10	20 ± 5
23	6 ± 2	5 ± 2	2.0 ± 0.5	5 ± 2	25 ± 8	6 ± 2
25	0.5 ± 0.1	1.0 ± 0.2	5 ± 2	4 ± 1	45 ± 10	1.0 ± 0.5

* The average values calculated from the results of at least three repeated experiments.

mation of additional contacts between the protein and the substituent could potentially influence the inhibitory mechanism. Therefore, compounds **6**, **9** and **18** were selected from the 4-nitro-BFX/BFZ group; compound **23**, from the group of 4,6-dinitro-BFX, and compound **25**, from the group of 5-nitro-BFX/BFZ (*Table 1*).

It should be mentioned that all of the strand transfer inhibitors act through the same mechanism: they bind to the active site of IN, which forms a complex with the viral DNA and prevent its interaction with cellular DNA [5, 15, 28]. The compounds equally efficient at inhibiting both stages of integration can have different mechanisms of action. They can either interact with the C-terminal domain disrupting the binding of DNA, or they can bind to the catalytic domain of IN affecting or not affecting the correct folding of viral DNA, or they can interact with the other parts of IN; e.g., acting as allosteric inhibitors [5, 29].

Initially, the effects of inhibitors on the DNA-binding activity of IN were studied. The C-terminal domain of IN is mainly responsible for the binding to DNA [30]. Therefore, the inhibitor that suppresses both DNA binding and 3'-processing when taken at equal concentrations affects the C-terminal domain. The action of the inhibitors on the DNA binding was studied at 25°C, since IN completely binds to the DNA-substrate under these conditions to form an enzyme-substrate complex, but does not perform a catalytic function [31]. It was found that almost all the investigated compounds affect DNA binding to IN to a much lesser extent than they affect the 3'-processing (*Table 3*, columns 5 and 1). This fact led to the assumption that the inhibitors interact with the catalytic domain of IN.

An inhibitor binding to the catalytic domain of IN can prevent "correct" interaction between the viral DNA and the active site of the enzyme without affecting the overall DNA-IN binding. The influence of the inhibitors on the correct folding of DNA-substrate at the active site of IN was studied using the method of covalent attachment of the aldehyde-containing analog of DNA-substrate to IN [32]. The aldehyde group was introduced into the structure of the modified thymidine analogue (T^m), which occupied position 3 counting from the 5'-end of oligonucleotide U5A (*Figure, A*), since it was located close to the amino acid residues of the IN catalytic domain [33]. The feasibility of this approach was described in [34, 35].

The U5B/U5A^m duplex containing a radioactive label in the U5A^m chain was covalently attached to the IN in the presence of increasing concentrations of inhibitors; the influence of inhibitors on the efficiency of the reaction was analyzed (*Figure, B*). No inhibition of the covalent attachment was observed in the case of Raltegravir (*Table 3*, column 6), which is consistent with the findings that strand transfer inhibitors do not affect the interaction between IN and viral DNA [5, 15]. The IC₅₀ values for all nitro-BFX/BFZ derivatives for the inhibition of the covalent DNA binding at the IN active site were similar to those obtained for the catalysis (*Table 3*, columns 6 and 1). This fact indicates that the inhibitors interact with the active site of IN and prevent the correct folding of the DNA-substrate within it. However, the binding of inhibitors does not cause such changes in the IN structure that can completely block its DNA binding activity.

Under the assumption that the derivatives of nitro-BFX/BFZ bind at the active site of IN, we decided to

Table 4. The spectra of potential toxicity/side effects of nitro-BFZ and nitro-BFX as compared to Raltegravir

Compound, №	Predicted toxic and side effects (Pa > 0.5)		
	Pa*	Pi*	Activity
6	0.536	0.068	Hypotension
	0.503	0.085	Vessel toxicity
9	-	-	-
18	0.595	0.015	Carcinogenicity (rats, males, kidneys)
	0.551	0.014	Carcinogenicity (rats, males)
	0.519	0.020	Stimulator of tear secretion
23	0.653	0.005	Mutagenic
	0.556	0.006	Mutagenic
25	0.816	0.014	Vessel toxicity
	0.679	0.007	Carcinogenicity (rats, males)
	0.661	0.008	Carcinogenicity (rats, females)
	0.632	0.019	QT-interval prolongation
	0.571	0.013	Carcinogenicity (rats, females, mammary gland)
	0.603	0.049	Hypotension
	0.588	0.034	Allergic dermatitis
	0.583	0.047	Cyanosis
	0.570	0.045	Ototoxicity
	0.568	0.074	Hemotoxicity
Raltegravir	0.933	0.003	Hyperkinesia
	0.932	0.004	Ataxia
	0.923	0.004	Anxiety
	0.861	0.013	Vertigo
	0.850	0.010	Thrombocytopenia
	0.830	0.017	Sensory impairments
	0.796	0.023	Vomiting
	0.780	0.016	Dyskinesia
	0.787	0.025	Dermatitis
	0.783	0.022	Headache
	0.781	0.024	Allergic reaction
	0.744	0.031	Pain
	0.702	0.040	Nausea
	0.683	0.032	Nephrotoxicity
	0.693	0.042	Sleeping disorders
	0.603	0.065	Hemotoxicity
0.589	0.073	Gastro-intestinal toxicity	
0.556	0.065	Hepatotoxicity	

* Pa – probability of observing activity; Pi – probability of observing inactivity.

clarify whether they interact with the metal-cofactor ions, which are bound at the IN active site and are essential for its catalytic activity [36]. Mg^{2+} is a native cofactor of IN, but *in vitro* IN efficiently catalyzes both reactions in the presence of Mn^{2+} ions as well. If the inhibitor interacts with the metal ion, its effects on the IN activity in the presence of these metal ions will differ due to the differences in the coordinating ability of Mg^{2+} and Mn^{2+} ions. This very effect was observed for Raltegravir (Table 3, columns 1–4). The results of inhibition of 3'-processing and the strand transfer reaction in the presence of various metal ions demonstrate that the type of the metal does not affect the efficiency of the action of nitro-BFX/BFZ derivatives. It is obvious that the interaction between these inhibitors and the active site of IN is not mediated by binding to the metal ion.

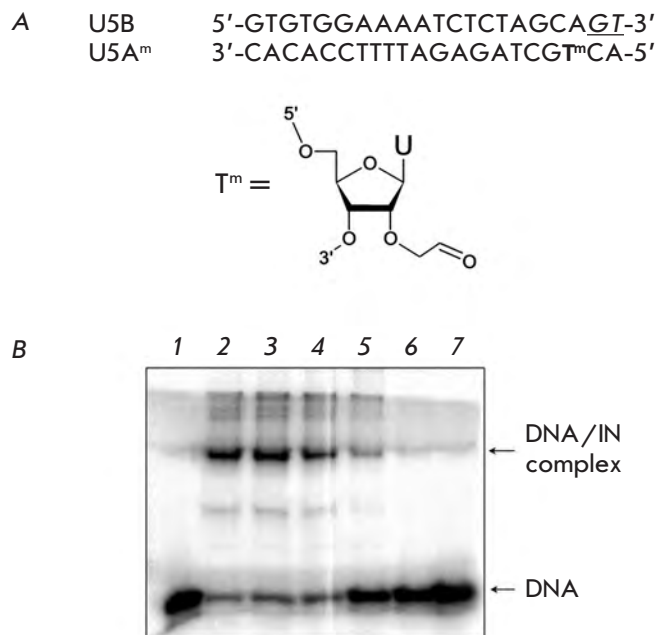
Prediction on the pharmacodynamic and pharmacokinetic characteristics of nitro-BFX/BFZ derivatives

The standard version of the PASS program (version 12.06.22) was used to predict the possible toxic and side effects of compounds **6**, **9**, **18**, **23**, **25**, and Raltegravir (Table 4). It should be mentioned that 15 out of 18 predicted ($Pa > 0.5$) toxic and side effects of Raltegravir correspond to the data obtained during experimental and clinical studies [37]. No side/toxic effects have been identified in the predicted spectra of biological activity of compound **9**. Compounds **6**, **18**, **23** and **25** can cause some undesirable side effects, although it should be borne in mind that the side effects predicted by PASS may occur at concentrations exceeding therapeutic doses.

The calculation of the ADME characteristics using QikProp showed that all 18 parameters of compounds **6**, **9**, **18**, **23** and **25** correspond to the recommended range [13]. The estimated IC_{50} for blockage of HERG K^+ channels is obtained from this range for Raltegravir (less than -5) [14]. This corresponds to the data obtained in [38], according to which Raltegravir at high concentrations acts as a blocker of HERG K^+ channels, which can result in prolongation of the QT-interval and, consequently, in the development of heart failure.

CONCLUSIONS

Thus, the new class of IN inhibitors identified using computer prediction, nitro-BFX and nitro-BFZ, was characterized in the present work. It was demonstrated that these compounds inhibit the 3'-processing equally or more efficiently than the strand transfer. The influence of the structure of nitro-BFX and nitro-BFZ on their inhibitory activity was studied. The most active integration inhibitors were identified to be 4-nitro-BFZ/BFX containing a methyl group at positions 5 and 7, as well as 5-nitro-BFZ. The described inhibitors also



The influence of compound **6** on the efficiency of covalent binding of a DNA-substrate analog containing the aldehyde group to IN. **A** – the structure of the U5B/U5A^m DNA-substrate analog and modified thymidine T^m . GT dinucleotide cleaved by IN during the 3'-processing is underlined and shown in italics. **B** – the analysis of the influence of inhibitor **6** on the covalent binding of the U5B/U5A^m duplex to IN using Laemmli gel-electrophoresis. Lanes: 1 – control; 2 – 0 μM of **6**; 3 – 0.1 μM of **6**; 4 – 0.5 μM of **6**; 5 – 1 μM of **6**; 6 – 10 μM of **6**; 7 – 100 μM of **6**

exhibited activity against mutant forms of IN resistant to Raltegravir. The study of the mechanism of IN inhibition by nitro-BFZ and nitro-BFX showed that these compounds prevent the binding of DNA-substrate at the enzyme active site and do not interact with the metal-cofactor ion. The comparison of the pharmacodynamic and pharmacokinetic characteristics of the investigated substances and Raltegravir show promise with respect to further investigations of these compounds as inhibitors of HIV-1 IN. ●

The authors wish to express their sincere appreciation to Marc Nicklaus and colleagues (National Cancer Institute/National Institutes of Health) for the calculations of the ADME parameters of the investigated compounds using QikProp program.

The work was supported by the Ministry of Education and Science of the Russian Federation (contract № 16.512.11.2193) and the Russian Foundation for Basic Research (grants № 11-04-01004_a and № 11-04-01586_a).

REFERENCES

1. Cara A., Guarnaccia F., Reitz M.S. Jr., Gallo R.C., Lori F. // *Virology*. 1995. V. 208. P. 242–248.
2. Marcelin A.G., Ceccherini-Silberstein F., Perno C.F., Calvez V. // *Curr. Opin. HIV AIDS*. 2009. V. 4. P. 531–537.
3. FDA approves raltegravir tablets. // *AIDS Patient Care STDS*. 2007. V. 21. № 11. P. 889.
4. Cooper D.A., Steigbigel R.T., Gatell J.M., Rockstroh J.K., Katlama C., Yeni P., Lazzarin A., Clotet B., Kumar P.N., Eron J.E., et al. // *N. Engl. J. Med.* 2008. V. 359. № 4. P. 355–365.
5. Korolev S.P., Agapkina Y.Y., Gottikh M.B. // *Acta Naturae*. 2011. V. 3. № 3. P. 12–28.
6. Kobayashi M., Nakahara K., Seki T., Miki S., Kawauchi S., Suyama A., Wakasa-Morimoto C., Kodama M., Endoh T., Oosugi E., et al. // *Antiviral Res.* 2008. V. 80. № 2. P. 213–222.
7. Keseru G.M., Makara G.M. // *Nature Reviews Drug Discovery*. 2009. V. 8. P. 203–212.
8. Johnson B.C., Metifiot M., Pommier Y., Highes S.H. *Antimicrob. Agents Chemother.* 2012. V. 56. P. 411–419.
9. Ma K., Wang P., Fu W., Wan X., Zhou L., Chu Y., Ye D. *Bioorg. Med. Chem. Lett.* 2011. V. 21. № 22. P. 6724–6727.
10. Ko G.M., Reddy A.S., Garg R., Kumar S., Hadaegh A.R. // *Curr. Comput. Aided Drug Des.* 2012. V. 8. № 4. P. 255–270.
11. Filimonov D.A., Poroikov V.V. Probabilistic approach in activity prediction. In: *Chemoinformatics Approaches to Virtual Screening*. Eds. Alexandre Varnek and Alexander Tropsha. Cambridge (UK): RSC Publishing. 2008. P. 182–216.
12. Filimonov D.A., Poroikov V.V. // *Rus. Khim. Zhurn.* 2006. V. 50. № 2. P. 66–75.
13. Akimov D.V., Filimonov D.A., Prikazchikova T.A., Gottikh M.B., Poroikov V.V. // *Biomed. Khim.* 2005. V. 51. № 3. P. 335–340.
14. Druzhilovskiy D.S., Filimonov D.A., Liao C., Peach M., Nicklaus M., Poroikov V.V. *Biochemistry (Moscow) Supplemental Series B. Biomedical Chemistry*. 2010. V. 4. №1. P. 59–67.
15. Summa V., Petrocchi A., Bonelli F., Crescenzi B., Donghi M., Ferrara M., Fiore F., Gardelli C., Gonzalez Paz O., Hazuda D.J., et al. // *J. Med. Chem.* 2008. V. 51. № 18. P. 5843–5855.
16. <http://www.schrodinger.com/products/14/17/>
17. Handzlik J., Bajda M., Zygmunt M., Maciąg D., Dybała M., Bednarski M., Filipek B., Malawska B., Kieć-Kononowicz K. // *Bioorg. Med. Chem.* 2012. V. 20. № 7. P. 2290–2303.
18. Shukla S., Kumar P., Das N., Moorthy N.S., Shrivastava S.K., Trivedi P., Srivastava R.S. // *Med Chem.* 2012. V. 8. № 5. P. 834–845.
19. Ghose A.K., Herbertz T., Hudkins R.L., Dorsey B.D., Malamo J.P. // *ACS Chem. Neurosci.* 2012. V. 3. № 1. P. 50–68.
20. Ghosh P.B., Whitehouse M.W. // *J. Med. Chem.* 1968. V. 11. P. 305–311.
21. Ghosh P.B. // *J. Chem. Soc. B*. 1968. P. 334–338.
22. Terrier F., Croisat D., Chatrousse A.-P., Pouet M.-J., Halle J.-C., Jacob G. // *J. Org. Chem.* 1992. V. 57. P. 3684–3689.
23. Zatsepin T.S., Kachlova A.V., Romanova E.A., Stetsenko D.A., Gait M.J., Oretskaya T.S. *Russian J. Bioorg. Chem.* 2001. V. 27. №1. P. 39–44.
24. Leh H., Brodin P., Bischerour J., Deprez E., Tauc P., Brochon J.-C., LeCam E., Coulaud D., Auclair C., Mouscadet J.-F. // *Biochemistry*. 2000. V. 39. P. 9285–9294.
25. Malet I., Delelis O., Valantin M.A., Montes B., Soulie C., Wiriden M., Tchertanov L., Peytavin G., Reynes J., Mouscadet J.-F., et al. // *Antimicrob. Agents Chemother.* 2008. V. 52. № 4. P. 1351–1358.
26. FDA approves new 4-drug once-a-day HIV treatment // *AIDS Policy Law*. 2012. V. 27. № 11: 1.
27. Delelis, O., Malet, I., Na, L., Tchertanov, L., Calvez, V., Marcelin, A.G., Subra, F., Deprez, E., Mouscadet, J.-F. // *Nucleic Acids Res.* 2009. V. 37. P. 1193–1201.
28. Hare S., Vos A.M., Clayton R.F., Thuring J.W., Cummings M.D., Cherepanov P. // *Proc. Natl. Acad. Sci. USA*. 2010. V. 107. P. 20057–20062.
29. Quashie P.K., Sloan R.D., Wainberg M.A. // *BMC Med.* 2012. V. 10:34
30. Puras Lutzke R.A., Vink C., Plasterk R.H. // *Nucleic Acids Res.* 1994. V. 22. № 20. P. 4125–4131.
31. Smolov M., Gottikh M., Tashlitskii V., Korolev S., Demidyuk I., Brochon J.-C., Mouscadet J.-F., Deprez E. // *FEBS J.* 2006. V. 273. P. 1137–1151.
32. Michel F., Crucifix C., Granger F., Eiler S., Mouscadet J.-F., Korolev S., Agapkina J., Ziganshin R., Gottikh M., Nazabal A., et al. // *EMBO J.* 2009. V. 28. P. 980–991.
33. Krishnan L., Li X., Naraharisetty H.L., Hare S., Cherepanov P., Engelman A. // *Proc. Natl. Acad. Sci. U S A.* 2010. V. 107. № 36. P. 15910–15915.
34. Johnson A.A., Marchand C., Patil S.S., Costi R., Di Santo R., Burke T.R.-Jr., Pommier Y. // *Mol. Pharmacol.* 2007. V. 71. № 3. P. 893–901.
35. Korolev S.P., Tashlitskii V.N., Smolov M.A., Gromyko A.V., Zhuze A.L., Agapkina Yu.Yu., Gottikh M.B. HIV-1 integrase inhibition by dimeric bisbenzimidazoles with different spacers. // *Russian J. Mol. Biol.* 2010. V. 44. №4. P. 718–727.
36. Neamati N., Lin Z., Karki R.G., Orr A., Cowansage K., Strumberg D., Pais G.C., Voigt J.H., Nicklaus M.C., Winslow H.E., et al. // *J. Med. Chem.* 2002. V. 45. № 26. P. 5661–5670.
37. http://www.merck.com/product/usa/pi_circulars/i/isentress/isentress_pi.pdf
38. http://www.ema.europa.eu/docs/en_GB/document_library/EPAR_-_Scientific_Discussion/human/000860/WC500037408.pdf

Recombinant Human Butyrylcholinesterase As a New-Age Bioscavenger Drug: Development of the Expression System

D.G. Ilyushin^{1*}, O.M. Haertley¹, T.V. Bobik¹, O.G. Shamborant¹, E.A. Surina¹, V.D. Knorre¹, P. Masson², I.V. Smirnov¹, A.G. Gabibov¹, N.A. Ponomarenko¹

¹Shemyakin and Ovchinnikov Institute of Bioorganic Chemistry, Russian Academy of Sciences, Miklukho-Maklaya Str., 16/10, Moscow, Russia, 117997

²Département de Toxicologie, Centre de Recherches du Service de Santé des Armées, BP 87, 38702 La Tronche Cedex, France

*E-mail: IlyushinDenis@gmail.com

Received 25.04.2012

Copyright © 2013 Park-media, Ltd. This is an open access article distributed under the Creative Commons Attribution License, which permits unrestricted use, distribution, and reproduction in any medium, provided the original work is properly cited.

ABSTRACT Butyrylcholinesterase (BChE) is a serine hydrolase (EC 3.1.1.8) which can be found in most animal tissues. This enzyme has a broad spectrum of efficacy against organophosphorus compounds, which makes it a prime candidate for the role of stoichiometric bioscavenger. Development of a new-age DNA-encoded bioscavenger is a vital task. Several transgenic expression systems of human BChE were developed over the past 20 years; however, none of them has been shown to make economic sense or has been approved for administration to humans. In this study, a CHO-based expression system was redesigned, resulting in a significant increase in the production level of functional recombinant human butyrylcholinesterase as compared to the hitherto existing systems. The recombinant enzyme was characterized with Elman and ELISA methods.

KEYWORDS bioscavenger; butyrylcholinesterase; CHO cell line; recombinant protein; organophosphorus toxins.

ABBREVIATIONS a.a.r. – amino acid residue; BChE – butyrylcholinesterase; PAGE – polyacrylamide gel electrophoresis; OPT – organophosphate toxin; CHO – Chinese hamster ovary cells; DMEM – Dulbecco's Modified Eagle Medium.

INTRODUCTION

Butyrylcholinesterase (BChE) is a serine hydrolase [EC 3.1.1.8] that has been found in almost all mammalian tissues (in particular, in the lungs, intestine, liver, and blood serum) [1]. The physiological function of BChE has not been determined thus far; however, it is believed to play a key role in maintaining and regulating the activity of neurotransmitter acetylcholine in the central nervous system and neuromuscular endings [2].

BChE can bind stoichiometrically to various acetylcholinesterase-inhibiting toxins. In particular, BChE interacts with organophosphorus compounds, such as sarin, soman, VX and VR gases, as well as with some pesticides. Such data were obtained during experiments on rodents [3] and primates [4]. The animals showed long-term resistance to the action of nerve paralytic agents after intravenous or intramuscular injections of BChE isolated from human serum [5].

Drug therapy methods for treating organophosphorus toxin (OPT) poisoning have been constantly devel-

oping for over 60 years. Yet, all of them are far from perfect. Such methods ensure the survival of a patient but cannot help avoid irreversible brain damage and disability. An alternative approach for treatment and prophylaxis of OPT poisoning is the use of bioscavengers [6]. Antibodies, various functional enzymes, and cyclodextrins, which isolate and inactivate highly toxic compounds before they reach their biological targets, can act as bioscavengers [7]. Among all bioscavengers against OPT, only BChE isolated from human plasma has received the status of a “New development drug” from the FDA: in 2006.

Human butyrylcholinesterase is a glycoprotein composed of four identical subunits. Each subunit consists of 574 amino acid residues and 9 polysaccharide chains. The molecular weight of a BChE subunit is 85 kDa, of which 23.9% is attributed to polysaccharide chains [8]. There are several oligomeric forms of BChE: 95% of the BChE in human plasma exists in the tetrameric form; the remaining 5% is represented with trimeric, dimeric,

and monomeric forms [9]. The BChE heterodimer with serum albumin is occasionally detected [10]. The oligomeric forms of BChE possess identical, specific activity but differ considerably in terms of their pharmacodynamic characteristics [3].

Human butyrylcholinesterase is nowadays isolated from blood plasma. The purification protocol published in 2005 was designed to process 100 l of human blood plasma in a single cycle [4]. According to experts, the annual supply of blood plasma of the USA has to be processed to obtain 1,000 doses of BChE [11]. Moreover, the use of donor plasma may lead to contamination of the drug with dangerous pathogens.

An alternative method consists in obtaining the recombinant protein. Expression in prokaryotic cells is the simplest (in terms of technology) and the most economically sensible method for producing recombinant proteins. However, attempts to express BChE in *Escherichia coli* have turned out unsuccessful [12].

CHO cells are now widely used to obtain correctly folded and functionally active recombinant products. More than 20 recombinant protein drugs have been produced and approved by the FDA over the past 25 years, including α -glucosidase (Myozyme) [13], the anti-hemophilic factor (ReFacto) [14], coagulation factor IX (BeneFIX) [15], interferon- β (Avonex) [16], α -galactosidase (Fabrazyme) [17], erythropoietin A (Eprex, Epogen), etc. A number of technical means (such as roller systems, spinners, and bioreactors allowing production of the target protein to an amount of several grams per liter of culture medium) have been developed in order to ensure efficient expression of recombinant proteins in animal cells [18–20]. In addition, expression efficiency is achieved by using strong promoters, such as the elongation factor 1 α promoter (EF-1) [21] or the cytomegalovirus (CMV) promoter [22].

In 2002, a recombinant, low-glycosylated BChE was obtained in a nonlymphoid CHO cell line [23]. The yield of the target protein produced in roller bottles was 2–5 mg per liter of the growth medium, whereas production levels need to be at least 50–100 mg/l of the growth medium in order to make economic sense.

Beside increasing the production levels of recombinant BChE, researchers are also focusing on obtaining a product with improved pharmacodynamic properties. Peptides of unknown origin with molecular weights ranging from 2072 to 2878 Da and the overall amino acid sequence PSPPLPPPPPPPPPPPPPPPPPPPPPLP have been detected recently as a fragment of human butyrylcholinesterase tetramer. These peptides are believed to play an important role in the formation of the quaternary structure of BChE by binding to the C-terminal domains of its subunits [24]. A proline-rich peptide of

N-terminal domain of the collagen-like protein ColQ (PRAD, proline-rich attachment domain) was demonstrated to play an essential role in BChE oligomerisation: the coexpression of peptide PRAD consisting of 45 a.a.r. and the recombinant BChE in CHO cells increases the production of tetrameric BChE isoforms to 70% [25].

In 2007, the American researchers Huang Y.J. *et al.* managed to produce transgenic goats whose milk contained recombinant BChE. It was demonstrated that 1 liter of milk obtained from the transgenic animals contained 1–5 g of active BChE. However, the obtained enzyme was not glycosylated enough, which greatly reduced its pharmacological activity [26].

In 2010, a group of American, Canadian, and Israeli scientists proposed to express recombinant BChE in transgenic plants [27]. After excessive PEGylation, the pharmacodynamic characteristics of the recombinant enzyme were comparable to those of human plasma BChE. Unfortunately, the clinical use of this drug is complicated as transgenic plants are not allowed by the FDA as a source of recombinant enzymes for therapeutic purposes.

Thus we conclude that, there is no efficient, economically sensible system for the expression of recombinant BChE today. The purpose of this work was to create such an expression system.

EXPERIMENTAL

Reagents and materials

Reagents produced by the following companies were used: Panreac, Amresco and Sigma, (USA); Merck (Germany); DNA plasmid isolation kit, PCR fragment purification kit, Agarose gel DNA extraction kit (Qiagen, USA); restriction enzymes and DNA-modifying enzymes (Fermentas, Lithuania), growth media and components of growth media (Gibco, USA); pcDNA3.1/Hygro, pBudCE4.1 (Invitrogen, USA), pET28a (Novogen, USA) vectors. Plasmids pGS / BChE and pRc/RSV-rQ45 were kindly provided by P. Masson (Centre de Recherches du Service de Santé des Armées, Toxicology Department, La Tronche, France) and O. Lockridge (UNMC, Omaha, USA).

Bacterial strains

The following *E. coli* strains were used: DH5 α , BL21 (DE3) and XL2-Blue (Novagen, USA).

Cell lines

A CHO-K1 cell line (Sigma, USA) utilizing the conventional methods for maintaining animal cell lines was used [28]. The cells were grown in culture flasks or plates in a DMEM medium containing 10% fetal bovine serum and 2 mM L-glutamine in an incubator at 37°C, 5% CO₂.

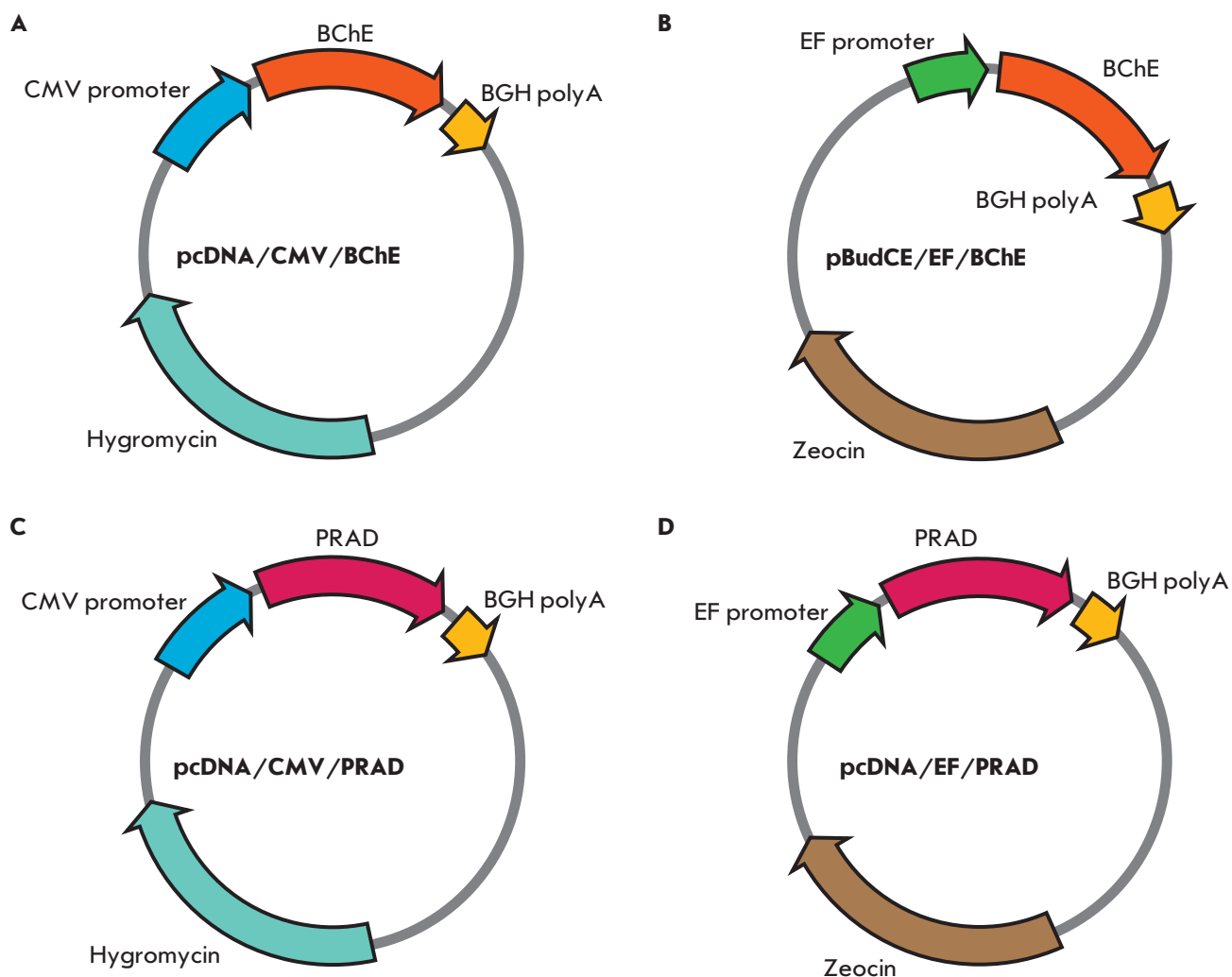


Fig. 1. Expression vectors used in this study. (A) pcDNA/CMV/BChE, (B) pBudCE/EF/BChE, (C) pcDNA/CMV/PRAD, (D) pcDNA/EF/PRAD

Construction of the expression vectors

1) Construction of the expression vector pcDNA/Hygro/CMV/BChE (Fig. 1A).

Plasmid pGS/BChE carrying the DNA fragment encoding human butyrylcholinesterase was treated with the restriction endonucleases *HindIII* and *ApaI*. A 1914-bp-long DNA fragment was purified by electrophoresis in a 1% agarose gel, followed by elution using the QIAquick Gel Extraction Kit and cloning into the dephosphorylated vector pcDNA3.1/Hygro.

2) Construction of the expression vector pBudCE/EF/BChE (Fig. 1B).

In order to obtain this construct, the vector pBudCE4.1 was modified; the DNA fragment corresponding to the CMV promoter was removed, thus allowing one to construct the vector pBudCE/EF. Plasmid

pGS/BChE was treated with restriction endonuclease *BglIII*. The required 1832-bp-long DNA fragment was purified as per the procedure described above and cloned into the similarly digested and dephosphorylated vector pBudCE/EF. Positive clones with the correct orientation of the fragments were determined by PCR using primers 1 and 2 (Table 1).

3) Construction of the expression vector pcDNA/CMV/PRAD (Fig. 1C).

Plasmid pRc/RSV-rQ45 [29] containing a sequence encoding the PRAD peptide and FLAG epitope was treated with the endonucleases *HindIII* and *XhoI*. A 252-bp-long fragment was purified by electrophoresis in a 10% polyacrylamide gel, followed by electroelution and cloning into the predigested and dephosphorylated vector pcDNA3.1/Hygro.

Table 1. Oligonucleotide primers used for cloning

Primer 1	TCA AGC CTC AGA CAG TGG TTC
Primer 2	GAA GAA GCT TGT ACA ATA TGC ATA GCA AAG TCA CAA TC
Primer 3	AAG TGG TTC CTT TAA TGC TCC T
Primer 4	ATA TGC GGC CGC TCA TTC TAA GAC ACT TGA TTA TTT CAG T
Primer 5	ATA TGC TAG CGA AGA TGA CAT CAT AAT TGC AAC A
Primer 6	ATA TGC GGC CGC TCA CAG AAA CTT GCC ATC ATA AAC ATG
Primer 7	ATA TGC TAG CGC TCG GGT TGA AAG AGT TAT TGT

4) Construction of the expression vector pcDNA/EF/PRAD (Fig. 1D).

Plasmid pBudCE/EF containing the EF promoter was treated with restriction endonuclease BglII. The digested DNA was filled in using DNA polymerase I Large (Klenow) Fragment; the reaction mixture was treated with endonuclease NheI. A 1223-bp-long fragment was purified by electrophoresis in a 1% agarose gel, followed by electroelution. Plasmid pcDNA/CMV/PRAD was treated with restriction endonuclease *HindIII*, filled in using DNA polymerase I Large (Klenow) Fragment, and the reaction mixture was treated with endonuclease SpeI. The vector obtained was purified as per the procedure described above, dephosphorylated and ligated with the previously obtained DNA fragment corresponding to the EF promoter.

5) Construction of the expression vectors pET28-C, pET28-N1 and pET28-N2 (Fig. 3A).

The nucleotide sequences encoding the C-terminal fragment of BChE (322 a.a.r.) and two fragments of the N-terminal peptide of BChE-N1 and N2 (133 and 119 a.a.r., respectively) were obtained by PCR. Plasmid pGS/BChE was used as a template. The following primer pairs were used in the reaction: fragment C – primers 3 and 4, fragment N1 – primers 5 and 6, fragment N2 – primers 7 and 8 (Table 1). The PCR products C, N1 and N2 were treated with the restriction endonucleases *NheI* and *NotI*, followed by cloning into the pET28a vector (digested and dephosphorylated) in the same fashion, yielding the expression vectors pET28-C, pET28-N1 and pET28-N2, respectively.

Electrocompetent DH5 α or XL2-Blue strain *E. coli* cells were transformed using ligation mixtures. The primary screening of clones from colonies was performed by PCR. The plasmids isolated from positive clones were further characterized by restriction analysis. The correctness of the assembly of expression vectors and constructs was confirmed by Sanger sequencing. Preparation of electrocompetent cells, transformation, and

treatment with restriction enzymes, ligation, PCR and DNA electrophoresis were performed in accordance with the standard procedures [30, 31]. The plasmids were isolated according to [32].

Expression and purification of the recombinant BChE peptides

BL21(DE3) strain *E. coli* cells were transformed with the vectors pET28-C, pET28-N1 or pET28-N2 by electroporation. The BChE peptides encoded by plasmids contained six histidine residues at the C-terminus, which enabled their isolation using metal-chelate affinity chromatography.

The cells were cultured at 37°C to OD₆₀₀ = 0.6, followed by induction with an isopropylthio- β -D-galactoside (IPTG) solution added to a concentration of 1mM. Six hours after the induction, the cells were centrifuged at 5000 rpm for 10 min; the precipitate was re-suspended in a buffer containing 50 mM Tris-HCl pH 8.0, 2 mM EDTA, and 0.1% Triton X-100 in 10% of the initial volume.

All the recombinant BChE polypeptides were expressed in the insoluble form. Lysozyme was added to the cell suspension until a final concentration of 0.1 mg/ml, followed by incubation at 30°C for 15 min under constant stirring to obtain a fraction of the inclusion bodies. MgCl₂ and DNase were then added to the lysate until concentrations of 8 mM, and 0.1 mg/ml, respectively. Cell lysate was centrifuged for 15 min at 13000 rpm. The precipitate containing the insoluble protein fraction was consecutively washed in solutions containing 50 mM Tris-HCl pH 8.0, 150 mM NaCl, 1% Triton X-100, 50 mM Tris-HCl pH 8.0, 150 mM NaCl, 2 M urea and 50 mM Tris-HCl pH 8.0, 150 mM NaCl, 8 M urea. The resulting fractions were analyzed by protein electrophoresis in 15% PAGE under reducing conditions. Polypeptides C and N1 were detected in the fraction containing 2 M urea; polypeptide N2 was detected in the insoluble protein fraction.

The N1 and C polypeptides were then purified by metal-chelate affinity chromatography under denaturing conditions using IMAC Sepharose 6FF resin (GE Healthcare, USA) in accordance with standard manufacturer's instructions. The eluates were dialyzed against water produced on a mQ installation (Millipore, USA); the precipitate was pelleted by centrifugation and re-suspended in 50% aqueous ethanol to obtain a finely dispersed suspension.

Polypeptide N2 was purified by repeated washing of the insoluble fraction with a solution containing 50 mM Tris-HCl pH 8.0, 150 mM NaCl, 8 M urea, and 1 mM β -mercaptoethanol. The precipitate was dialyzed against water produced on the mQ installation (Millipore, USA), precipitated by centrifugation and re-suspended in 50% aqueous ethanol to produce a finely dispersed suspension.

Immunization of mice using full-length human plasma BChE

BALB/c mice were obtained from the Harlan nursery (UK) and kept in the vivarium of the Pushchino Branch of the Institute of Bioorganic Chemistry (Russian Academy of Sciences), under sterile conditions minimizing contact of the immune system with external antigens (Specific Pathogen-Free status). The age of mice ranged from 6 to 8 weeks. Immunization was carried out by administering 100 μ g of BChE per mice in a complete Freund's adjuvant twice at weekly intervals. Booster immunization of mice was performed intraperitoneally 3 days prior to splenocyte collection by administering 50 mg of BChE in phosphate-buffered saline (PBS) per mice.

Production of mouse monoclonal antibodies

Monoclonal antibodies were obtained by the standard methods using cell hybridomas and ascites [33, 34]. Monoclonal antibodies were purified by affinity chromatography on resin HiTrap Protein-A (GE Healthcare, USA) according to the manufacturer's procedure. Biotinylation of the antibodies was performed using NHS-biotin (GE Healthcare, USA), in accordance with the manufacturer's methodology.

Immunization of rabbits with recombinant polypeptides BChE

Immunization of rabbits was carried out in the vivarium of the Institute of Bioorganic Chemistry, Russian Academy of Sciences. The recombinant polypeptides N1 and N2 of BChE were administered subcutaneously as follows: the first injection contained a suspension of the peptide in a complete Freund's adjuvant, the second injection (after 28 days) contained a suspension of the peptide in an incomplete Freund's adjuvant, and the third injection (after 14 days) contained a suspension of the peptide in an

incomplete Freund's adjuvant. Each animal was injected with 200 μ g of the peptide. Seven days following the immunization, a total of 10 ml of blood was collected from the ear vein of each animal to obtain a blood serum. The antibody titers were determined by indirect ELISA.

Immunoenzyme assay (ELISA)

Various ELISA methods using conventional testing protocols were used in the present work [33, 34].

1) Indirect ELISA was used to determine the antibody titer. For this purpose, 96-well plates MaxiSorp (Nunc, USA) were used to adsorb the purified human plasma BChE, and monoclonal antibodies were subsequently introduced to BChE in various dilutions, or human BChE peptides were adsorbed onto plates, followed by the introduction of monoclonal antibodies or polyclonal rabbit sera in various dilutions. The complex was detected using anti-goat antibodies conjugated with horseradish peroxidase.

2) Competitive ELISA was used to search for a pair of monoclonal anti-human BChE antibodies. For this purpose, 96-well plates MaxiSorp (Nunc, USA) were used to adsorb human plasma BChE and were subsequently incubated with monoclonal anti-BChE antibodies in various dilutions in the presence of 10 ng/ml biotinylated monoclonal antibody 4C6D8. The interaction was detected using a streptavidin-HRP conjugate. The starting concentration of the test antibodies was 100 ng/ml.

3) Sandwich ELISA was performed to determine the BChE concentration. The monoclonal antibodies 4C6D8 were adsorbed onto 96-well plates MaxiSorp (Nunc, USA) and incubated with the BChE samples denatured under various conditions (*Fig. 3B*). The interaction was detected using polyclonal anti-N1 BChE rabbit serum (titer 1:1000). Anti-goat antibodies conjugated with horseradish peroxidase were used to detect the reaction.

Transfection of eukaryotic cells by lipofection

Prior to the transfection, impurities and salts were removed from the plasmid DNAs, which were preliminarily linearized using the restriction endonuclease PvuI and BglII (in the case of the vector pcDNA/EF/PRAD). The lipofection was performed using Lipofectamine™ Reagent and Plus™ Reagent (Invitrogen, USA) according to the manufacturer's recommendations.

EXPRESSION OF RECOMBINANT BChE BY THE CHO CELLS

The cells were cultured in flasks in DMEM containing a 2% fetal bovine serum and 2 mM L-glutamine at 37°C, 5% CO₂ (25 cm²). After the 50–70% monolayer was achieved, the conditioned growth medium was re-

moved and the cells were washed with an equal volume of sterile $1 \times$ PBS, followed by the addition of an equal volume of the protein-free growth medium Peptotech (Peptotech, USA), EX-Cell (Sigma, USA) or ProCHO4 (Lonza, Switzerland). The cells were then incubated in a protein-free growth medium for 5 days at 37°C and 5% CO_2 . Every 24 hours, a sample of the culture medium was taken to determine the content of the active form of butyrylcholinesterase by Ellman's test.

Determining the content of the active form of human BChE by Ellman's test [35]

The culture liquid ($50 \mu\text{l}$) was mixed with $100 \mu\text{l}$ of sterile $1 \times$ PBS, $100 \mu\text{l}$ of the resulting solution was transferred into a well of the 96-well plate. Butyrylcholinesterase isolated from human plasma (Sigma, USA) was used as a control to build the calibration curve. Prior to taking measurements, a $100 \mu\text{l}$ solution of $50 \mu\text{M}$ dithionitrobenzoic acid and $100 \mu\text{M}$ butyrylthiocholine iodide in $1 \times$ PBS were introduced into the wells containing the samples and controls. The measurements were performed on a TECAN GENios instrument at a wavelength of 405 nm .

Purification of the recombinant human BuChE from the growth medium

The growth medium containing CHO cells was centrifuged at $800 g$ for 5 min to remove cells and at $3500 g$ for 15 min to remove cellular debris. The supernatant was filtered through Millipore HPWH membranes with a pore diameter of $0.22 \mu\text{m}$ to remove residual impurities. The purified supernatant was ultra concentrated 3 times using Pellicon PLCTK30 membranes (Millipore, USA), followed by dilution with the coating buffer (a 50 mM potassium phosphate buffer, $\text{pH } 7.2$, 1 mM EDTA). The resulting concentrated medium was applied to the Procainamide-Sepharose 4B affinity resin [4] in the recirculation mode at a speed of 0.5 ml/min overnight at $+4^\circ\text{C}$. The recombinant BChE was eluted from the resin using a NaCl gradient ($0\text{--}500 \text{ mM}$, 15 column volumes) at a flow rate of 0.5 ml/min . The resulting protein fraction was concentrated on Centricon 10 membranes (Millipore) and additionally purified by gel filtration on a Superdex 200 column (GE Healthcare).

Determination of the content of BChE isoforms by Karnovsky's method [36]

Electrophoretic separation of proteins under native conditions was carried out using the standard Laemmli method [31] with minor modifications. An aqueous stock solution with a 29:1 ratio of acrylamide- N,N,N',N' -methylene-bisacrylamide was used to prepare the gel. The concentrating (upper) 4% gel was prepared in 0.125

M Tris-HCl, $\text{pH } 6.9$. The separating (lower) 8% gel was prepared in 0.125 M Tris-HCl, $\text{pH } 8.8$. Electrophoretic separation was carried out in a buffer containing 50 mM glycine, 5 mM Tris-HCl $\text{pH } 8.0$. The samples were loaded on a buffer containing 10% glycerol, 0.2 M Tris-HCl $\text{pH } 7.5$. Electrophoresis in a concentrating gel was performed at a current of $8\text{--}10 \text{ mA}$ per gel plate and in the separating gel at $15\text{--}20 \text{ mA}$. After the proteins were separated in a nondenaturing polyacrylamide gel, the gel plate was transferred into a solution containing 125 mM NaOH, 125 mM maleic acid, 11.6 mM sodium citrate, 10 mM CuSO_4 , $550 \mu\text{M}$ potassium hexacyanoferrate (III), and 2 mM butyrylthiocholine iodide. The gel was incubated in the solution on an orbital shaker at room temperature for $3\text{--}8 \text{ h}$.

Determination of the kinetic constants of recombinant BChE by Ellman's test

A modified Ellman's reaction was used to determine the kinetic constants. A known amount of BChE was added into a solution containing 1 mM dithionitrobenzoic acid in a 0.1 M potassium phosphate buffer $\text{pH } 7.2$; the butyrylthiocholine iodide concentration was varied from $10 \mu\text{M}$ to 1 mM . The number of BChE active sites was determined by titration in diisopropylfluorophosphate (DFP). The reaction was carried out at 25°C ; the absorbance was recorded at 412 nm .

RESULTS AND DISCUSSION

Development of a recombinant human butyrylcholinesterase expression system

The aim of our work was to construct an efficient recombinant human BChE expression system. Since BChE is intended for prophylaxis and treatment of OPT exposure, the CHO line cells were selected as well studied and approved by the FDA recombinant protein expression system.

In order to select a promoter that would provide the most efficient production of BChE, the CHO cell line was transfected via lipofection of the circular plasmid DNA vectors with pGS/BChE [37], pcDNA/CMV/BChE (Fig. 1A) and pBudCE/EF/BChE (Fig. 1B), which carry the human butyrylcholinesterase gene under the control of various promoters. Samples of the culture media were collected to determine the content of the active form of BChE using Ellman's test 48 and 72 h following the lipofection. Conditioned medium of the CHO cells line grown under the same conditions as transfectomas were used as the control. The results shown in Fig. 2A demonstrate that the expression levels of the vectors pGS/BChE and pcDNA/CMV/BChE were comparable and were equal to approximately $0.2 \mu\text{g/ml}$, whereas the expression level of pBudCE/EF/BChE was almost

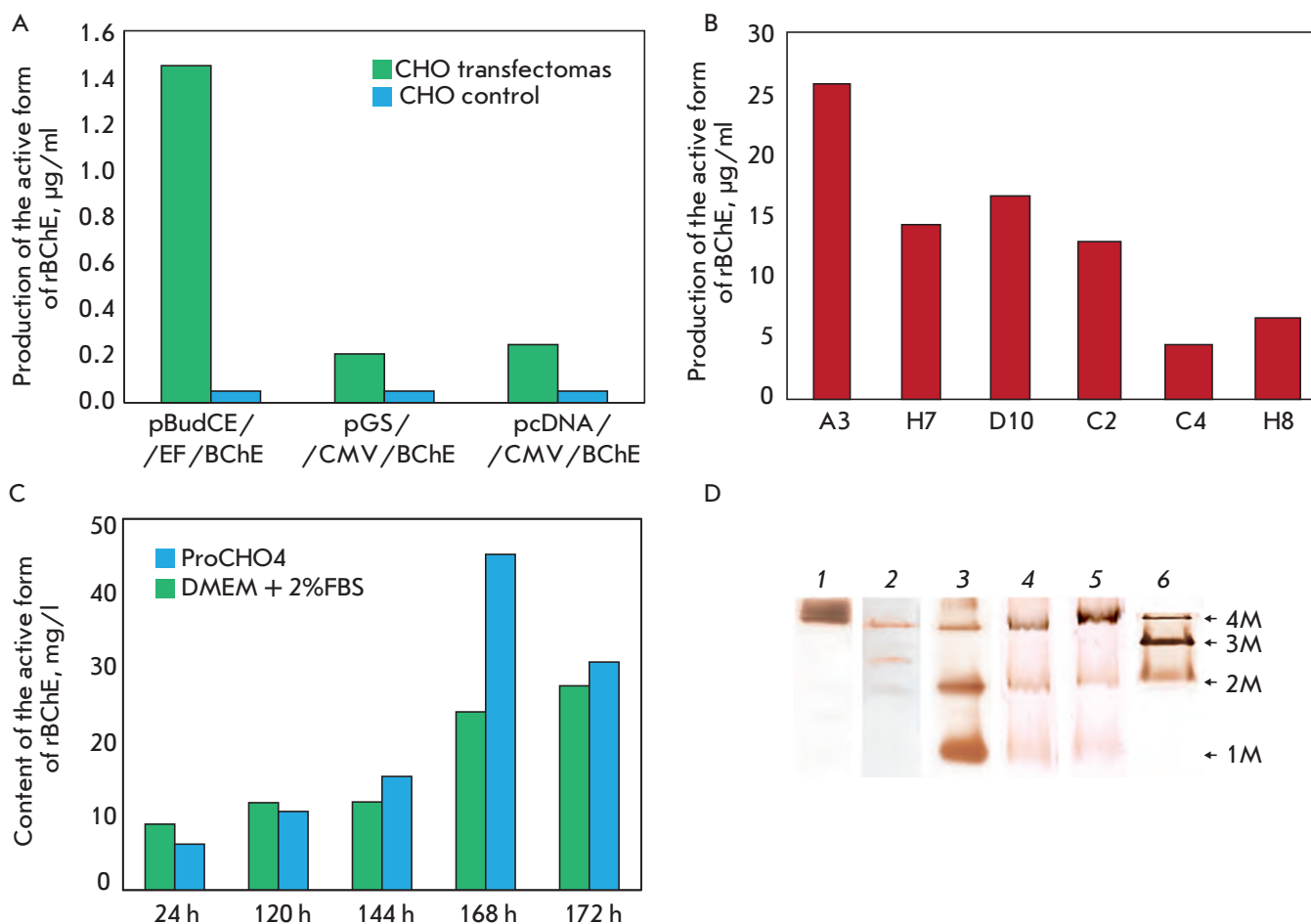


Fig. 2. (A) Analysis of the transient transfection of CHO cells with the BChE-containing expression vectors pBudCE/EF/BChE, pGS/CMV/BChE and pcDNA/CMV/BChE. (B) Analysis of recombinant BChE produced by CHO monoclonal cells after stable transfection with a linearized pBudCE/EF/BChE vector. (C) 8% Native PAGE stained by Karnovsky's method. 1 – Human plasma, 2 – Purified human BChE, 3 – cultural medium of A3 clone, 4 – cultural medium of A3 clone transfected with pcDNA/CMV/PRAD, 5 – clone transfected with pcDNA/EF/PRAD, 6 – cultural medium of A3H9 clone; 4M – tetramer, 3M – trimer, 2M – dimer, 1M – monomer

an order of magnitude higher (1.45 µg/ml). Thus, the vector pBudCE/EF/BChE containing the BChE gene under the control of the EF-1 promoter (elongation factor 1) was the most promising construct.

Plasmid DNA of the vector pBudCE/EF/BChE was linearized and transfected via lipofection into the CHO cells in order to obtain stable expression clones. The cells were spread over 24-well plates (1:12) to obtain stable transfectomas 72 h after the lipofection. The selection was performed using Zeocin, which was added to the growth medium at a concentration of 600 µg/ml. After the selection and analysis, the cells were spread over the 96-well plates to obtain monoclonal cells. The production of an active form of BChE at all stages was determined using Ellman's test. Af-

ter a comparative analysis of the BChE expression (Fig. 2B) the clone A3 was selected for further manipulations. The A3 clone proved a stable producer of recombinant BChE in five generations. The next step was to adapt this clone to produce BChE using special protein-free media.

A number of special culture media were tested, including Peprtech (Peprtech), EX-Cell (Sigma), and ProCHO4 (Lonza, Switzerland). In order to adjust the expression conditions, the cells of clone A3 were pre-cultured in a DMEM medium containing 2% fetal bovine serum. After the cells reached a 70–90% monolayer, the medium was replaced with one of the tested protein-free media, and the cells were incubated for several days. Incubation in Peprtech and EX-Cell media re-

sulted in cell death on the 1st or 2nd day of incubation. These media were deemed unsuitable for this monoclonal. During cell incubation in a ProCHO4 medium, a significant increase in rBChE output was observed by the 96th hour of incubation (4 days) (*Fig. 2C*). A decrease in BChE activity on the 5th day can be attributed to the proteolytic activity caused by cell death.

The analysis of the oligomeric composition of rBChE produced by clone A3/CHO using Karnovsky's method (*Fig. 2D, 3*) demonstrated that rBChE was primarily present in the monomeric form, and that the amount of the tetrameric form was minimal. The BChE tetramer is of interest from the pharmacological point of view, since its half-elimination time is 3 to 4 days, while that of the monomer is several hours [4]. It was previously demonstrated that the amount of the tetramerized product increased during the co-expression of the BChE and PRAD peptides (collage-like protein ColQ domain) [37]. Furthermore, addition of a chemically synthesized peptide (a component of BChE) to the growth medium results in tetramerization of the recombinant protein [24]. PRAD peptides and the proline-rich peptide of BChE are very similar in terms of their structure and, therefore, can have similar properties. However, the synthesis of peptides containing tandem proline residues is complicated and characterized by a low yield, and is unprofitable under conditions of biotechnological production. Hence, we decided to use the co-expression of BChE and the PRAD peptide under the control of different promoters. For this purpose the expression vectors pcDNA/CMV/PRAD (*Fig. 1C*) and pcDN/EF/PRAD (*Fig. 1C*) carrying PRAD under the control of the EF or CMV promoter were transfected into the cells of clone A3 by lipofection. 72 h following the transfection, the presence of the tetrameric form of BChE in the medium was controlled electrophoretically using Karnovsky's method. The cells of clone A3, which were transfected with plasmid pcDNA3.1/EF/PRAD, were selected based on the results of the analysis (*Fig. 2D, 4, 5*). The use of the EF promoter in this case allows one to obtain cells capable of producing the tetrameric form of BChE in larger quantities. The expression vector pcDNA/EF/PRAD was linearized using restriction endonuclease *BglIII* and transfected into the cells of clone A3 by lipofection in order to obtain stable producer clones. The selection was carried out by adding 1.5 mg/ml of hygromycin B and 600 µg/ml of Zeocin to the growth medium. After the selection and analysis, the cells were spread over the 96-well plates to obtain monoclonal. Production of BChE isoforms by the monoclonal was determined using Karnovsky's method; the clone A3H9 was selected based on the results. Following the optimization of expression conditions in the ProCHO4 growth medium (Lonza), a stable producer clone, A3H9, characterized by the production of tetra-

meric and dimeric forms of BChE and complete absence of monomer production was obtained in accordance with the previously described scheme (*Fig. 2D, 6*).

Development of a system for detecting and assessing the production of the recombinant protein

In the present work, the evaluation of the efficiency of the transfection and selection of the CHO cell line clones producing recombinant BChE was conducted with respect to the functional activity of the enzyme using Ellman's [35] and Karnovsky's [36] methods. These techniques are based on the ability of BChE to hydrolyze butyrylthiocholine, which makes them inapplicable in cases when BChE is inactive or inhibited [38, 39].

It is a well-known fact that high-level expression of recombinant products in eukaryotic cells is sometimes accompanied by a decrease in their specific activity (i.e. production of a certain amount of inactive protein). This can be often attributed to the fact that the system of post-translational modifications of a cell cannot cope with the amount of protein produced; hence, inactive products are formed, which are either misfolded, or contain uncleaved propeptide, or other defects. Such problems can be resolved by co-expression of the product with the required chaperones or the enzymes involved in post-translational modifications [40–44]. Thus, it was critical to measure the specific activity of the enzyme during expression.

Thus, our task was to develop a system of direct assessment of the BChE content in the samples. The system was planned to be used to characterize recombinant BChE, quantitatively detect inactive BChE in the growth medium, and to determine the specific activity of the enzyme during purification. The sandwich – ELISA assay is the simplest and most informative method that can be used to determine the concentration of protein in the samples. The analysis of the commercially available anti-human BChE antibodies demonstrated that pairs of noncompeting monoclonal antibodies which can be used to perform sandwich ELISA have not been produced yet.

The sequences corresponding to the C- and N-terminal fragments of BChE (*Fig. 3A*): C (322 a.a.r.), N1 and N2 (133 and 119 a.a.r.) were produced using the prokaryotic expression system and purified. The monoclonal anti-BChE (full-length human) antibodies 3C6D8, 1A1F1, 1B4F4, 1B4D12, 1A1F7, 4C6D8 and 1A1D11 were obtained using the conventional procedures [33]. Competitive ELISA demonstrated that all the antibodies interacted with the C-terminal region of BChE, while competing with each other (*Fig. 3B*). Western hybridization using BChE fragments confirmed the ELISA results (data not shown). In order to overcome the existing problem, polyclonal rabbit sera

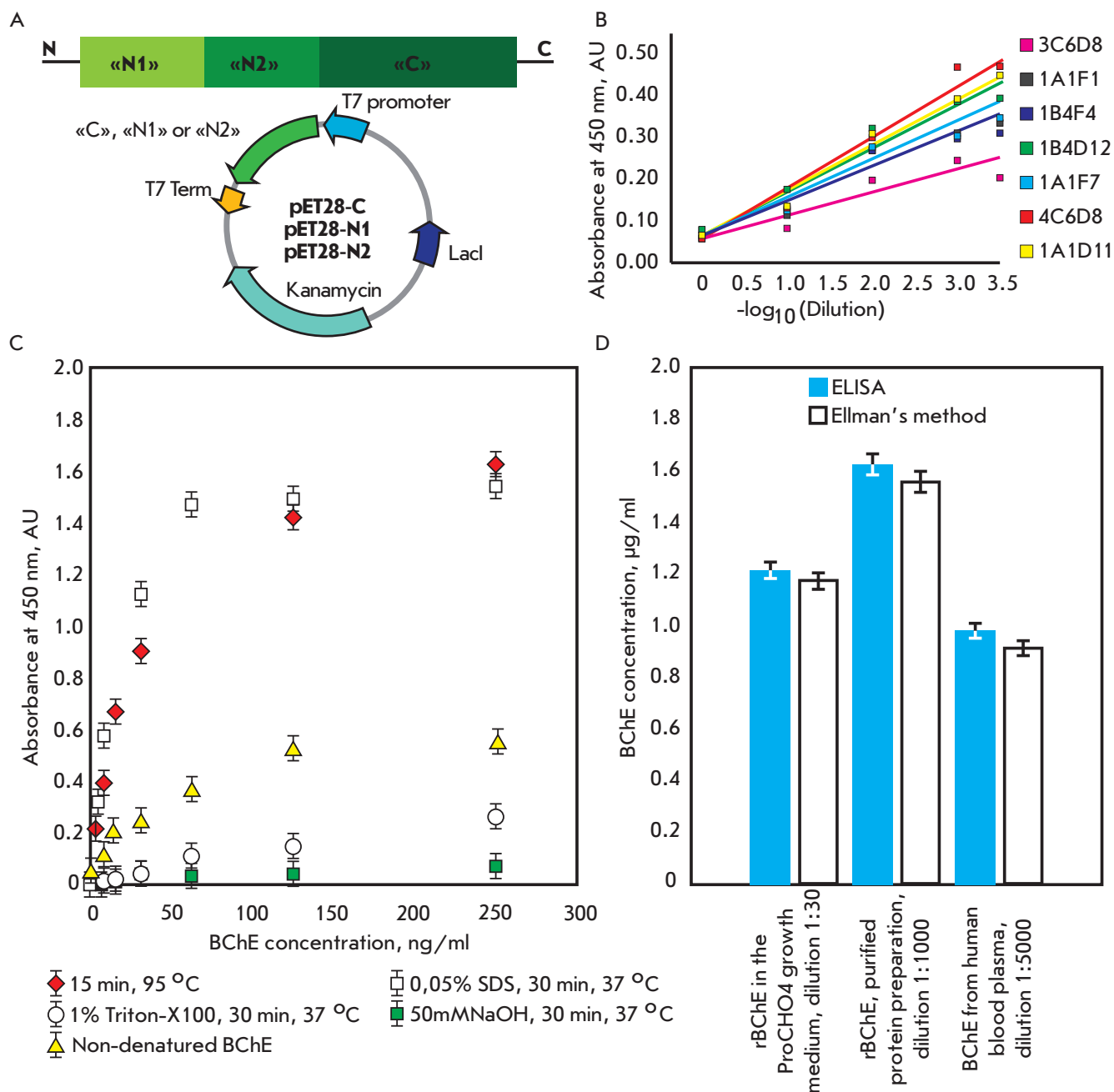


Fig. 3. (A) Expression vectors pET28-C, pET28-N1 and pET28-N2 encoding the respective polypeptides of human BChE (B) Competitive ELISA of anti-BChE mouse monoclonal antibodies. The X-axis represents $-\log_{10}(\text{Dilution})$; starting antibody concentration was 100 ng/ml. All antibodies were tested in pair with the biotinylated 4C6D8 antibody. (C) Determination of the most appropriate method for recombinant BChE denaturation for elaboration of the sandwich ELISA (D) Analysis of the BChE concentration using the Ellman and sandwich ELISA methods gives similar values

were obtained using the BChE recombinant polypeptide fragments N1 and N2 as antigens. Identical titers of antibodies against both N-terminal fragments of BChE were detected in sera using ELISA. However, higher ability to bind to full-length BChE was demonstrated by the anti-N1 antibodies. Despite the high

level of specific interaction between the antibodies and BChE during the indirect ELISA, the maximum signal during sandwich ELISA did not exceed 0.6 rel. units. A hypothesis was put forward that partial denaturation of the antigen would increase the availability of the epitopes and thereby increase the sensitivity of the

Table 2. Purification of the recombinant BChE from the growth medium

Extraction phase	General BChE activity, AU	Yield, %	Total amount of BChE, mg	Specific activity, AU/mg
Culture medium	915	100	2.03	451
Culture concentrate	890	97	1.96	454
Column effluent from affinity chromatography	825	90	1.81	456
Gel filtration, 21 min fraction	650	71.5	1.41	461

method. Among the tested techniques for denaturing BChE (heating, adding detergents or alkali), incubation at 95°C for 15 min turned out to be the most efficient (Fig. 3C). Based on the results of the analysis, the antibody 4C6D8 was selected from a panel of monoclonal antibodies. It showed the highest sensitivity when combined with polyclonal rabbit anti-N1-polypeptide antibodies.

A quantitative method for determining the BChE content in samples of the culture medium, purified preparations, and human plasma was developed. The comparison of the BChE concentration in the samples determined using this method with the results obtained using Ellman's method demonstrated that over 95% of the BChE expressed by clone A3H9 into the growth medium exhibited enzymatic activity (Fig. 3D).

Isolation and functional analysis of the purified rBChE

rBChE was purified from the growth medium in order to study its functional activity. The developed purification protocol included such stages as ultrafiltration, concentration, affinity purification, and gel filtration. A sample was selected for each purification stage, was analyzed for content of the active form of BChE by Ellman's test, and total amount of recombinant enzyme by ELISA. The analysis data are listed in Table 2. The final yield of the protein obtained with a purity of 95% (according to the electrophoresis) was about 70%.

The kinetic parameters of the purified recombinant BChE were determined using BTC within a concentration range of 10 to 1000 μM at an enzyme concentration of 5 nM. The individual kinetic parameters of the BTC hydrolysis reaction were calculated based on these data (Table 3). The comparison of the kinetic constants of rBChE and BChE isolated from human plasma demonstrated that the K_M values were identical within the calculation error and were equal to 25 and 23 μM [37], respectively. The constants k_2 (49200 and 39900 min^{-1} , respectively) were only slightly different,

which apparently is associated with the methods used to determine the concentration of the active sites of the enzymes under study. It has also been determined that butyrylcholinesterase isolated from human blood plasma is characterized by substrate activation in reactions with compounds of choline series. A similar effect is also observed in the case of the hydrolysis of butyrylcholine iodide of the recombinant BChE at substrate concentrations higher than 500 μM . This allowed to carry out estimation of the constant K_{ss} and parameter b . Parameter b for recombinant BChE did not differ (2.4 \pm 0.27) from the standard value of 2.5 \pm 0.1 [37] considering the error. Thus, it can be concluded that the obtained recombinant BChE is functionally active, and that the structure of the active site is identical in the natural and recombinant molecules of the enzyme.

CONCLUSIONS

This study allowed us to construct an efficient system for the expression of active human butyrylcholinesterase in CHO cells. The use of the EF-1 promoter made it possible to significantly increase production of the recombinant protein (from 3–5 to 40 mg/l). The calculated kinetic constants indicate that the active site of the enzyme is intact. The analysis of the isoforms

Table 3. Kinetic constants of hydrolysis of the recombinant BChE butyrylthiocholine iodide and BChE isolated from human blood plasma

Constant	rBChE	BChE isolated from human plasma [37]
$K_M, \mu\text{M}$	25 \pm 1	23 \pm 2
k_{cat}, min^{-1}	49200 \pm 800	39900 \pm 1800
$K_{ss}, \mu\text{M}$	250 \pm 30	140 \pm 20
b	2.4 \pm 0.2	2.5 \pm 0.1

of rBChE in the growth medium showed that the enzyme is mainly produced in the dimeric and tetrameric forms.

The developed ELISA technique allowed us to quantitatively assess the BChE content in samples of these culture medium, the purified enzyme, and in human plasma. The comparison of the BChE concentrations in the samples with those obtained using Ellman's method demonstrated that over 95% of the BChE expressed by the A3H9 clone was active and that the specific activity of rBChE was not reduced during purification.

The next phase of the work will be focused on further improvement of the pharmacodynamic properties of the recombinant enzyme by chemical modifications,

such as PEGylation [45] or sialylation [46]. ●

The authors are grateful to Prof. Oksana Lockridge (UNMC, Omaha, USA) for generously providing the vectors pGS/CMV/BChE and pRc/RSV-rQ45.

This work was supported by the Russian Foundation for Basic Research (grant № 10-04-00673-a), the Federal Target-oriented Program (№ 2046.2012.4) of the Scientific School "The Chemical Foundations of Biocatalysis", the Program of the Presidium of RAS № 24 "Nanotechnologies and Nanomaterials," and the Foundation for assistance to small enterprises in the field of science and technology (Program "U.M.N.I.K.").

REFERENCES

- Jbilo O., L'Hermite Y., Talesa V., Toutant J.P., Chatonnet A. // *Eur. J. Biochem.* 1994. V. 225. P. 115–124.
- Mesulam M. // *Neuroscience.* 2002. V. 110. P. 627–639.
- Saxena A., Sun W., Fedorko J.M., Koplovitz I., Doctor B.P. // *Biochem. Pharmacol.* 2011. V. 81. P. 164–169.
- Lockridge O., Schopfer L.M., Winger G., Woods J.H. // *J. Med. Chem. Biol. Radiol. Def.* 2005. V. 3. P. 1–23.
- Raveh L. // *Toxicol. Appl. Pharmacol.* 1997. V. 145. P. 43–53.
- Patrick M., Daniel R. // *Acta Naturae.* 2009. V. 1. № 1. P. 68–78.
- Masson P., Nachon F., Broomfield C.A., Lenz D.E., Verdier L., Schopfer L.M., Lockridge O. // *Chem. Biol. Interact.* 2008. V. 175. P. 273–280.
- Lockridge O., Bartels C.F., Vaughan T.A., Wong C.K., Norton S.E., Johnson L.L. // *J. Biol. Chem.* 1987. V. 262. P. 549–557.
- Lenz D.E., Yeung D., Smith J.R., Sweeney R.E., Lumley L.A., Cerasoli D.M. // *Toxicology.* 2007. V. 233. P. 31–39.
- Masson P., Carletti E., Nachon F. // *Protein Pept. Lett.* 2009. V. 16. P. 1215–1224.
- Geyer B.C., Kannan L., Cherni I., Woods R.R., Soreq H., Mor T.S. // *Plant Biotechnol. J.* 2010. V. 8. P. 873–886.
- Masson P., Steve A., Philippe P.-T., Oksana L. // *Multidisciplinary approaches to cholinesterase functions. Expression and refoldin of functional human butyrylcholinesterase in E. coli.* N.Y.: Plenum Press, 1992.
- Kishnani P.S., Corzo D., Nicolino M., Byrne B., Mandel H., Hwu W.L., Leslie N., Levine J., Spencer C., McDonald M., et al. // *Neurology.* 2007. V. 68. P. 99–109.
- Schwartz R.S., Abildgaard C.F., Aledort L.M., Arkin S., Bloom A.L., Brackmann H.H., Brettler D.B., Fukui H., Hilgartner M.W., Inwood M.J. // *N. Engl. J. Med.* 1990. V. 323. P. 1800–1805.
- White G.C., Beebe A., Nielsen B. // *Thromb. Haemost.* 1997. V. 78. P. 261–265.
- Jacobs L.D., Cookfair D.L., Rudick R.A., Herndon R.M., Richert J.R., Salazar A.M., Fischer J.S., Goodkin D.E., Granger C.V., Simon J.H., et al. // *Ann. Neurol.* 1996. V. 39. P. 285–294.
- Barngrover D. // *J. Biotechnol.* 2002. V. 95. P. 280–282.
- Tabuchi H., Sugiyama T., Tanaka S., Tainaka S. // *Biotechnol. Bioeng.* 2010. V. 107. P. 998–1003.
- Porter A.J., Dickson A.J., Racher A.J. // *Biotechnol. Progr.* 2010. V. 26. P. 1446–1454.
- Strnad J., Brinc M., Spudić V., Jelnicar N., Mirnik L., Carman B., Kravanja Z. // *Biotechnol. Progr.* 2010. V. 26. P. 653–663.
- Mizushima S., Nagata S. // *Nucl. Acids Res.* 1990. V. 18. P. 5322.
- Boshart M., Weber F., Jahn G., Dorsch-Häsler K., Fleckenstein B., Schaffner W. // *Cell.* 1985. V. 41. P. 521–530.
- Nachon F., Nicolet Y., Viguie N., Masson P., Fontecilla-Camps J.C., Lockridge O. // *Eur. J. Biochem.* 2002. V. 269. P. 630–637.
- Li H., Schopfer L.M., Masson P., Lockridge O. // *Biochem. J.* 2008. V. 411. P. 425–432.
- Altamirano C.V., Lockridge O. // *Biochemistry.* 1999. V. 38. P. 13414–13422.
- Huang Y.-J., Huang Y., Baldassarre H., Wang B., Lazaris A., Leduc M., Bilodeau A.S., Bellemare A., Côté M., Herskovits P., Touati M., Turcotte C., Valeanu L., et al. // *Proc. Natl. Acad. Sci. USA.* 2007. V. 104. P. 13603–13608.
- Geyer B.C., Kannan L., Garnaud P.-E., Broomfield C.A., Cadieux C.L., Cherni I., Hodgins S.M., Kasten S.A., Kelley K., Kilbourne J., Oliver Z.P., Otto T.C., Puffenberger I., et al. // *Proc. Natl. Acad. Sci. USA.* 2010. V. 107. P. 20251–20256.
- Freshney R.I. *Culture of animal cells.* Oxford, N.Y.: Wiley-Blackwell, 2005. P. 642.
- Duysen E.G., Bartels C.F., Lockridge O. // *J. Pharmacol. Exp. Ther.* 2002. V. 302. P. 751–758.
- Sambrook J., Russell D.W. *Molecular Cloning.* Cold Spring Harbor, N.Y.; Cold Spring Harbor Lab. Press, 2001.
- Sambrook J., Fritsch E.F., Maniatis T. *Molecular Cloning: A Laboratory Manual.* Cold Spring Harbor, N.Y.; Cold Spring Harbor Lab. Press, 1989.
- Schlesinger N., Baker D.G., Schumacher H.R. // *J. Rheumatol.* 1997. V. 24. P. 1018–1019.
- Harlow E., Harlow E., Lane D. *Antibodies: A Laboratory Manual.* Cold Spring Harbor, N.Y.; Cold Spring Harbor Lab. Press, 1988.
- Ausubel F.M. // *Current Protocols.* 2002. Unit 2.7.
- Ellman G.L., Courtney K.D., Anders V., Feather-Stone R.M. // *Biochem. Pharmacol.* 1961. V. 7. P. 88–95.
- Karnovsky M.J., Roots L. // *J. Histochem. Cytochem.* 1964. V. 12. P. 219–221.
- Xie W., Altamirano C.V., Bartels C.F., Speirs R.J., Cashman J.R., Lockridge O. // *Mol. Pharmacol.* 1999. V. 55. P. 83–91.
- Bartels C.F., Jensen F.S., Lockridge O., van der Spek A.F., Rubinstein H.M., Lubrano T., La Du B.N. // *Am. J. Hum.*

RESEARCH ARTICLES

- Genet. 1992. V. 50. P. 1086–1103.
39. Wang Y., Boeck A.T., Duysen E.G., van Keuren M., Saunders T.L., Lockridge O. // *Toxicol. Appl. Pharmacol.* 2004. V. 196. P. 356–366.
40. Preininger A., Schlokat U., Mohr G., Himmelspach M., Stichler V., Kyd-Rebenburg A., Plaimauer B., Turecek P.L., Schwarz H.P., Wernhart W., Fischer B.E., Dorner F. // *Cytotechnology.* 1999. V. 30. P. 1–15.
41. Wajih N., Hutson S.M., Owen J., Wallin R. // *J. Biol. Chem.* 2005. V. 280. P. 31603–31607.
42. Jossé L., Smales C.M., Tuite M.F. // *Biotechnol. Bioeng.* 2010. V. 105. P. 556–566.
43. Meleady P., Henry M., Gammell P., Doolan P., Sinacore M., Melville M., Francullo L., Leonard M., Charlebois T., Clynes M. // *Proteomics.* 2008. V. 8. P. 2611–2624.
44. Roncarati R., Seredenina T., Jow B., Jow F., Papini S., Kramer A., Bothmann H., Dunlop J., Terstappen G.S. // *Assay Drug Dev. Technol.* 2008. V. 6. P. 181–193.
45. Chilukuri N., Sun W., Naik R.S., Parikh K., Tang L., Doctor B.P., Saxena A. // *Chem. Biol. Interact.* 2008. V. 175. P. 255–260.
46. Jain S., Hreczuk-Hirst D.H., McCormack B., Mital M., Epenetos A., Laing P., Gregoriadis G. // *Biochim. Biophys. Acta.* 2003. V. 1622. P. 42–49.

Overexpression of MRPS18-2 in Cancer Cell Lines Results in Appearance of Multinucleated Cells

Z. Shevchuk¹, M. Y. Yurchenko², S. D. Darekar¹, I. Holodnuka-Kholodnyuk³, V. I. Kashuba⁴, E. V. Kashuba^{1,2*}

¹Department of Microbiology, Tumor and Cell Biology (MTC), Karolinska Institutet, Stockholm, 17177, Sweden

²Kavetsky Institute of Experimental Pathology, Oncology and Radiobiology of NASU, 45 Vasylkivska str., Kyiv-22, 03022, Ukraine

³Kirichenstein Institute of Microbiology and Virology, Riga Stradins University, 5 Ratsupites, Riga, LV-1067, Latvia

⁴Institute of Molecular Biology and Genetics of NASU, 150 Zabolotnogo str., Kyiv-143, 03680, Ukraine

*E-mail: Elena.Kashuba@ki.se

Received 01.10.2012

Copyright © 2013 Park-media, Ltd. This is an open access article distributed under the Creative Commons Attribution License, which permits unrestricted use, distribution, and reproduction in any medium, provided the original work is properly cited.

ABSTRACT Human mitochondrial ribosomal protein MRPS18-2 (S18-2) is encoded by a cellular gene that is located on the human chromosome 6p21.3. We discovered that overexpression of the S18-2 protein led to immortalization and de-differentiation of primary rat embryonic fibroblasts. Cells showed anchorage-independent growth pattern. Moreover, pathways characteristic for rapidly proliferating cells were upregulated then. It is possible that the S18-2 overexpression induced disturbance in cell cycle regulation. We found that overexpression of S18-2 protein in human cancer cell lines led to an appearance of multinucleated cells in the selected clones.

KEY WORDS Mitochondrial ribosomal protein S18-2 (MRPS18-2), multinucleated cells, cancer cell line, cell cycle, RB binding protein.

INTRODUCTION

Mitochondrial ribosomal protein S18-2 (MRPS18-2, NP_05476, S18-2 in the text) is encoded by a cellular gene located on human chromosome 6p21.3. S18-2 cDNA was cloned after an analysis of the differentially expressed genes in CD34⁺ hematopoietic progenitor cells [1]. The human genome contains three different S18 genes, in contrast to two in *C. elegans* and one in bacteria [2, 3]. The proteins of the S18 family are localized on the surface of the small subunit (28S) of the mammalian mitochondrial ribosome [3]. The function of these proteins is largely unknown.

Recently we shown that overexpression of the human mitochondrial ribosomal protein S18-2 led to immortalization of primary rat embryonic fibroblasts, REFs [4]. Cells of the derived cell line named 18IM lost contact inhibition. Moreover, they acquired the ability for anchorage-independent growth in soft agar with a high cloning efficiency (more than 90%). Immortalized 18IM cells expressed the embryonic stem cell markers SSEA-1, Sox2, and Oct4 that were not detected in the original REFs. Noteworthy, the 18IM cells lost the expression of mesodermal markers like vimen-

tin and smooth-muscle actin. Part of them expressed ecto- and endoderm-specific pan-keratin, ectoderm-specific beta-III-tubulin, and mesoderm-specific MHC class II markers; some of the cells differentiated into fat cells in confluent cultures. The 18IM cells produced excessive amounts of pyruvate, suggesting an enhanced ATP synthesis. Moreover, as was shown by microarray analysis and Q-PCR, many genes encoding enzymes that are involved in redox reactions, such as ATP synthases, mitogen activated kinases, and NADH dehydrogenases, are greatly upregulated in the immortalized cells [5]. Pathways of oxidative phosphorylation, ubiquinone biosynthesis, PI3K/AKT signaling, and fatty acid elongation in mitochondria, characteristic for rapidly proliferating cells, were also upregulated in the 18IM cells.

Earlier we had found that S18-2 specifically binds to the retinoblastoma protein, RB [6]. S18-2 competes with E2F1 for the RB binding, thus S18-2 might play a role in the control of G₁-S phase transition [7].

In the present work we show that overexpression of S18-2 in the human tumor cell lines MCF7 and KRC/Y leads to the appearance of multinucleated cells.

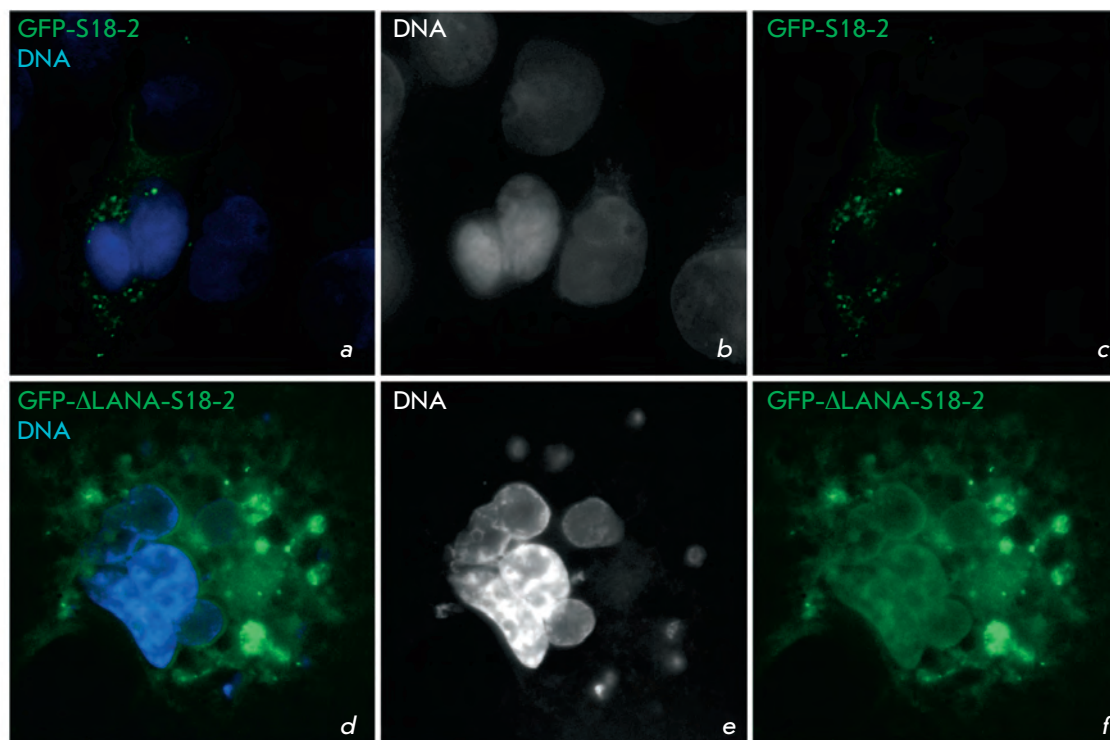


Fig. 1. Cellular localization of GFP-S18-2 (panels a–c) and GFP- Δ LANA-S18-2 (panels d–f) in the transfected MCF7 (top row) and KRC/Y (bottom row) cells. Note that in all transfected cells the exogenous S18-2 protein (panels a, c, d, and f) is localized in the cytoplasm

EXPERIMENTAL PROCEDURES

Plasmids

Cloning of S18-2 cDNA into the pEGFPC-1 and pCMV-Tag3A (c-myc-tagged) vectors was described earlier [7]. S18-2 cDNA was also cloned in the pEGFPC-1 vector, coding for a fusion protein GFP- Δ LANA-S18-2, with the first 35 amino acids of LANA, encoded by the human herpes virus 8 (HHV8, Kaposi sarcoma associated herpes virus) at the 5' end. The sequence was verified by direct sequencing, using commercial forward and reverse primers (Stratagene, Santa Clara, CA, USA) and Applied Biosystems sequencer (Perkin Elmer, Wellesley, MA, USA).

Antibodies

The following primary antibodies were used: mouse monoclonal anti-c-myc (clone 9E10, Zymed Laboratories Inc., San Francisco, CA, USA), anti-BrdU (Becton Dickinson (BD), San Jose, CA, USA), and anti-actin (Sigma-Aldrich, St. Louis, MO, USA); rabbit anti-S18-2 serum (described in [7]) and anti-MRPS18B (Proteintech Group inc, Chicago, IL, USA), and FITC-conjugated swine anti-rabbit and rabbit anti-mouse (Dako, Glostrup, Denmark).

Cells, cell culture, immunostaining and imaging

MCF7 breast carcinoma and KRC/Y renal carcinoma cell lines were cultured at 37°C in a Iscove's medium

that contained 10% fetal bovine serum and appropriate antibiotics (penicillin (100 μ U/ml) and streptomycin (100 μ g/ml)). Periodic staining with Hoechst 33258 (Sigma-Aldrich) monitored the absence of mycoplasma. Prior to transfection experiments, the cells were grown on coverslips. The MCF7 cells were transfected with GFP- and c-myc-tagged constructs (GFP-S18-2 and MT-S18-2, correspondingly), and the KRC/Y cells were transfected with GFP- Δ LANA-S18-2 construct, in parallel with empty vectors, using Lipofectamine and Plus Reagent (Life Technology, Carlsbad, CA), according to the manufacturer's protocol. Immunostaining and digital image capturing was performed as described elsewhere. Briefly, cells on coverslips were fixed in a 1 : 1 mixture of cold methanol and acetone (-20°C). After rehydration in phosphate-buffered saline (PBS), the cells were stained with antibodies. Hoechst 33258 was added at a concentration of 0.4 μ g/ml for DNA staining. Images were captured using DAS microscope Leitz DM RB with a Hamamatsu dual mode cooled charge-coupled device (CCD) camera (C4880; Hamamatsu, Japan).

Cell cycle analysis by flow cytometry.

One million of living cells were labeled with bromodeoxyuridine (BrdU, 30 μ M) for 30 min at 37°C, trypsinized, collected, and fixed in ethanol (75% in PBS) at 4°C for at least 10 hours. After this, the cells were treated with pepsin (1 mg/ml in 30 mM HCl) for 30 min at 37°C and with 2 M HCl for 15 min. The cell were labeled with

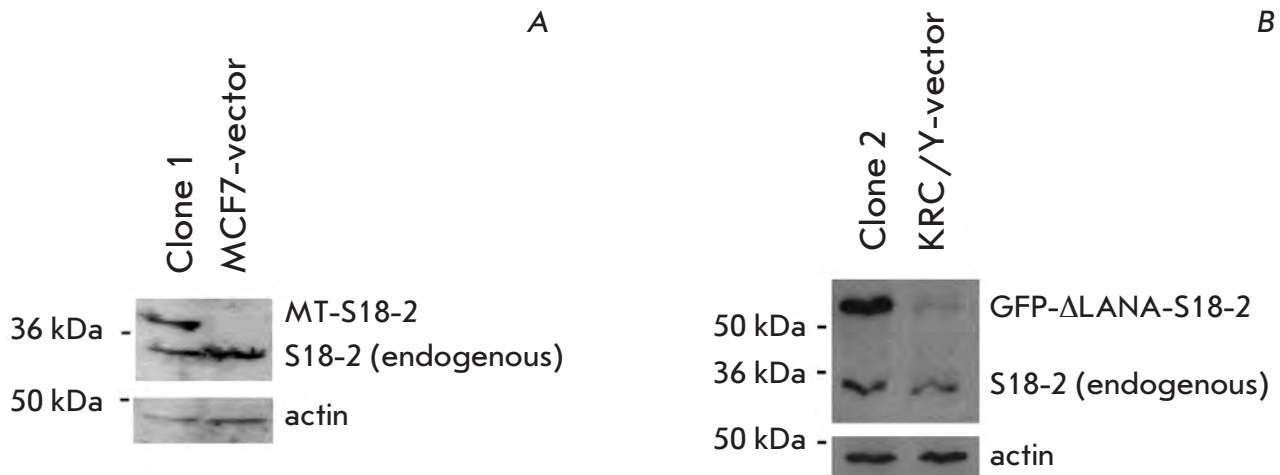


Fig. 2. A constitutive expression of S18-2 protein in the MCF7 and KRC/Y cells as compared to vector-transfected cells. The membrane was probed with anti-S18-2 rabbit serum and mouse anti-actin antibodies. Secondary antibodies (sheep anti-rabbit and anti-mouse horse radish peroxidase conjugated, GE-Healthcare, Uppsala, Sweden) and Enhanced chemiluminescence kit (GE-Healthcare) were used to monitor protein bands. *A*, transfection of MCF7 cells with MT-S18-2 plasmid; *B*, transfection of KRC/Y cells with GFP-ΔLANA-S18-2 plasmid. Note the expression of endogenous S18-2 protein in all cells

anti-BrdU and FITC-conjugated rabbit anti-mouse antibodies and stained with propidium iodide (25 μg/ml in PBS). Cells (1×10^4) were analyzed by flow cytometry, using a FACScan flow cytometer (BD), and the percentage of cells in each phase of the cell cycle was determined with the help of CellQuest software (BD).

RESULTS AND DISCUSSION

Establishment of MCF7 and KRC/Y sub-lines, expressing S18-2 constitutively

Cells were grown in 6-well-plates prior transfection. 5 μg of MT-S18-2 or GFP-ΔLANA-S18-2 plasmid was used for transfection. MT-S18-2 and GFP-S18-2 signal was observed in the cytoplasm of the transfected MCF7 cells (*Fig. 1*, the top row, panels *a* and *c*). Earlier we have shown that GFP-S18-2 could be targeted to the nucleus upon cell transformation [4]. In order to achieve a nuclear localization of S18-2, its cDNA was cloned in the GFP-ΔLANA fusion vector that contained the first 35 amino acids of LANA, the HHV8-encoded latent nuclear antigen. It was shown that N-terminus of LANA binds to histones H2A and H2B to tether a HHV8 episome to a chromosome [8]. Despite that, the GFP-ΔLANA-S18-2 fusion protein was observed mainly in the cytoplasm of KRC/Y cells (*Fig. 1*, the lower row, panels *d* and *f*). 48 hours after transfection the cells were transferred to a Petri dish (7.5 cm in diameter) and the selective medium that contained 2 mg/ml G418 was applied. Three weeks later, some of the clones

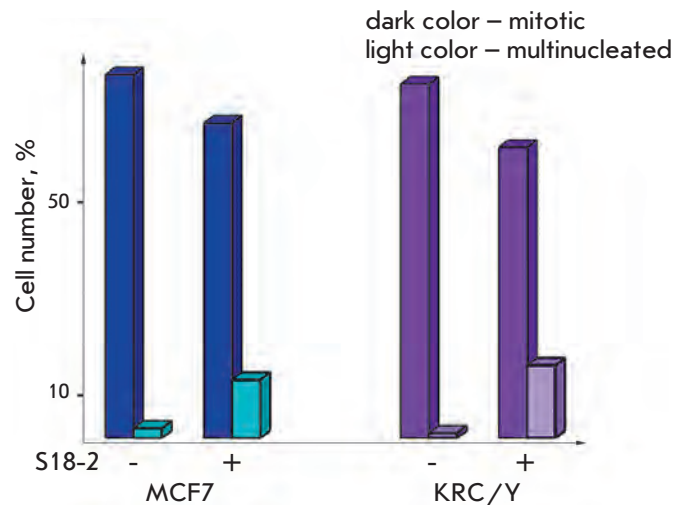


Fig. 3. MCF7 and KRC/Y cell cultures, expressing exogenous S18-2 constitutively, show a high proportion of multinucleated cells. Dark-color bars represent the percentage of mitotic cells and light-color bars, percentage of multinucleated cells in the culture

that had survived (12 clones for MT-S18-2 and GFP-ΔLANA-S18-2 plasmids) were isolated and analyzed by Western blotting and immunostaining. Three clones of MCF7 and four clones of KRC/Y expressed exogenous S18-2 at a high level. For the further study, clone 1 of MCF7 and clone 2 of KRC/Y were selected (*Fig. 2A* and

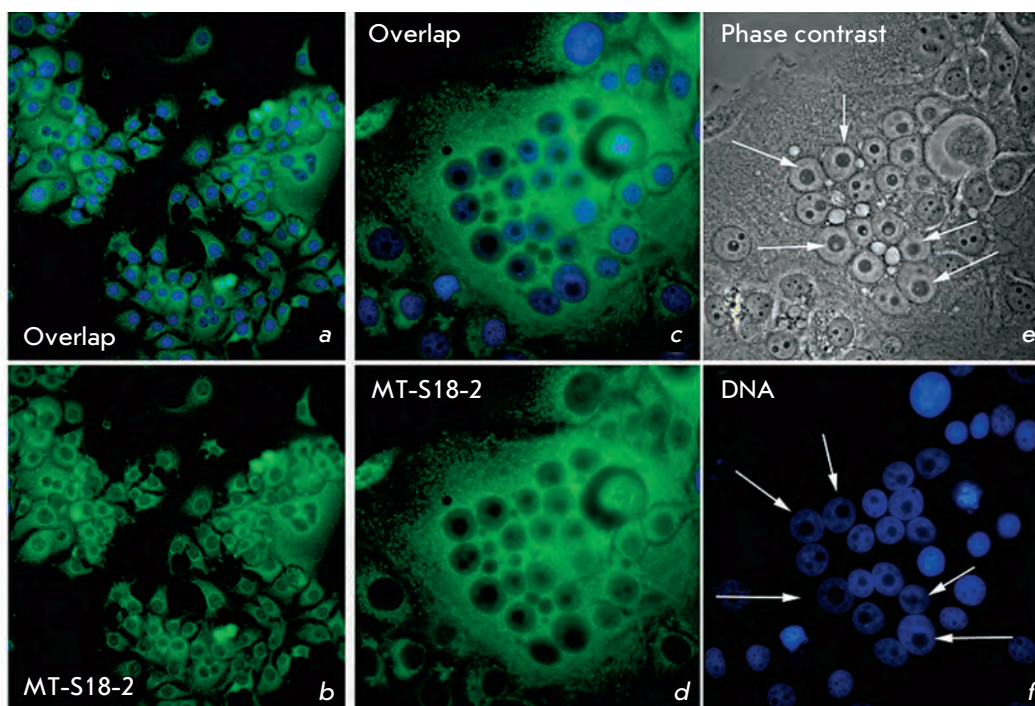


Fig. 4. Multinucleated cells in the MCF7 cell culture expressing S18-2 constitutively. The percentage of multinucleated cells is shown in panels a and b (20 \times). At higher magnification (63 \times), large single nucleoli in multinucleated cells can be seen (panels c–f). Signal of MT-S18-2 fusion protein stained with anti-c-myc antibody is shown in green; DNA is stained blue

B). Noteworthy, the endogenous S18-2 was expressed at low levels in both cell lines.

MT-S18-2 overexpression leads to the appearance of multinucleated cells

MCF7-clone 1 and KRC/Y-clone 2 cells that expressed S18-2 constitutively, along with vector-transfected cells, were passaged for more than 20 population doublings. We have observed an extremely high frequency of multinucleated cells (*Fig. 3*). Approximately 12% of MCF7 cells and 15% of KRC/Y cells that expressed exogenous S18-2 protein at a high level, were multinucleated. Such cells were observed after sequential freezing and thawing of the culture. Noteworthy, the nucleoli in multinucleated cells were enlarged (*Fig. 4*, panels c, e, and f), suggesting an enhanced protein synthesis.

In order to investigate a possible mechanism of multinucleated cell formation, we analyzed the cell cycle distribution in 18IM cells. The percentage of cells in S-phase was much higher in 18IM cells than that in REFs (*Fig. 5*). A corresponding reduction in the cell number in G₁-phase was also observed. A smaller number of cells in G₂/M phase in 18IM cell culture may suggest that S18-2 protein, when expressed at a high level, leads to elevated transcription/translation, causing impaired mitosis.

How the mitochondrial ribosomal protein S18-2 can influence cell cycle regulation? Actually, it is well known that a crucial role in the G₁/S checkpoint con-

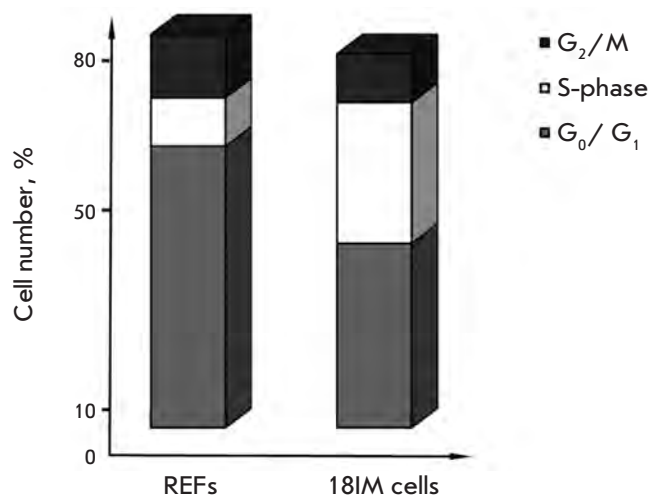


Fig. 5. Cell cycle distribution in 18IM cells and control primary fibroblasts (REFs). The percentage of cells in S-phase is clearly elevated in 18IM cells, suggesting the deregulation of cell cycle upon the S18-2 overexpression

trol is performed by retinoblastoma protein (RB) [9]. A hypo-phosphorylated form of RB binds to E2F1-5 transcription factors and prevents the S-phase entry. Hyper-phosphorylation of RB results in freeing of E2F1-5 and activation of the E2F-dependent transcription. As we mentioned earlier, we have found that S18-2 protein binds to RB and frees E2F1 from inhibitory

complexes with RB, inducing the S-phase [6, 7]. It may explain the increased number of cells in S-phase (Fig. 5) and, eventually, the formation of multinucleated cells.

There could be other mechanisms leading to a creation of cells with more than one nucleus. For example, enhanced expression of nucleoporin (Nup153, NP_005115) led to the appearance of multinucleated HeLa cells, due to its binding to the MAD1 protein controlling mitotic spindle-assembly checkpoint [10]. Another example of similar action is overexpression of BCSG1 protein (gamma-synuclein, NP_003078) in breast cancer cell lines, leading to inactivation of BubR1 regulating mitotic checkpoint [11]. Can S18-2 influence the cell division due to its binding to proteins controlling a mitotic pole formation? This question has no answer yet, however. There are more than 70 mitochondrial ribosomal proteins encoded by the human genome (for review see [12]), and their functions are largely unknown. Some studies suggested multiple functions of ribosomal proteins in mammalian cells. It was shown, for example, that MRPS29, one of the proteins of the small mitochondrial ribosome subunit, is not only in-

involved in the ribosome assembly but can also induce apoptosis [13, 14]. The mitochondrial ribosomal protein of large subunit, L41 (MRPL41), can induce G₁ arrest [15, 16]. To further explore the functions of S18-2, we are currently looking for S18-2 binding proteins.

CONCLUSIONS

We have shown that overexpression of the mitochondrial ribosomal protein S18-2 in the human cancer cell lines MCF7 and KRC/Y results in the appearance of multinucleated cells. This can be due to enhanced transcription/translation and, probably, impaired mitosis. Further studies should be performed to analyze this phenomenon. ●

This work was supported by the Swedish Cancer Society, by matching grants from the Concern Foundation (Los Angeles) and the Cancer Research Institute (New York), by the Swedish Institute, Karolinska Institutet Research Foundation and by Lilian Sagens & Curt Eriksson Research Foundation.

REFERENCES

- Zhang Q.H., Ye M., Wu X.Y., Ren S.X., Zhao M., Zhao C.J., Fu G., Shen Y., Fan H.Y., Lu G. // *Genome Research*. 2000. V. 10. № 10. P. 1546–1560.
- Suzuki T., Terasaki M., Takemoto-Hori C., Hanada T., Ueda T., Wada A., Watanabe K. // *J. Biol. Chem*. 2001. V. 276. № 35. P. 33181–33195.
- Cavdar Koc E., Burkhart W., Blackburn K., Moseley A., Spremulli L.L. // *J. Biol. Chem*. 2001. V. 276. № 22. P. 19363–19374.
- Kashuba E., Pavan Yenamandra S., Deoram Darekar S., Yurchenko M., Kashuba V., Klein G., Szekely L. // *Proceedings of the National Academy of Sciences of the United States of America*. 2009. V. 106. № 47. P. 19866–19871.
- Yenamandra S.P., Darekar S.D., Kashuba V., Matskova L., Klein G., Kashuba E. // *Cell Death Dis*. 2012. V. 3. e357.
- Snopok B., Yurchenko M., Szekely L., Klein G., Kashuba E. // *Anal. and Bioanal. Chem*. 2006. V. 386. № 7–8. P. 2063–2073.
- Kashuba E., Yurchenko M., Yenamandra S.P., Snopok B., Isagulians M., Szekely L., Klein G. // *Proceedings of the National Academy of Sciences of the United States of America*. 2008. V. 105. № 14. P. 5489–5494.
- Barbera A.J., Chodaparambil J.V., Kelley-Clarke B., Luger K., Kaye K.M. // *Cell Cycle*. 2006. V. 5. № 10. P. 1048–1052.
- Classon M., Harlow E. // *Nat. Rev. Cancer*. 2002. V. 2. № 12. P. 910–917.
- Lussi Y.C., Shumaker D.K., Shimi T., Fahrenkrog B. // *Nucleus*. 2010. V. 1. № 1. P. 71–84.
- Gupta A., Inaba S., Wong O. K., Fang G., Liu J. // *Oncogene*. 2003. V. 22. № 48. P. 7593–7599.
- O'Brien T.W. // *IUBMB Life*. 2003. V. 55. № 9. P. 505–513.
- Saini N., Balhara J., Adlakha Y.K., Singh N. // *Int. J. Integ. Biol*. 2009. V. 5. № 5. P. 49–57.
- Khanna N., Sen S., Sharma H., Singh N. // *Biochem. Biophys. Res. Commun*. 2003. V. 30. № 1. P. 26–35.
- Kim M.J., Yoo Y.A., Kim H. J., Kang S., Kim Y.G., Kim J.S., Yoo Y.D. // *Biochem. Biophys. Res. Commun*. 2005. V. 338. № 2. P. 1179–1184.
- Yoo Y.A., Kim M.J., Park J.K., Chung Y.M., Lee J.H., Chi S.G., Kim J.S., Yoo Y.D. // *Mol. Cell. Biol*. 2005. V. 25. № 15. P. 6603–6616.

Genetic Diversity of *Bacillus thuringiensis* from Different Geo-Ecological Regions of Ukraine by Analyzing the 16S rRNA and *gyrB* Genes and by AP-PCR and saAFLP

N. V. Punina^{1,2*}, V. S. Zotov¹, A. L. Parkhomenko³, T. U. Parkhomenko³, A. F. Topunov¹

¹Bach Institute of Biochemistry, Russian Academy of Sciences, Leninsky prospect, 33, bld. 2, Moscow, Russia, 119071

²Research Centre for Medical Genetics, Russian Academy of Medical Sciences, Moskvorechje str., 1, Moscow, Russia, 115478

³Institute of Agriculture of Crimea, National Academy of Agrarian Sciences of Ukraine, Kievskaya str., 150, Simferopol, Ukraine, 95453

*E-mail: hin-enkelte@yandex.ru

Received 02.10.2012

Copyright © 2013 Park-media, Ltd. This is an open access article distributed under the Creative Commons Attribution License, which permits unrestricted use, distribution, and reproduction in any medium, provided the original work is properly cited.

ABSTRACT The *Bacillus cereus* group consists of closely related species of bacteria and is of interest to researchers due to its importance in industry and medicine. However, it remains difficult to distinguish these bacteria at the intra- and inter-species level. *Bacillus thuringiensis* (*Bt*) is a member of the *B. cereus* group. In this work, we studied the inter-species structure of five entomopathogenic strains and 20 isolates of *Bt*, which were collected from different geo-ecological regions of Ukraine, using various methods: physiological and biochemical analyses, analysis of the nucleotide sequences of the 16S rRNA and *gyrB* genes, by AP-PCR (BOX and ERIC), and by saAFLP. The analysis of the 16S rRNA and *gyrB* genes revealed the existence of six subgroups within the *B. cereus* group: *B. anthracis*, *B. cereus* I and II, *Bt* I and II, and *Bt* III, and confirmed that these isolates belong to the genus *Bacillus*. All strains were subdivided into 3 groups. Seventeen strains belong to the group *Bt* II of commercial, industrial strains. The AP-PCR (BOX and ERIC) and saAFLP results were in good agreement and with the results obtained for the 16S rRNA and *gyrB* genes. Based on the derived patterns, all strains were reliably combined into 5 groups. Interestingly, a specific pattern was revealed by the saAFLP analysis for the industrial strain *Bt* 0376 p.o., which is used to produce the entomopathogenic preparation “STAR-t”.

KEYWORDS *Bacillus cereus* group; *B. thuringiensis*; 16S ribosomal RNA; *gyrB*; saAFLP; taxonomy; phylogeny.

ABBREVIATIONS *Bt* – *Bacillus thuringiensis*; ICPs – δ -endotoxins; b.p. – base pair; MLST – multilocus sequence typing; MEE – multilocus enzyme electrophoresis; saAFLP, AFLP – single adapter amplified fragment length polymorphism; RFLP – restriction fragment length polymorphism; AP-PCR – arbitrarily primed polymerase chain reaction; rep-PCR – repetitive sequence-based PCR; BOX, ERIC – DNA repeats; ME – minimum evolution; NJ – neighbor joining.

INTRODUCTION

Bacillus thuringiensis (*Bt*) are gram-positive bacteria that exhibit bioinsecticide activity due to their ability to produce δ -endotoxins (ICPs), or Cry proteins, during sporulation [1]. These toxins are active for a wide range of insect species and genera, including agricultural pests and human parasites [2, 3]. Due to the high specificity of ICPs, entomopathogenic *Bt* bacteria can be used, instead of pesticides, and are widely employed in designing bioengineered crop protection agents [4, 5].

Based on a phenotypic and genotypic analysis, *Bt* species were attributed to the *B. cereus* group. This group also comprises the closely related species

B. cereus, *B. anthracis*, *B. mycoides*, *B. pseudomycoides*, and *B. weihenstephanensis*. The *B. cereus* and *Bt* species cannot be distinguished using the morphological [6], phenotypic [7], or genetic methods [8–11]. It has been hypothesized that these species can belong to the same species, *B. cereus sensu lato* [12, 13]. Since this group of closely related bacteria is of significant interest for agriculture and medicine, a thorough investigation into their taxonomy, as well as an elaboration of new tools and technologies for their differentiation and isolation, remains a rather urgent task.

Bt strains were conventionally isolated and further divided into subspecies according to either the pres-

ence or absence of ICP crystals or the genes encoding them (*cry* and *cty*) [1, 3]. However, this method has a drawback: the ICP's genes are localized on the plasmid, and bacteria can lose them or pass them to the other *Bt* strains or closely related bacterial species during conjugation [14]. Over 82 *Bt* serovars were revealed by a serological analysis of the flagellar antigen (H-serotyping) [15, 16]. However, such classification did not always correlate with the actual phylogenetic relationships for this species [17–19].

The genetic diversity of *Bt* bacteria and the possibility to distinguish between the two species, *Bt* and *B. cereus*, were studied using different methods: DNA-DNA hybridization [20] and the analysis of the nucleotide sequences of 16S rRNA, 23S rRNA, 16S–23S rRNA [8, 11], MLST [21], MEE [12, 18], AFLP [22–24], RFLP [25], AP-PCR [26–29], etc. However, the actual phylogenetic relationships between *Bt* have not been determined by these methods.

This work was aimed at assessing how the modified genomic fingerprinting technique (saAFLP) could be applied to reveal the phylogenetic differences between *Bacillus* sp. isolates and strains from various geo-ecological regions of Ukraine. The nucleotide sequences of the 16S rRNA and *gyrB* genes were analyzed in order to determine the taxonomic relationships at the genus-species level. The saAFLP method, along with other informative methods (rep-PCR), was used to study the structure at the intra-species level. This complex diagnostics, together with the results of physiological and biochemical assays, offers broad opportunities for studying the taxonomic structure of these closely related organisms. However, it should be borne in mind that the sampling of *Bt* strains requires further broadening.

MATERIALS AND METHODS

Bacterial strains

Five entomopathogenic strains and 20 isolates of *Bt* bacteria exhibiting unique biochemical properties from a collection of useful microorganisms of various Ukrainian and Russian research institutions (Institute of Agriculture of Crimea, National Academy of Agrarian Sciences of Ukraine, Simferopol, Autonomous Republic of Crimea, Ukraine; Institute of Agricultural Microbiology, National Academy of Agrarian Sciences of Ukraine, Chernigov, Ukraine; All-Russian Collection of Industrial Microorganisms “GosNIIGenetika”, Moscow, Russia) were used in this study. Five strains from the collection of the All-Russian Collection of Industrial Microorganisms “GosNIIGenetika” were used as standard strains. Isolates from the collection of the Institute of Agriculture of the Crimea, National Acad-

emy of Agrarian Sciences of Ukraine, were isolated in different geo-ecological regions of Ukraine.

DNA isolation

The overall cellular DNA specimens were isolated from strains cultured on agarized TY medium (g/l): yeast extract – 1.0; peptone – 10.0; CaCl₂ – 0.4; agar – 20.0. DNA was isolated from fresh cultures on days 1–2 of growth via sorption onto magnetic particles (Mini-prep kit, Silex, Russia).

Phenotypic characterization

The morphological and physiological-biochemical characteristics of the pure bacterial cultures were determined based on the general strategy of phenotypic differentiation described in *A Guide for Bacterial Identification* [30] and *Methods for General Bacteriology* [31].

PCR amplification and sequencing of the 16S rRNA gene

The PCR analysis and subsequent determination of the nucleotide sequences of the 16S rRNA gene [32] were conducted on a genetic analyzer using the universal primers 27f (5'-GTTTGATCMTGGCTCAG-3') and 1492R (5'-TACGGYTACCTTGTTACGACTT-3') [33]. The amplified fragments were detected by electrophoresis in 1.5% agarose gel. Sequencing was carried out on a Genetic Analyzer 3130xl ABI automated sequencing machine (Applied Biosystems, USA).

PCR amplification and sequencing of the *gyrB* gene

The *gyrB* gene was amplified and sequenced using the previously constructed primer systems UP1 and UP2r [34], the *Bacillus* genus-specific primers designed by us, *gyrB_F* (5'-CTTGAAGGACTAGARGCAGT-3') + *gyrB_Rf* (5'-CCTTCACGAACATCYTCACC-3') and *gyrB_Fr* (5'-GGTGARGATGTTTCGTGAAGG-3') + *gyrB_R* (5'-TGGATAAAGTTACGACGYGG-3'), and the protocol. The temperature–time profile of the reaction was as follows: the initial denaturation at 94°C – 2 min; then, 30 cycles: 94°C – 30 s, 62°C – 30 s, 72°C – 1 min; final elongation – 5 min at 72°C. The amplified fragments were revealed by electrophoresis in 1.5% agarose gel. Sequencing was carried out on a Genetic Analyzer 3130xl ABI (Applied Biosystems, USA).

PCR using primers to different repeating elements (rep-PCR)

The previously described primer systems [26, 27] ERIC1R 5'-ATGTAAGCTCCTGGGGATTCAC-3'; ERIC2 5'-AAGTAAGTGACTGGGGTGAGCG-3'; and BOXA1R 5'-CTACGGCAAGGCGACGCTGACG-3' were used for rep-PCR.

Amplification was carried out in 25 µl of the following mixture: 1× polymerase buffer BioTaq (17 mM (NH₄)₂SO₄, 6 mM Tris-HCl, pH 8.8, 2 mM MgCl₂), 5 nM dNTP, 50 ng of DNA template, 12.5 pM of the primer, and 1.25 AU of BioTaq DNA polymerase (Dialat Ltd., Russia). The temperature-time profile of the reaction: first cycle – 94°C, 2 min; subsequent 40 cycles – 94°C, 20 s; 40°C, 30 s and 72°C, 90 s; final elongation – 7 min at 72°C. The PCR products were analyzed by electrophoresis in a 1.5% agarose gel stained with ethidium bromide at a field intensity of 6 V/cm and documented using the BioDoc Analyze system (Biometra, Germany).

saAFLP analysis [35]

We had modified the AFLP method developed and patented by M. Zabeau and P. Vos [36]; its suitability for the analysis of closely related *Bt* strains was assessed in this study. The phylogenetic relationships between closely related strains of various species belonging to the genus *Rhizobium* had been successfully analyzed using this modified saAFLP method [35]. The saAFLP procedure comprises three steps: (I) simultaneous treatment of the extracted bacterial DNA in the same tubes using one of the restriction endonucleases (XmaJI, XbaI, PstI) and ligation with a single-stranded adapter Ad.CTAG1; (II) PCR amplification with a single primer complementary to the Ad.CTAG1 sequence; (III) electrophoretic separation of the PCR products in agarose gel. The fundamentally new aspects for this saAFLP method include conducting the restriction analysis and the ligase reaction in the same tube, using restriction endonucleases XmaJI (XbaI, PstI) to study the phylogenetic relationships between the *Bt* strains isolated in various geo-ecological regions of Ukraine, and using only the single-stranded adapter Ad.CTAG1.

The restriction analysis was carried out simultaneously with the ligation in 10 µl of the mixture containing 80 ng of the DNA sample, the ligase buffer (Fermentas, USA), 10 pM of the single-stranded adapter Ad.CTAG1 (5'-ctagCTGGAATCGATTCCAG-3'), 5 AU of T4 DNA ligase (Fermentas, USA), and 1 AU of restrictase XmaJI (XbaI, PstI). The resulting mixture was incubated at 37°C for 2 h. The reaction volume was then brought up to 100 µl. PCR was carried out on a Mastercycler Gradient Eppendorf amplifier in 25 µl of the mixture containing 1× PCR buffer, 2.8 mM MgCl₂, 0.2 mM dNTP, 2 µl of the restrictase–ligase mixture as a DNA template, 0.4 µl of primer Pr.CTAG1 (5'-CTGGAATCGATTCCAGctag-3') complementary to the adapter, and 1 AU BioTaq DNA polymerase (Dialat Ltd., Russia). PCR amplification was carried out in the following mode: initial denaturation – 94°C, 2 min,

followed by 30 cycles – 94°C, 30 s; 40°C, 30 s; 72°C, 3 min; final elongation – 5 min at 72°C.

Analysis of nucleotide sequences

The primary comparative analysis of the nucleotide sequences determined in this study and represented in the GenBank database was carried out using the NCBI Blast software [37]. Sequence alignment was performed using the CLUSTALW 1.75v. software [38]; the sequences were verified and edited using BioEdit 7.0.5.3 [39] and Mega 3.1 [40] editors. The phylogenetic trees were constructed in the Mega 3.1 software [40] using the neighbor joining (NJ) [41] and minimum evolution (ME) [42] methods. The statistical significance of the branching order of the resulting trees was determined using the bootstrap analysis by constructing 1,000 alternative trees.

RESULTS AND DISCUSSION

Analysis of the nucleotide sequences of the 16S rRNA gene

The analysis of the nucleotide sequences of the 16S rRNA gene is frequently used for taxonomic localization and the identification of the bacterial genus/species. We amplified and sequenced the PCR fragments of the 16S rRNA gene (the size of the sequenced region was 1386 bp) of five typical strains of genus *Bacillus* and 20 Ukrainian isolates to verify their taxonomic attribution to the genus *Bacillus*. Similar nucleotide sequences of the 16S rRNA gene of *B. cereus*, *Bt*, *B. anthracis*, *B. mycoides*, *B. pseudomycoides*, and *B. weihenstephanensis* were obtained from the database of the National Center for Biotechnology Information (NCBI, USA) and used for comparative purposes. The nucleotide sequences of *B. pumilus*, *B. licheniformis*, and *B. subtilis* were selected as the remote control for the phylogenetic analysis. A phylogenetic tree representing the evolution of the analyzed gene was constructed based on the aligned sequences using the ME algorithm (Fig. 1). The pairwise genetic distances were calculated using the Kimura's two-parameter model.

The topology of the resulting tree was consistent with the phylogenetic structure of the genus determined by DNA–DNA hybridization [43] and established for the *B. cereus* group by the analysis of the 16S rRNA, 23S rRNA gene fragments [8, 11], and the 16S–23S rRNA intergenic region [44], rep-PCR [29], and AFLP [23].

The attribution of the isolates to the genus *Bacillus* has been verified by analysing the nucleotide sequences of the 16S rRNA gene. However, this method did not allow one to reliably distinguish individual species within the *B. cereus* group due to the fact that the sequence of

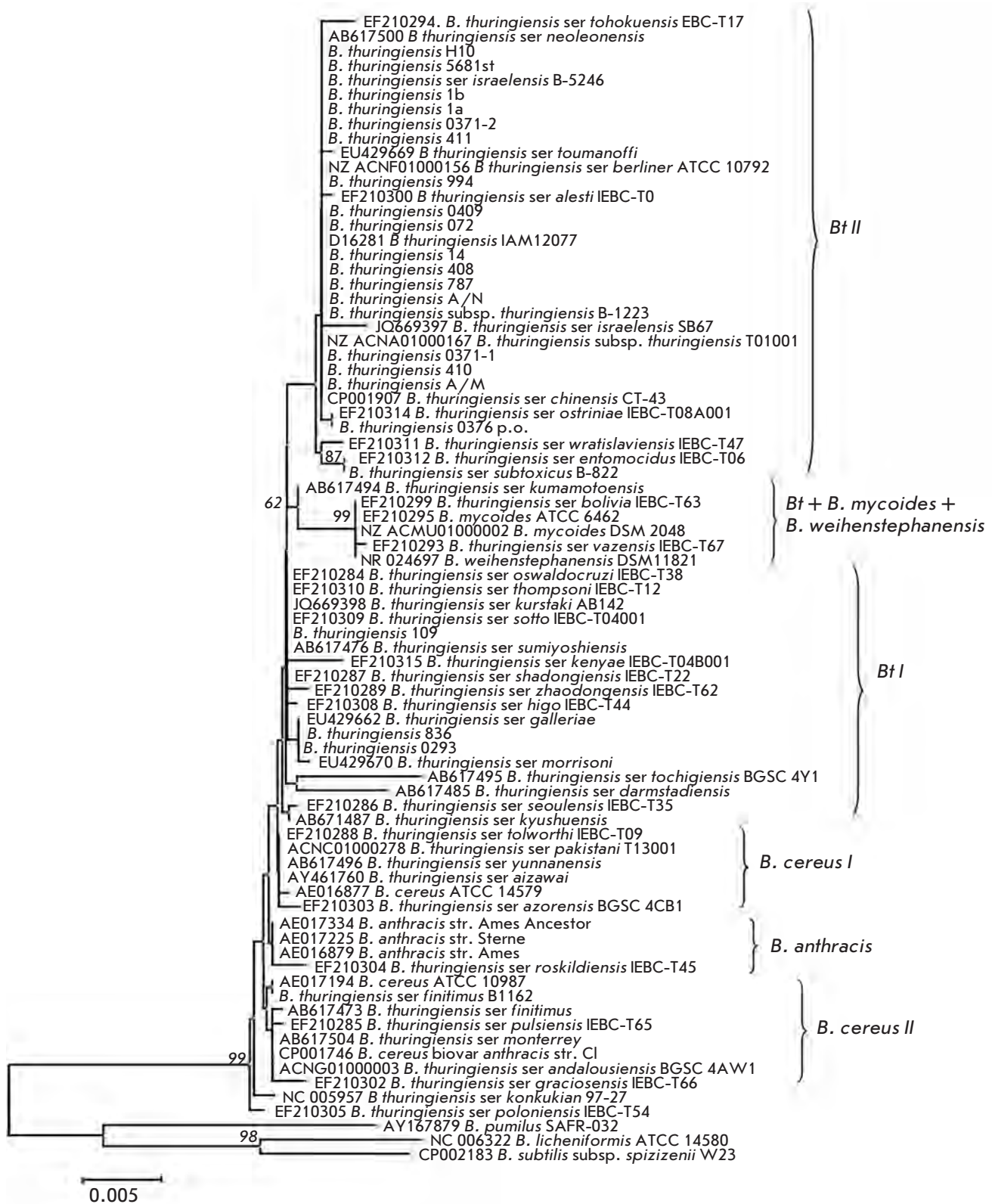


Fig. 1. Phylogenetic tree constructed based on the sequences of the 16S rRNA gene for bacteria of the *B. cereus* group using the ME algorithm. The scale corresponds to 0.5 substitutions per 100 bp (genetic distances). The bootstrap confidence values were generated using 1,000 permutations and showed in % under the branches. Branches absent in more than 50% of the trees are not shown



Fig. 2. Phylogenetic tree constructed based on the sequences of the *gyrB* rRNA gene for bacteria of the *B. cereus* group using the ME algorithm. The scale corresponds to 5 substitutions per 100 bp (genetic distances). The bootstrap confidence values were generated using 1,000 permutations and showed in % under the branches. Branches absent in more than 50% of trees are not shown

the 16S rRNA gene was highly conserved (99.7–100.0% homology), which has also been repeatedly mentioned in other studies [8, 29].

The *B. anthracis* strains were grouped into a single cluster; however, the level of significance was low. *Bt* strains were also attributed to this cluster *B. anthracis*. We distinguished two *B. cereus* groups (I and II), identically to the study by Bavykin *et al.* [45]. This branching has not been statistically confirmed (statistical significance of the branching order < 50%). The *B. cereus* I group included the pathogenic *B. cereus* strain ATCC 14579^T and a number of nonpathogenic *Bt* serovars. The *B. cereus* II group consisted of various *Bt* serovars and nonpathogenic *B. cereus* strain ATCC 10987^T. Most of the *Bt* strains with a low significance level of branching formed a single cluster, which brought together different serovars of this species. The *B. mycoides* and *B. weihenstephanensis* strains were attributed to a separate subgroup.

The potential commercial strains and the typical strain *Bt ser. berliner* ATCC 10792^T were put together and attributed to the *Bt* II group with a branching significance of 56%. This group comprised seventeen Ukrainian isolates of different serotypes isolated from different host insects, mostly from the Lugansk and Kherson regions, and the Krasnogvardeisk and Simferopol districts. Strain *Bt* 0376 p.o. (serotype 1) was proposed for the production of the eco-friendly entomopathogenic preparation “STAR-t” (OOO Simbitor) intended to control the number of Colorado potato beetle (*Leptinotarsa decemlineata*) larvae, potato tuber moth (*Phthorimea operculella* Zel.), and chickpea leaf-miner (*Liriomiza cicerina* Rd.) during vegetation and storing potato and chickpea and was attributed to this group and had the group-specific substitutions A/G77, T/C90, T/A92, C/T192, C/A1015 in the 16S rRNA gene. All the investigated isolates from the *Bt* II group had completely identical nucleotide sequences of the 16S rRNA gene. Strain *Bt var. thuringiensis* 994 (serotype 1, analogue of the bioagent of bacterial preparation “Bitoxybacillin”) used to produce the preparation “Akbitur,” strain *Bt* 408 (serotype 3) exhibiting high entomopathogenic activity against *L. decemlineata*, and strain *Bt var. darmstadiensis* H10 (serotype X) were also attributed to the *Bt* II group.

Strains *Bt* 836 (serotype 4), *Bt var. kurstaki* 0293 (serotype 3, analogue of the strain used as a bioagent in the preparation “Lepidocid”), and *Bt var. morrisoni* 109 (serotype X) were attributed to the *Bt* I group. Both specific nucleotide substitutions typical and unique for the *Bt* strains were found within each group. A total of 16, 30, 32, 28, and 21 substitutions were found in *B. anthracis*, *B. cereus* I, *B. cereus* II, *Bt* I, and *Bt* II, respectively. However, it should be men-

tioned that most nucleotide substitutions were random and strain-specific.

Thus, the 16S rRNA gene cannot be used to assess and study the phylogenetic relationships of the *B. cereus* group at a levels below genus/species, since it does not allow one to determine the species-specific nucleotide substitutions for this group.

Genetic diversity of the sequences of the *gyrB* gene

The nucleotide sequence of the *gyrB* gene is used along with the 16S rRNA gene in taxonomic studies and for bacterial identification [34]. A number of studies have recently been published where the variability of the sequence of this gene in different bacterial species belonging to the genus *Bacillus* was studied (e.g., *B. subtilis* [46], *B. cereus* groups [47]). The universal primers proposed earlier [34] and the primer systems constructed by us and specific for the 3'-terminus of the *gyrB* gene of bacteria belonging to the *B. cereus* group were used to amplify and sequence the PCR fragments of this gene (the size of the sequenced region was 1800 bp, 81.82% of the entire gene). We selected this fragment of the gene on the basis of the distribution of the polymorphism (entropy) level of the *gyrB* nucleotide sequence using the DNAsp v. 5 software [48]. The level of polymorphism was above average on the regions 150–700 and 1650–200 bp from the beginning of the gene (data not shown). However, due to the fact that there was a limited number of *gyrB* DNA sequences of a certain length of strains belonging to the *B. cereus* group in GenBank, we selected the region from 385 to 1507 bp from the beginning of the gene (the annotation is provided for the strain *Bt ser. berliner* ATCC 10792^T), which comprised 60% of the total length of the gene, for the analysis. The phylogenetic tree shown in Fig. 2 was constructed using the ME algorithm for 25 investigated strains, isolates, and reference sequences of the *Bacillus* sp. strains included in GenBank. The nucleotide sequences of species *B. pumilus*, *B. licheniformis*, and *B. subtilis* were used as remote controls for the phylogenetic analysis.

The topology of the constructed tree was similar with that of the phylogenetic trees constructed earlier for the 16S rRNA gene, and for the intergenic region 16S–23S rRNA; it showed no dependence on the algorithms used for the construction (NJ, ME). The inter- and intraspecies differences between the species *B. anthracis* and the *B. cereus* – *Bt* group have been identified. The results of the studies demonstrated that the nucleotide sequence of the *gyrB* gene possesses a higher resolving power than the 16S rRNA gene and the intergenic region 16S–23S rRNA sequences [34, 46] and, hence, is more suitable for the taxonomic studies of closely related species.

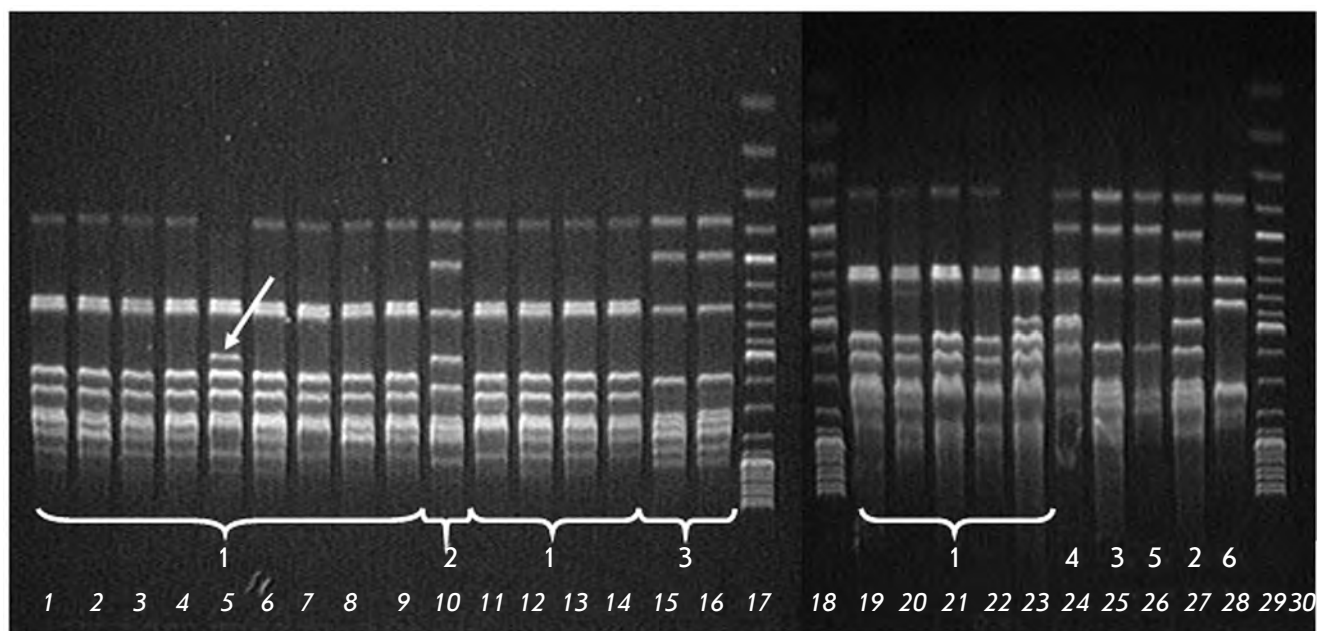


Fig. 3. Electrophoretic analysis of the saAFLP products obtained for the DNA samples of *B. thuringiensis* strains. Lanes: **17, 18, 29** – 1 kb GeneRuler™ DNA molecular mass marker (Fermentas); **1** – *Bt* H10, R-type; **2** – *Bt* A/N; **3** – *Bt* 408; **4, 19** – *Bt* 5681st; **5, 23** – *Bt* 0376 p.o.; **6** – *Bt* 787; **7** – *Bt* 411; **8** – *Bt* 72; **9** – *Bt* 0371-1; **10, 27** – *Bt* 109; **11** – *Bt* 14; **12** – *Bt* 994; **13** – *Bt* 1b; **14** – *Bt* A/M; **15** – *Bt* 836; **16, 25** – *Bt* 0293; **20** – *Bt* sbsp. *israelensis* B-5246; **21** – *Bt* 0371; **22** – *Bt* sbsp. *thuringiensis* B-1223; **24** – *Bt* sbsp. *subtoxicus* B-822; **26** – *Bt* sbsp. *galerae* B-197; **28** – *Bt* sbsp. *finitimus* B-1162; **30** – control PCR without template DNA

Identically to the data obtained for the 16S rRNA gene (but with a higher significance level), five subgroups can be distinguished within the *B. cereus* group: *B. anthracis*, *B. cereus* I and II, *Bt* I and II. Another group, *Bt* III, was distinguished in the phylogenetic cladogram with a 92% statistical significance of the branching order. It comprised the following strains: *Bt* ser. *bolivia* IEBC-T63 and *Bt* ser. *finitimus* IEBC-T02. With a high significance level, most strains formed the *Bt* II group, which also comprised the strains used for the production of entomopathogenic preparations. However, as previously assumed based on published data, the *B. cereus* and *Bt* species were indistinguishable [45]. Thus, the *Bt* strains, along with the strains belonging to the species *B. anthracis*, *B. cereus*, and *B. weihenstephanensis*, were grouped into the subgroups *B. anthracis*, *B. cereus* I and II and *B. weihenstephanensis*. The *gyrB* gene of strain *Bt* 0376 p.o. and other strains of this group were compared; due to the higher resolving power and variability of the *gyrB* nucleotide sequence, two substitutions specific to this strain (A/G861 and A/G1149) have been identified. In general, the level of similarity between the nucleotide and amino acid sequences in the *B. cereus* group was 87.1–95.2% and 95.1–99.2%, respectively.

Clusterization of the strains into two groups with a high statistical significance of the branching order is worth mentioning. Cluster I was formed by groups A and B. Group A consisted of the reliably grouped pathogenic strains *B. anthracis*, the nonpathogenic strain *B. cereus* ATCC 10987^T, entomopathogenic strains *Bt* ser. *finitimus* B1162 and *Bt* ser. *poloniensis* IEBC-T54 belonging to the *B. cereus* II group, and entomopathogenic strains belonging to the *Bt* III group. Group B was formed by strain *B. cereus* ATCC 14579^T (pathogenic for humans), entomopathogenic strains *Bt* belonging to the *B. cereus* I group, and entomopathogenic strains belonging to the *Bt* I group. Cluster II included bacteria belonging to the species *B. weihenstephanensis* and *B. mycooides*, and the *Bt* II group comprising most of the strains used for industrial production of entomopathogenic preparations. This clusterization of bacteria probably attests to a paraphyletic structure of both the *B. cereus* group in general and the separate species of this group.

Polymorphism among *Bt* detected using saAFLP and rep-PCR markers

Along with the housekeeping genes, genomic fingerprinting methods are used to reveal the differences be-

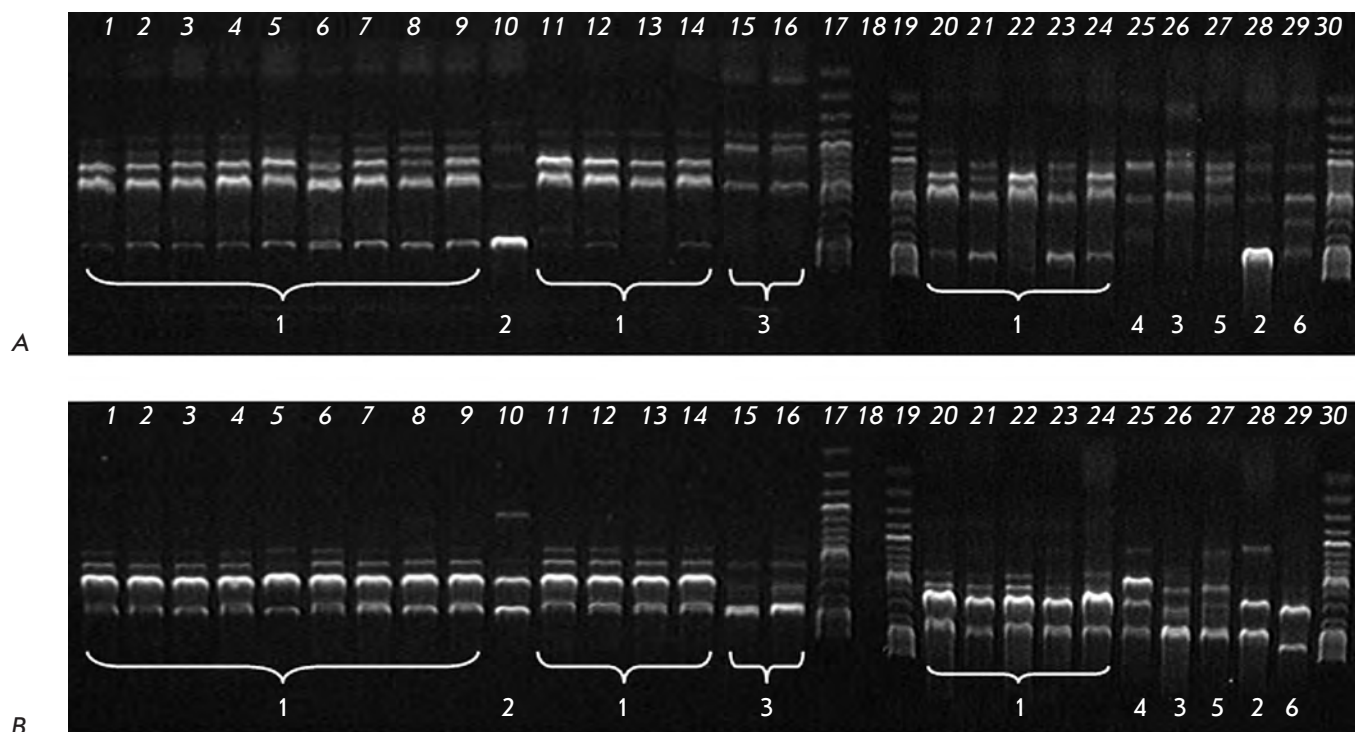


Fig. 4. Electrophoretic analysis of the PCR products obtained for DNA samples of *B. thuringiensis* strains with primers ERIC (A) and BOX (B). Lanes: **17, 19, 30** – 1 kb GeneRuler™ DNA molecular mass marker (Fermentas); **1** – *Bt* H10, R-type; **2** – *Bt* A/N; **3** – *Bt* 408; **4, 19** – *Bt* 5681st; **5, 23** – *Bt* 0376 p.o.; **6** – *Bt* 787; **7** – *Bt* 411; **8** – *Bt* 72; **9** – *Bt* 0371-1; **10, 28** – *Bt* 109; **11** – *Bt* 14; **12** – *Bt* 994; **13** – *Bt* 1b; **14** – *Bt* A/M; **15** – *Bt* 836; **16, 26** – *Bt* 0293; **18** – control PCR without template DNA; **21** – *Bt* sbsp. *israelensis* B-5246; **22** – *Bt* 0371; **22** – *Bt* sbsp. *thuringiensis* B-1223; **25** – *Bt* sbsp. *subtoxicus* B-822; **27** – *Bt* sbsp. *galerae* B-197; **29** – *Bt* sbsp. *finitimus* B-1162

tween closely related bacterial species and strains. Rep-PCR is the most frequently used. This method is based on using oligonucleotide primers homologous to the sequences of various intergenic repeats. In our study, the differences between the closely related *Bt* strains were identified using rep-PCR (BOX-, ERIC-PCR) and saAFLP. The results obtained are shown in *Figs. 3, 4*.

All the strains under study were analyzed by saAFLP applying three restriction endonucleases (XmaJI, XbaI, and PstI). The informative spectra for all the *Bt* strains were recorded using XmaJI only. The modified saAFLP method allowed to distinguish the strains at the species–group level. All investigated *Bt* strains were divided into six group according to these spectra (*Fig. 3*). All strains presumably belonged to different subspecies of the *Bt* species. Group 1 comprised the typical strains *Bt* sbsp. *thuringiensis* and *Bt* 0376 p.o. This strain contained a unique saAFLP pattern (1,000 bp long), which distinguished it from the other strains belonging to group 1 (marked with a white arrow in *Fig. 3*). Groups 2, 3, 4, and 5 were represented by either a small number of strains or a single strain. It

should be mentioned that this grouping corresponded to the data obtained previously by the analysis of 16S rRNA and *gyrB* genes sequences. It is significant that each strain of the same group was characterized by a group-specific saAFLP spectrum and pattern, which distinguished it from the strains belonging to the other groups. We also found patterns (markers) that are unique for individual strains (e.g., the commercial strain *Bt* 0376 p.o.), which distinguished them among all the strains belonging to group 1. Thus, the proposed method is more specific and can be used for a quick search for strain/group-unique markers and for the study of polymorphism in populations.

The ERIC-PCR (*Fig. 4A*) and BOX-PCR (*Fig. 4B*) methods were also used in this study to compare the results obtained using these reference primers and by saAFLP analysis modified by us. Based on the analysis of the obtained ERIC and BOX patterns, all investigated *Bt* strains were subdivided into six groups. However, no differences between the ERIC and BOX spectra detected within each group for every strain. The number of specific PCR markers and the total number

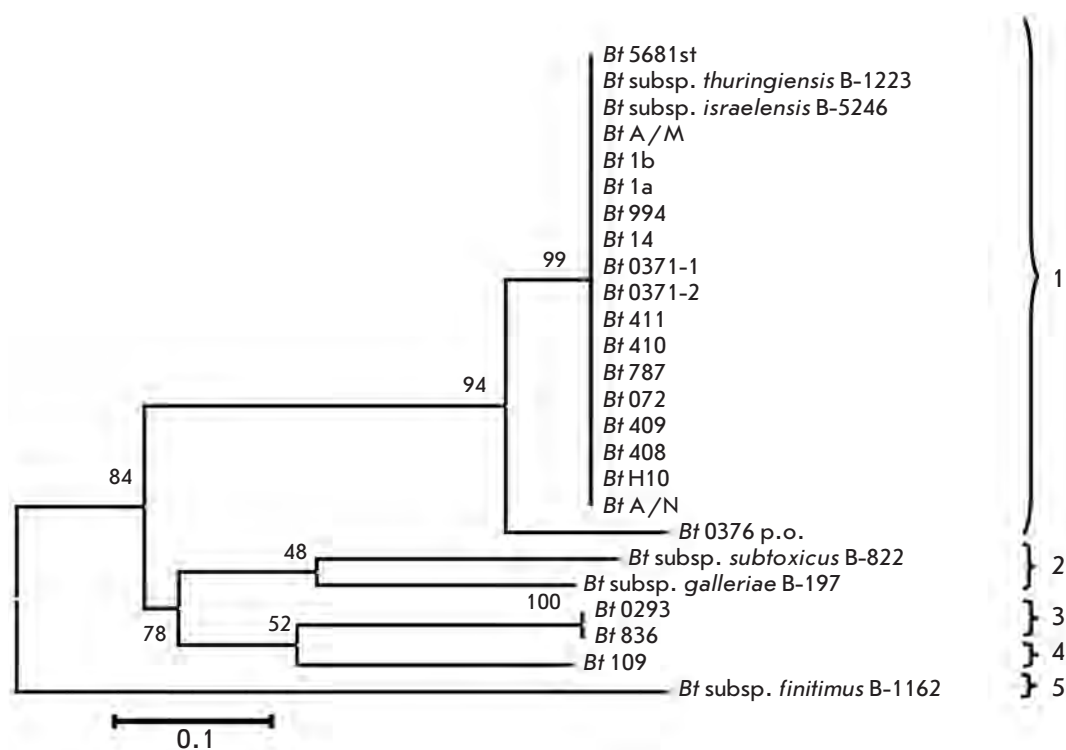


Fig. 5. Dendrogram of 25 *Bt* strains isolated on the territory of Ukraine. The dendrogram was constructed using the NJ algorithm based on the total results of ERIC and BOX PCR and saAFLP for 36 polymorphic markers. The numbers denote the statistical significance of the branching order (%) determined by a bootstrap analysis of 1,000 permutations

of fragments obtained by saAFLP were greater than those obtained using the ERIC and BOX primers. This fact attests to the higher sensitivity, specificity, and informativity of the saAFLP method. The character of the results could be attributed to the fact that the ERIC and BOX-PCR allow one to analyze only separate genomic regions, which are rather conserved (promoter regions (ERIC1R-ERIC2, BOX, REP2-I-REP1R-I) or the regions of functional genes (e.g., tRNA)). Hence, the spectra obtained by these methods contain general, rather than strain-specific, information and could be more useful for passportization of strains. The spectra recorded by saAFLP, which is not confined to any particular genomic region, show the individuality of each microorganism. The differences between all the analyzed strains could be identified on the basis of fingerprints (patterns) based on this method [34]. The specificity of the spectra allows one to conclude that the saAFLP method is probably appropriate for investigating and distinguishing the true phylogenetic relationships between bacteria without using the data obtained through other primers or methods, with the exception of determining the genus of a microorganism using the 16S rRNA or *gyrB* gene.

However, in order to verify the reliability of these results and obtain a complete view of the genetic relationships between closely related bacteria, it is necessary to analyze the overall data obtained by both the saAFLP method and ERIC- and BOX-PCR.

In our study, we used three methods (ERIC-, BOX-PCR, and saAFLP) to identify 36 polymorphic markers (unique fragments) among the analyzed strains. The resulting data were used to construct a dendrogram (Fig. 5). The genetic distances between the strain pairs were determined using Pearson's correlation, the Simple difference, and the Cosine distance (data not shown). The resulting matrix distances were used to conduct a cluster analysis using the NJ method. According to the results obtained, all the investigated strains were subdivided into five clusters. The statistical significance of the branching order varied from 58 to 99%. The clusters were isolated based on a similarity of $\geq 80\%$ and/or a significance level of branching $\geq 50\%$. Cluster 1 comprised the strains *Bt* H10 R-type, *Bt* A/N, *Bt* 408, *Bt* 409, *Bt* 410, *Bt* 5681st, *Bt* 787, *Bt* 411, *Bt* 072, *Bt* 0371-1, *Bt* 14, *Bt* 994, *Bt* 1a, *Bt* 1b, *Bt* A/M, *Bt* subsp. *israelensis* B-5246, *Bt* 0371-1, *Bt* 0371-2, and the typical strain *Bt* subsp. *thuringiensis* B-1223. Within this cluster, the strain *Bt* 0376 p.o. was isolated with a high statistical significance of the branching order. Cluster 2 was formed by two subspecies, *Bt* subsp. *galleriae* and *Bt* subsp. *subtoxicus*. A significance of branching of $< 50\%$ demonstrates that these strains presumably belong to two different subspecies and may represent separate clusters if the strain sampling is enlarged. In order to verify or refute this hypothesis, the strain sample should be broadened. Cluster 3 consisted of the strains *Bt* 0293 and *Bt* 836; clusters 4 and 5 were rep-

resented by the strains *Bt* 109 and *Bt* subsp. *finitimus* B-1162, respectively.

Based on the published data and the results obtained by us, it can be concluded that a complex approach combining an analysis of both the biochemical properties of the strain and molecular-biological methods, is required to study and identify the *Bt* species belonging to the *B. cereus* group. The *Bt* species can be successfully studied using the nucleotide sequence of the *gyrB* gene. At the intraspecies level, it can be studied by saAFLP, along with the other AP-PCR methods (rep-PCR). These methods were used to subdivide the strain sample into five groups, which also corresponded

to their unique biochemical properties that had previously been determined in studies conducted by our colleagues [49]. The elaborated saAFLP method enabled to identify the DNA fragment, which is unique for the strain *Bt* 0376 p.o., isolated first by our colleagues from the Institute of Agriculture of the Crimea (National Academy of Agrarian Sciences of Ukraine) and used to produce the entomopathogenic preparation "STAR-t". We intend to increase the size of the strain sampling, to study the composition of the *cry* genes, and to determine the nucleotide sequences of the unique DNA fragments revealed for the separate saAFLP groups and strains. ●

REFERENCES

- Hofte H., Whiteley H.R. // *Microbiol. Rev.* 1989. V. 53. P. 242–255.
- Feitelson J.S. // *Advanced engineered pesticides* / Ed. Kim L. N.Y.: Marcel Dekker, 1993. P. 63–72.
- Crickmore N., Zeigler D.R., Feitelson J., Schnepf E., Vanrie J., Lereclus D., Baum J., Dean D.H. // *Microbiol. Rev.* 1998. V. 62. P. 807–813.
- Aronson A.I., Beckman W., Dunn P. // *Microbiol. Rev.* 1986. V. 50. P. 1–24.
- Rowe G.E., Margaritis A. // *Crit. Rev. Biotechnol.* 1987. V. 6. P. 87–127.
- Baumann L., Okamoto K., Unterman B.M., Lynch M.J., Baumann P. // *J. Invertebr. Pathol.* 1984. V. 44. P. 329–341.
- Aronson A.I. // *Bacillus subtilis* and other gram-positive bacteria: biochemistry, physiology, and molecular genetics / Eds. Sonenshein A.B., Hoch J.A., Losick R. Washington, D.C.: Amer. Soc. Microbiol., 1993. P. 953–963.
- Ash C., Farrow J.A.E., Dorsch M., Stackebrandt E., Collins M.D. // *Int. J. Syst. Bacteriol.* 1991. V. 41. P. 343–346.
- Carlson C.R., Caugant D.A., Kolsto A.-B. // *Appl. Environ. Microbiol.* 1994. V. 60. P. 1719–1725.
- Wunschel D., Fox K.F., Black G.E., Fox A. // *Syst. Appl. Microbiol.* 1994. V. 17. P. 625–635.
- Bourque S.N., Valero J.R., Lavoie M.C., Levesque R.C. // *Appl. Environ. Microbiol.* 1995. V. 61. P. 1623–1626.
- Helgason E., Okstad O.A., Caugant D.A., Johansen H.A., Fouet A., Mock M., Hegna I., Kolsto A.-B. // *Appl. Environ. Microbiol.* 2000. V. 66. P. 2627–2630.
- Chen M.L., Tsen H.Y. // *J. Appl. Microbiol.* 2002. V. 92. P. 912–919.
- Thorne C.B. // *Bacillus subtilis* and other gram-positive bacteria / Ed. Sonenshein A.L. Washington, D.C.: Amer. Soc. Microbiol., 1993. P. 113–124.
- de Barjac H., Franchan E. // *Entomophaga.* 1990. V. 35. P. 233–240.
- Lecadet M.-M., Frachon E., Cosmao Dumanoir V., Ripou-teau H., Hamon S., Laurent P., Thiery I. // *J. Appl. Microbiol.* 1999. V. 86. P. 660–672.
- Hansen B.M., Damgaard P.H., Eilenberg J., Pedersen J.C. // *J. Invertebr. Pathol.* 1998. V. 71. P. 106–114.
- Helgason E., Caugant D.A., Lecadet M.-M., Chen Y., Mahillon J., Hegna I., Kvaloy K., Kolsto A.-B. // *Curr. Microbiol.* 1998. V. 37. P. 80–87.
- Priest F.G., Barker M., Baillie L.W.J., Holmes E.C., Maiden M.C.J. // *J. Bacteriol.* 2004. V. 186. № 23. P. 7959–7970.
- Somerville H.J., Jones M.L. // *J. Gen. Microbiol.* 1982. V. 73. P. 257–265.
- Ko K.S., Kim J.M., Kim J.W., Jung B.Y., Kim W., Kim I.J., Kook Y.H. // *J. Clin. Microbiol.* 2003. V. 41. P. 2908–2914.
- Kiem P., Kalif A., Schupp J., Hill K., Travis S.E., Richmond K., Adair D.M., Hugh-Jones M., Kuske C.R., Jackson P. // *J. Bacteriol.* 1997. V. 179. P. 818–824.
- Hill K., Ticknor L., Okinaka R., Asay M., Blair H., Bliss K., Laker M., Pardington P., Richardson A., Tonks M., et al. // *Appl. Environ. Microbiol.* 2004. V. 70. P. 1068.
- Ticknor L.O., Kolsto A.-B., Hill K.K., Keim P., Laker M.T., Tonks M., Jackson P.J. // *Appl. Environ. Microbiol.* 2001. V. 67. P. 4863–4873.
- Joung K.-B., Cote J.-C. // *J. Appl. Microbiol.* 2001. V. 90. P. 115–122.
- Epplen J.T., Ammer H., Epplen C. / *Oligonucleotide Fingerprinting Using Simple Repeat Motifs: A Convenient, Ubiquitously Applicable Method To Detect Hypervariability for Multiple Purposes* // Eds Burke G., Dolf G., Jeffreys A.J., Wolff R. Basel: Birkhauser, 1991. P. 50–69.
- Louws F.J., Fulbright D.W., Stephens C.T., de Bruijn F.J. // *Appl. Environ. Microbiol.* 1994. V. 60. P. 2286–2295.
- Chaley M.B., Korotkov E.V., Skryabin K.G. // *DNA Res.* 1999. V. 6. P. 153–163.
- Boulygina E.S., Ignatov A.N., Tsygankova S.V., Korotkov E.V., Kuznetsov B.B. // *Microbiology.* 2009. V. 78. № 6. P. 703–710.
- Bergey's Manual of Systematic Bacteriology*, 2nd Ed. // Eds Logan N.A., De Vos P. N.Y.: Springer, 2009. № 3. P. 21–128.
- Manual of Methods for General Bacteriology* // Eds Gerhardt P., Murray R.G., Costilow R.N., Nester E.W., Wood M.W., Krieg N.R., Phillips G.B. Washington, DC: Am. Soc. Microbiol., 1981. P. 232–234.
- Sanger F., Air G.M., Barrell B.G. // *Nature.* 1977. V. 265. P. 687–695.
- Lane D.J. / *16S/23S rRNA sequencing. Nucleic Acid Techniques in Bacterial Systematics* // Eds Stackebrandt E., Goodfellow M. N.Y.: Wiley, 1991. P. 115–175.
- Yamamoto S., Harayama S. // *Appl. Environ. Microbiol.* 1995. V. 61. P. 1104–1109.
- Zotov V.S., Punina N.V., Khapchaeva S.A., Didovich S.V., Melnichuk T.N., Topunov A.F. // *Ekologicheskaya genetika.* 2012. V. 2. P. 49–62.
- Zabeau M., Vos P. Selective restriction fragment amplification: a general method for DNA fingerprinting //

RESEARCH ARTICLES

- European Patent Office. Munich. Germany. 1993. Publication 0534858A1.
37. Altschul S.F., Gish W., Miller W. // *J. Mol. Biol.* 1990. V. 215. P. 403–410.
38. Thompson J.D., Higgins D.G., Gibson T.J. // *Nucl. Acids Res.* 1994. V. 22. P. 4673–4680.
39. Hall T.A. // *Nucl. Acids Symp. Ser.* 1999. V. 41. P. 95–98.
40. Kumar S., Tamura K., Nei M. // *Briefings in Bioinformatics.* 2004. V. 5. P. 150–163.
41. Nei M., Kumar S. *Molecular evolution and phylogenetics.* N.Y.: Oxford Univ. Press, 2000. P. 336.
42. Rzetsky A., Nei M. // *Mol. Biol. Evol.* 1992. V. 9. P. 945–967.
43. Priest F.G. / DNA homology in the genus *Bacillus*. In *The Aerobic Endospore-Forming Bacteria* // Eds Berkeley R.C.W., Goodfellow M. London: Acad. Press, 1981. P. 33–57.
44. Daffonchio D., Cherif A., Borin S. // *Appl. Environ. Microbiol.* 2000. V. 66. P. 5460–5468.
45. Bavykin S.G., Lysov Y.P., Zakhariyev V., Kelly J.J., Jackman J., Stahl D.A., Cherni A. // *J. Clin. Microbiol.* 2004. V. 42. № 8. P. 3711–3730.
46. Wang L.T., Lee F.L., Tai C.J., Kasai H. // *Int. J. Syst. Evol. Microbiol.* 2007. V. 57. P. 1846–1850.
47. La Duc M.T., Satomi M., Agata N., Venkateswaran K. // *J. Microbiol. Meth.* 2004. V. 56. P. 383–394.
48. Librado P., Rozas J. // *Bioinformatics.* 2009. V. 25. P. 1451–1452.
49. Parkhomenko A.L., Parkhomenko T.U., Lesovoy N.M. // *Scientific notes of Taurida V. Vernadsky National University. Series: Biology, Chemistry.* 2009. V. 22. № 3. P. 96–100.

GENERAL RULES

Acta Naturae publishes experimental articles and reviews, as well as articles on topical issues, short reviews, and reports on the subjects of basic and applied life sciences and biotechnology.

The journal is published by the Park Media publishing house in both Russian and English.

The journal *Acta Naturae* is on the list of the leading periodicals of the Higher Attestation Commission of the Russian Ministry of Education and Science

The editors of *Acta Naturae* ask of the authors that they follow certain guidelines listed below. Articles which fail to conform to these guidelines will be rejected without review. The editors will not consider articles whose results have already been published or are being considered by other publications.

The maximum length of a review, together with tables and references, cannot exceed 60,000 symbols (approximately 40 pages, A4 format, 1.5 spacing, Times New Roman font, size 12) and cannot contain more than 16 figures.

Experimental articles should not exceed 30,000 symbols (20 pages in A4 format, including tables and references). They should contain no more than ten figures. Lengthier articles can only be accepted with the preliminary consent of the editors.

A short report must include the study's rationale, experimental material, and conclusions. A short report should not exceed 12,000 symbols (8 pages in A4 format including no more than 12 references). It should contain no more than four figures.

The manuscript should be sent to the editors in electronic form: the text should be in Windows Microsoft Word 2003 format, and the figures should be in TIFF format with each image in a separate file. In a separate file there should be a translation in English of: the article's title, the names and initials of the authors, the full name of the scientific organization and its departmental affiliation, the abstract, the references, and figure captions.

MANUSCRIPT FORMATTING

The manuscript should be formatted in the following manner:

- Article title. Bold font. The title should not be too long or too short and must be informative. The title should not exceed 100 characters. It should reflect the major result, the essence, and uniqueness of the work, names and initials of the authors.
- The corresponding author, who will also be working with the proofs, should be marked with a footnote *.
- Full name of the scientific organization and its departmental affiliation. If there are two or more scientific organizations involved, they should be linked by digital superscripts with the authors' names. Abstract. The structure of the abstract should be very clear and must reflect the following: it should introduce the reader to the main issue and describe the experimental approach, the possibility of practical use, and the possibility of further research in the field. The average length of an abstract is 20 lines

(1,500 characters).

- Keywords (3 – 6). These should include the field of research, methods, experimental subject, and the specifics of the work. List of abbreviations.

- INTRODUCTION
- EXPERIMENTAL PROCEDURES
- RESULTS AND DISCUSSION
- CONCLUSION

The organizations that funded the work should be listed at the end of this section with grant numbers in parenthesis.

- REFERENCES

The in-text references should be in brackets, such as [1].

RECOMMENDATIONS ON THE TYPING AND FORMATTING OF THE TEXT

- We recommend the use of Microsoft Word 2003 for Windows text editing software.
- The Times New Roman font should be used. Standard font size is 12.
- The space between the lines is 1.5.
- Using more than one whole space between words is not recommended.
- We do not accept articles with automatic referencing; automatic word hyphenation; or automatic prohibition of hyphenation, listing, automatic indentation, etc.
- We recommend that tables be created using Word software options (Table → Insert Table) or MS Excel. Tables that were created manually (using lots of spaces without boxes) cannot be accepted.
- Initials and last names should always be separated by a whole space; for example, A. A. Ivanov.
- Throughout the text, all dates should appear in the “day.month.year” format, for example 02.05.1991, 26.12.1874, etc.
- There should be no periods after the title of the article, the authors' names, headings and subheadings, figure captions, units (s – second, g – gram, min – minute, h – hour, d – day, deg – degree).
- Periods should be used after footnotes (including those in tables), table comments, abstracts, and abbreviations (mon. – months, y. – years, m. temp. – melting temperature); however, they should not be used in subscripted indexes (T_m – melting temperature; T_{pt} – temperature of phase transition). One exception is mln – million, which should be used without a period.
- Decimal numbers should always contain a period and not a comma (0.25 and not 0,25).
- The hyphen (“-”) is surrounded by two whole spaces, while the “minus,” “interval,” or “chemical bond” symbols do not require a space.
- The only symbol used for multiplication is “×”; the “×” symbol can only be used if it has a number to its right. The “.” symbol is used for denoting complex compounds in chemical formulas and also noncovalent complexes (such as DNA·RNA, etc.).
- Formulas must use the letter of the Latin and Greek alphabets.

GUIDELINES FOR AUTHORS

- Latin genera and species' names should be in italics, while the taxa of higher orders should be in regular font.
- Gene names (except for yeast genes) should be italicized, while names of proteins should be in regular font.
- Names of nucleotides (A, T, G, C, U), amino acids (Arg, Ile, Val, etc.), and phosphonucleotides (ATP, AMP, etc.) should be written with Latin letters in regular font.
- Numeration of bases in nucleic acids and amino acid residues should not be hyphenated (T34, Ala89).
- When choosing units of measurement, SI units are to be used.
- Molecular mass should be in Daltons (Da, KDa, MDa).
- The number of nucleotide pairs should be abbreviated (bp, kbp).
- The number of amino acids should be abbreviated to aa.
- Biochemical terms, such as the names of enzymes, should conform to IUPAC standards.
- The number of term and name abbreviations in the text should be kept to a minimum.
- Repeating the same data in the text, tables, and graphs is not allowed.

GUIDENESS FOR ILLUSTRATIONS

- Figures should be supplied in separate files. Only TIFF is accepted.
- Figures should have a resolution of no less than 300 dpi for color and half-tone images and no less than 500 dpi.
- Files should not have any additional layers.

REVIEW AND PREPARATION OF THE MANUSCRIPT FOR PRINT AND PUBLICATION

Articles are published on a first-come, first-served basis. The publication order is established by the date of acceptance of the article. The members of the editorial board have the right to recommend the expedited publishing of articles which are deemed to be a priority and have received good reviews.

Articles which have been received by the editorial board are assessed by the board members and then sent for external review, if needed. The choice of reviewers is up to the editorial board. The manuscript is sent on to reviewers who are experts in this field of research, and the editorial board makes its decisions based on the reviews of these experts. The article may be accepted as is, sent back for improvements, or rejected.

The editorial board can decide to reject an article if it does not conform to the guidelines set above.

A manuscript which has been sent back to the authors for improvements requested by the editors and/or reviewers is reviewed again, after which the editorial board makes another decision on whether the article can be accepted for publication. The published article has the submission and publication acceptance dates set at the beginning.

The return of an article to the authors for improvement does not mean that the article has been accepted for publication. After the revised text has been received, a decision is made by the editorial board. The author must return the improved text, together with the original text and responses to all comments. The date of acceptance is the day on which the final version of the article was received by the publisher.

A revised manuscript must be sent back to the publisher a week after the authors have received the comments; if not, the article is considered a resubmission.

E-mail is used at all the stages of communication between the author, editors, publishers, and reviewers, so it is of vital importance that the authors monitor the address that they list in the article and inform the publisher of any changes in due time.

After the layout for the relevant issue of the journal is ready, the publisher sends out PDF files to the authors for a final review.

Changes other than simple corrections in the text, figures, or tables are not allowed at the final review stage. If this is necessary, the issue is resolved by the editorial board.

FORMAT OF REFERENCES

The journal uses a numeric reference system, which means that references are denoted as numbers in the text (in brackets) which refer to the number in the reference list.

For books: the last name and initials of the author, full title of the book, location of publisher, publisher, year in which the work was published, and the volume or issue and the number of pages in the book.

For periodicals: the last name and initials of the author, title of the journal, year in which the work was published, volume, issue, first and last page of the article. Must specify the name of the first 10 authors. Ross M.T., Grafham D.V., Coffey A.J., Scherer S., McLay K., Muzny D., Platzer M., Howell G.R., Burrows C., Bird C.P., et al. // Nature. 2005. V. 434. № 7031. P. 325–337.

References to books which have Russian translations should be accompanied with references to the original material listing the required data.

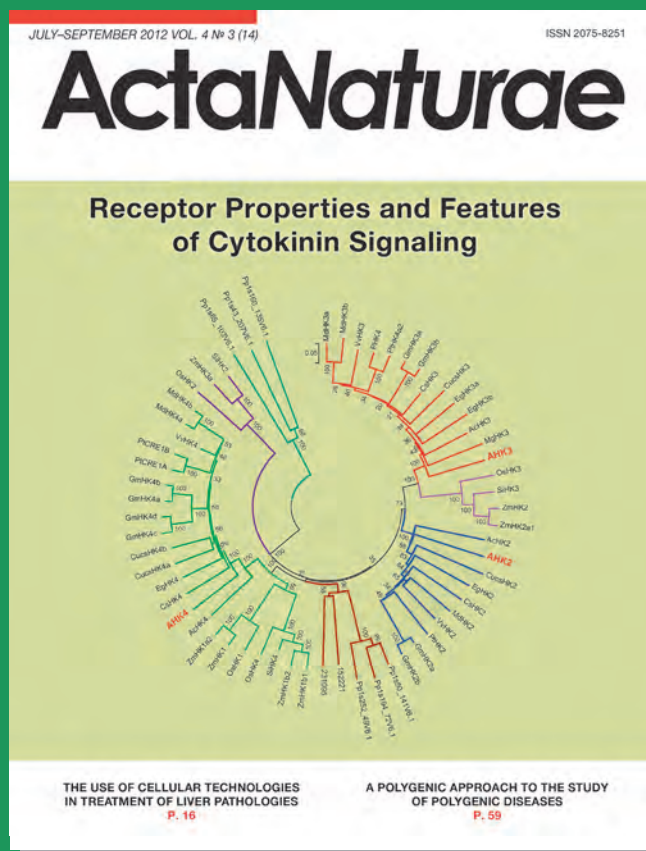
References to doctoral thesis abstracts must include the last name and initials of the author, the title of the thesis, the location in which the work was performed, and the year of completion.

References to patents must include the last names and initials of the authors, the type of the patent document (the author's rights or patent), the patent number, the name of the country that issued the document, the international invention classification index, and the year of patent issue.

The list of references should be on a separate page. The tables should be on a separate page, and figure captions should also be on a separate page.

The following e-mail addresses can be used to contact the editorial staff: vera.knorre@gmail.com, actanaturae@gmail.com, tel.: (495) 727-38-60, (495) 930-87-07

Acta Naturae is a new international journal on life sciences based in Moscow, Russia. Our goal is to present scientific work and discovery in molecular biology, biochemistry, biomedical disciplines and biotechnology. *Acta Naturae* is also a periodical for those who are curious in various aspects of biotechnological business, intellectual property protection and social consequences of scientific progress.



For more information and subscription please contact us at journal@biorf.ru

NANOTECHNOLOGIES

in Russia

Peer-review scientific journal

Nanotechnologies in Russia
(*Rossiiskie Nanotekhnologii*)

focuses on self-organizing structures and nanoassemblages, nanostructures including nanotubes, functional nanomaterials, structural nanomaterials, devices and facilities on the basis of nanomaterials and nanotechnologies, metrology, standardization, and testing in nanotechnologies, nanophotonics, nanobiology.

→ **Russian edition:** <http://nanoru.ru>

→ **English edition:** <http://www.springer.com/materials/nanotechnology/journal/12201>

Issued with support from:



The Ministry of Education and Science of the Russian Federation